# Chemistry and reaction kinetics of biowaste torrefaction

# Chemistry and Reaction Kinetics of Biowaste Torrefaction

PROEFSCHRIFT

ter verkrijging van de graad van doctor aan de Technische Universiteit Eindhoven, op gezag van de rector magnificus, prof.dr.ir. C.J. van Duijn, voor een commissie aangewezen door het College voor Promoties in het openbaar te verdedigen op dinsdag 15 maart 2011 om 16.00 uur

door

Marcelis Jacob Cornelis van der Stelt

geboren te Werkendam

Dit proefschrift is goedgekeurd door de promotor:

prof.dr. H.J. Veringa

Technische Universiteit Eindhoven, 2010
A catalogue record is available from the Eindhoven University of Technology Library.

ISBN: 978-90-386-2435-8

This thesis is printed by Gildeprint, Enschede, The Netherlands.
The cover page is designed by Jeroen Ramakers

# Chemistry and Reaction Kinetics of Biowaste Torrefaction


## Summary

This thesis addresses the question of how the chemistry and reaction kinetics of torrefaction are influenced by reaction conditions and the effects occurring during the reaction. This research question can be specified by questions such as, what controls their kinetics during torrefaction and what does this mean, which products are formed, what are the mass - and energy balances, and what is the endothermal and/or exothermal behaviour.

In future energy scenarios an important role in the (renewable) energy supply is given to biomass. The unique position of biomass as the only renewable source for sustainable carbon carrier makes biomass an attractive energy source. Biomass as energy source has some typical characteristics making it a specific, but complicated fuel for the future. Some biomass properties are inconvenient, particularly its high oxygen content, a low calorific value, the hydrophilic nature and there with connected high moisture content. Other disadvantages of biomass are its tenacious and fibrous structure and its inhomogeneous composition. This makes process design and process control complicated. Torrefaction is a technology that can improve biomass properties and therefore offers solutions to the above problems. Torrefaction is a thermal pre-treatment technology to upgrade ligno-cellulosic biomass to a higher quality and more attractive biofuel. The main principle of torrefaction, from a chemical point of view, is the removal of oxygen leading to a final solid product: the torrefied biomass having a lower O/C ratio compared to the original biomass.

The heart of the torrefaction technology is the reactor concept. In the development of the torrefaction system knowledge it is important to obtain a good insight into the mechanisms of torrefaction at fundamental level. Torrefaction is a complex process which involves many physical and chemical processes such as heat transfer, moisture evaporation, decomposition kinetics, heat of torrefaction, pressure build up in the solid, changes in material properties all in relation with

torrefaction temperature. Further the material is inherently anisotropic. Research at this level can give better information about the quality of the torrefaction.

The thesis can be divided into three parts. In the first part a broad literature review about pyrolysis and torrefaction is carried out. The second part gives the experimental section in which the chemistry and reaction kinetics have been studied extensively with the help of different experimental methods. The final part gives an overview on the-state-of-the-art of different commercial torrefaction initiatives to further assist reactor technology.

Although pyrolysis and torrefaction operate in a different temperature regime, pyrolysis type research is applied for exploring torrefaction of biowaste resources. The chemical principles and different reaction mechanisms are to get insight into the torrefaction characteristics. Due to the different reaction temperatures differences between pyrolysis and torrefaction are observed in the final product composition and reaction rates.

The weight loss kinetics of different biowaste resources and its constituents are determined by thermogravimetric analysis at a milligram scale. The reaction kinetics are modeled based on existing pyrolysis reaction models. On the basis of the mathematical results only, it cannot be stated how the biomass decomposes during torrefaction. Different assumptions on the kinetics lead to identical mathematical formulations. Hence, it is found that biomass torrefaction follows the classical methods of reaction kinetics. During biomass torrefaction two different phases on these categories react independently of each other. The slow reacting phase has high availability and the fast reacting phase has an apparent temperature dependence of the (low) availability.

The products formed during torrefaction of different biowaste streams have been determined in a small scale fixed bed reactor (0 – 10 g) and thermogravimetric analysis coupled with mass spectroscopy and Fourier Transformed Infrared. In the fixed bed reactor the torrefied wood, the condensable and non-condensable gases are quantified offline with elemental analysis, gas chromatography/mass spectroscopy and micro gas chromatography. The fast reacting phase with low availability produces small molecular products even as the slow reacting phase with high availability, but this phase also produces higher molecular weight

products and aromatic compounds. Finally, the energy balance of the torrefaction of beech wood is determined. The heat of reaction that is found is between 0.7 MJ/kg biomass endothermic and -0.8 MJ/kg biomass exothermic for reaction temperatures between 230 and 280°C.

Finally, the influence of torrefaction on large cylindrical wood particles with diameters between 10 and 28 mm for beech and willow wood has been investigated. Fixed bed experiments are carried out at temperatures between 200 - 300°C to determine the product composition and the intra particle temperature profile depending on location, time and temperature. The condensable products are characterized and the exothermal effect is quantified. It is shown that the maximum temperature increase due to this exothermal effect is between 40°C inside a large particle. Also an analytical mathematical model has been developed based on the reaction mechanism found with thermogravimetric analysis and for the kinetic modelling to describe this internal temperature profile. Some modifications are applied to the model found to describe the weight loss kinetics. The model describes the temperature profile in the particle as a function of time, temperature, location and the progress of the reaction. The high number of required numerical parameters limits the numerical validation of the torrefaction model and makes biomass modeling complicated.

# Table of Contents

# Chapter 1

# Introduction


## Abstract

*This chapter highlights the challenge of the transition to a bio-based economy in which bio-energy can play an important role. Co-firing of biomass is seen as an important step in the renewable energy mix. In this chapter the role of torrefaction for co-firing is described briefly. The main objective of this study and the structure of this thesis are outlined.*

## 1.1 Background

Nowadays, there is an increased interest in the transition from a petrochemical based industry towards a bio-based economy. Biomass is getting increased attention as a potential source for non-food applications such as fuel-, chemical-, material- and electricity production. In a bio-based economy biomass replaces partially the fossil based resources as oil, natural gas and coal. Rising prices of fossil fuels, climate change discussions, instability of oil producing countries and increasing pressure on the environment are drivers for green engineering. Sustainable chemical processes, products and system designs must lead to a diversified economy in which less energy is consumed, less $CO_2$ is emitted and greener resources are applied [Ten Pierick &Van Mill, 2009].

The challenge for the long-term development of the bio-based economy is enormous since there is a strong interaction with themes like climate, energy, trade, agriculture policy, food facilities, knowledge based economy, biodiversity, logistics and transport fuels is clearly present. The advantages of a bio-based economy are much known, but at the other side attention is necessary for barriers such as sustainability in relation to biomass use, market failures, still the lack of required technologies and biomass availability. Also the impact of large scale biomass use must guarantee the application of sustainable produced biomass from anywhere in the world.

The Netherlands is considered to play an important role in the transition to a bio-based economy because of its large port facilities, chemical industry, refinery facilities and sophisticated agro industry. 30% of the fossil resources should be replaced by biomass feedstock in the year 2030 according the working program of the Dutch government [Schoon en Zuinig, 2007]. [Sues, 2011] shows that biomass waste streams (or residues) are an interesting sustainable option for conversion into energy in Europe. These tertiary biomass resources do not show competition with food production, but the availability is marginal with a range between 1.4 and 3.4 EJ/year. The same study shows that with these proportions it is inevitable to import biomass from other continents to reach the targets for transportation fuels and biomass co-firing for the production of electricity. This is supported by [de Wit and Faaij, 2010] looking at the agricultural residues from food and feed production.

**Table 1.1:** Total biomass use as part of avoided primary fossil energy use in % in The Netherlands

| | Avoided primary energy use (%) | | | |
|---|---|---|---|---|
| | 1995 | 2000 | 2005 | 2008 |
| Biomass total | 0.59 | 0.88 | 1.81 | 2.16 |
| Waste incineration | 0.21 | 0.39 | 0.37 | 0.41 |
| Co-firing biomass | 0 | 0.06 | 0.93 | 0.59 |
| Wood stoves for heat, companies | 0.06 | 0.06 | 0.06 | 0.08 |
| Wood stoves, households | 0.16 | 0.15 | 0.18 | 0.21 |
| Other biomass combustion | 0.02 | 0.08 | 0.14 | 0.28 |
| Biogas | 0.14 | 0.14 | 0.13 | 0.22 |
| Biofuels | - | - | 0 | 0.36 |

It is supposed that 20% of the energy in Europe is being produced from renewable sources in 2020. Bio-energy is a part of the bio-based economy that can partly replace the energy application of fossil resources, but [Faaij, 2006] mentions that the use of available biomass resources could become a problem and limitation. Biomass import from South America is proposed as a tool to reach the targets [Sues, 2011]. According the Transition Biomass bioenergy can comprise 30% of the total energy consumption in 2040. An important role is ascribed to the electricity production by co-firing biomass waste streams in existing coal fired stations [Sues, 2011]. In the covenant about coal as energy resource [Kolenconvenant, 2002] it is stated that around 30 PJ/year co-firing of biomass could be achieved in the period 2008 – 2012. The goal of 10% energy supply by renewable sources will be covered for around 50% by biomass use in 2020. This means around 190 PJ/year [Tortech, 2006]. At the moment the use of biomass in The Netherlands for energy purposes is not that large. Table 1.1 summarises the evolution of biomass use as pronounced in avoided primary energy use (%) in The Netherlands from 1995 – 2008. It is shown that the contribution of biomass is still only 2.16%. Almost half of the contribution is derived from waste incineration and co-firing of biomass.

Co-firing is seen as an important step in the energy transition, but the application of biomass in the bio-energy chain for the production of energy in the form of electricity offers some difficulties. Particle size reduction of woody feedstocks is necessary for co-firing in coal fired power stations or for application in entrained

flow gasification. Due to the fibrous and tenacious structure of biomass this offers problems for the grindability and makes large scale biomass co-firing problematic. Also the transportation of biomass (which is necessary to reach the renewable energy targets) comprises difficulties such as low energy density of the biomass, hydrophilic behaviour, sensitivity for rotting and bad fluidization behaviour.

The technology of torrefaction can improve the characteristics mentioned above. By thermal treatment of the biomass in the temperature range 200 - 300°C (between drying and pyrolysis) the biomass shows improved characteristics like:

- Improved grindability
- Increased energy density
- Better hydrophobic properties
- Improved homogeneity of the biomass

The torrefied product can be easily grinded and pelletized so that a high quality fuel is produced that can be co-fired into the existing coal power stations or entrained flow gasification. Nowadays, the often mentioned name for torrefied biomass is biocoal. Next to co-firing, pelletized torrefied biomass can also be applied into wood stoves for small scale combustion in the private market. Small scale combustion systems can be used as an alternative to oil-fired central heating in developed areas with a lot of biomass waste streams such as Sweden, Norway and Austria, but small scale combustion systems are also used in developing areas such as parts of Africa. Easily access to sustainable use of biomass can contribute to rural development.

## 1.2 Co-firing biomass in the Netherlands

Co-firing of biomass is an important activity in The Netherlands. The idea behind it is to replace fossil fuels with renewable resources in existing coal fired power plants. Co-firing reduces the $CO_2$ emissions and enhances recycling of material so land filling is minimized. Among the different combustion techniques like pulverised coal combustion, fluidised bed combustion and grate combustion, pulverised coal combustion is the most common technology to produce power in large scale power plants up to 1000 $MW_{el}$. A fine grinded fuel with particles smaller than 100μm is pneumatically injected into a furnace. High moisture content

and the fibrous nature of biomass make it difficult to achieve this particle size. [Spliethof et al., 2001] mentions the main problems of biomass co-firing which are fuel supply, fuel handling, behaviour inside the boiler and the quality of the ash. Fuel supply is related to the several pre-treatment steps that are necessary for application such as harvesting, drying, milling and densification. Fuel handling is related to the particle size of the biomass. According to [van Loo & Koppejan, 2002] the maximum size for renewable fuels in PF boilers is 10 – 20 mm. [Hein & Bemtgen, 1998] states that wood particles should be milled to less than 1 mm to reach a satisfactory burn-out within the residence times [Heikkinen, 2005]. Blockages and self-ignition are the main possible problems. Also the flow behaviour of biomass is different than coal and the lower energy density requires larger streams of biomass. If the biomass particle is too large for complete burnout in the boiler it could start glowing. This leads to the formation of CO which is responsible for corrosion effects in the boiler. Corrosion can be enlarged by the alkali containing ash of the biomass.

Co-firing of biomass has certainly also advantages [Dai et al., 2008]. Often mentioned advantages next to decrease of $CO_2$ emissions and reduction of land waste fill are the flexibility in fuel supply and types of resources. Making the power station attractive for a diverse stream of resources creates more flexibility in handling secondary fuels. Seasonal fuel streams become easier to be handled in the coal station. Therefore co-firing of biomass and waste can be carried out by three different methods, namely:

- Direct co-firing: coal and biomass are handled together before the burner and fed through the coal burners into the boiler.
- Indirect co-firing: coal and biomass are gasified in a different unit and the product gas is injected into the coal furnace.
- Parallel combustion: biomass and coal infrastructure consists of complete separate combustion unit, but than the heat to power equipment

Next to co-firing with biomass, pulverized fuel combustion can also contribute to decreasing the greenhouse gas emissions by improving its efficiency, capturing and storing the $CO_2$. Large efficiency improvements are difficult to achieve and $CO_2$ capturing is costly and technically complicated [Heikkinen, 2005].

**Table 1.2:** Co-firing locations in The Netherlands

| Power plant | Owner | Capacity (MWth) | Co-fired fuel | Type |
|---|---|---|---|---|
| Hemweg Centrale (HW8) | Nuon | 670 | Sewage sludge | Direct |
| Borssele 12 | EPZ | 403 | Wood pellets, olive pulp | Direct |
| Amercentrale 8 | Essent | 600 | Wood pellets, olive pulp | Direct |
| Amercentrale 9 | Essent | 600 | Wood pellets, olive pulp | Indirect + direct |
| Gelderland | Electrabel | 602 | Demolition wood | Direct |
| Buggenum | Nuon | 253 | Sewage sludge, wood | Direct |
| Maasvlakte 1+2 | E-ON Benelux | 1062 | Biomass pellets | Direct |

The co-firing activities in The Netherlands are mentioned in Table 1.2. At the moment there are eight power plants in The Netherlands in which pulverized coal and a secondary fuel are used for the production of electricity with a total capacity more than 4000 $MW_{el}$. For the Amercentrale 8 320kton/a biomass is co-fired and Amercentrale 9 it will be contribution of 600kton/a biomass [Kiel, 2010]. For Borssele 112 it is 100 kton/a, for Buggenum the contribution is around 5 kton/a gasification of biomass and in the Maasvlakte units the contribution is together around 200 kton/a. The Dutch municipal solid waste is currently being incinerated in the existing grate-fired incineration plants and is not mixed with the coal in the coal power stations for co-firing.

[Kiel, 2010] states that for the middle- and long term the energy production will depend on oil and gas. Co-firing biomass can be an easy and cheap possibility to increase the renewable energy share. Nowadays, around 30 wt% is co-fired in the existing power stations, with concrete plans (Amercentrale 9) to achieve 50%. It is expected that co-firing biomass becomes more attractive if large amounts of torrefied biomass will enter the renewable resources market. The improved grindability due to torrefaction makes it possible to co-fire larger shares of (pelletized) biomass taking into account the current infrastructure and burnout behaviour of the biomass particle.

## 1.3 Biomass torrefaction

This thesis deals with the role of torrefaction as pre-treatment technology in the production of bio-energy. Torrefaction is a thermo-chemical conversion method in the temperature range between drying and pyrolysis operating at 200 – 300°C under inert atmospheric conditions. Other names for the torrefaction process are roasting, slow- and mild pyrolysis, wood cooking and high-temperature drying. In this temperature range the biomass decomposes and during this decomposition a gas is produced.

The chemical principle of torrefaction is the removal of oxygen containing compounds out of the biomass. Typically, a solid product is formed which is called torrefied biomass, bio-char or bio-coal. The modified solid product contains like 70% of the mass and 90% of the energy of the original raw biomass leading to an increased energy density (because of the removal of oxygen). The produced gas can be used to supply the necessary process heat for torrefaction. An increased energy density makes the bio-coal interesting as intermediate product for large distance transportation. Also due to the removal of oxygen after torrefaction the biomass has more hydrophobic characteristics that make storage of torrefied biomass more attractive above non-torrefied biomass, because of the rotting behavior.

The thermal treatment also destructs the fibrous structure and tenacity of biomass, which makes it interesting for grinding. Grinding of the biomass offers an even higher increased volumetric energy density. Due to biomass grinding also higher shares of co-firing of coal/biomass mixtures can be achieved. Another advantage of torrefied biomass that increases co-firing possibilities is its uniformity in product quality. Woodcuttings, demolition wood, waste wood have after torrefaction quite similar physical and chemical properties including hydrophobicity.

Although the advantages of torrefaction are known, nowadays, there is no commercial reactor technology available for torrefaction purposes. At the moment several initiatives with a capacity ranging between 10 and 100 kton annual are in development.

## 1.4 Research activities

In the development of the torrefaction knowledge it is important to get a good insight in the mechanisms behind torrefaction at fundamental level. Torrefaction is a complex process which involves many physical and chemical processes such as heat transfer, moisture evaporation, decomposition kinetics, heat of torrefaction, pressure build up in the solid, changes in material properties with the extent of torrefaction temperature, anisotropic property behavior. Research at this level can give better information about the quality of the torrefied product. The most important technological issues that remain to be solved at fundamental level before large-scale use becomes more efficient are related to the complex torrefaction kinetics.

The study of the basic reaction mechanism is the priority of the present research which intends to make an experimental, theoretical and modelling contribution to the development of torrefaction. Therefore it concentrates on the determination of the operating conditions in relevant experimental research, the kinetic constants of biomass torrefaction, the reaction heat of biomass torrefaction and (volatile and solid) product information related to the torrefaction conditions. The different approaches to investigate the torrefaction of biowastes are:

- Thermogravimetric Analysis (TGA) is applied on a generally small particle, so that the heat transfer is neglible compared to the decomposition rate and useful information on the kinetics of biowaste torrefaction can be gained by monitoring the mass loss of the particle. The information obtained by TGA can be applied in different kinetic models to study different reaction mechanisms.

- Thermogravimetric Analysis coupled with Mass Spectroscopy (TG-MS) or Fourier Transformed Infrared (FTIR) is applied on small particles so that the online analysis of product formation can be monitored.

- Fixed bed experiments have been carried out on generally small particles to study the product formation of biowaste, so that the heat transfer in the particle is limited.

- Fixed bed experiments are applied on large cylindrical particles of wood. The heat transfer is then the limiting step and this study deal with the modelling of the thermal properties of the wood. Thermocouples are set inside the particle to measure temperature profiles.

This thesis addresses the question how the chemistry reaction mechanism of torrefaction is influenced by its reaction conditions and what effects occur during the reaction.

## 1.5 Scope and outline of this thesis

This research is carried out within the framework of the project "EOS-LT Tortech Torrefaction as key technology for the production of solid fuels from biomass and waste". Torrefied pellets are considered an important feedstock in the co-firing of biomass in existing coal fired stations for the production of electricity and in the transportation of biomass in the bio-based economy. The project is financed by SenterNovem and is cooperation between the Energy research Centre of The Netherlands, Eindhoven University of Technology and GF Energy. Other companies involved in the project are Imtech Technology, CPM Europe BV, HVC Alkmaar, Technisch Bureau MTM BV, NUON, Delta Milieu Biofuels BV and EPZ. This part of the research is carried out at Eindhoven University of Technology, The Netherlands.

The goal of this thesis is to identify the reaction mechanism of biowastes during torrefaction for the production of solid biofuels. **This thesis addresses the question how the chemistry and reaction kinetics of torrefaction are influenced by its reaction conditions and what effects occur during the reaction.** This research question can be more specified with the subquestions such as, how are the kinetics during torrefaction and what does this mean, which products are formed, what are the mass - and energy balances, what is the endo- and or exothermal behaviour, etc. Understanding the reaction mechanism during torrefaction could increase the fundamental knowledge for torrefaction as new thermochemical technology between drying and pyrolysis. The research is focused on the kinetic mechanism of biowaste decomposition and the product formation between 200 - 300°C.

In **Chapter 2** an overview is presented about the thermo chemical conversion of biomass. The chapter deals mainly with the relation of pyrolysis with torrefaction research. The characteristics of pyrolysis and its products and product applications of these fractions are shown. Also an overview of the kinetic pyrolysis models which will be used in Chapter 4 is presented. Finally, some different reactor technologies for pyrolysis are discussed.

In **Chapter 3** a review is given about the upgrading of biomass for the production of biofuels by torrefaction. In this review the characteristics of torrefaction are described and a short history of torrefaction is given. Torrefaction is based on the removal of oxygen from biomass which aims to produce a fuel with increased energy density by decomposing the reactive hemicellulose fraction. Different reaction conditions (temperature, inert gas, reaction time) and biomass resources lead to various solid, liquid and gaseous products. A short overview of the different mass and energy balances is presented. Finally, the technology options and the most promising torrefaction applications and their economic potential are described.

In **Chapter 4** a method is presented to study the reaction mechanism of biomass decomposition during torrefaction. The question that is answered is how the reaction mechanism of the torrefaction process is depending on different process conditions such as temperature and residence time. Thermo gravimetric experiments are carried out to get information about the weight loss of several biowastes and biomass constituents. Four different models are analyzed and validated with the experimental results. The model is verified by reactivity plots of the torrefaction of torrefied biomass which means that the weight loss kinetics of torrefied biomass have been researched by torrefaction at higher temperatures.

**Chapter 5** summarizes the results of investigation upon the product formation during biomass torrefaction for different biomass feedstocks and its constituents in a small scale fixed bed reactor. The mechanism found in Chapter 4 has been studied more extensively looking at the products. Also the reaction mechanism is research by the analytical method of combined dynamic thermo gravimetric mass spectroscopy (TG-MS) and thermo gravimetric Fourier transformed infrared (TG-

FTIR). Based on these experiments the mass and energy balances are constructed and more qualitative information is gained about the mechanism.

**Chapter 6** summarizes the results of investigation upon the torrefaction of large wood particles comprising the product formation and the intra particle temperature profile. Fixed bed experiments have been carried out at different temperatures to determine the product composition and the intra particle temperature profile depending on location, time and temperature. The condensable products have been characterized and the exothermal effect quantified. Finally an analytical model has been developed based on the reaction mechanism found in Chapter 4. Some modifications are applied regarding reaction kinetics, reaction coordinates and the heat transfer. The model describes the temperature profile in the particle as function of time, temperature, location and the progress of the reaction.

In **Chapter 7** an overview is given about the commercial state of the art of the torrefaction technology. The different reactor technologies will be outlined and the initiatives in The Netherlands will be discussed. Finally, in **Chapter 8** the main conclusions of this study are presented and some recommendations about future work are proposed. Also an outlook to the future of torrefaction is given.

## References

Dai J, Sokhansanj S, Grace JR, Bi X, Lim CJ, Melin S. (2008) Overview and some issues related to co-firing biomass and coal**.** Canadian Journal of Chemical Engineering 86 (3); 367 - 386

De Wit, M. Faaij, A. (2010). European biomass resource potential and costs. Biomass and Bioenergy 34; 188 - 202

Faaij, A (2006). Bio-energy in Europe; changing technology choices. Energy Policy 34; 322 - 342

Heikkinen JM. (2005) Characterisation of Supplementary Fuels for Co-combustion with Pulverised Coal. PhD Thesis; Delft University of Technology

Hein KRG, Bemtgen JM. EU clean coal technology — co-combustion of coal and biomass. Fuel Processing Technology; 54:159–169; 1998.

Kiel J, (2010) Vergroening van kolencentrales – Technische mogelijkheden en uitdagingen. Biomassa Meestook Symposium, Amsterdam, 27 Mei 2010

Kolenconvenant (2002). Convenant kolencentrales en $CO_2$ reductie, zoals afgesloten tussen de Nederlandse overheid en de eigenaren van kolencentrales in Nederland op 24 april 2002

Schoon en Zuinig, werkgroep (2007). www.vrom.nl/schoonenzuinig last checked 27 april 2010

Spliethoff H, Unterberger S, Hein KRG. (2001). Status of co-combustion of coal and biomass in Europe. In 6th International Conference on Technologies and Combustion for a Clean Environment; Porto; Portugal; 575–584; 9-12 July 2001

Sues A, (2011). Are European bio-energy targets achievable? An evaluation based on thermo economics and environmental indicators. PhD Thesis; Eindhoven University of Technology

Ten Pierik E, Van Mill, E. (2009). Multi-level perspective nader beschouwd; Aangrijpingspunten voor transitie richting bio-based economy? Lei Wageningen UR; Den Haag; Rapport 2009-035; Projectcode 31267

Tortech (2006). Projectplan EOS-LT onderzoeksproject “TORTECH – Torrefactie als sleuteltechnologie voor de productie van (vaste) brandstoffen uit biomassa en afval” ; SenterNovem

Van Loo S, Koppejan J. Handbook of biomass combustion and co-firing. Twente University Press, Enschede, 2002.

# Chapter 2

# Fundamentals of thermo chemical conversion of biomass


## Abstract

*In this chapter an overview is presented about the fundamentals of thermo chemical conversion of biomass. Different topics such as biomass composition, biomass decomposition chemistry, reaction kinetics and product applications are presented. A specific outlook is given to the technology of pyrolysis to understand the basic principles of torrefaction. Finally, an overview is given about the available reactor technologies for the thermal treatment of biomass.*

## 2.1 Introduction

The conversion of biomass comprises a whole range of technologies from a wide spectrum of feedstocks to several energy carriers and products. In this chapter an overview is presented about the main principles of thermo chemical conversion technologies in general and pyrolysis in detail. This thesis deals with the question what the chemistry and reaction kinetics of torrefaction are. Torrefaction is a thermo chemical conversion method that focuses on a high quality solid fuel. A different name for torrefaction is low temperature pyrolysis; both technologies, pyrolysis and torrefaction, respectively, operate at inert conditions. The difference is that pyrolysis operates at temperatures above 400°C and torrefaction below 300°C. Depending on the composition of the biomass resource, the reaction conditions and the reactor technologies different pyrolysis products can be formed. An overview is given about the different choices that can be made. Also a literature review is presented about the reaction mechanisms of biomass during pyrolysis which will be used for the modelling of biomass torrefaction in Chapter 4. Because extensive literature reviews on the subject have appeared over the years [Mohan et al., 2006] [Hubert et al., 2006] [Czernik & Bridgwater, 2004] [Bridgwater, 1999] only the major aspects of the pyrolysis mechanism are discussed. Finally, the most important reactor technologies are discussed.

## 2.2 Biomass composition

The chemical structure and major constituents in biomass are important in the several thermo chemical processes and development for producing biofuels and biochemicals. Biomass is a solid fuel and, like most of the solid fuels, it consists of the elements carbon, oxygen and hydrogen. The presence of large amounts of oxygen in biomass means that the (pyrolytic) chemistry differs extensively from fossil fuels [Mohan et al., 2006]. Herbaceous and woody biomass can both be classified as lignocellulosic biomass, which consists mainly of cellulose, hemicelluloses and lignin. Other chemical fractions in biomass are small amounts of inorganic material (which upon thermal decomposition transforms into ash) and low molecular extractives such as resins, terpenes, fats and waxes.

The main role of lignocellulose is to build up the cellular structure of plants as a foundation and connection agent of cell walls, providing mechanical strength and toughness to the plant. On microscopic scale, the wood is composed of micro

fibrils. The cellulose is concentrated in the interior of the fiber, the outer wall of the fiber is composed of lignin and hemicelluloses and the lamellas to connect the fibers are composed in general of lignin. The lignin connects the wood fibers with each other and the hemicelluloses link the cellulose with the lignin. In the rest of this paragraph the (chemical) characteristics of the three lignocellulosic compounds are described.

## 2.2.1 Cellulose

Cellulose is a linear polysaccharide $(C_6H_{10}O_5)_n$ of D-glucose $(C_6H_{12}O_6)$ linked by β-1,4-glycosidic bonds with a degree of polymerization between 1000 - 10000. The chemical structure of cellulose is shown in Figure 2.1. The basic repeating unit of the cellulose polymer consists of two glucose anhydride units containing hydroxyl groups. Both molecules adopt a stable chair conformation which allows the formation of hydrogen bonds between the adjacent oxygen and hydrogen atoms. This intra and inter molecular hydrogen bonds forces a linear arrangement and increases the crystalline character of the material. Cellulose derives its strength from its fibrous structure, which is mainly coming from its hydrogen bondings within the polymer chain. Cellulose fibers form the skeletal structure of - and give strength to the biomass.

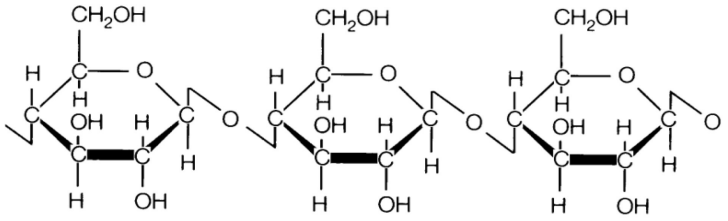

**Figure 2.1:** Chemical structure of cellulose

## 2.2.2 Hemicelluloses

Hemicelluloses are complex hetero polysaccharides consisting out of pentoses $(C_5H_8O_4)_n$ and hexoses $(C_6H_{10}O_5)_n$. The different saccharides are glucose, galactose, mannose, xylose, arabinose and glucuronic acid and vary in the composition of soft- and hardwood. Examples of glucomannan and xylan are shown in Figure 2.2. Hemicelluloses have an amorphous structure rich of branches

and are the least stable constituent in the biomass due to their lack of crystallinity. Hemicelluloses are shorter chains than the cellulose since the degree of polymerization varies mainly between 50 – 300 monomer units.

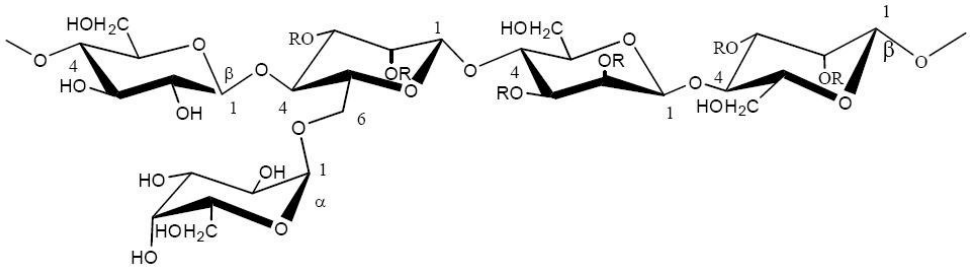

**Figure 2.2:** Different components of hemicelluloses

## 2.2.3 Lignin

The third major component of lignocellulosic biomass is lignin. Lignin has an amorphous and highly cross-linked structure, without a well defined order or clearly repeated aromatic units. This irregular structure of lignin is a direct consequence of its biosynthesis, whose last step is constituted by a random recombination. Different polymerization of phenylpropenyl units results in lignin. There are three different types of phenylpropane units such as coniferyl, sinapyl and *p*-coumaryl alcohol according to the different side groups. Softwood is mainly composed of coniferyl phenylpropane units. On the other hand, hardwood is mainly composed of coniferyl and sinapyl alcohol units.

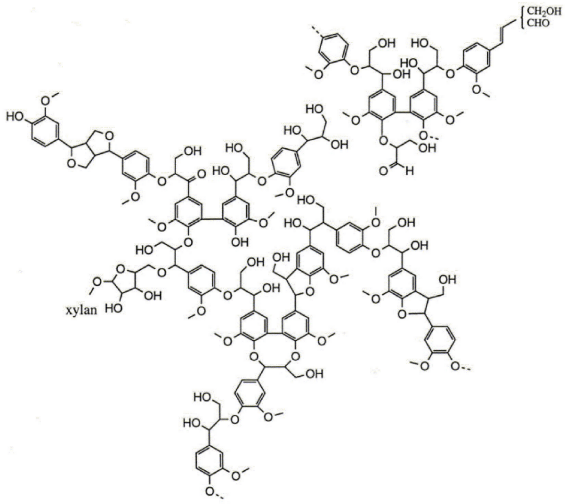


**Figure 2.3:** Chemical structures of lignin

## 2.3 Biomass conversion

Biomass can be converted into different useful products by biochemical and thermo chemical pathways. Biochemical conversion comprises the technologies of anaerobic digestion and fermentation. This thesis deals mainly about the thermo chemical conversion in the low temperature regime, which is torrefaction. This chapter deals about the higher temperature range. The temperature difference between both technologies is clearly shown in Figure 2.4. Lignocellulosic biomass can be used in different thermo chemical ways to provide energy:

- Direct combustion to produce heat for use in heating and steam for electricity generation.
- Gasification to produce a syngas which can be combusted for heat and electricity generation (indirect combustion). Gasification operates basically at temperatures higher than 800°C.
- Pyrolysis to produce a solid, liquid and gaseous fuel which can be used for a wide spectrum of applications (including chemicals).

With direct combustion and gasification the products must be used immediately since storage is difficult and costly. The advantage of pyrolysis is that the liquid product can be stored, although the liquid produced is not completely stable [Diebold, 2000]. [De Wild, 2009] expressed very clearly the differences between the various thermo chemical conversion processes as in Figure 2.4. The biomass constituents decompose in the torrefaction and/or pyrolysis temperature regime between 200 and 600°C. At lower temperatures the biomass loses almost entirely

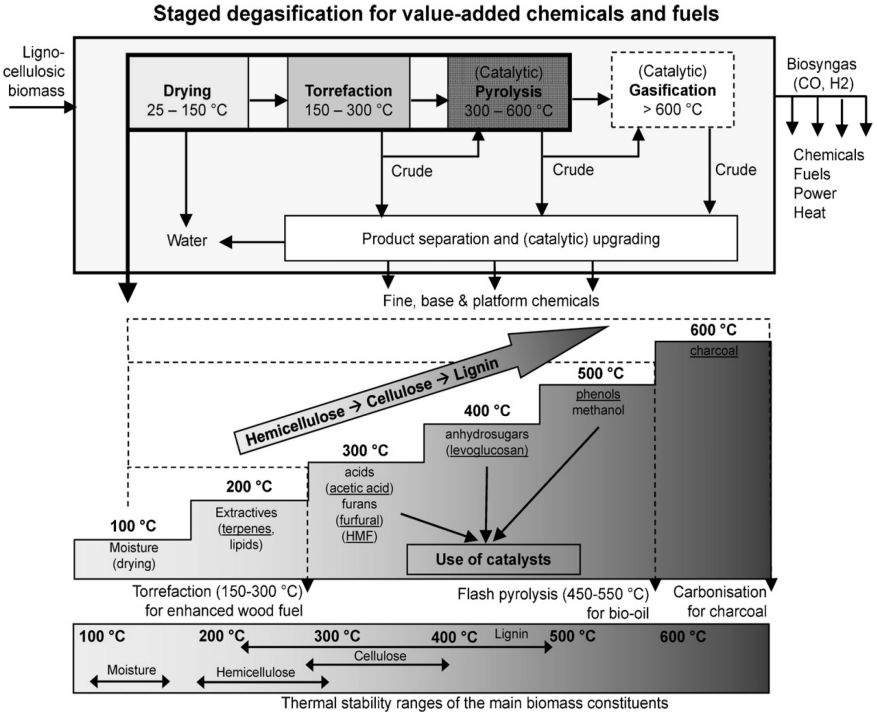


**Figure 2.4:** Staged degasification concept within the thermo chemical biorefinery [De Wild et al., 2009]

water and at higher temperatures the biomass is gasified to a syngas consisting out of CO, $CO_2$, $H_2$ and $CH_4$. It is shown that at different temperatures different products are formed from hemicellulose, cellulose and lignin. Combustion is not shown in this figure since it operates at oxygen conditions stoechiometrical higher

than 1. Gasification, pyrolysis and torrefaction operate under (partial) inert conditions.

The several technologies produce their final energy carriers in different forms with several possible applications, but there is also a difference in efficiency. Bio-energy conversion efficiencies for biomass combustion power plants, producing electricity, range from 20 to 40% [McKendry, 2002], for biomass gasification between 75 to 80%, as chemical energy in the gas produced and pyrolysis efficiencies vary extremely in the energy content of the final liquid product. In the next paragraph a more detailed description is given about the pyrolysis process which stands close to the principles of torrefaction.

## 2.4 Pyrolysis

### 2.4.1 Description and process parameters

The focus of torrefaction is to produce a high quality solid fuel, pyrolysis is meant to convert biomass to (a maximum quantity of) liquids (bio-oil). This thesis deals mainly about the thermo chemical conversion in the low temperature which is torrefaction. This paragraph deals about the higher temperature range above 300°C. Both processes have in common that the biomass feedstock is densified in its energy content to reduce storage space and transport costs [Venderbosch & Prins, 2010]. Pyrolysis is a thermo chemical conversion method (of biomass) operating between 300 - 600°C in the absence of oxygen to produce renewable fuels and chemicals. It is also always the first step in combustion and gasification, but in these processes it is followed by total or partial oxidation of the primary products. Pyrolysis is a combination of the Greek words *pyros* and *lysis* which mean fire and breaking [Cornelissen, 2009]. It leads to an array of useful solid, liquid and gaseous products. Pyrolytic oil (synthetic oil) has a strategic value because, as a liquid, its handling, storage, transportation and utilization are similar to that of petroleum based oil.

Pyrolysis is an old process that was already applied in ancient times to produce tar in combination with caulking boats and embalming agents. In the past pyrolysis was mainly focused on the carbonization of biomass resources, but nowadays the main concept behind pyrolysis is the production of a liquid bio-oil which can be used for combustion, gasification and extraction of chemicals.

Pyrolysis is the breaking apart of the chemical bonds by the use of thermal energy only. The degradation of a molecule is caused by the dissociation of a chemical bond and the production of free radicals. Scission of the volatiles is dependent on the chemical bond strengths of the different groups. The weakest bindings will break up first and can be found in the side groups of the natural polymers hemicellulose, cellulose and lignin. The process parameters that determine the yield of the pyrolysis products are reaction temperature, residence time, heating rate, physicochemical pretreatment, particle size, geometrical configuration of the reactor, heat carrier and biomass species [Lievens, 2007].

The different pyrolysis principles are fast, intermediate and slow pyrolysis based on different reaction conditions mentioned. Table 2.1 shows the typical product yields (dry wood basis) obtained by different modes (fast, intermediate and slow) of pyrolysis of wood [Bridgwater, 2003]. Fast pyrolysis has a high conversion into liquid products at temperatures between 300 and 600°C. Fast pyrolysis is focused on the production of a maximum amount of condensable gas which can be reached with high heating rates and fast quenching of the volatiles. Slow pyrolysis can be subdivided into conventional slow pyrolysis and torrefaction. Conventional slow pyrolysis has a high conversion in condensable and gaseous products at temperatures between 300 and 500°C, but a higher char rate than for fast pyrolysis is produced. Slow pyrolysis is the process that comes closest to the technology of torrefaction. Torrefaction can be regarded as low temperature pyrolysis with a low conversion of biomass operating below 300°C. The heating rates between slow pyrolysis and torrefaction are similar. There is more char formation during slow pyrolysis than during fast pyrolysis. A slightly lower reaction temperature, lower heating rate and secondary reactions due to longer residence time are the main reasons for this char formation.

**Table 2.1:** Typical product yields (dry wood basis) obtained by different modes of pyrolysis of wood

| Process | Temperature | Vapour residence time | Liquid (%) | Char (%) | Gas (%) |
|---|---|---|---|---|---|
| Fast | Moderate | mili sec | 75 | 12 | 13 |
| Intermediate | Moderate | sec | 50 | 25 | 25 |
| Slow | Low | min | 30 | 35 | 35 |

The composition of the biomass is also an important parameter determining the amounts of pyrolysis products. As the cellulose content decreases the char yield increases and the liquid and gas yield decrease [Zanzi et al., 2002]. A higher yield of lignin in the biomass leads to more char formation, since the aromatic structure is very stable. This char formation is stimulated by a high carbon ratio in the lignin in relation to the other biomass constituents. The ash in the biomass contains the inorganic elemental constituents which occur as oxides, silicates, carbonates and sulphates. A higher yield of ash leads to more char formation, less liquid production, faster reaction rates and lower reaction temperatures [Piskorz et al., 1998]. Also, the heating value of the gas phase decreases with a higher ash yield.

## 2.4.2 Pyrolysis fractions

The solid fraction of the pyrolysis of biomass contains char and ash. This fraction can be used for combustion, gasification and as activated carbon with a high internal surface area and porosity. From the elemental analysis of the chars it can be concluded that the energy values of the carbons must be high between 26 and 36 MJ/kg based on the higher heating value (HHV) [Demirbas, 1999].

The main product of pyrolysis is a vapour that condenses resulting into a liquid phase which is called the bio-oil. [Czernik & Bridgwater, 2004] studied the fuel properties of pyrolysis oils from several biomass resources. Depending on the resource and the pyrolysis temperature 21.1 – 49.3 wt% on dry and ash-free basis bio-oil is produced with a HHV between 32 - 40 MJ/kg. The higher heating values of pyrolysis oil increase with increasing lignin content in the biomass samples. The bio-oil is a complex mixture of oxygenated hydrocarbons with large water content. In Chapter 5 it is explained how most of the products are formed during

pyrolysis. The elemental composition is mainly 54 – 58 % carbon, around 6% hydrogen and the rest is mainly oxygen. Heavy fuel already contains like 85 – 90% carbon and the rest is hydrogen with a HHV of almost 50 MJ/kg.

The gas fraction of pyrolysis products contains mainly the small permanent gases such CO, $CO_2$, $H_2$ and $CH_4$. It can be used in combustion engines for power generation necessary for the pyrolysis process, but the HHV of the gas is much lower than for methane, propane and LPG, but higher than conventional gasification gas.

### 2.4.3 BEST Energies slow pyrolysis technology[1]

The slow pyrolysis process is a process which comes closest to the reaction conditions of torrefaction. Although the temperature is higher than for torrefaction the heating rate for both processes are almost similar. In this and next paragraph two different types of slow pyrolysis will be described focused on the production of biochar and energy.

A well known slow pyrolysis process has been developed by BEST Energies from the United States of America. The slow pyrolysis process recycles waste biomass such as animal manure and green waste to produce energy and a stable form of carbon which can be sequestered beneficially over the long-term in soils. As a proof of concept BEST Energies has a fully operation demonstration plant with a capacity of 300kg/hr of biomass intake. Approximately 35% by weight of the dry feed material is converted to a high-carbon char material that is collected on the discharge of the kiln, called the Agrichar.

The BEST Energies slow pyrolysis technology consists out of a drier, pyrolysis kiln, gasifier, syngas clean-up and engine. The biomass resource is dried and fed into an externally heated kiln. As the material passes through the kiln, it reacts to produce an off-gas (syngas) which is utilized for the internal heat circulation. The commercial production plant will be based on 4kton per hour of continuous dry biomass supply.

[1] www.bestenergies.com

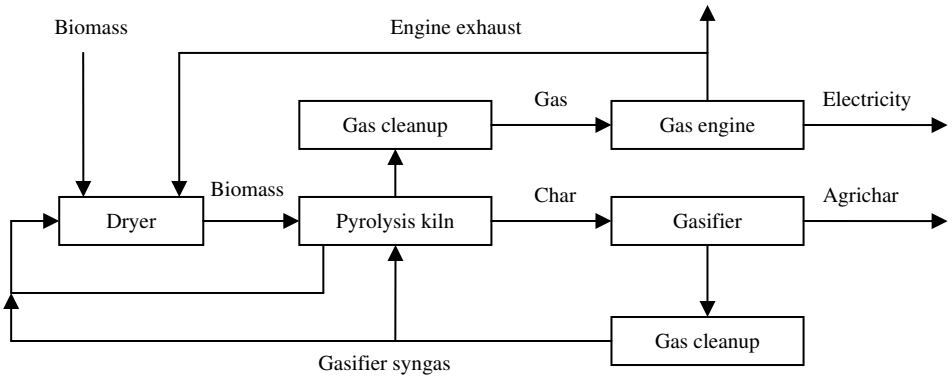


**Figure 2.5:** The BEST Energies slow pyrolysis technology for the production of Agrichar

### 2.4.4 Slow pyrolysis CHOREN technology

CHOREN Industries is a company focused on the biomass-to-liquid production via a multistage gasification process. It is possible to convert solid biomass and other feed materials containing carbon into combustion and synthesis gas. At the heart of the CHOREN technology is the Carbo-V Process. The Carbo-V Process is a three-stage process involving the following sub-processes:

- low temperature slow pyrolysis,
- high temperature gasification
- endothermic entrained bed gasification.

In the first step, the low temperature slow pyrolysis, the biomass is heated to 400 – 500°C and broken down into tar rich volatiles and solid char. The volatiles pass into the high temperature combustion chamber of the Carbo-V-gasifier where they are partially oxidized with oxygen and steam. Above 1400°C the ash particles melt and the long chain hydrocarbons are broken down to CO and $H_2$ resulting in a tar free gas.

The milled and pulverized char is blown into the hot gases beneath the combustion chamber. The endothermic gasification of the char causes an almost instantaneous drop in temperature to 800°C producing a raw gas with a high heating value. The

tar free gas is cooled by the heat exchanger yielding steam for industrial processes or generation of power. Ash particles and char, that have not been entirely converted, are separated from the raw gas in the deduster. These are then recycled back in the Carbo-V-combustion chamber. After scrubbing the gas the Fischer-Tropsch synthesis can start.

### 2.4.5 Fast pyrolysis Bioliq technology[2]

In cooperation with LURGI AG, Frankfurt, a flash pyrolysis pilot plant with a capacity of 500 kg/h biomass was built at Forschungszentrum Karlsruhe with funds from BMELV. Operation of the plant started in 2007. In a twin-screw reactor, the crushed biomass is heated to 500°C using hot sand. In the absence of air, the biomass reacts to gases and coke within seconds. Most of the gas condenses to liquids after cooling. Then, the coke is mixed into these liquids. This results in an energy-rich mix that may be transported and handled rather well and is transferred to the next process step. A small amount of burnable gas is used to reheat the sand.

## 2.5 Pyrolysis kinetics

### 2.5.1 Thermal degradation

This section reports the state of the art in modelling chemical decomposition processes of wood - and wood constituents pyrolysis. It is assumed that the mechanisms of pyrolysis and torrefaction are closely linked, but that the different operating temperatures and heating rates influence the product formation and reaction path; the pathways can be used for the different pyrolytic conversion methods, but yields will differ. Torrefaction operates at lower temperature with low carbon conversion, slow pyrolysis operates at higher temperature with slow, but high carbon conversion and fast pyrolysis operates at high temperature with fast and high conversion. A literature study about the pyrolysis kinetics and reaction path can give a first insight into the torrefaction kinetics. The pyrolysis kinetics is used as foundation for the description of torrefaction. The difference between slow and fast pyrolysis has not been taken into account, since in both processes a gas, a condensable fraction and char is formed, but the yields and composition are different.

[2] http://www.bioliq.com/schnell.html

Chemical kinetics is important in the description of the pyrolysis mechanism and to arrive at a good understanding of the process. It helps to control the process and optimize the design. A wealth of research data is available about the pyrolysis of wood, especially about reaction mechanism, reaction kinetics, and optimization of process condition, selection of particle size and influence of process technology [Gronli, 1996]. The thermal degradation process of wood at average temperature can be subdivided into primary and secondary pyrolysis:

- Primary pyrolysis is the first stage of the solid degradation in which condensable volatiles, permanent gases and a char are produced.

- Secondary pyrolysis is the next stage in which homo- and heterogeneous reactions take place between the products that are formed during the primary pyrolysis such as thermal cracking, repolymerisation and recondensation.

The thermal degradation of biomass is a process in which a set of several degradation reactions occur which makes it a rather complex process, so simplified kinetic models are applied to describe and determine the reactivity and its kinetics. Di Blasi mentions that the problem exists of a not available classification of biomass fuels based on thermo gravimetric analysis and general mechanisms to interpret such results [Di Blasi, 2008]. Varhegyi also reports the general problem of numerical modelling for pyrolysis of biomass which is the number of the unknown parameters [Varhegyi, 1980]. If the number of parameters is too large, different sets of values of the parameters can provide an acceptable fit between the experimental data and the corresponding calculated data. In such instances, special chemical considerations or hypotheses should be used to reduce the number of parameters.

At molecular level biomass consists of different natural polymers such as hemicellulose, cellulose and lignin that all show different thermal reactivity [Gaur & Reed, 1998], so three different temperature ranges may be distinguished in biomass that comprises different fractions of these components. In this thesis it is assumed that hemicellulose is the main reaction component in the biomass, although there are many different hemicelluloses (xylans, glucomannans,

galactoses, pectin). Hemicelluloses decompose in general at temperatures between 225 - 325°C, cellulose at 305 - 375°C and lignin over a broad temperature range between 250 - 500°C. Some studies suggest that primary decomposition of biomass is the superstition of the thermal behaviour of the relative reactivity ratios of the different lignocelluloses constituents.

A general one-component mechanism of primary wood pyrolysis is presented by [Shafizadeh & Chin, 1976] in Figure 2.6. In this model three competing reactions occur at different reaction rate. This model is applicable if high heating rates or high temperatures are applied in the pyrolysis process so that differentiation between reaction steps becomes complicated. Parallel or consecutive reactions in the biomass occur then at high reaction rates so that intermediate products are complicated to analyse. The effect of heating the biomass becomes stronger than the reactivity effect. Di Blasi mentions that the wide range of activation energies that has been found for this model can be a result of the different heating conditions established in different experimental devices, the different sample characteristics and the mathematical treatment of the data [Di Blasi, 2008. If the data is structured according the reaction temperature three different sets of data are found, but still with a wide range of activation energies.

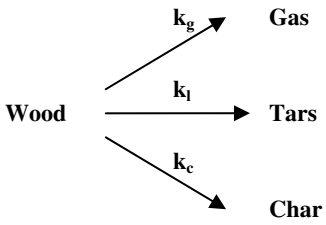


**Figure 2.6:** One-component mechanism of primary wood pyrolysis

Another general model is proposed by [Chan et al., 1985] [Chan et al., 1988] that added tar cracking to the competing reaction model. Also dehydration is included in the reaction model. This model can be seen in Figure 2.7.

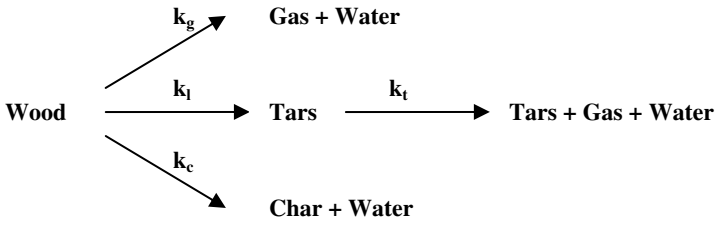


**Figure 2.7:** Competing reactions with secondary tar cracking and dehydration

Next to the model proposed by [Chan et al., 1985] [Chan et al., 1988] Di Blasi and others included tar cracking and repolymerisation to the reaction model with three competing reactions [Di Blasi et al., 1999]. This model can be seen in Figure 2.8.

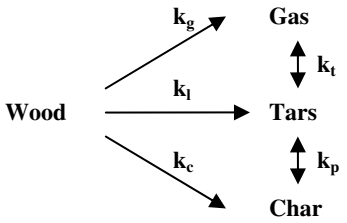


**Figure 2.8:** Competing reactions with secondary tar cracking and repolymerisation

Di Blasi subdivided the many chemical mechanisms in one-component mechanisms of primary pyrolysis, multi-component devolatilisation mechanisms, multi-component decomposition mechanisms of primary pyrolysis and secondary reaction models. In the first case a simplified model of primary decomposition process is based on a one component (or one-stage) reaction process with additional measurements of the yields of the product formation.

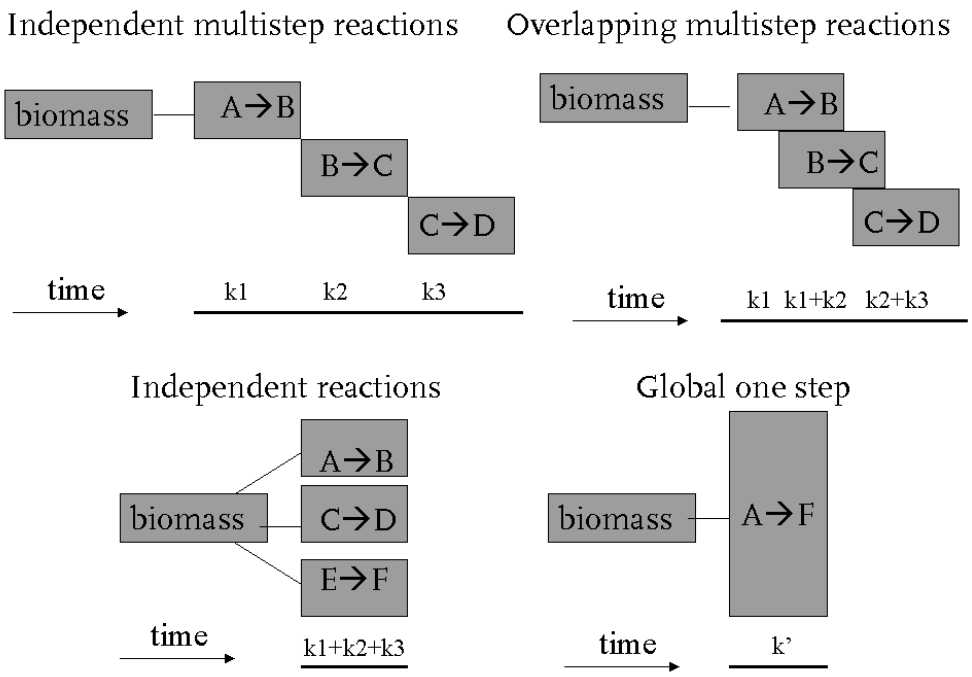


**Figure 2.9:** Various kinetic models for biomass decomposition according to Prins et al.

Multi component decomposition or volatilization models describe the dynamics of several zones or pseudo-components. These multi components are often described with the reactivity of the biomass constituents hemicelluloses, cellulose and lignin. Secondary reaction models take into account the reactions that occur between the primary pyrolysis products. For torrefaction [Prins et al., 2006] subdivided the different mechanisms of biomass kinetics in a global one step mechanism, independent multistep reactions, overlapping multistep reactions and independent reactions. Although four different mechanisms are found two mechanisms are chemically the same, namely the independent and the overlapping multistep reactions. It is not logic that first reaction A to B will occur completely before reaction product C is formed. More about these different mechanisms can be read in the chapter about the mechanistic pathway for biomass decomposition during torrefaction at isothermal conditions.

In the rest of this paragraph a few specific pyrolysis models and its assumptions will be outlined and described in detail. Generally two different approaches are used in modelling the pyrolysis of biomass. The first consists of predicting the total behaviour of wood starting from its principal components. The other method is called the "Lumped Parameter Approach" which is more a strategy that consists of classifying the products resulting from the degradation [Turner et al., 2010]. The models discussed are the following:

1. The Broido-Shafizadeh model
2. Di-Blasi & Lanzetta model
3. Rousset model

## 2.5.2 The Broido-Shafizadeh model

A commonly accepted model for the decomposition of celluloses during pyrolysis is the Broido-Shafizadeh model [Bradbury et al., 1979]. Broido showed that cellulose decomposes by a six step reaction mechanism at low temperatures. [Broido & Weinstein, 1971] described the pyrolysis of cellulose as a multistep reaction mechanism in which an endothermal reaction step forms an active anhydrocellulose (A*). This intermediate anhydrocellulose reacts in the second step to gas and char (C) which can be seen in Figure 2.10. Next to these two reaction steps a competitive reaction occurs resulting in the formation of volatile organic tars. D and E are modified solid residues.

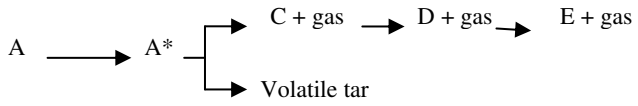


**Figure 2.10:** Cellulose decomposition as is proposed by [Broido & Weinstein, 1971]

[Bradbury et al., 1979] simplified the reaction network. This model describes pyrolysis at low pressure in the temperature range 259 - 341°C by a three step reaction model. An initiation step leads to the formation of "active" cellulose (A*) that further decomposes by two mutually competitive first-order reactions leading

to (i) a condensable fraction and (ii) a char and gaseous fraction including (C and gas). At lower temperatures the initial period can be explained by a high activation energy process converting the cellulose from an inactive to an active form. At higher temperatures the initial period results from the time required for the cellulose sample to reach temperature equilibrium. The thermal degradation of cellulose undergoes intermediate physical and chemical changes such as a glass transition and depolymerisation. These changes are ascribed to the activation of the cellulose macromolecules. The description of this model assumes ash free reactions without secondary reactions and transport processes.

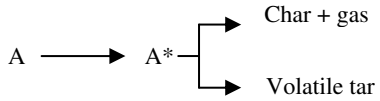


**Figure 2.11**: Broido-Shafizadeh model which describes the decomposition of cellulose (A) by pyrolysis with the formation of active cellulose (A*)

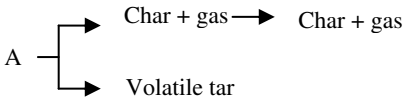


**Figure 2.12:** Broido-Shafizadeh model modified by [Varhegyi et al, 1994] which describes the decomposition of cellulose (A) by pyrolyis

In Chapter 4 it will be shown that this activation step can also be the result of heating the biomass with a causal effect of mass loss. The phenomenon seen at 312°C is possibly an error in the measurements. Also [Varhegyi et al., 1994] seriously questioned the Broido-Shafizadeh model for cellulose pyrolysis and modified the model slightly. Their criticism focused on the first initiation step which is according to them too extensive in the temperature range 250 - 370°C. Activation into active cellulose is something that cannot be detected. According to [Varhegyi et al., 1989] [Varhegyi et al., 1994] other researchers weight loss curves

show only a single step first-order rate law. Although this activation step is not found a high temperature (370°C) decomposition step is observed. A reaction pathway by two competitive reactions followed by a decomposition step is proposed for high temperature reactions. Possible explanations for an initiative step could be the effect of secondary reactions due to bigger particle size and the effect of pyrolytic vapors in the work of [Bradbury et al., 1979]. The simplified model by [Varheghyi et al., 1994] is generally accepted today as reference point for the thermal degradation of pyrolysis. The modified Broido-Shafizadeh model is presented in Figure 2.12. Out of the biomass char + gas are formed mutually with competitive tar formation. The char and gas can react further via secondary reactions to modified char and gas.

### 2.5.3 Di Blasi model

The model developed by [Di Blasi & Lanzetta., 1997] was originally developed to describe the thermal decomposition of hemicellulose which is the most reactive constituent of wood. More present the method has also been applied to the pyrolysis of wood in the low temperature regime [Branca & Di Blasi, 2003]. It is mentioned that the thermal degradation of xylan and model compounds show the existence of a two-step decomposition mechanism. An important role is assigned to the cleavage of the glycosidic group, polymerization of the glycosyl units and the decomposition of the sugar moiety. Figure 2.13 shows the biomass pyrolysis model of xylan according to Di Blasi.

It is shown that xylan reacts via an intermediate modified solid B to a final char product C. Volatile products from side chains are the main contributors to the mass loss that occurs in the biomass or xylan. It is shown that the first step is much faster than the second step based on the parameters that have been derived by the Arrhenius law. The main drawback of the model is that this model (and other two step mechanisms) can predict the global solid degradation rate, but no information can be obtained on the dependence of product yield on reaction temperature. [Demirbas, 2000] considered three different steps during the pyrolysis of wood, see Figure 2.14. In the first step moisture and volatiles are released under formation of a solid residue that did not react. This first step is followed by the formation of volatiles and gases by devolatilisation from the residue resulting in a solid bio char. The last step in the pyrolysis mechanism is the decomposition of the bio-char into a

carbon rich secondary char. The model proposed can be seen as a multi-component mechanism of primary pyrolysis.

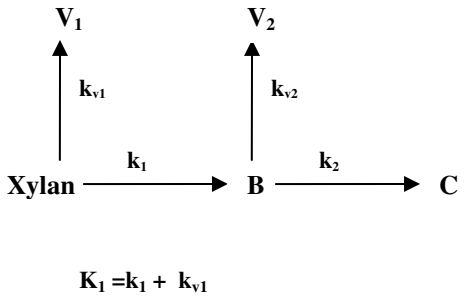


**Figure 2.13:** Schematic representation of the biomass pyrolysis model according to di Blasi

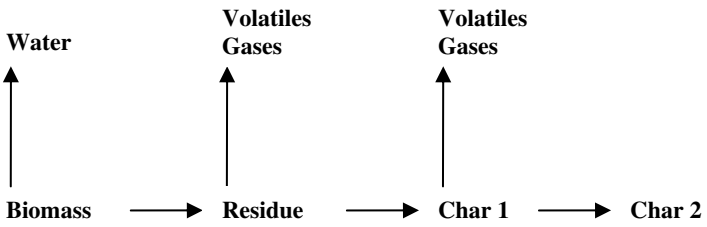


**Figure 2.14:** Schematic representation of the biomass pyrolysis model according to Demirbas et al.

## 2.5.4 Rousset model

A model developed by [Rousset, 2004] [Rousset et al., 2006] [Turner et al., 2010] describes the low temperature thermal decomposition as a superposition of the decomposition of the biomass main constituents (cellulose, hemicelluloses and lignin) as a ratio of their content in the wood. The Rousset model is a combination of the Broido-Shafizadeh model (BS) and the Di Blasi-Lanzetta model (BL). The cellulose decomposition is described according the BS model and the hemicelluloses decomposition follows the BL model. This combination results in an enormous disadvantage in the number of parameters that can be derived

resulting in seven reaction constants with the same number of kinetic constants and activation energies based on the Arrhenius law.

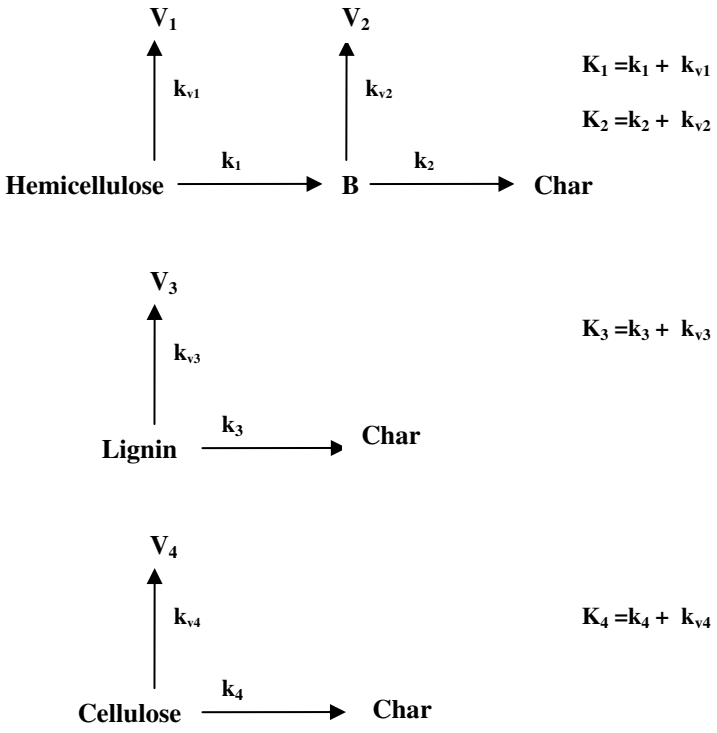


**Figure 2.15:** Reaction model for the decomposition of wood as superposition of the lignocellulose constituents hemicellulose, cellulose and lignin as a ratio of their content in the wood according to Rousset [Rousset,2004][Repellin et al., 2010]. The model is a combination of the modified Broido-Shafizadeh model and the Di Blasi and Lanzetta model with the extension of a simple model for the degradation of lignin

## 2.6 Pyrolysis oil

### 2.6.1 Composition and stability

Pyrolysis oil consists of the condensable fraction of the volatiles formed during thermal treatment and makes it possible to decouple the biomass conversion and the generation of energy. An essential aspect for this decoupling is, however, that the oil is thermodynamically stable which is not the cases due to the large fraction of reactive oxygenates in the liquid. [Diebold, 2000] reviews the chemical and physical mechanisms of the storage stability of fast pyrolysis oils. The oxygen content of the bio-oils is usually 35 – 40% and is predominantly present in most of more than 300 compounds. The most important reactions that occur between these compounds within the bio-oil involve:

1. Organic acids with alcohols to form esters and water
2. Organic acids with olefins to form esters
3. Aldehydes and water to form hydrates
4. Aldehydes and alcohols to form hemiacetals, or acetals and water
5. Aldehydes to form oligomers and resins
6. Aldehydes and phenolics to form resins and water
7. Aldehydes and proteins to form oligomers
8. Organic sulfur to form oligomers
9. Unsaturated compounds to form polyolefins

An important problem of the pyrolysis product is the large amount of water, although the fluidization of the oil is increased by the water since the viscosity of the organic phase is high. Distillation is not a solution for water removal as already at water evaporation temperatures, the above mentioned reactions will occur at higher rate forming all kind of sticky products. Polymerisation of pyrolysis liquids is strongly accelerated when heated up to 80°C or higher [Scholze, 2002] [Boucher et al., 2000]. These polymerization reactions also make it difficult to characterize and quantify all components formed during thermo chemical conversion. Selective condensation may reduce the water content of one or more fractions but at the expense of operating problems [Bridgwater et al., 1999].

## 2.6.2 Applications

Pyrolysis oil can be used for a wide variety of applications, because of its decoupling of production in time, scale and place from its application. The bio-oils have been successfully tested in engines, turbines and boilers and upgraded to high-quality hydrocarbon fuels [Czernik & Bridgwater, 2004]. The bio-oil can be used for energetic, chemical and commodity purposes depending on the upgrading technology. An overview is presented in

**Table 2.2:** Bio-oil applications after upgrading

| Energy | Commodity | Chemicals |
|---|---|---|
| Fuel for power | Bio-lime | Acetic acid |
| Fuel for heat | Hydrogen | Acetone |
| Energy carrier | Fatty acids | Adhesives and resins |
| | Food flavourings | Alkanes |
| Diesel | Glyoxal | Anhydrosugars |
| Fuel oil | Hydroxyacetaldehyde | Anisole |
| Gasoline | Levoglucosan | Aromatics |
| Reformulated gasoline | Oxychemicals | Aryl ethers |
| Olefins | Phenols | Calcium acetate |
| Emulsions | Polyphenols | Carboxylic acids |
| | Fertiliser | Cresols |
| | Wood preservative | |

## 2.6.3 Upgrading to chemicals

Pyrolysis oil is also seen as an important resource for the production of different bio-based chemicals [Mohan et al., 2006]. There is an increased interest since chemicals have a higher economic value than fuel products. Although not all compounds in the bio-oil have been characterized yet, still hundreds of compounds can be identified as fragments of the biomass fractions lignin, cellulose and hemicellulose [Mohan et al., 2006]. The non-characterized compounds are related with the polymerization reactions of the oxygenates (phenols and carbohydrates). All types of oxygen functionalities with different molecular weight are present: acids, sugars, alcohols, ketones, aldehydes, phenols and furans. A large fraction of

the oil is the phenolic fraction, consisisting of small amounts of phenol, eugenol, cresols and xylenols. Research has been applied on the valorisation of the lignin fraction of pyrolysis oil, called the pyrolitic lignin [De Wild et al., 2009b]. [Bridgwater et al., 1999] states that also the small concentrations of typical organics can be economic viable in the future.

[Cornelissen, 2009] made an overview of bio-oil upgrading technologies, which are related with the incompatibility with conventional fuels, stability, odour options, high viscosity and the water content. At the moment the only commercially attractive application is that of food flavouring or liquid smoke. A red-coloured product is used to brown and flavour sausages, bacon and fish. The browning agents include: glucoaldehyde (and other aldehydes), and acetone. These products can be produced by adding water to the bio-oil. Another attractive application is the production of calcium salts of carboxylic acids which are used for road de-icers. Aspects to be considered for economical attractiveness are that the original feedstock, the process conditions, and condensing parameters are of major importance for het type of chemicals [Venderbosch & Prins, 2010]. Pre-treatment may influence the chemical production.

[Venderbosch & Prins, 2010] described the fractions of the bio-oil that can be isolated for chemical production which are technical feasible, but economically not yet attractive. These fractions are for example the phenol compounds for wood preservation and wood panels such as plywood, MDF and particle board, sugar fractions in the bio-oil for further fermentation by hydrolysis and the synthesis of antibiotics, carboxylic acid fraction for its catalyst functionality. Phenolic compounds can also be used as natural resin, but variability in the lignin fraction makes production difficult.

An important project going on at the moment is the project set up by the European Union which is called the BIOCOUP project[3]. Forest residues are used as a cheap resource for the production of bio-liquids for the application in bio-refinery, due to that oxygenated compounds can be recovered as valuable bio-chemicals. For

[3] www.biocoup.com, last checked 5th August 2010

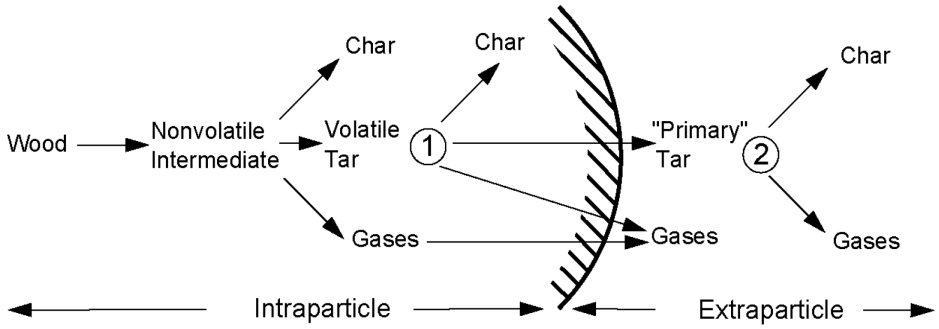


**Figure 2.16:** Tar formation during biomass pyrolysis and gasification

example the isolation of acids from aqueous streams and the use of residual phenolic fractions in phenol-formaldehyde resins and the possibilities of extraction and separation of bio-chemicals have been studied. Separating and purifying valuable bio-chemicals may help increase the viability of the overall process.

Solvent fractionation of bio-oil is an important step in the upgrading to high quality biobased chemicals. Effective separation methods must be developed to concentrate different fractions. Several reaction schemes are proposed based on column separation and solvent extraction [Mohan et al., 2006]. In general, the first step of purification is the separation of the aqueous fraction and the organic fraction by adding water to the bio-oil. Overlap of components in the different phases may exist due to polarity of the compounds.

## 2.7 Tar formation during thermo chemical conversion

A negative side effect during thermo chemical conversion of biomass is the formation of tar. There is no clear and uniform definition for tar, but basically it means the formation of hydrocarbons that can condensate in the reactor under operating conditions. The most precise definition is that “tar is a mixture of organics being produced during thermochemical biomass conversion processes”. Primary tars, in general the hydrocarbons that are released during pyrolysis, can react with each other to form more developed secondary products with higher

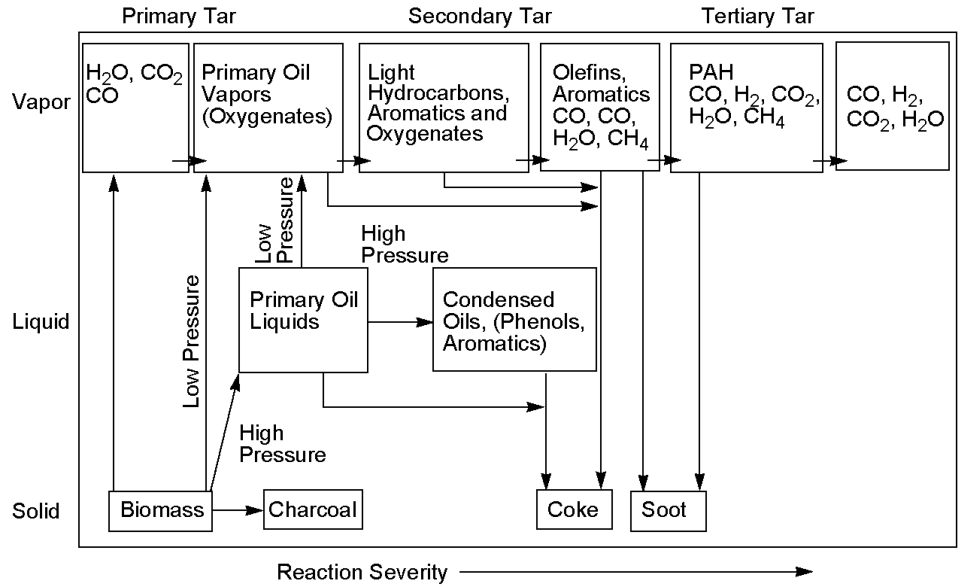


**Figure 2.17:** Pyrolysis pathways, according to [Milne & Evans, 1998]

molecular weight. Primary tars can also react with the biomass and form char, see Figure 2.16.

An extensive overview of reaction pathways of (secondary) tar reactions is reported by [Milne & Evans, 1998]. This molecular pathway is shown in Figure 2.17. Depending on reaction conditions such as temperature, pressure, reaction time and progress different products are formed. In this overview a subdivision is made between primary, secondary and tertiary tar. The Energy research Centre of the Netherlands (ECN) proposed a tar classification system based on the compounds larger than benzene; an overview is given in [Devi, 2004]. The different classes consist out of tars containing hetero atoms, light hydrocarbons with single ring, hydrocarbons with two and three ring compounds and heavy polyaromatic ring compounds larger than three rings.

Primary tar is the direct volatilization product of pyrolysis, which is formed between 300 and 600°C containing the oxygenates formed out of hemicellulose, cellulose and lignin. Secondary tar is formed out of the primary oil vapors which

contains small polymers and aromatics; the formation starts around 500°C [Milne & Evans, 1998]. Tertiary tar contains polycyclic aromatic hydrocarbons (PAH) and is formed between 800 - 1000°. Finally, all tars can be cracked into the permanent gases CO, $CO_2$, $CH_4$, $H_2$ and $H_2O$ by primary and secondary measures [Devi, 2004].

## 2.8 Pyrolysis reactor technologies

The centre of the torrefaction and pyrolysis process is the reactor. The overall objective is to improve the speed of reactor implementation and success of fast pyrolysis for fuels and chemicals by contributing to the resolution of critical technical areas and disseminating relevant information particularly to industry and policy makers[4]. In the development of pyrolysis reactors the main consideration is heat transfer [Bridgwater, 1999] [Bridgwater et al., 1999] [Venderbosch & Prins, 2010]. There are two important features of heat transfer in a pyrolysis reactor:

1. to the heat transfer medium (solid reactor wall, gas and solid, or gas)
2. from the heat transfer medium to the biomass particle which can be subdived in:
    - gas - solid heat transfer where heat is transferred from the hot gas to the pyrolysing biomass particle by convection
    - solid - solid heat transfer with conduction heat transfer

Since the thermal conductivity of biomass is very poor, reliance on gas – solid heat transfer means that biomass particles have to very small to fulfill the requirements of rapid heating. For fast pyrolysis already some commercially available continuous reactor designs have been developed. In Figure 2.18 these reactors are shown:

1. Ablative
2. Circulating fluidized bed
3. Vacuum reactors
4. Bubbling Fluidized bed
5. Auger reactor
6. Rotating cone

[4] www.iea.org

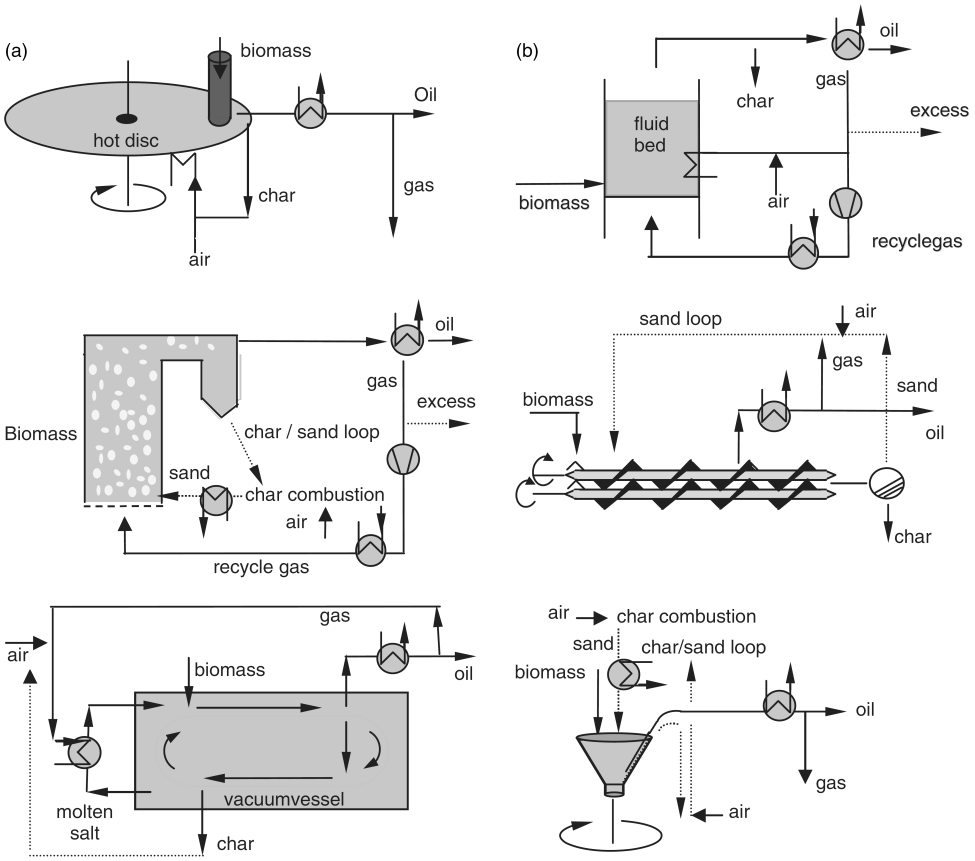


**Figure 2.18:** Pyrolysis Technologies for the production of bio-oils. a) Ablative, CFB and vacuum technologies. b) Fluidized bed, screw (auger) and rotating cone

**Table 2.3:** Advantages and disadvantages of several reactor technologies for pyrolysis

| Reactor type | Mode of heat transfer | (Dis)advantages |
|---|---|---|
| Ablative | 95% Conduction | Accepts large size feedstock |
| | 4% Convection | High mechanical char abrasion |
| | 1% Radiation | Compact design |
| | | Heat supply problematic |
| | | Heat transfer gas not required |
| | | Transport gas not always required |
| Circulating Fluidized Bed | 80% Conduction | High heat transfer rates |
| | 19% Convection | High char abrasion and erosion |
| | 1% Radiation | Char/solid heat carrier separation required |
| | | Solids recycle required |
| | | Maximum particle size up to 6 mm |
| | | Possible liquids cracking by hot solids |
| | | Possible catalytic activity from char |
| | | Greater reactor wear possible |
| Fluidized Bed | 90% Conduction | High heat transfer rates |
| | 9% Convection | Heat supply to fluidizing gas |
| | 1% Radiation | Limited char abrasion |
| | | Very good solids mixing |
| | | Particle size limitation up to 2 mm |
| | | Simple reactor configuration |
| Entrained flow | 4% Conduction | Low heat transfer rates |
| | 95% Convection | Particle size limitation |
| | 1% Radiation | Limited gas/solid mixing |

Ad. 1. In an ablative pyrolysis reactor the surface, heated by a hot flue gas is rotating and the biomass is pressed onto the hot surface. This means that the wood "melts" and leaves an oil film behind which evaporates. [Cornelissen, 2009] compares this with the melting of butter in a frying pan. The shearing action creates more surface area increasing the heat transfer. The mechanical action and centrifugal force causes the particle to pyrolyse and it is very dependent on the pressure, the relative velocity of the wood, shear forces that reduce the particle size and the reactor's surface temperature. The application of ablative pyrolysis leads to

compact and intensive reactors that do not need a carrier gas. In general the following limitations for the ablative technology can be expected [Venderbosch & Prins, 2010]:

- Limited heat transfer rates to the hot surface due to the indirect heating principle. There is only a limited temperature difference between the hot flue gas (800°C) and the pyrolysis reactor (500 - 600°C).
- Restrictions in feedstock morphology since the material needs to be pressed against the hot surface.

Ad. 2. A circulating fluidized bed (CFB) have many of the characteristics of bubbling fluidized beds (Ad 4.), except that the residence time of the char is almost the same as that for the vapors [Mohan et al., 2006]. A solid heat carrier (hot sand) is circulated between the combustor and the pyrolysis reactor to supply the heat. The sand is heated by blowing hot air at the bottom of the reactor which makes gas – solid heat transfer by convection an important part of the heat transfer. The heat is supplied by the burning char, which lead to more attrition. These reactors easily achieve short residence times for volatiles, but biomass residence times are not uniform and only a little greater than the volatiles residence times [Cornelissen, 2009]. Recycling of the partly reacted char is necessary, but recirculation leads to the building up of ash. The ash can crack the volatiles and lead to a lower yield of the bio-oil. The heat transfer limitation is within the particle, like the bubbling fluidized bed reactor, which requires also small particle sizes up to a few mm. CFB reactors are suitable for large throughput of biomass, because the hot recirculated sand is often contacted with the biomass.

Ad. 3. Vacuum pyrolysis involves the thermal decomposition of biomass under reduced pressure (15kPa) [Cornelissen, 2009]. The biomass is moved by gravity and rotating scrapers through multiple hearth pyrolyzers with the temperature increasing from 200 to 400/500°C. These horizontal plates are heated up by molten salts which are heated by a burner that is supplied with the non-condensable gases. Additional heating could be necessary. In comparison to the other pyrolysis techniques larger particles can be used, but it has smaller heating rates. The pyrolytic vapours are quickly removed from the reactor under vacuum conditions, so the amount of secondary reactions and products is small, representing more the

original structures of the complex constituents in the biomass. The application of a vacuum pump and the difficulty to scale up makes it a difficult technology [Bridgwater & Peacocke, 2000].

Ad. 4. A bubbling fluidized bed is the most common used reactor type for fast pyrolysis [Bridgwater et al., 1999]. Bubbling fluidized provide good temperature control and very efficient heat transfer to biomass particles, because of the high solid density in the bed [Bridgwater & Peacocke, 2000]. The heat is transferred from an external heat source to the biomass by a mixture of convection and conduction, requiring very small particles of typically not more than 3 mm to obtain good liquid yields [Bridgwater et al., 2009] [Brown and Holmgren[5]]. In the reactor the sand heats the biomass by solid – solid heat transfer. The heat transfer limitation is within the particle, requiring small particles. A carrier gas is needed for fluidization and transport [Mohan et al., 2006]. Char has a higher residence time than the gases and acts as an effective vapour cracking catalyst. Cyclonic separators are place after the reactor to separate rapidly and effectively the char. [Cornelissen, 2009] states the important difference between CFB and BFB as follows that in a CFB sand and char are removed by the reactor and in BFB only the char.

Ad 5. In auger pyrolysis reactor the screw mechanisms plays an important role in the pyrolysis process looking at the heat transfer and transportation through the reactor tube. The reactor design is adopted from the Lurgi process in which a twin-screw mixer reactor is developed for oil shale, tar sand and refinery vacuum residues [Venderbosch & Prins, 2010]. In general it contains the following features: it is compact and does not require any carrier gas, it operates at lower process temperatures and operates as a continuous process [Cornelissen, 2009]. Char is produced and gases are condensed as bio-oil, while non condensables are collected as biogas. Chopped biomass is mixed with hot sand and decomposed to vapors and char. Heat transfer takes place by intimate contact with a heat carrier, with no need for an inert carrier gas [Venderbosch & Prins, 2010].

Ad. 6. The rotating cone is a reactor in which the biomass is mixed with the heat transfer medium (mostly sand). It is developed by BTG and the University of

[5] pdf file with presentation at http://www.ars.usda.gov last checked May 17, 2010

Twente in The Netherlands. By rotation of the cone the biomass is mixed which makes compact design possible and it does not need carrier gas. The vapours and aerosols are not diluted and their flow is upwards, but minimal. It requires very small particles and is hard to scale-up. The original idea was to achieve ablative pyrolysis where biomass particles were heated on a surface, but nowadays an enormous ratio between sand and biomass is used [Bridgwater & Peacocke, 2000] Bridgwater et al., 1999] [Bridgwater, 1999] summarized the advantages and disadvantages for different reactor types for (fast) pyrolysis, which are shown in Table 2.3.

Finally, Figure 2.19 shows the market attractiveness and the technology strength of different pyrolysis reactor systems as adopted from [pyne.co.uk]. It is shown that fluidized beds and auger reactors have high market attractiveness and a strong technology strength. Entrained flow concepts have low market attractiveness and a weak technology strength for pyrolysis of biomass.

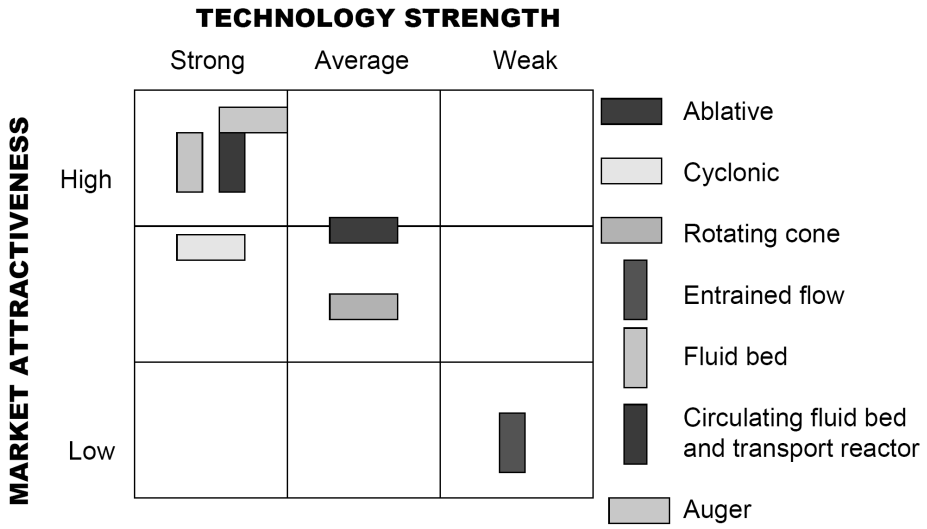


**Figure 2.19:** Market attractiveness and technology strength of different pyrolysis reactor techniques. Adopted from pyne.co.uk

## References

Bradbury AGW, Sakai Y, Shafizadeh F (1979). A kinetic model for pyrolysis of cellulose. Journal of Applied Polymer Science 23; 3271 - 3280

Branca C, Di Blasi C (2003). Kinetics of the isothermal degradation of wood in the temperature range 528 – 708K. Journal of Analytical and Applied Pyrolysis 67(2); 207 - 219

Bridgwater AV (1999). Principles and practice of biomass fast pyrolysis processes for liquids. Journal of Analytical and Applied Pyrolysis 51; 3 - 22

Bridgwater AV, Meier D, Radlein D. (1999). An overview of fast pyrolysis of biomass Organic Geochemistry 30; 12; 1479-1493

Bridgwater AV, Peacocke GVC (2000). Fast pyrolysis processes for biomass. Renewable & sustainable energy reviews 4; 1; 1-73

Bridgwater AV (2003**).** Renewable fuels and chemicals by thermal processing of biomass. Chemical Engineering Journal 9; 2-3; 87-102

Broido A, Weinstein M (1971). Low temperature isothermal pyrolysis of cellulose. In Proceedings of the 3rd International Conference on Thermal Analysis; Wiedemann, E; Birkhauser Verlag; Basel; 285 - 296

Chan WCR, Kelbon M, Krieger BB (1985). Modelling and experimental verification of physical and chemical processes during pyrolysis of a large biomass particle. Fuel 64; 11; 1505-1513

Chan WCR, Kelbon M, Krieger BB (1988). Single-particle biomass pyrolysis: Correlations of reaction products with process conditions. Industrials and Engineering Chemistry Research 27; 12; 2261-2275

Cornelissen T (2009). Flash pyrolysis of biomass and co-pyrolysis with biopolymers. PhD thesis – research group: Applied Chemistry. Hasselt University, Belgium

Czernik S, Bridgwater AV. Overview of applications of biomass fast pyrolysis oil**.** Energy and Fuels 18; 2; 590-598

De Wild PJ, Uil H, Reith JH, Kiel JHA, Heeres HJ (2009). Biomass valorisation by staged degasification. A new pyrolysis-based thermochemical conversion option to

produce value-added chemicals from lignocellulosic biomass. Journal of Analytical and Applied Pyrolysis 85; 1-2; 124-133

Demirbas A (2000). Mechanism of liquefaction and pyrolysis reactions of biomass. Energy Conversion & Management 41; 633 – 646.

Demirbas A, Arin G (2002) An overview of biomass pyrolysis. Energy Sources, 24; 471 – 472

Demirbas A (2009). Fuel properties of pyrolysis oils from biomass. Energy Sources Part A, 31; 412-419

Devi L (2004). Catalytic removal of biomass tars; Olivine as prospective in-bed catalyst for fluidized-bed biomass gasifiers, PhD Thesis, Eindhoven University of Technology

Di Blasi C, Lanzetta M (1997). Intrinsic kinetics of isothermal xylan degradation in inert atmosphere. Journal of Analytical and Applied Pyrolysis 1997;40;287-303

Di Blasi C, Signorelli G, Di Russo C, Rea G (1999). Product distribution from pyrolysis of wood and agricultural residues. Industrial and Engineering Chemistry Research 38; 6; 2216-2224

Di Blasi C (2008). Modelling chemical and physical processes of wood and biomass pyrolysis. Progress in Energy and Combustion Science 2008;34(1);47-90

Diebold JP (2000). A review of the chemical and physical mechanisms of the storage stability of fast pyrolysis bio-oils; NREL 2000;1-51

Gaur S, Reed TB (1998). Thermal data for natural and synthetic fuels. Marcel Dekker, New York, 1998

Gronli MG (1996). A theoretical and experimental study of the thermal degradation of biomass. PhD. Thesis; Norwegian University of Science and Technology; Trondheim; Norway

Hubert GW, Iborra S, Corma A (2006). Synthesis of transportation fuels from biomass: chemistry, catalysts, and engineering. Chemical Reviews 106; 4044 - 4098

Janse AMC, Westerhout RWJ, Prins W (2000). Modelling of flash pyrolysis of a single wood particle. Chemical Engineering and Processing 2000; 39; 239-252

Lievens C (2007). Valorization of heavy metal contaminated biomass by fast pyrolysis. PhD thesis – research group: Applied Chemistry. Hasselt University; Campus Diepenbeek

McKendry P (2002). Energy production from biomass (part 1): Overview of biomass. Bioresource Technology 83; 1; 37 - 46

McKendry P (2002). Energy production from biomass (part 2): Conversion technologies. Bioresource Technology 83; 1; 47 - 54

McKendry P (2002). Energy production from biomass (part 3): Gasification technologies. Bioresource Technology 83; 1; 55 - 63

Milne TA, Evans RJ (1998). Biomass gasification "tars": their nature, formation and conversion. NREL, Golden, Colorado, USA. Report no. NREL/TP-570-25357

Mohan D, Pittman CU, Steele PH (2006). Pyrolysis of wood/biomass for bio-oil: A critical review. Energy Fuels; 20; 848 - 889

Piskorz, J., Majerski, P., Radlein, D., Scott, D.S., Bridgwater, A.V. (1998). Fast pyrolysis of sweet sorghum and sweet sorghum bagasse. Journal of Analytical and Applied Pyrolysis 46; 1; 15-29

Prins MJ, Ptasinski KJ, Janssen FJJG (2006a). Torrefaction of wood Part: 1. Weight loss kinetics. Journal of Analytical and Applied Pyrolysis 2006; 77; 1; 28-34

Repellin V, Govin A, Rolland M, Guyonnet R (2010). Modelling anhydrous weight loss of wood chips during torrefaction in a pilot kiln. Biomass and Bioenergy

Rousset P (2004). Choix et validation experimentale d'un modele de pyrolyse pour le bois traite parr haute temperature: de la micro-particule au bois massif. PhD Thesis; ENGREF; Nancy

Rousset P, Turner I, Donnot A, Perre P (2006). Choix d'un modèle de pyrolyse ménagée du bois à l'échelle de la microparticule en vue de la modélisation macroscopique. Annals of Forest Science 63; 213 – 229

Shafizadeh F, Chin PPS (1976). Pyrolytic production and decomposition of 1,6-anhydro-3,4-dideoxy-β-d-glycero-hex-3-enopyranos-2-ulose**.** Carbohydrate Research 46; 1; 149-154

Turner I, Rousset P, Remond R, Perre P (2010). An experimental and theoretical investigation of the thermal treatment of wood in the range 200 - 260°C. International Journal of Heat and Mass transfer 53; 715 - 725

Várhegyi G (1980). A basic problem in mathematical modelling in pyrolysis: The number of the unknown parameters. Journal of Analytical and Applied Pyrolysis 2; 1; 1-6

Varhegyi G, Antal Jr MJ, Szekely T, Szabo P (1989). Kinetics of the thermal decomposition of cellulose, hemicellulose, and sugar cane bagasse. Energy & Fuels 3; 3; 329-335

Varhegyi G, Jakab M, Antal Jr. MJ (1994). Is the Broido-Shafizadeh model for cellulose pyrolysis true? Energy & Fuels 8; 1345 - 1352

Varhegyi G, Antal Jr. MJ, Jakab E, Szabo P (1997). Kinetic modelling of biomass pyrolysis. Journal of Analytical and Applied Pyrolysis 42; 73 - 87

Venderbosch RH, Prins W (2010). Fast pyrolysis technology development. Biofuels, Bioproducts and Biorefining 4; 178-208

Williams PT, Besler S (1996). The influence of temperature and heating rate on the slow pyrolysis of biomass. Renewable Energy, 1996;7(3);233-250

Zanzi R, Sjöström K, Björnbom E (2002). Rapid pyrolysis of agricultural residues at high temperature. Biomass and Bioenergy 23; 5; 357-366

# Chapter 3

# Biomass upgrading by torrefaction for the production of biofuels: a review


## Abstract

*An overview of the research on biomass upgrading by torrefaction for the production of biofuels is presented. Torrefaction is a thermal conversion method of biomass in the low temperature range of 200 - 300ºC. Biomass is pre-treated to produce a high quality solid biofuel that can be used for combustion and gasification. In this review the characteristics of torrefaction are described and a short history of torrefaction is given. Torrefaction is based on the removal of oxygen from biomass which aims to produce a fuel with increased energy density by decomposing the reactive hemicellulose fraction. Different reaction conditions (temperature, inert gas, reaction time) and biomass resources lead to various solid, liquid and gaseous products. A short overview of the different mass and energy balances is presented. Finally, the technology options and the most promising torrefaction applications and their economic potential are described.*

## 3.1 Introduction

The transition to a society driven by renewable energy sources such as solar, wind, biomass, tide, wave and geothermal energy next to energy savings becomes even more an important alternative in our energy consumption. According to the World Energy Outlook [IEA, 2006] renewable energy sources are expected to be the fastest growing energy sources. In this spectrum of several different energy sources biomass is the only source that is based on sustainable carbon.

In future energy scenarios an important role in the (renewable) energy supply has been addressed to biomass. The unique position of biomass as the only renewable source as sustainable carbon carrier makes biomass an attractive energy source. Biomass can be converted into energy via thermo chemical conversions, biochemical conversions and extraction of oil from oil bearing seeds. Among various thermo chemical conversion methods gasification is the most promising. Gasification is the partial oxidation of carbonaceous feedstock above 800°C to produce a syn-gas that can be used for many applications such as gas turbines, engines, fuel cells, producing methanol and hydrocarbons. Due to its higher efficiency, it is desirable that gasification becomes increasingly applied in future rather than direct combustion.Coupling gasification with power systems increases the efficient use of thermal energy streams [Prins et al., 2005] [Prins et al., 2006a] [Prins et al., 2006b].

Biomass as energy source shows some typical characteristics which make it a special, but rather complicated fuel for the future. Biomass is available in a wide range of resources such as waste streams, woody and grassy materials and energy crops. Woody materials are preferred above food crops, because of several reasons. Woody materials contains much more energy than food crops, the amount of fertilizers and pesticides necessary for wood is much lower and the production of woody materials is much higher than for food crops which means that the land use becomes smaller. Another characteristic of biomass is its climate neutral behavior. If biomass is grown in a sustainable way, its production and application produces no net amount of $CO_2$ in the atmosphere. The $CO_2$ released by the application of biomass is stored in the biomass resource during photosynthesis and is extracted from the atmosphere which means a climate neutral carbon cycle of $CO_2$.

On the other hand, some biomass properties are inconvenient, particularly its high oxygen content, a low calorific value, a hydrophilic nature and a high moisture content. Also the energy production from biomass resources shows reduced overall energy efficiency due to photosynthesis. The overall energy efficiency from solar energy to biomass energy is 1 – 3% [Hermann, 2005]. The high amount of oxygen also results in smoking during combustion. Other disadvantages of biomass are its tenacious and fibrous structure and its heterogeneous composition that makes process design and process control more complicated.

The use of biomass is also subjected to limitation of land, water and competition with food production. The agricultural production of biomass is relatively land intensive and involves high logistics costs due to low energy density of biomass. For biomass based systems a key challenge is to develop efficient conversion technology which can also compete with fossil fuels.

Torrefaction is a technology which can improve biomass properties and therefore offers some solutions to above problems. Torrefaction is a thermal pre-treatment technology to upgrade ligno-cellulosic biomass to a higher quality and more attractive biofuel. The main principle of torrefaction from a chemical point of view is the removal of oxygen with a final solid product: the torrefied biomass which has a lower O/C ratio compared to the original biomass.

The aim of this review is to present recent developments in the torrefaction technology. In the next part the main torrefaction characteristics such as operating conditions, mass – and energy balances and particle size reduction are described. Finally, this chapter shows the applications of torrefaction and an economic evaluation of the production of torrefied biomass pellets.

## 3.2 Torrefaction characteristics

### 3.2.1 General process description

Torrefaction is a thermal method for the conversion of biomass operating in the low temperature range of 200 to 300ºC. It is carried out under atmospheric conditions in absence of oxygen. Other names for the torrefaction process are roasting, slow- and mild pyrolysis, wood cooking and high-temperature drying. In recent history torrefaction has only been applied to various types of woody

biomass, but already around 1930 the torrefaction process was studied in France. The amount of publications on torrefaction is relatively small. Literature about torrefaction of diverse biomass resources can be found, namely: maritime pine , chestnut, oak and eucalyptus, Caribbean pine [Arcate, 2002], birch, pine, bagasse [Pach et al., 2002], bamboo [IIS, 2006], wood briquette [Felfli et al., 2005] and willow and beech [Prins et al., 2006a] [Prins et al, 2006c] [Prins et al., 2006d]. Just below 200 ºC thermal methods are used for wood preservation [Hakkou et al., 2006] [Windeisen et al., 2007] [Sundqvist et al., 2006] [Tjeerdsma et al., 1998] [Rousset et al., 2004], while torrefaction is applied for energy purposes.

Torrefaction is used as a pre-treatment step for biomass conversion techniques such as gasification and cofiring. The thermal treatment not only destructs the fibrous structure and tenacity of biomass, but is also known to increase the calorific value. Also after torrefaction the biomass has more hydrophobic characteristics that make storage of torrefied biomass more attractive above non-torrefied biomass, because of the rotting behavior. During the process of torrefaction the biomass partly devolatilises leading to a decrease in mass, but the initial energy content of the torrefied biomass is mainly preserved in the solid product so the energy density of the biomass becomes higher than the original biomass which makes it more attractive for i.e. transportation.

A typical mass and energy balance for woody biomass torrefaction is that 70% of the mass is retained as a solid product, containing 90% of the initial energy content. The other 30% of the mass is converted into torrefaction gas, which contains only 10% of the energy of the biomass [Bergman et al., 2005]. An energy densification with typically a factor of 1.3 can be attained. This is one of the main fundamental advantages of the torrefaction process. As the energy density of torrefied wood is significantly higher compared to untreated wood, larger transportation distances can be allowed. Another advantage of torrefied biomass is its uniformity in product quality. Woodcuttings, demolition wood, waste wood have after torrefaction quite similar physical and chemical properties including hydrophobicity.

Research focused on torrefaction has been started in France in the 1930's, but publications about this research are limited. [Pentanunt et al., 1990] studied the combustion characteristics of (torrefied) wood in a bench scale torrefaction unit. It

was shown that torrefied wood has a significantly higher combustion rate and produces less smoke than wood. Also it was found that torrefied briquettes were practically water resistant and torrefaction appeared a good technique for upgrading briquettes. The structure of the torrefied biomass is changed in comparison to the raw biomass which makes it brittle and hydrophobic [Bourgeois & Guyonnet., 1988] [Bourgeois et al., 1989] [Li & Gifford., 2001].

[Ferro et al., 2004] studied the effect of the raw material, temperature, residence time and nitrogen flow on the properties of the torrefied products. The experiments were performed in a reactor tube with pine, lucern, sugar cane bagasse, wood pellets and straw pellets. It was concluded that the type of biomass influenced the product distribution in its gas, liquid and solid ratio. The same research has been done for birch [Pach et al., 2002].

The Energy research Centre of the Netherlands (ECN) has been working on the principle of torrefaction since 2002 and published various reports [Bergman et al., 2005] [Bergman, 2005] [Bergman et al., 2004] [Pels & Bergman., 2006]. So far, their research has been focused on various woody biomass and herbaceous species as straw and grass. In particular the influence of feed, particle size, torrefaction temperature and reaction time on torrefaction characteristics such as mass and energy yield and product properties has been investigated. As torrefaction is not available commercially at the moment, much of the generated knowledge still is used to develop this technology. On the basis of the principles of torrefaction it is strongly believed that is has high potential to become a leading biomass pretreatment technology [Weststeyn, 2004].

Prins et al. performed thermodynamic analysis of coupled biomass gasification and torrefaction [Prins et al., 2006acd] [Prins, 2005]. This work is in line by what is done by the Energy research Centre Netherlands [Bergman et al., 2005] [Bergman, 2005]. The research was focused on weight loss kinetics of wood torrefaction [Prins et al., 2006c], analysis of products from wood torrefaction [Prins et al., 2006d] and more efficient biomass gasification via torrefaction. It was shown that weight loss kinetics for torrefaction of willow can be accurately described by a two-step reaction in series model and deciduous wood types, such as beech and willow, were found to be more reactive than coniferous wood. Prins concluded that

the overall mass and energy balances for torrefaction at 250 and 300ºC showed that the process of torrefaction is mildly endothermic. The general conclusion was that the concept of wood torrefaction, followed by high temperature entrained flow gasification of the torrefied wood, is very promising [Prins, 2005].

The mass and energy losses of torrefaction in nitrogen of two energy crops, reed canary grass and short rotation willow coppice (SRC), and wheat straw showed that the torrefied fuel can contain up to 96% of the original energy content in the solids [Bridgeman et al., 2008]. Also the combustion behavior of raw and torrefied was studied by differential thermal analysis. It is shown that both volatile and char combustion of the torrefied sample become more exothermic compared to the raw fuels. TGA experiments have shown that the torrefied product exhibited different volatile release and burning profiles. Combustion behavior of (torrefied) willow showed that the initiation of volatile release for willow torrefied at 290ºC is approximately 60ºC higher than for untreated willow For willow treated at 250 and 270ºC it is shown that the initiation of the combustion starts at temperatures 30ºC and 40-50ºC higher. Finally, it is demonstrated that torrefied particles start char combustion quicker than the raw SRC particles, although char combustion is slower for the torrefied fuel.

In the work of [Arias et al., 2008] the influence of torrefaction on the grindability and reactivity of woody biomass has been investigated to improve its properties for pulverized systems. After torrefaction at 220, 260 and 280ºC the grindability of raw biomass and the treated samples was compared and an improvement in grindability was observed after torrefaction. In order to evaluate the grindability of the raw biomass in comparison to the torrefied biomass the samples were handled in a cutting mill with a bottom sieve of 2 mm. The samples were then sieved and it is shown that the torrefied biomass has a particle size distribution in which the amount of smaller particles is larger than in the non torrefied sieved particles.

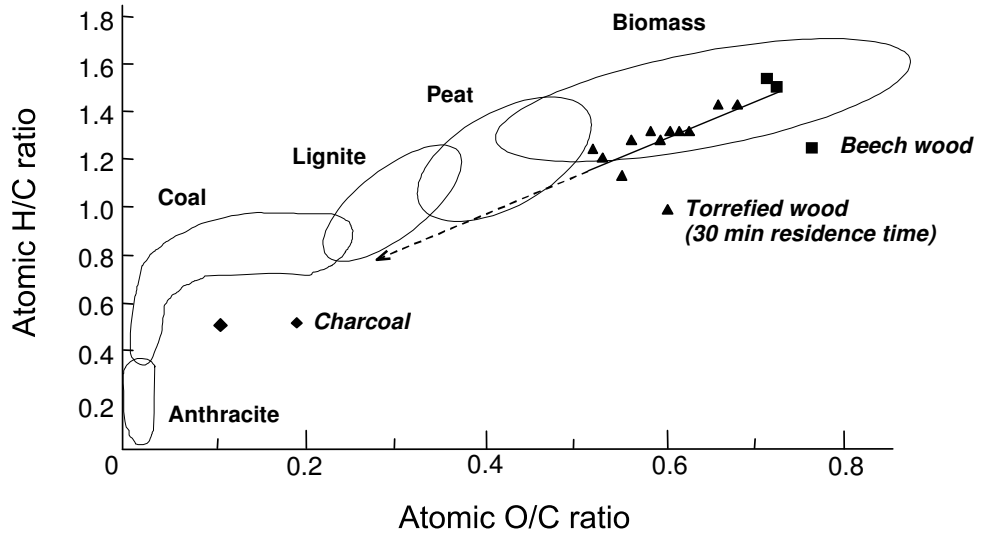


**Figure 3.1:** The Van Krevelen diagram which shows the atomic H/C ratio and the atomic O/C ratio of several different kinds of biowastes and torrefied wood

### 3.2.2 Process stages

The overall torrefaction process can be divided into several steps, such as heating, drying, torrefaction and cooling. The definitions provided by [Bergman et al., 2005] have been used as a basis to further define the temperature-time stages in torrefaction. Five main stages that have been defined in the total torrefaction process are:

- Initial heating: the biomass is initially heated until the stage of drying of the biomass is reached. In this stage, the temperature is increased, while at the end of this stage moisture starts to evaporate.
- Pre-drying: at 100ºC the free water is evaporated from the biomass at constant temperature.
- Post-drying and intermediate heating: the temperature of the biomass is increased to 200 ºC. Physically bound water is released. During this stage some mass loss can occur as light fractions can evaporate.

- Torrefaction: during this stage the actual process occurs. The torrefaction will start when the temperature reaches 200ºC and ends when the process again is cooled down from the specific temperature to 200ºC. The torrefaction temperature is defined as the maximum constant temperature. During this period most of the mass loss of the biomass occurs.
- Solids cooling: the torrefied product is further cooled below 200ºC to the desired final temperature, which is the room temperature.

### 3.2.3 Mass and energy balances

During torrefaction numerous different products are formed depending on the torrefaction conditions such as reaction temperature, residence time and biomass properties. As result of partial decomposition of biomass during this process, the chemical composition of original biomass changes as is shown in the Van Krevelen diagram [Prins, 2005]. The Van Krevelen diagram gives information about the differences in the elemental composition (C,H,O ratio). In this figure the composition of typical fuels such as coal, lignite, peat biomasses are shown. It is clear that biomass compared to coal contains more oxygen.

Torrefaction has a big influence on the properties of the solid product, mainly caused by the removal of oxygen from the original solid biomass resource. In the Van Krevelen diagram for torrefied wood it is shown how the properties of the solid product are influenced and become more coal like [Prins et al., 2006a] It can be seen that biomass loses relatively more oxygen and hydrogen than carbon and properties changes in the direction of carbon. In this way the net calorific value (LHV) is influenced and the product becomes energy denser.

Various products are formed as torrefied solid product, condensable volatiles and gas as the biomass reacts under different conditions. An important parameter is the composition of the biomass resource since the content of hemicellulose, cellulose and lignin differs influencing the product distribution. The effect of process conditions (residence time and torrefaction temperature) was studied by Prins and Bergman, respectively.

[Prins et al., 2006d] studied the product distribution during the torrefaction of larch, willow and straw at different temperatures and reaction times. Table 3.1

presents the composition of wood and torrefied wood, derived at two different experimental conditions. Table 3.1 also shows that the lower atomic ratio between hydrogen and carbon and the lower oxygen to carbon ratio result into a higher LHV. It was found that the yield of solid product decreases with temperature and residence time.

The observed weight loss for straw is comparable to willow and beech wood. The volatiles were subdivided into condensable and non-condensable volatiles. Acetic acid and water are the main condensable torrefaction volatiles. These products were ascribed to the decomposition of hemicellulose. The non-condensable volatiles formed were mainly carbon dioxide and carbon monoxide. At higher temperatures, both condensables and non-condensables are produced in a higher amount.

Figure 3.2 - Figure 3.5 show the product distribution for torrefaction at different reaction conditions and several biomass resources such as birch, straw pellets, miscanthus and pine [Pach et al., 2002] [Ferro et al., 2004]. During torrefaction the relative amounts of solid, liquid and gas can be determined. The liquid is formed after gases are condensed. As the temperature and residence time rises torrefaction forms more condensables and gasses. The amount of torrefied solid biomass left ranges between 65 – 95%. It can be seen that a temperature rise has more influence on product distribution than a longer residence time which means that reactivity of the biomass becomes smaller after 1 or 2 hours. It can be seen that in case of pine more volatiles are formed compared to birch and straw. However, the differences in torrefied behavior of researched biomass sources are relatively small.

**Table 3.1:** Composition of wood and torrefied wood

| | **Wood** | **Torrefied wood (250°C, 30 min.)** | **Torrefied wood (300°C,10min.)** |
|---|---|---|---|
| Carbon | 47.20% | 51.30% | 55.80% |
| Hydrogen | 6.10% | 5.90% | 5.60% |
| Oxygen | 45.10% | 40.90% | 36.30% |
| Nitrogen | 0.30% | 0.40% | 0.50% |
| Ash | 1.30% | 1.50% | 1.90% |
| LHV (MJ/kg) | 17.6 | 19.4 | 21 |

**Table 3.2:** Mass and energy balances for torrefaction of (dry) willow at a temperature of 250°C (reaction time of 30 minutes) and 300°C (reaction time of 30 minutes). Data per kg of wood input

| | **Torrefaction (250°C, 30 min.)** | | | **Torrefaction (300°C, 10 min.)** | | |
|---|---|---|---|---|---|---|
| | Mass (kg/kg) | LHV (kJ/kg) | Sensible heat (kJ/kg) | Mass (kg/kg) | LHV (kJ/kg) | Sensible heat (kJ/kg ) |
| Torrefied wood | | | | | | |
| Org. material | 0.859 | | | 0.655 | | |
| Ash | 0.013 | | | 0.013 | | |
| Total | 0.872 | 16883 | 202 | 0.668 | 14024 | 189 |
| Volatiles | | | | | | |
| Steam | 0.057 | 0 | 24 | 0.066 | 0 | 35 |
| Acetic acid | 0.021 | 300 | 6 | 0.072 | 1001 | 28 |
| Other organics | 0.018 | 258 | 6 | 0.142 | 2280 | 59 |
| Carbondioxide | 0.029 | 0 | 6 | 0.04 | 0 | 11 |
| | 0.003 | 30 | 1 | 0.012 | 121 | 3 |
| Carbonmonoxide | | | | | | |
| Hydrogen | trace | 1 | 0 | trace | 1 | 0 |
| Methane | negl. | 0 | 0 | trace | 2 | 0 |
| Total | 0.128 | 589 | 43 | 0.332 | 3405 | 136 |

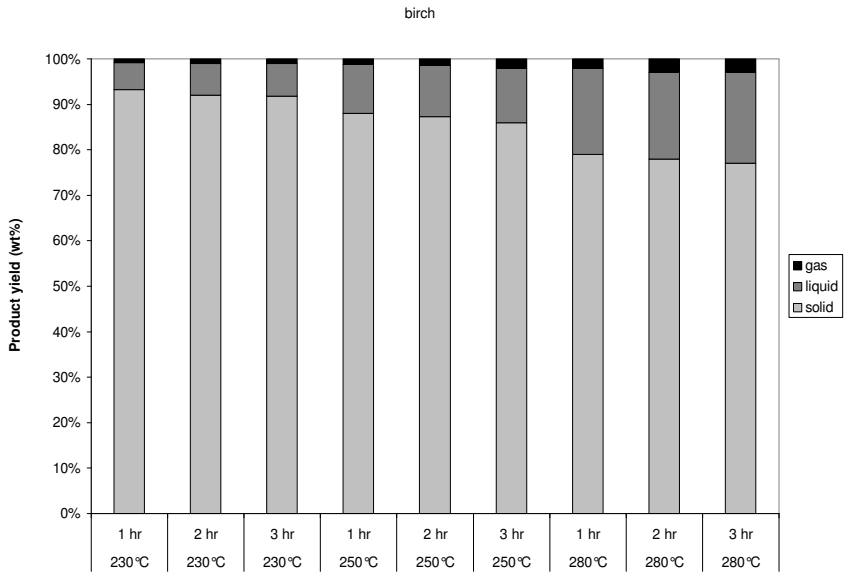


**Figure 3.2:** Product yield torrefaction of birch after 1, 2 and 3 hr at 230, 250 and 280°C

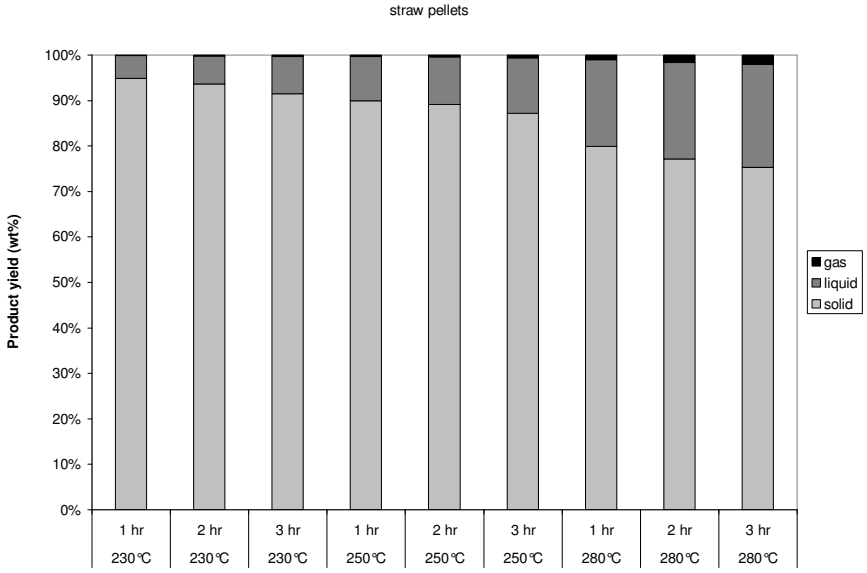


**Figure 3.3:** Product yield torrefaction of straw pellets after 1, 2 and 3 hr at 230, 250 and 280°C

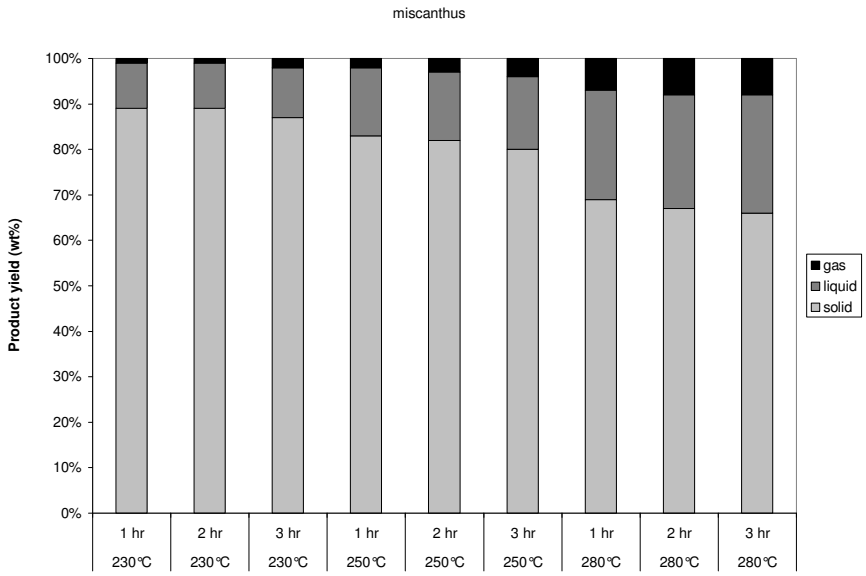


**Figure 3.4:** Product yield torrefaction of miscanthus after 1, 2 and 3 hr at 230, 250 and 280°C

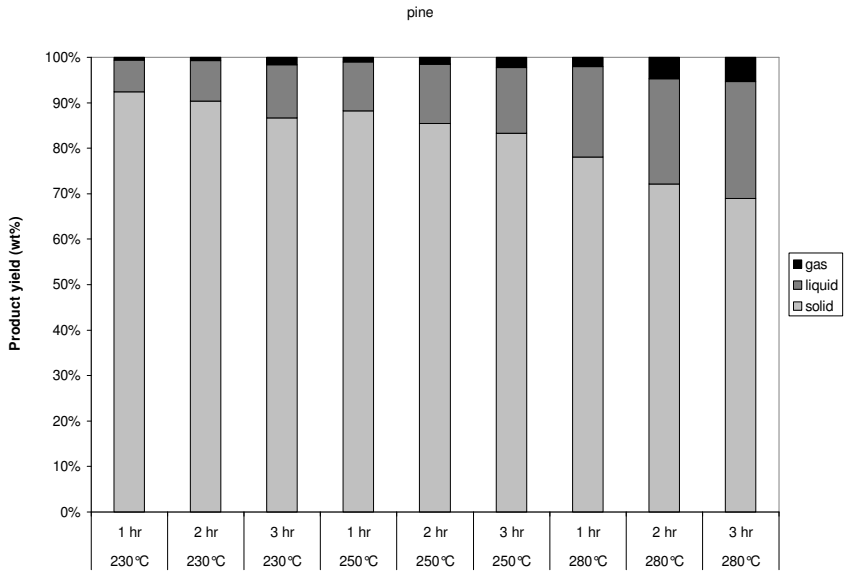


**Figure 3.5:** Product yield torrefaction of pine after 1, 2 and 3 hr at 230, 250 and 280°C

The mass and energy balances for the data shown in Table 3.1 and Figure 3.6 present the overall mass and energy balances for both experiments. It is shown that several organic (acid) condensable volatiles are formed such as acetic acid, furfural, formic acid, methanol, lactic acid and phenol. At 250°C less volatiles are formed compared to torrefaction at 300°C. Also the torrefied wood at 250°C is energy denser than the torrefied wood produced at 300°C, mainly because of the acetic acid and other organics formed at high temperature. Non-condensable volatiles such as $CO_2$ and CO are the main gas products.

Figure 3.6 shows that, depending on the temperature, the solid torrefied product contains 95% (250°C) and 79% (300°C) of the energy input based on the LHV [Prins et al., 2006a] Energy densifications of 1.1 and 1.19 are determined for torrefied wood in relation to raw wood for the two experiments. It can be seen that the torrefaction process is slightly endothermic at different reaction conditions.

In Figure 3.7 [Pach et al., 2002] [Ferro et al., 2004] the influence of different torrefaction conditions (reaction temperature and residence time) for several other biomass streams on the energy densification are shown. The energy densification numbers vary between 1.00 for straw pellets and 1.45 for miscanthus[1] torrefied at 280°C for 3hr.

[1] http://hem.fyristorg.com/zanzi/paper/zanziV2A-17.pdf 18th April 2008

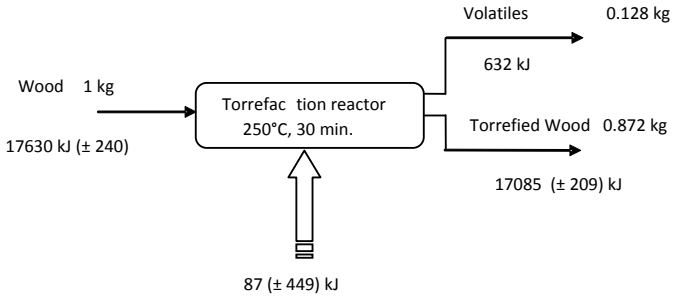


**(a)**

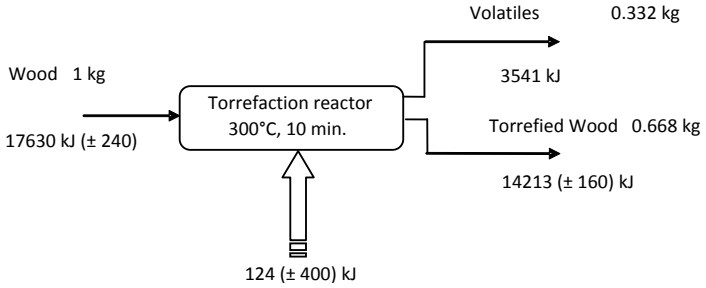


**(b)**

**Figure 3.6:** Overall mass and energy balances for torrefaction of (dry) willow at temperature and reaction time of (a) 250°C and 30 minutes (b) 300°C and 10 minutes [Prins et al., 2006a]

## 3.2.4 Particle size reduction

In existing entrained flow gasification, as currently used for coal, a small particle size is necessary. Biomass resources have a tenacious and fibrous structure which makes it rather difficult to grind and suitable for co-firing in existing coal fired stations or other pulverized systems. Nowadays large energy consumption is necessary to get small particle size of typical biomass, such as wood. Torrefaction is a technology that improves the grindability of biomass resources. The Energy Research Centre Netherlands studied the grindability of several (woody) biomass feedstock, torrefied biomass and coal. Size reduction experiments show that the

power consumption needed for grinding torrefied biomass can be reduced with 80 – 90% in comparison with untreated biomass [Bergman et al., 2005]

In Figure 3.8 the power consumption necessary for grinding several samples of biomass to small particles is shown. Size reduction experiments were carried out for coal, torrefied woodcuttings (C), willow (W) and demolition wood (D) for different torrefaction conditions (temperature and residence time) and wet woodcuttings, willow and demolition wood. It is shown that the power consumption for grindability of torrefied biomass is reduced and is compared to that of coal.

[Arias et al., 2008] also studied the influence of torrefaction on the grindability and reactivity of woody biomass. The grindability was studied using a cutting mill, after which the particle size distribution of torrefied biomass was evaluated after torrefaction in the temperature regime of 240-280°C. Different sieve fractions are used to determine the effect of milling on the particle size and particle size distribution. It is shown that there is an improvement in the grindability characteristics of the torrefied biomass. The percentage of particles in the smallest sieve size increases after torrefaction.

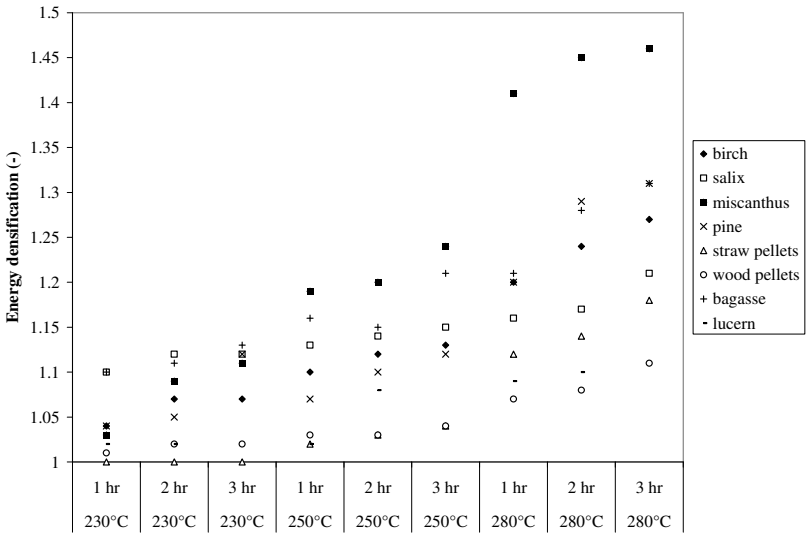


**Figure 3.7:** Energy densification several biomass resources at different temperature and with different residence time [Pach et al., 2002] [Ferro et al., 2004].

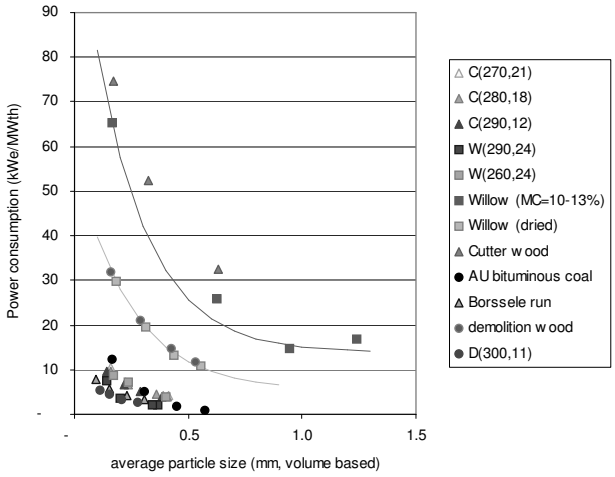


**Figure 3.8:** Size reduction several untreated biomass, torrefied biomass and coal resources [Bergman et al, 2005]

## 3.3 Technological applications

### 3.3.1 Pelletisation

It is commonly known that various biomass resources differ in composition and so in behaviour. Pelletisation of biomass is an interesting option to improve biomass properties to get more uniformity. Densification by means of pelletisation is considered to be a proven technology to improve biomass properties for its conversion into heat and power. Pellets from torrefied biomass are attractive with respect to heating value, grindability, combustion nature, storage, transport and handling which make them attractive as replacement for coal in existing power stations. The Energy Research Centre Netherlands (ECN) developed the so called $BO_2$ process (in initial literature also referred to as the TOP process) in which pellets are processed with torrefied biomass. Compared to non-torrefied pellets $BO_2$ pellets show better hydrophobic behaviour, strength and higher density. The main characteristics of different pellets are shown in Table 3.3 [Bergman, 2005].

**Table 3.3:** Properties of wood, torrefied biomass, wood and $BO_2$ pellets

| **Properties** | **Unit** | **Wood** | **Torrefied biomass** | **Wood pellets** | | **TOP pellets** | |
|---|---|---|---|---|---|---|---|
| Moisture | %wt | 35% | 3% | 10% | 7% | 5% | 1% |
| LHV | | | | | | | |
| normal | MJ/kg | 10.5 | 19.9 | 15.6 | 16.2 | 19.9 | 21.6 |
| dry | MJ/kg | 17.7 | 20.4 | 17.7 | 17.7 | 20.4 | 22.7 |
| Bulk density | $kg/m^3$ | 550 | 230 | 500 | 650 | 750 | 850 |
| Energy density | $GJ/m^3$ | 5.8 | 4.6 | 7.8 | 10.5 | 14.9 | 18.4 |

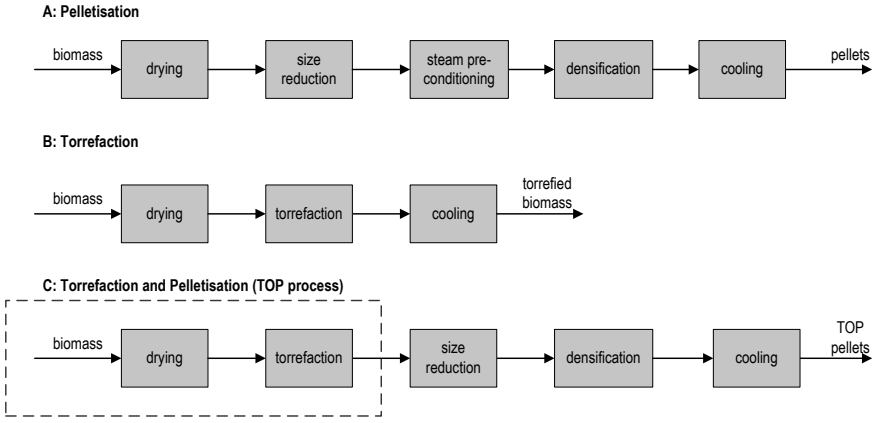


**Figure 3.9:** Pelletisation, torrefaction and the TOP process schemes [Bergman et al., 2006]

The $BO_2$ process combines torrefaction and pelletisation and according to Figure 3.9 torrefaction is introduced into the system as a unit after drying and before size reduction in comparison to a typical biomass pelletisation process. The torrefaction process consists of several steps such as drying, torrefaction and cooling. The pelletisation process comprises the steps of drying, size reduction, steam pre-conditioning, densification and cooling. Combining the torrefaction and pelletisation process leads to the introduction of torrefaction in the pelletisation step and the removal of the steam pre-conditioning from the pelletisation step.

### 3.3.2 Torrefaction and gasification

Torrefaction is mainly used as pre-treatment technology to upgrade the biomass to a higher quality bio-fuel. This biofuel can be used in other conversion methods to produce bio-energy. The main application of torrefied biomass (wood) is as a renewable fuel for combustion or gasification. [Prins et al., 2006a] studied the possibility of more efficient biomass gasification via torrefaction in different systems; air-blown circulating fluidized bed gasification of wood, wood torrefaction and circulating fluidized bed gasification of torrefied wood, and wood torrefaction integrated with entrained flow gasification of torrefied wood.

The main idea behind combining biomass torrefaction and gasification is that the heat produced during gasification in the form of steam is recovered for application in the torrefaction stage. The advantages of torrefaction as a pre-treatment prior to gasification in three concepts are compared with each other. In Figure 3.10 abc three different gasification schemes are presented.

- Figure 3.10a shows biomass (wood) gasification in circulating fluidized bed (CFB). The CFB gasifier is operated below 1000°C at atmospheric conditions to avoid problems with ash softening and melting. Air is used as gasifying medium. The steam is exported at 280°C at 45 bar.

- Figure 3.10b shows torrefied biomass (wood) gasification in an air-blown CFB gasifier. The volatile product is not used in the process. The acidic water can be condensed and the non-condensable gases combusted.

- Figure 3.10c shows torrefied biomass (wood) gasfication in an oxygen blown entrained flow gasifier. The torrefied wood is gasified at very high temperatures. At these high temperatures the volatiles will decompose into carbon monoxide and hydrogen. According to Prins et al. this method avoids the loss of organic material, because all product streams are effectively integrated in the gasification system and contribute to the production of syn-gas.

The processes were modeled with Aspen Plus, version 11 and the main interest was to estimate the effect of modifying the chemical composition prior to gasification Prins et al. The other assumptions used are:

- The mass and energy balances as shown in Table 3.1 are used as input for the simulation
- The torrefied wood is pulverized into particles of 100µm and the energy requirement for this is 10-20 kWe/MWth, this amounts value of 3% and 2.5% of the fuel for torrefaction at 250°C and 300°C.

- Cryogenic air separation is used with an electricity requirement of 380 kWh/ton oxygen.

- Operating temperatures of 950°C and 1200°C were assumed for CFB and EF gasification, respectively. The operating pressure was atmospheric.

- The hot product gases from the gasifier are quenched with cold product gas to a temperature of 800°C. Steam produced is partially used to provide heat for the torrefaction process.

In Figure 3.11 the overall gasification efficiency at varying gasification temperature for different process schemes on exergetic basis is shown; air-blown circulating fluidized bed gasification of wood, wood torrefaction and circulating fluidized bed gasification of torrefied wood, and wood torrefaction integrated with entrained flow gasification of torrefied wood. Compared to energy, exergy is not only taking the amount of energy into account, but also the quality of the energy. Exergy is the maximum work possible during a process. Energy is never destroyed, but exergy accounts for the irreversibility of a process that occurred due to a production of entropy.

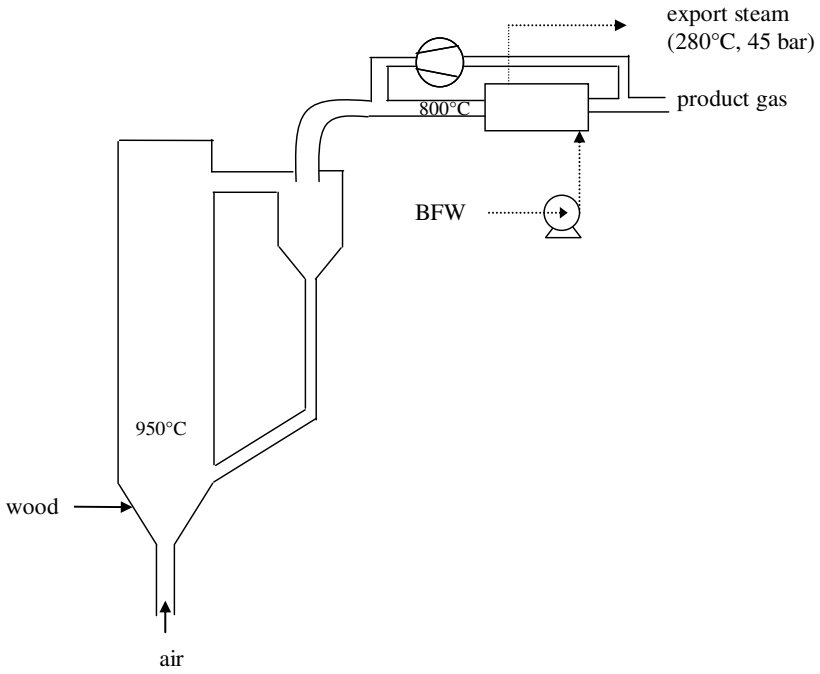


**(a)**

**Figure 3.10:** Gasification process schemes (a) Circulating Fluidized Bed gasification of wood, (b) wood torrefaction and CFB gasification of torrefied wood, (c) wood torrefaction integrated with EF gasification of torrefied wood

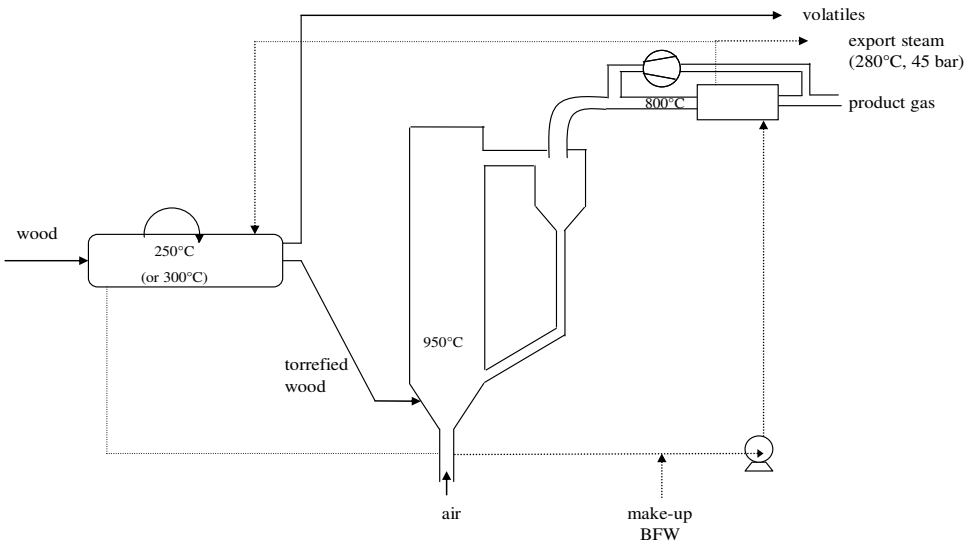
volatiles
export steam
(280°C, 45 bar)
800°C
product gas
wood
250°C
(or 300°C)
950°C
torrefied
wood
air
make-up
BFW
Torrefaction reactor
Circulating Fluidized
Bed gasifier
Heat Recovery /
Steam Generator

**(b)**

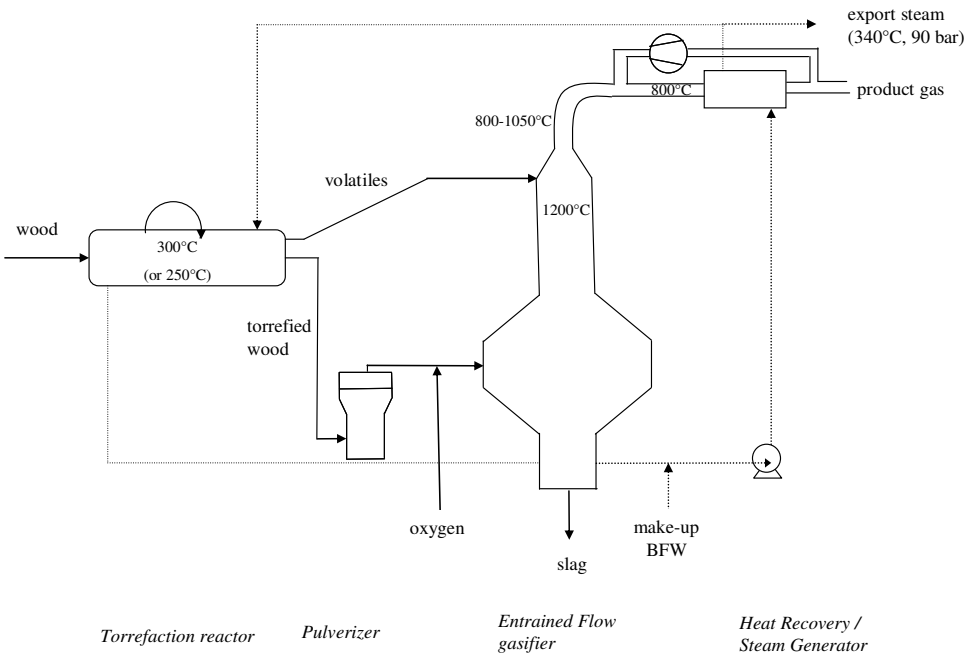
export steam
(340°C, 90 bar)
800°C
product gas
800-1050°C
volatiles
1200°C
wood
300°C
(or 250°C)
torrefied
wood
oxygen
slag
make-up
BFW
Torrefaction reactor
Pulverizer
Entrained Flow
gasifier
Heat Recovery /
Steam Generator

**(c)**

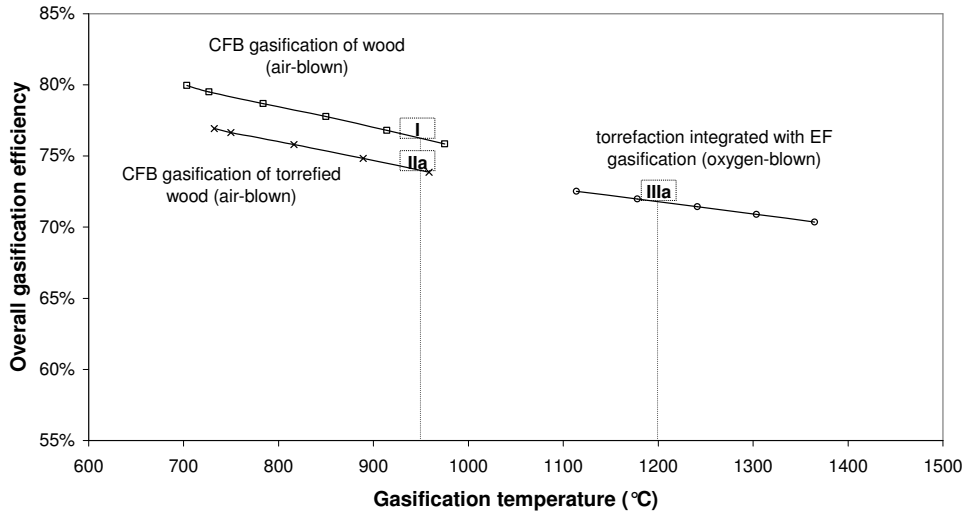


**(a)**

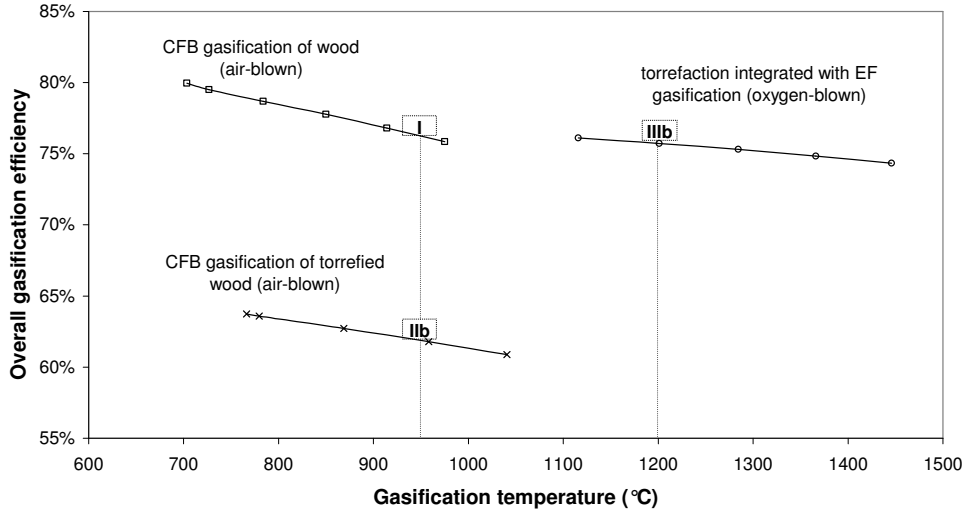


**(b)**

**Figure 3.11:** Overall gasification efficiency on exergetic basis at varying gasification temperature for different process schemes at a) 250°C torrefied wood and b) 300°C torrefied wood

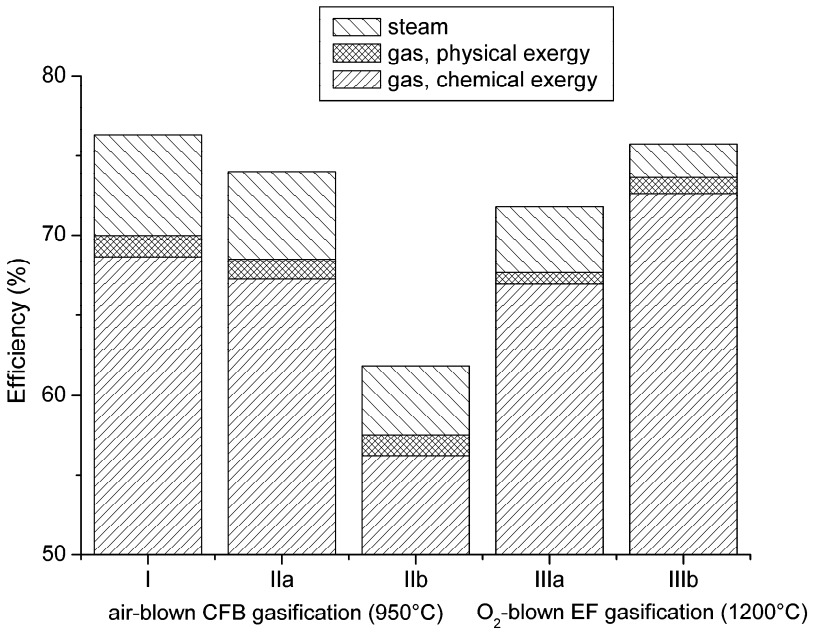


**Figure 3.12:** Exergetic efficiency of different process schemes, see also Figure 16 for the explanation of the cases

It is shown that the integration of torrefaction and gasification results into higher exergy efficiency than stand-alone gasification. Torrefaction integrated into gasification leads always to the usage of a bone-dry solid product in the gasifier which always leads to higher efficiencies. The overall efficiency of air-blown CFB gasification is lower for torrefied wood than for wood, especially at a high torrefaction temperature when a lot of energy is contained in the volatiles, which are not used in the process. Prins et al. concluded that "if the heat produced in the gasifier is used to drive the wood torrefaction reactions, the chemical exergy preserved in the product gas has been shown to increase provided that both torrefied wood and volatiles are introduced into the gasification process".

In Figure 3.12 the exergetic efficiency of different process schemes are shown. The efficiency is based on the exergy of product gas and steam relative to the exergy of the wood fuel. It is shown that overall efficiency comprises contributions

of the exergy of the steam, physical and chemical exergy of the product gas in relation to the input of the exergy of wood. Torrefaction at 300°C integrated with gasification at 1200°C conserves the highest amount of chemical exergy in the product gas, the maximum possible amount of work that can be provided by the substance itself. On the other hand physical exergy depends only on physical conditions that are pressure and temperature.

## 3.4 Economics

The torrefaction step represents an additional unit operation in the biomass utilization chain. The attendant capital and operating costs, as well as conversion losses are, however, off-set by savings elsewhere. The advantages of torrefaction are particularly pronounced for three applications at present, namely entrained flow gasification, small scale combustion using pellets and co-firing in pulverized coal fired power stations.

For small scale combustion applications, logistics and storage are the key areas where $BO_2$ pellets have a competitive advantage over ordinary first generation wood pellets. For the other two applications just listed grindability is of particular significance, as it is quite difficult to obtain the right particle size and properties with virgin biomass. Size reduction is also energy intensive, as is transportation of low density biomass over long distances.

Recent cost estimates [Bergman et al., 2007] for the ECN torrefaction technology indicate that the total capital investment of a stand-alone 75 ktonne/a plant will be in the range 6.1 to 7.3 M€. The assumed feedstock is wet softwood chips. The plant consists of a conventional rotary drum for drying the biomass, ECN torrefaction technology and conventional grinding equipment and pellet mill. No feedstock preparation (e.g. chipping) before drying was included

About 75 ktonne/a production rate (design), the total production costs are calculated at 37 €/tonne product (2.0 €/GJ), produced from a feedstock with 35% moisture content. At 50% and 25% moisture content this is about €/tonne (2.6 €/GJ) and 34 €/tonne (1.9 €/GJ) of product respectively. The moisture content is one of the most influential parameters of the torrefaction process as it predominantly determines the energy input of the process. These data represent the

added cost for the torrefaction process, assuming a zero cost of the feedstock. biomass, ECN torrefaction technology and conventional grinding equipment and pellet mill. No feedstock preparation (e.g. chipping) before drying was included

Table 3.4 summarises the main outcomes of an economic analysis performed for four cases comparing torrefied pellets (TOP) and conventional pelletisation. The main cost items shown are the total capital investment (TCI) and the total production costs (TPC). Although depreciation and financing are items contributing to the TPC, they are also summarised individually, as these items may be treated differently in discounted cash flow analyses.

Table 3.5 shows the importance of economy of scale for torrefaction technology. These economic characteristics clearly offer opportunities to achieve profitable biomass- to-energy chains.

A recent study [Zwart et al., 2005] also includes a comparison of torrefaction and another pre-treatment option for the production of liquid fuels via entrained flow gasification and Fischer-Tropsch. Its main conclusions are that pre-treatment significantly enhances the economic viability of synthetic transportation fuels, and that among the pre-treatment options studied, torrefaction has an edge over fast pyrolysis and conventional pelletisation. The main conclusion of the assessment of ten various biomass-to-liquids production routes is that overseas torrefaction is the most attractive pre-treatment technology. The additional investments related to this pretreatment step are less than the associated logistic cost reduction.

This view is supported by a study about pre-treatment technologies, and their effects on the international bioenergy supply chain logistics [Uslu et al., 2008]. It is indicated that torrefaction as pre-treatment technology seems a very promising option for minimizing logistic costs and energy use for long distance bio-energy transport. A chain analysis in this work including local biomass production, central gathering point where pretreatment takes place, export and import terminals and final conversion unit is considered. The final conversion methods considered were Fischer Tropsch (FT) fuels and power production by means of biomass integrated gasification combined cycle (BIGCC), combustion and co-firing.

**Table 3.4:** Economic performance characteristics of the pelletisation of sawdust and green wood (hardwood) for the conventional pelletisation process and the $BO_2$ process

| Item | unit | Conventional Pelletisation | $BO_2$ process | Conventional Pelletisation | $BO_2$ process |
|---|---|---|---|---|---|
| Feedstock | | Sawdust | Sawdust | Green wood | Green wood |
| Production rate | kton/a | 80 | 56 | 80 | 56 |
| Total Capital Investment* | M€ | 3.9 | 5.6 | 5.9 | 7.4 |
| Total production costs** | €/ton | 41 | 45 | 54 | 50 |
| | €/GJ | 2.6 | 2.2 | 3.4 | 2.5 |
| Financing | €/ton | 2.0 | 4.4 | 3.2 | 5.9 |
| Depreciation | €/ton | 4.0 | 8.8 | 6.5 | 11.7 |

*: including working capital of about 0.5 to 0.7 M€

**: Including cost items financing and depreciation

Capacities and costs are related to tonnages of product

**Table 3.5:** Economies of scale for torrefaction technology

| | 36 ktonne/a | 75 ktonne/a | 112 ktonne/a |
|---|---|---|---|
| Investment | 4.7 M€ | 6.7 M€ | 7.3 M€ |
| Total production costs | 3.1 €/GJ | 2.5 €/GJ | 1.6 €/GJ |

Energy crops produced in Latin America were transported to The Netherlands. The costs of delivering biomass in the form of $BO_2$ pellets and pellets is 3.3 €/GJ and 3.9 €/GJ, respectively. This includes the biomass source, transport and pre-treatment. Transportation of torrefied pellets is much cheaper than pellets. Delivering liquid energy carriers at an intermediate harbor is more expensive than solid torrefied pellets. The delivery costs of bio-oil vary between 4.7 and 6.6 €/GJ including biomass production, transportation, storage and pretreatment. Delivering power in the form of electricity costs at least 4.4 €/kWh from an existing cofiring plant and 4.6 €/kWh from a BIGCC.

It is also shown that economy of scale plays an important role in costs of pre-treatment. A torrefaction and pelletisation capacity of more than 40 MWth does not gain more on the economy of scale. On a scale of 19 MWth the delivery costs increase with 16%.

It is concluded that torrefaction in combination with pelletisation is the optimum supply chain from economic and energy efficiency perspective, $BO_2$ supply converted to FT-liquid is the optimal synfuel production chain and $BO_2$ supply converted to power either by BIGCC or existing co-firing facility are the optimal chains.

## 3.5 Conclusions

Some biomass properties, particularly high O/C ratios and difficulties to get small particle size, form problems for technological application of biomass. Torrefaction has the potential to become an important biomass pretreatment technology and so improve the biomass to a high quality solid fuel with good characteristics in energy density, homogeneity, grindability and hydrophobic behavior. The main advantage of torrefaction is improvement of energy density and grindability. Further research on kinetics is recommended to get data needed for reactor design in large scale. Also further research on the product characteristics is recommended. Characteristics such as pelletisation, biological degradation and dust forming of the solid biomass need more attention. It is shown that torrefaction offers efficiency advantage when used as a pretreatment step before entrained flow gasification.

## References

Arcate JR (2002). Torrefied wood, an enhanced wood fuel. Bioenergy 2002; Boise; Idaho; September 22-26

Arias B, Pevida C, Fermoso J, Plaza MG, Rubiera F, Pis JJ (2008). Influence of torrefaction on the grindability and reactivity of woody biomass. Fuel Processing Technology 89; 2; 169 - 175

Bergman PCA, Boersma, Kiel JHA, Prins MJ, Ptasinski KJ, Janssen FJJG (2004). Torrefaction for entrained flow gasification of biomass. Report ECN-RX—04-046; ECN Petten; The Netherlands

Bergman PCA (2005). Combined torrefaction and pelletisation: the TOP process. Report ECN-C—05-073; ECN Petten; The Netherlands

Bergman PCA, Boersma, AR, Zwart RWR, Kiel JHA (2005). Torrefaction for biomass co-firing in existing coal-fired power stations "Biocoal". Report ECN-C--05-013, 2005, ECN, Petten, The Netherlands

Bergman PCA, Boersma AR, Kiel JHA (2007). Torrefaction for biomass conversion into solid fuel. 15th European Biomass Conference and Exhibition ICC Berlin; Germany; 7 – 11 May 2007

Bourgeois J, Guyonnet R (1988). Characterization and analysis of torrefied wood. Wood Science and Technology 22; 2; 143 – 155

Bourgeois J, Bartholin MC, Guyonnet R (1989). Thermal treatment of wood: analysis of the obtained product. Wood Science and Technology 23; 4; 303 – 310

Bridgeman TG, Jones JM, Shield I, Williams PT (2008). Torrefaction of reed canary grass, wheat straw and willow to enhance solid fuel qualities and combustion properties. Fuel 87; 6; 844 - 856

Felfli FF, Luengo CA, Suarez JA, Beaton PA (2005). Wood briquette torrefaction. Energy for Sustainable Development 9; 3; 19 - 22

Ferro TD, Vigouroux V, Grimm A, Zanzi Z (2004). Torrefaction of Agricultural and Forest Residues. Cubasolar; Guantanamo; Cuba; April 12 – 16 2004

Hakkou M, Petrissians M, Gerardin P, Zoulalian A (2006). Investigations of the reasons for fungal durability of heat-treated beech wood. Polymer Degradation and Stability 91; 2; 393 - 397

Hermann WA (2006). Quantifying global exergy resources. Energy 31; 12; 1685 - 1702

Indian Institue of Science (2006). Project completion on torrefaction of bamboo

Internation Energy Agency (2006). World Energy Outlook 2006

Li J, Gifford J (2001). Evaluation of woody biomass torrefaction. Forest Research; Roturua; New Zealand

Pach M, Zanzi Z, Bjornbom E (2002). Torrefied biomass a substitute for wood and charcoal. 6th Asia-Pacific International Symposium on Combustion and Energy Utilization

Pels JR, Bergman PCA (2006). Torwash: proof of principle. Report ECN-E--06-021; ECN Petten; The Netherlands

Pentananunt R, Rahman ANMM, Bhattacharya SC (1990). Upgrading of biomass by means of torrefaction. Energy 15; 12; 1175 – 1179

Prins MJ (2005). Thermodynamic analysis of biomass gasification and torrefaction. PhD Thesis; Technische Universiteit Eindhoven; The Netherlands

Prins MJ, Ptasinski KJ, Janssen FJJG (2005). Energy and exergy analyses of the oxidation and gasification of carbon. Energy 30; 7; 982 – 1002

Prins MJ, Ptasinski KJ, Janssen FJJG (2006a). More efficient biomass gasification via Torrefaction. Energy 31; 15; 3458 - 3470

Prins MJ, Ptasinski KJ, Janssen FJJG (2006b). From coal to biomass gasification via torrefaction. Energy 32; 7; 1248 - 1259

Prins MJ, Ptasinski KJ, Janssen FJJG (2006c). Torrefaction of wood Part: 1. Weight loss kinetics. Journal of Analytical and Applied Pyrolysis 77; 1; 28-34

Prins MJ, Ptasinski KJ, Janssen FJJG (2006d). Torrefaction of wood Part: 2. Analysis of products. Journal of Analytical and Applied Pyrolysis 77; 1; 35-40

Rousset P, Perre P, Girard P (2004). Modification of mass transfer properties in poplar wood by a thermal treatment at high temperature. Holz als Roh- und Werkstoff 62; 2; 113 - 119

Sundqvist B, Karlsson O, Westermark U (2006). Determination of formic-acid and acetic acid concentrations formed during hydrothermal treatment of birch wood and its relation to colour, strength and hardness. Wood Science and Technology 40; 7; 549 – 561

Tjeerdsma BF, Boonstra M, Pizzi A, Tekely P, Militz H (1998). Characterisation of thermally modified wood: molecular reasons for wood performance improvement. Holz als Roh- und Werkstoff 56; 3; 149 – 153

Uslu A, Faaij A, Bergman PCA (2008). Pre-treatment technologies, and their effect on international bioenergy supply chain logistics. Techno-economic evaluation of torrefaction, fast pyrolysis and pelletisation. Energy 33; 8; 1206 – 1223

Weststeyn A (2004). First torrefied wood succesfuylly co-fired, PyNe Newsletter Issue 17

Windeisen E, Strobel C, Wegener G (2007). Chemical changes during the production of thermo-treated beech wood. Wood Science and Technology 41; 6; 523 – 536

Zwart RWR, Boerrigter H, Van Der Drift A (2006). The impact of biomass Pretreatment on the feasibility of overseas biomass conversion to Fischer-Tropsch Products. Energy & Fuels 20; 5; 2192 – 2197

# Chapter 4

## Mechanistic pathway for biomass decomposition during torrefaction at isothermal conditions


### Abstract

*This chapter describes the weight loss kinetics of biomass composition during torrefaction at isothermal conditions between 220 - 300°C for several biomass resources and its constituents such as beech, willow, spruce, straw, hay, bagasse, refuse derived fuel, xylan (hemicellulose), cellulose and (alkali lignin). Four different models are studied and validated for the thermal decomposition of beech wood. Also a causal model, which takes into account the effect of the reactor temperature and the biomass particle temperature on the biomass weight loss, is developed. It is shown that a model that describes the decomposition of biomass via two independent phases is an accurate decomposition mechanism.*

## 4.1 Introduction

Kinetic modelling produces advanced computational tools for the design and optimization of chemical reactors applied for thermo chemical conversion of biomass. The knowledge of the fuel reactivity is also needed for the formulation of simple design and scaling results.

The main principle of torrefaction is based on the reactivity of hemicellulose. The other two components (cellulose and lignin) are less reactive in the temperature range 200-300°C. Low stability organic compounds that are highly volatile at low temperatures such as most of the food contain an extended amount of starch [Heikkinen et al., 2004]. Due to these different fractions biomass can decompose in different ways under various conditions. Biomass torrefaction can be subdivided into four stages: moisture evaporation, hemicellulose decomposition, lignin decomposition and cellulose decomposition [Bergman et al., 2005].

Volatilization forms the major step in any thermo chemical conversion process involving biomass materials due to the fact that biomass materials comprise about 80% volatile fractions and 20% solid carbonaceous residue, namely char and ash, respectively [Gaur & Reed, 1998]. Torrefaction of biomass involves several reactions, which makes it a complex mechanism. Decomposition of biomass is actually a set of reactions taking place at the same time and these reactions can be analysed with complex kinetic models.

Knowledge of the torrefaction of the three main components cellulose, hemicellulose and lignin is important to get a fundamental base of understanding of torrefaction. If the temperature is increased to 200°C hemicellulose starts limited volatilization and carbonization (the biomass starts to become brown). Hemicellulose decomposes into volatiles and a char-like solid product. Extensive devolatilisation occurs when a temperature around 250 – 260°C is reached. In this temperature range also lignin and cellulose slightly decompose, which do not lead to a significant mass loss.

[Ferro et al., 2004] mentions that after drying at 100°C further heating removes chemically bound water due to evaporation and decomposition reactions, which occurs at temperatures over 160°C. At this temperature also the formation of $CO_2$

starts. While various biomass resources consist of various fractions of hemicellulose, lignin and cellulose a variation in reactivities can be found among these resources. [Bergman et al., 2005] states that even the reactivity of hemicellulose very much depends on its molecular structure so that a large difference is observed between deciduous and coniferous wood. Torrefaction of deciduous wood leads to more devolatilisation and carbonization than torrefaction of coniferous wood [Prins et al., 2006a].

Recently, [Prins et al., 2006a] described the weight loss kinetics of wood (willow) torrefaction with a model based on a two step reaction in series. The model is developed by Di Blasi and Lanzetta for the thermal decomposition of xylan [Di Blasi & Lanzetta, 1997]. It is shown that the model can describe accurately the weight loss kinetics for torrefaction between 230 - 300°C. Finally, Prins concluded that the first step to form an intermediate product is much faster than the formation of the final char. It is not known what the chemical structure and formula of this intermediate product is. The final elemental composition of the solid product is studied [Prins et al., 2006b].

A schematic representation of this Di Blasi model is shown in Figure 4.1 (model ii). Typical information about the torrefaction kinetics is reported by Prins et al. Biomass “A” decomposes in an intermediate product “B” which remains undefined and volatiles “V1” are formed. This intermediate product decomposes in a final char “C” and other volatiles “V2”. For the two decomposition steps activation energies of 76.0 and 151.7 kJ/mol, respectively, and pre-exponentional factors of $2.48 \times 10^{4}$ and $1.10 \times 10^{10}$ kg $kg^{-1}$ $s^{-1}$, respectively, were found for willow wood used as biomass resource. Di Blasi found activation energies of 76.0 and 143 kJ/mol for the decomposition steps [Di Blasi & Lanzetta, 1997].

[Repellin et al., 2010] modelled the anhydrous weight loss of beech and spruce chips during torrefaction in a pilot kiln. Three phenomenological models are applied to study the effect of torrefaction temperature and reaction time on the weight loss after 5, 20, 40 and 60 minutes. A simple global one step model, the Di-Blasi Lanzetta model and a third model by Rousset [Rousset, 2004] were used to describe the kinetics. They all showed good correlations between experimental and

calculated anhydrous weight loss. It is shown that the anhydrous weight loss took place in the first 20 minutes of torrefaction.

In this chapter, four different biomass decomposition models are presented to describe the isothermal weight loss kinetics; a general one step model, a two step reactions in series model, a two competitive reactions model and two parallel reactions model. Since it is the goal to describe the reaction kinetics at isothermal conditions a solution is presented for the stage in which the biomass heats up by the application of a causal model. This model describes the effect of the reactor temperature on the particle temperature and the effect of the particle temperature on the mass loss.

## 4.2 Biomass decomposition models applied for torrefaction

### 4.2.1 Model selection and description

In Chapter 2 the models that describe the pyrolysis reactivity and kinetics have been studied extensively. It is seen that there are two approaches to describe the mass loss. These approaches are based on a single homogeneous fuel or based on the three biomass constituents hemicellulose, cellulose and lignin. Also an overview is presented about commonly used models. In this paragraph the four models that have been selected for the modelling of biomass torrefaction are discussed, namely

- *model i*: a general one step model in which all reactions take place at once producing volatiles and a chemically changed solid. Only one phase "A" reacts during the torrefaction. This single phase can be the biomass as a whole or a constituent of the biomass.

- *model ii*: two reaction steps follow each other in series resulting in two (different) volatile phases. One solid phase reacts and an intermediate product is formed. This solid intermediate product "B" is a chemically changed solid that reacts further to produce a final solid char. This model is also proposed by [Di Blasi and Lanzetta , 1997]. In the Di Blasi model component "A" is defined as xylan. [Prins et al., 2006b] defined component "A" as willow wood.

- *model iii*: two reactions compete with each other to form a chemically modified solid product leading to two different phases. This single reacting phase can be the biomass or a constituent of the biomass.

- *model iv*: two different phases or constituents of the biomass react independently of each other to form a chemically changed solid product. For example hemicellulose and cellulose decompose during biomass torrefaction.

The models are a simplification of the real reaction mechanisms, because the structure of biomass is complex. This complex structure means that during the decomposition of biomass feedstocks during torrefaction different sets of reactions can occur at the same time. To keep the modelling of biomass decomposition controllable these four models are proposed. Different variations between and within the models can be thought about, but will make the modelling even more complicated. An example is that a combination of models ii and iv will automatically lead to three phases that react. Another possibility that can be proposed is the formation of volatiles "$V_2$" also out of solid phase "$A_1$" in model iv.

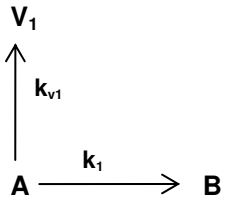


$K_1 = k_1 + k_{v1}$

Model i : Single step

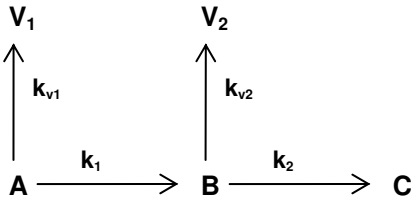


$K_1 = k_1 + k_{v1}$

$K_2 = k_2 + k_{21}$

Model ii : Successive reactions

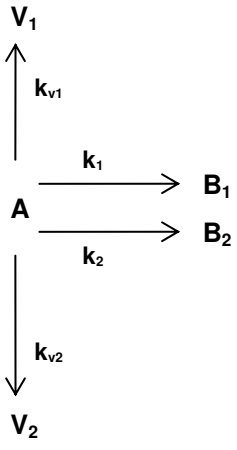


$K_1 = k_1 + k_{v1}$

$K_2 = k_2 + k_{v2}$

Model iii : Two competitive reactions

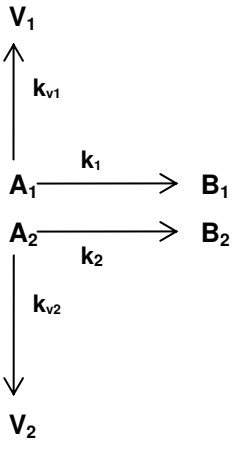


$K_1 = k_1 + k_{v1}$

$K_2 = k_2 + k_{v2}$

Model iv : Two parallel reactions

**Figure 4.1:** Different biomass decomposition models as applied in the evaluation of torrefaction weight loss kinetics between 220 - 300°C under inert conditions

### 4.2.2 Model equations and assumptions

Kinetics provides the framework for describing the rate at which a chemical reaction occurs and enables us to relate the rate to a reaction mechanism that describes how the molecules react via intermediates to the eventual product [Chorkendorff & Niemantsverdriet, 2003]. Kinetic models for the pyrolysis of biomass are often based on the Arrhenius law which describes the temperature dependence of the reaction rate. In order for the reaction to occur, the reactant molecules must become activated and there exists equilibrium between normal and activated molecules. In this part the four mechanistic models are explained with the equations and the assumptions.

Model i: Global one step

For each of the four mechanistic models, the reactivity equations of the different reactive phases can be derived. It is assumed that biomass reacts in sets of reactions since thermo chemical conversion of biomass comprises many different reactions. The reactivity rates and balances for model i are:

$$r_A = \frac{\partial A}{\partial t} = -K_1 A^{n_A} \tag{4.1}$$

$$r_B = \frac{\partial B}{\partial t} = k_1 A^{n_A} \tag{4.2}$$

In the reaction rate equation all reactions are assumed to be first order in A so the system of equations can be solved. If the mass balance for the total solid residue is solved by integration of the differential equations for the reaction rate, the following expression for the total relative mass loss is derived for the global one step reaction mechanism.

$$M = A + B \tag{4.3}$$

$$\frac{M_v}{M_0} = \left(1 - \frac{k_1}{K_1}\right)\left(1 - e^{-K_1 t}\right) \tag{4.4}$$

This expression to describe the mass loss can be simplified into an equation that describes the model phenomenologically. With this simplification the model becomes dependent on parameters that represent a (maximum) amount of a specific phase/group that can react and a parameter that has the characteristic of an activation energy. In the equation (4.5) these are parameters "*a*" and "*b*". So, the global one step model can be described with the following simplified expression:

$$\frac{M_v}{M_0} = a \cdot \left(1 - e^{-bt}\right) \tag{4.5}$$

Model ii : Two steps in series

The reaction rates and balances for model ii are:

$$r_A = \frac{\partial A}{\partial t} = -\left(k_1 + k_{v1}\right)A^{n_A} \tag{4.6}$$

$$r_B = \frac{\partial B}{\partial t} = k_1 A^{n_A} - \left(k_2 + k_{v2}\right)B^{n_B} \tag{4.7}$$

$$r_C = \frac{\partial C}{\partial t} = k_2 B^{n_B} \tag{4.8}$$

In the reaction rate equation all reactions are assumed to be first order in "A" and "B". If the mass balance for the total solid residue is solved by integration of the differential equations for the reaction rate, the following expression for the total relative mass loss is derived for the two steps in series reaction mechanism.

$$M = A + B + C \tag{4.9}$$

$$\frac{M_v}{M_0} = 1 - \left(1 + \left[\frac{k_1 K_1 - k_1 k_2}{K_1 (K_2 - K_1)}\right]\right) e^{-K_1 t} - \left[\frac{-k_1 K_2 + k_1 k_2}{K_2 (K_2 - K_1)}\right] e^{-K_2 t} - \frac{k_1 k_2}{K_1 K_2} \tag{4.10}$$

Like the simplification that has been carried out to derive equation (4.5) the same simplification can also be applied to a model that represents the reaction of two different phases. These components are mentioned *"a"* and *"b"* for a single reactive phase in the reaction process and for a second reactive phase "*c"* and *"d"*. This expression to describe the mass loss can be simplified into a simple equation that describes the model phenomenological, which is the same as:

$$\frac{M_v}{M_0} = a \cdot \left(1 - e^{-bt}\right) + c \cdot \left(1 - e^{-dt}\right) \tag{4.11}$$

Model iii : Two competitive reactions

The differential rate equations for the two competitive reactions are:

$$r_A = \frac{\partial A}{\partial t} = - K_1 \, A^{n_A} \tag{4.12}$$

$$r_{B_1} = \frac{\partial B_1}{\partial t} = k_1 \, A^{n_B} \tag{4.13}$$

$$r_{B_2} = \frac{\partial B_2}{\partial t} = k_2 \, A^{n_B} \tag{4.14}$$

In the reaction rate equation all reactions are assumed to be first order in A, $B_1$ and $B_2$. If the mass balance for the total solid residue is solved by integration of the differential equations for the reaction rate, the following expression for the total relative mass loss is derived for the two competitive one step reaction mechanisms.

$$M = A + B_1 + B_2 \tag{4.15}$$

$$\frac{M_v}{M_0} = \left(1 - \frac{k_1 + k_2}{K_1 + K_2}\right)\left(1 - e^{-(K_1 + K_2)t}\right) \tag{4.16}$$

This expression to describe the mass loss can be simplified into a simple equation that describes the model phenomenological. Also the two competitive one step reaction model can be described with the following simplified expression resulting in the same expression as for the global one step model:

$$\frac{M_v}{M_0} = a \cdot \left(1 - e^{-bt}\right) \tag{4.5}$$

Model iv : Two parallel reactions

The differential rate equations for model iv are:

$$r_{A_1} = \frac{\partial A_1}{\partial t} = -K_1 \, A_1^{n_A} \tag{4.17}$$

$$r_{B_1} = \frac{\partial B_1}{\partial t} = k_1 \, A_1^{n} \tag{4.18}$$

$$r_{A_2} = \frac{\partial A_2}{\partial t} = - K_1 A_2{}^{n_A} \tag{4.19}$$

$$r_{B_2} = \frac{\partial B_2}{\partial t} = k_2 \ A_2{}^{n_A} \tag{4.20}$$

In the reaction rate equation all reactions are assumed to be first order in $A_1$, $A_2$, $B_1$ and $B_2$. If the mass balance for the total solid residue is solved by integration of the differential equations for the reaction rate, the following expression for the total relative mass loss is derived for the two competitive one step reaction mechanisms.

$$M = A_1 + A_2 + B_1 + B_2 \tag{4.21}$$

In the reaction rate equation all reactions are assumed to be first order in A. If the mass balance for the total solid residue is solved by integration of the differential equations for the reaction rate, the following expression for the total relative mass loss is derived for the two parallel one step reaction mechanisms.

$$\frac{M_v}{M_0} = 1 - \frac{A_{1_0}}{A_{1_0} + A_{2_0}} \left( e^{-K_1 t} \left( 1 - \frac{k_1}{K_1} \right) + \frac{k_1}{K_1} \right) - \frac{A_{2_0}}{A_{1_0} + A_{2_0}} \left( e^{-K_2 t} \left( 1 - \frac{k_2}{K_2} \right) + \frac{k_2}{K_2} \right) \tag{4.22}$$

This expression to describe the mass loss can be simplified into a simple equation that describes the model phenomenologically, which is the same as:

$$\frac{M_v}{M_0} = a \cdot \left( 1 - e^{-bt} \right) + c \cdot \left( 1 - e^{-dt} \right) \tag{4.11}$$

This makes clear that effect of two parallel one step reactions is the same as the result of the summation of two one step reactions. The mathematics of model ii and iv can also be developed into a two step mechanism with a linear term. The second exponential is developed into the first term of the series.

$$\frac{M_v}{M_0} = a \cdot \left(1 - e^{-bt}\right) + c \cdot t \tag{4.23}$$

Model during heating up with causal effects

This part is concerned with the interactions between heat transfer during biomass torrefaction and its kinetics. It may contribute to the development of simple models to describe the torrefaction of (single) biomass particles and so create a better understanding of the influence of reaction time and temperature on the product quality.

According to [Pyle & Zaror, 1984], who studied the heat transfer and kinetics in the low temperature pyrolysis of solids; it is doubtful whether tractable models can be developed to incorporate all the features of pyrolysis since the process depends on a wide range of factors including particle size, heating rate and retention time at different temperatures. Torrefaction is a technology that can be compared with pyrolysis although the temperature is lower and the focus is on a high quality solid fuel. In the technology of torrefaction heat is applied to biomass particles with different particle size. During this process two effects occur. These are the heating up of the biomass and reactions that stimulate volatilization; the release of mass destructs the biomass structure and stimulates the increase of the energy density.

In kinetic analysis it is difficult to separate the effects of chemistry and heat- and mass transport phenomena [Di Blasi, 2008]. These two effects need to be separated from each other to get a good insight in the rate and influence of both effects. Below a description is given how this is achieved. It is important to keep in mind that the heating up of a biomass particle is a function of time and that the reactivity is a function of temperature and time. In other words, the heating of a particle has effect on the reactivity of the biomass. This principle is called a causal effect which means that one parameter has influence on another effect.

An effect $f_n\ (t)$ is not constant in time during a process changing in time so we should find an expression for $F_n\ (t)$ as a function of time and the sum of the different effects $f_n\ (t)$ on $F_n\ (t)$. Therefore we divide the time in which a process is supposed to be changed between time intervals and supposed to be constant during the intervals and given by $f_n(t)$. Below the basic equations are described [Veringa, 1981].

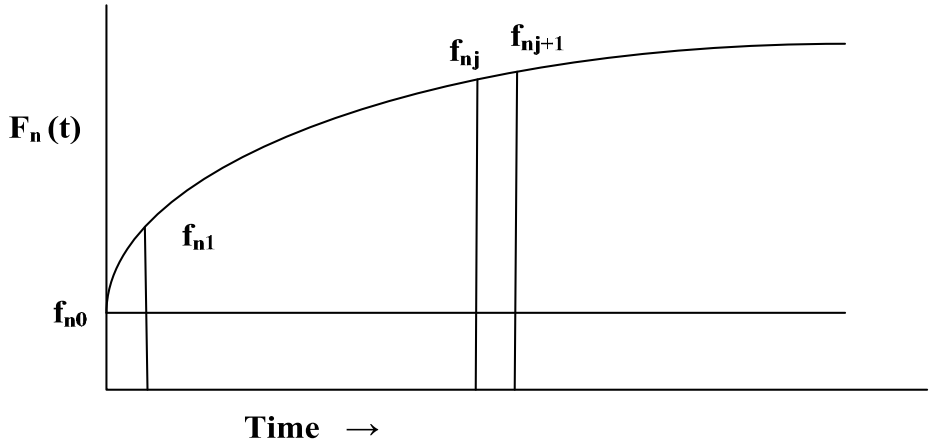


**Figure 4.2:** the effect $F_n$ in a filament approached by a cummulative step function $f_{nj+1} - f_{nj}$

For each interval a relaxation effect occurs which is given by:

$$\frac{d\left(F_n(t)\right)}{dt} = \frac{f_n(t)}{\tau}\exp\left(-\frac{t}{\tau}\right) \tag{4.24}$$

For the contribution of the $j^{th}$ time interval at time t and during $\Delta t$, it follows that:

$$\Delta F_n(t)_j = \frac{1}{\tau}\Delta_j f_n(t)\int_{j\Delta t}^{t}\exp\left(-\frac{1}{\tau}\left(t' - j\Delta t\right)\right)dt' \tag{4.25}$$

with

$$\Delta_j f_n(t) = f_n(t)_j - f_n(t)_{j-1} \tag{4.26}$$

and

$$\Delta_0 f_n(t) = f_n(t)_0 \tag{4.27}$$

so that

$$F_n(t) \equiv \lim_{N\to\infty} \sum_{j=0}^{N} \Delta F_n(t)_j = \lim_{N\to\infty} \sum_{j=0}^{N} \frac{1}{\tau} \Delta_j f_n(t) \int_{j\Delta t}^{t} \exp\left(-\frac{1}{\tau}\left(t' - j\Delta t\right)\right) dt' \tag{4.28}$$

which is

$$F_n(t) \equiv \frac{\exp\left(\frac{-t}{\tau}\right)}{\tau} \int_0^t f_n(t) \exp\left(\frac{t'}{\tau}\right) dt' \tag{4.29}$$

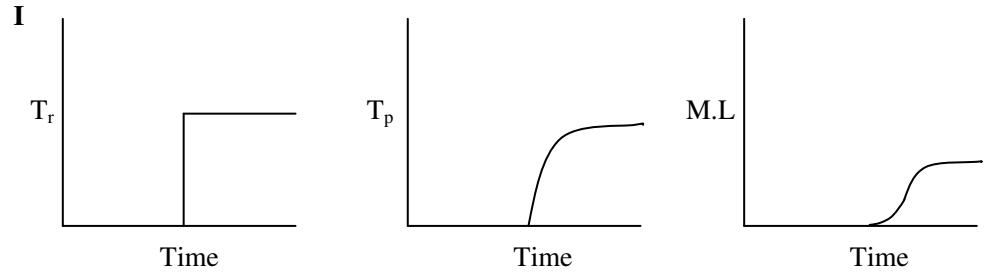


**Figure 4.3:** Causal effects during the heating up of biomass for situation I which means a infinite step wise heating up curve of the reactor ($T_r$) with effects on the biomass particle temperature ($T_p$) that causes a certain mass loss (M.L.)

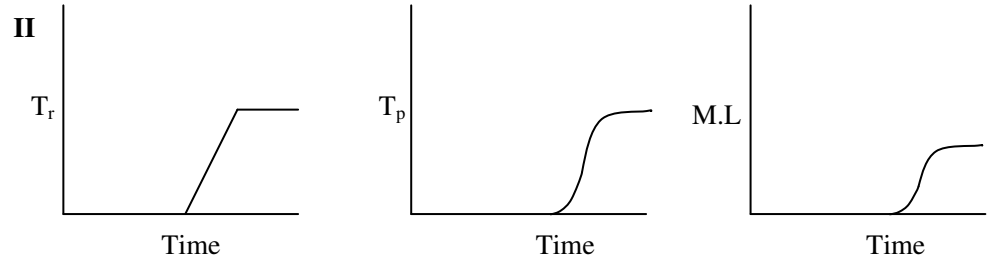


**Figure 4.4:** Causal effects during the heating up of biomass for situation I which means a linear heating up curve of the reactor ($T_r$) whict effects the biomass particle temperature ($T_p$) that causes a certain mass loss (M.L.)

This causal effect can be translated to the mass loss experiments carried out by TGA experiments. During TGA the apparatus is heated up to its final reactor temperature ($T_r$). This reactor temperature influences the heating up of the biomass particle ($T_p$) which causes thermal degradation of the biomass (M.L.) These causal effects for two situations I and II can be explained with a figure and described by related mathematical relations. The two situations can also be visualized by Figure 4.3 and Figure 4.4.

The two situations describe different heating profiles that can be applied to heat to desired torrefaction temperature and causal effects that follow as heating the biomass particle and the mass loss that occurs, because of the heat that is applied and the particle temperature that is reached.

The mathematics for both situations is described by the following equations:

- Equation $f_0$ describes the reactor temperature $T_{r,}$
- Equation $f_1$ describes the biomass particle temperature $T_p$
- Equation $f_2$ describes the thermal degradation/mass loss M.L.

Situation I is an imaginary situation in which an infinite heating rate step is applied to heat up to the desired torrefaction temperature; this is described with formula $f_0(T,t)^I$. The effects of heating up the biomass particle which is defined with function $f_1(T,t)^I$ and the mass loss defined with function $f_2(T,t)^I$ that occurs if biomass is torrefied between 200 and 300°C will follow the effect of the infinite heating rate step. Function $f_1(T,t)^I$ can also be applied to describe the mass loss if a constant temperature is reached after situation $f_2(T,t)^{II}$ has been . The final result is the same as the parameters "$a_1$" is substituted with "$a_2$".

Situation II is a more realistic situation in which a dynamic heating rate α is applied to achieve a specific torrefaction temperature, which is described with function $f_0(T,t)^{II}$. The heating rate α influences the functions for the heating profile of the biomass particle and for the mass loss during torrefaction. This can be seen in the extra terms that arise in functions $f_1(T,t)^{II}$ and $f_2(T,t)^{II}$.

Situation I

The reactor is heated up with a infinite stepwise heating pattern which can be described with:

$$f_0^I(T,t) = \int_{-\infty}^{t} \delta(t' - t_0)dt' \tag{4.30}$$

This heating up of the reactor results into a temperature increase of the biomass particle. The effect on the temperature of the biomass particle is described by:

$$f_1^I(T,t) = \left(1 - e^{-a_1 t}\right) \tag{4.31}$$

If the biomass heats up to torrefaction temperature biomass decomposition occurs. The effect on the mass loss of the biomass is described by the following functions:

$$f_2^I(T,t) = e^{-a_2 t}\int_0^t \left(1 - e^{-a_1 t'}\right) e^{a_2 t'} a_2 dt' = \tag{4.32a}$$

$$e^{-a_2 t}\left[e^{a_2 t}\right]_0^t - \frac{a_2}{a_2 - a_1} e^{-a_2 t}\left[e^{(a_2 - a_1)t}\right]_o^t = \tag{4.32b}$$

$$\left[1 - e^{-a_2 t}\right] - \frac{a_2}{a_2 - a_1}\left[e^{-a_1 t} - e^{-a_2 t}\right] \tag{4.32c}$$

This equation (4.32c) is symmetric in *"$a_1$"* and *"$a_2$"*, so does not matter which of the two parameters is connected to temperature relaxation or the subsequent mass release.

Situation II:
The reactor is heated up with a linear heating pattern with heating rate α which can be described with the following formula:

$$f_0^{II}(T,t) = \alpha t \tag{4.33}$$

This heating up of the reactor results into a temperature increase of the biomass particle. The effect on the temperature of the biomass particle is described by:

$$f_1^{II}(T,t) = e^{-a_1 t}\int_0^t f_0(T,t) a_1 e^{a_1 t} dt = \alpha t - \frac{\alpha}{a_1}[1 - e^{-a_1 t}] \tag{4.34}$$

If the biomass heats up to torrefaction temperature biomass decomposition occurs. The effect on the mass loss of the biomass is described by the following functions:

$$f_2^{II}(T,t) = e^{-a_2 t}\int_0^t (f_1(T,t))e^{a_2 t'} a_2 dt' = \tag{4.35a}$$

$$e^{-a_2 t}\int_0^t \alpha t e^{a_2 t'} a_2 dt' - e^{-a_2 t}\int_0^t \frac{\alpha}{a_1}[1-e^{-a_1 t'}]e^{a_2 t'} a_2 dt' = \tag{4.35b}$$

$$\alpha t - \frac{\alpha}{a_2}[1-e^{-a_2 t}] - \frac{\alpha}{a_1}\left([1-e^{-a_2 t}] - \frac{a_2}{a_2-a_1}[e^{-a_1 t} - e^{-a_2 t}]\right) \tag{4.35c}$$

This equation (4.35c) is symmetric in *"$a_1$"* and *"$a_2$"*, so does not matter which of the two parameters is connected to temperature relaxation or the subsequent mass release.

## 4.3 Experimental

### 4.3.1 Materials

Different biomass types have been treated isothermal by thermogravimetry between 200 - 300°C: beech, oregon, spruce, willow, straw, xylan (model compound for hemicellulose) and cellulose. The materials were obtained from the Energy Research Centre Netherlands (ECN). The biomass was grinded into small particles and the sizes were < 250 μm.

### 4.3.2 Equipment and procedure

The thermal analysis has been carried out with a TA Instruments Q500 Thermogravimetric analyzer with autosampler. The heating rate can be varied between 0.1 and 100°C, the weighing precision is 0.1μg and the isothermal temperature precision is 0.1°C.

The TGA experiments were carried out in an inert atmosphere with a nitrogen flow rate of 20 ml/min. The several biomass sample weights varied from 3 to 10 mg. The temperature range varied from 220 to 300°C. The heating procedure started with a dynamic heating rate of 10°C/min until 105°C to evaporate the moisture in an isothermal stage of 15 min. After drying, the biomass was heated with a dynamic heating rate of 10°C/min. The final torrefaction temperature is between 220 and 300°C. An isothermal heating period of two hours was applied at the final isothermal temperature. Table 4.1 summarizes the experimental conditions used to investigate the kinetics in this chapter.

If the heating rate is too high, the results may be affected by heat transfer limitations within the sample. If a too low heating rate is applied, the weight loss that occurs during the warming up phase is not negligible, which complicates the interpretation of kinetic data [Di Blasi & Lanzetta, 1997]. The weight loss kinetics is corrected to avoid variations in ash and moisture content, on dry and ash free basis.

$$\left(\frac{M_t}{M_0}\right)_{\exp} = \left(\frac{W_{TGA} - W_{ash}}{W_{initial} - W_{ash}}\right) \tag{4.36}$$

Where $W_{initial}$ is the solid weight of the dry sample, $W_{ash}$ the weight of the ash in the dry sample and $W_{TGA}$ is the solid weight that is measured as a function of time. According the definition torrefaction starts at 200°C, so $W_{initial}$ is the solid weight at this temperature [Bergman et al., 2005]. It is possible that there is mass loss below this temperature, but it will only be a few weight percentages. This loss can be ascribed to residual bound water that is released.

**Table 4.1:** Experimental conditions during the TG experiments

| | |
|---|---|
| Instrument | TA Instruments Q500 |
| Temperature | 220 - 300°C |

| | |
|---|---|
| Biomass types | Beech, Oregon, Spruce<br>Willow, straw, xylan<br>Cellulose, (Alkali)<br>Lignin |
| Gas flow rate | 20 ml/min nitrogen |
| Sample size | 3 - 10 mg |
| Particle size | < 250 μm |

## 4.4 Results

### 4.4.1 Thermogravimetry experiments

Figure 4.5 - Figure 4.12 show the mass loss of the biomass materials beech, oregon, spruce, willow, straw, xylan, cellulose and (alkali) lignin between 220 - 300°C. The mass loss is observed from 200°C at which a dynamic heating rate is applied of 10°C/min until the desired final isothermal temperature conditions. Torrefaction starts according the definition at 200°C, but below this temperature already a few percents of mass loss occurred. The thermogravimetry experiments show the fraction of the organic phase that can react at a specific temperature and show the ratio between the solid and volatile phase. It is a simple method to determine what can be expected from the mass loss. The mass loss is an important indicator in torrefaction technology, because it is one parameter that determines what the result will be on the energy densification in the torrefied biomass. Other techniques are necessary to determine what happens with the energy balance.

It is shown that all biomass resources have their highest decomposition rate in the first ten minutes. These first ten minutes describe the mass loss during the heating up of the TGA apparatus and the biomass from 200°C to the final torrefaction temperature which is maximum 300°C. During heating to 300°C already a mass loss around 25% for most of the wood feedstocks can occur. The mass loss of xylan in this interval can be even higher and results in an organic weight loss of around 40%. It can be concluded that the xylan is the most reactive component in the stage that the biomass heats up, but the fixed carbon content of the xylan is higher than that of all the wood feedstocks at 300°C. On the other hand cellulose reactivity is small in the lower temperature regime, but temperatures above 280°C

show that the maximum reactivity of the cellulose is higher than all the other feedstocks. It is shown that a mass loss of almost 90% can be reached at 300°C.

Looking at the mass loss curves of the wood resources (beech, oregon, spruce and willow) it can be seen that all different kinds of woods show the same mass loss curve. Some difference can be seen in the absolute values that represent the quantitative amount of organic fraction that is converted into the gas phase. Further it is shown that at each isothermal torrefaction temperature, even after two hours, the material is still reactive. Between 220 - 300°C after two hours the material still has a slowly increasing mass loss that shows almost a linear trend. Beech wood torrefaction between 310 - 330°C does not show this linear trend anymore which means that the maximum amount of material is volatilized. The fixed carbon content is reached and represents a volatile weight loss of around 80%. It is important to keep in mind that commercial torrefaction will never reach these long residence times. The volatile fraction that is released represents better the amount of volatiles that is formed during slow pyrolysis. Pyrolysis of biomass is mainly carried out at higher temperatures between 400 - 600°C to obtain a maximum amount of bio-oil. Finally, the reactivity of alkali lignin is very small. The final char yield that is reached after two hours is around 75 – 80% at 300°C and no reactivity can be observed anymore at this temperature.

In Figure 4.13 and Figure 4.14 the final mass loss of beech, xylan, cellulose and alkali lignin is shown after 30 min. and 120 min. of torrefaction. It is shown that during 30 min. torrefaction xylan is the most reactive component at all temperatures between 220 - 300°C. Therefore, it can be concluded that during 30 min. torrefaction most of the mass loss of wood is caused by the thermal decomposition of the hemicellulose in the biomass. If longer residence times are applied for the torrefaction beech wood at a certain moment the contribution of the cellulose to the mass loss of the beech wood becomes more important. At 270°C and 120 min. reaction time the loss due to cellulose decomposition is almost as extensive as due to the decomposition of xylan.

In the TG curves of the different wood species it can be observed that the curves comprise three different domains (or regimes) in which the biomass reacts. These three different domains that can be recognised are:

1. A parabolic mass loss curve in the first minutes in which the biomass heats up to the desired torrefaction temperatures. In section 4.4.2 this domain is studied more extensively.

2. A second domain in which the mass loss curve of the biomass shows exponential characteristics. In section 4.4.3 this domain is studied more extensively looking at different reaction models and the temperature dependence.

3. A third domain in which the biomass mass loss curve show a linear trend. In section 4.4.3 and 4.4.4 this domain is studied more extensively looking at different mass loss plots that describe the thermal behaviour of different phases in the biomass that react.

In the rest of this chapter the weight loss of beech wood is studied more extensively in these three different domains to derive a model that describes the torrefaction reaction kinetics. The figure schematically represents an s-curve. The results for beech wood will be compared with the other wood resources.

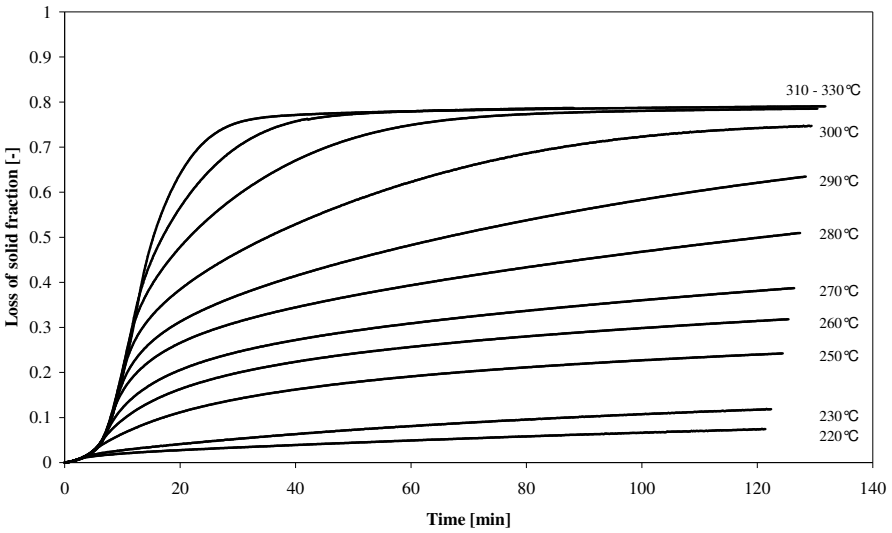


**Figure 4.5:** Isothermal TGA of beech at 220 - 330°C with heating rate 10°C/min until isothermal temperature. The mass loss is normalized at 200°C which is according the definition the starting temperature for torrefaction

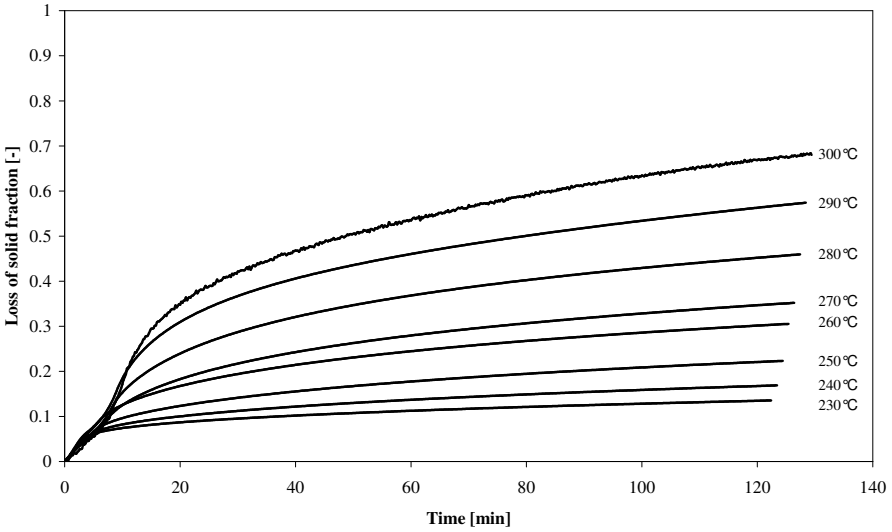


**Figure 4.6:** Isothermal TGA of oregon at 220 - 300°C with heating rate 10°C/min until isothermal temperature. The mass loss is normalized at 200°C which is according the definition the starting temperature for torrefaction

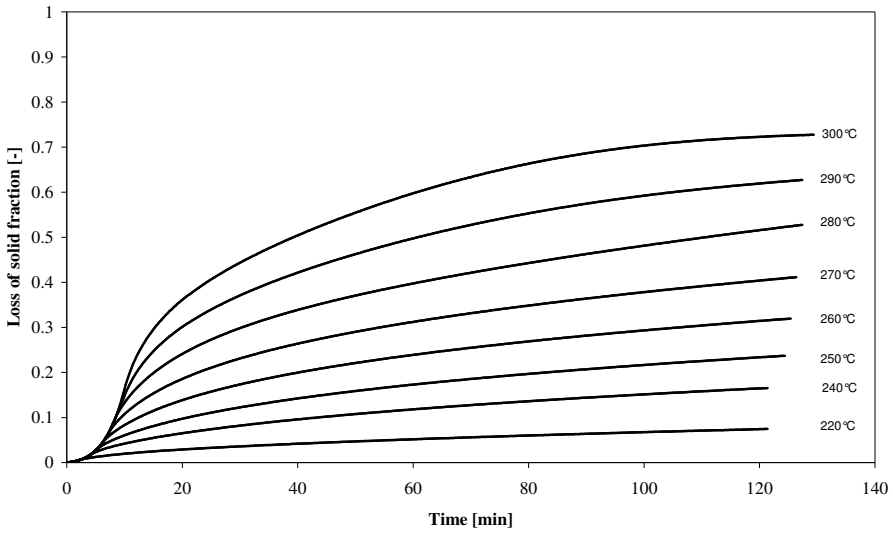


**Figure 4.7:** Isothermal TGA of spruce at 220 - 300°C with heating rate 10°C/min until isothermal temperature. The mass loss is normalized at 200°C which is according the definition the starting temperature for torrefaction

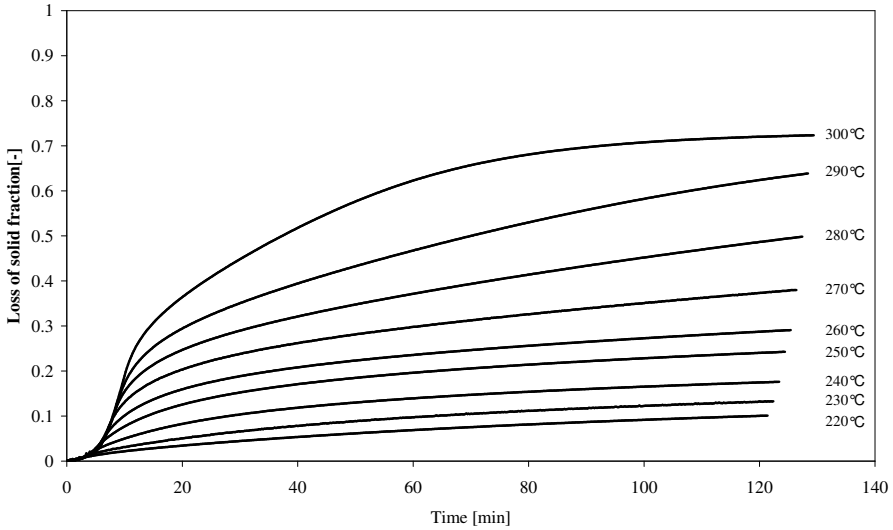


**Figure 4.8:** Isothermal TGA of willow at 220 - 300°C with heating rate 10°C/min until isothermal temperature. The mass loss is normalized at 200°C which is according the definition the starting temperature for torrefaction

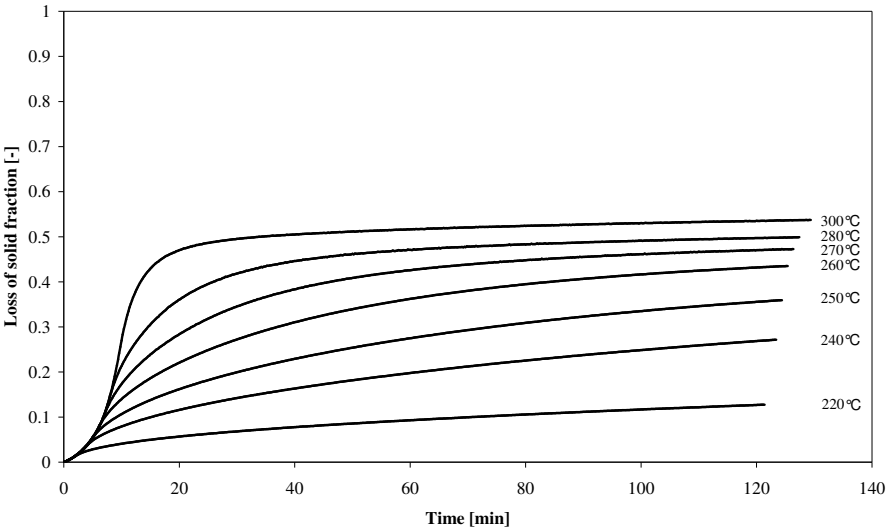


**Figure 4.9:** Isothermal TGA of straw at 220 - 300°C with heating rate 10°C/min until isothermal temperature. The mass loss is normalized at 200°C which is according the definition the starting temperature for torrefaction

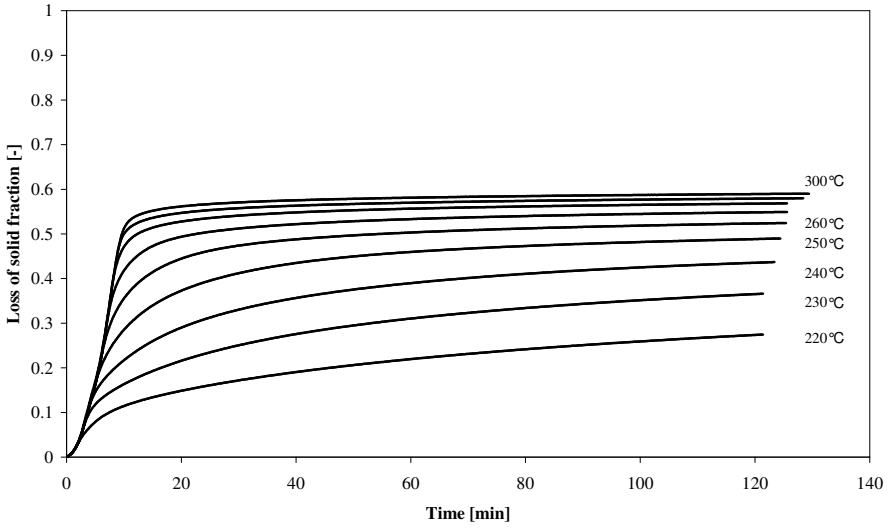


**Figure 4.10:** Isothermal TGA of xylan at 220 - 300°C with heating rate 10°C/min until isothermal temperature. The mass loss is normalized at 200°C which is according the definition the starting temperature for torrefaction

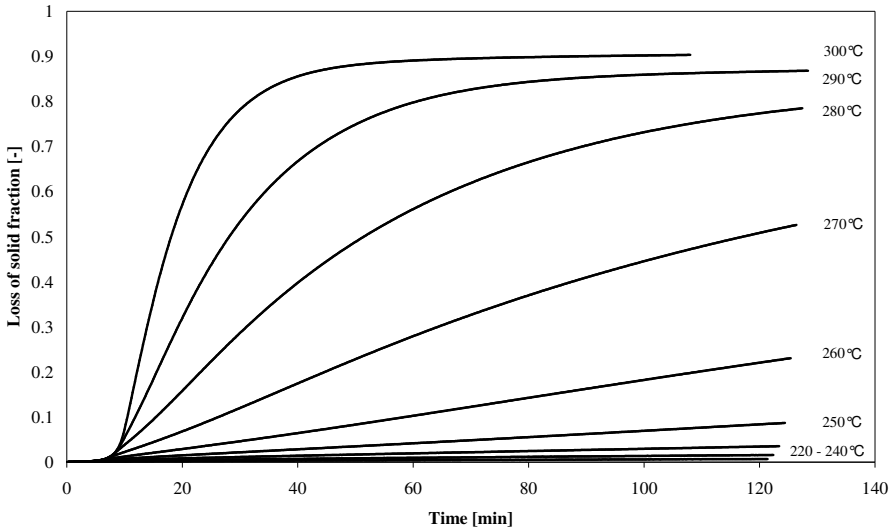


**Figure 4.11:** Isothermal TGA of cellulose at 220 - 300°C with heating rate 10°C/min until isothermal temperature. The mass loss is normalized at 200°C which is according the definition the starting temperature for torrefaction

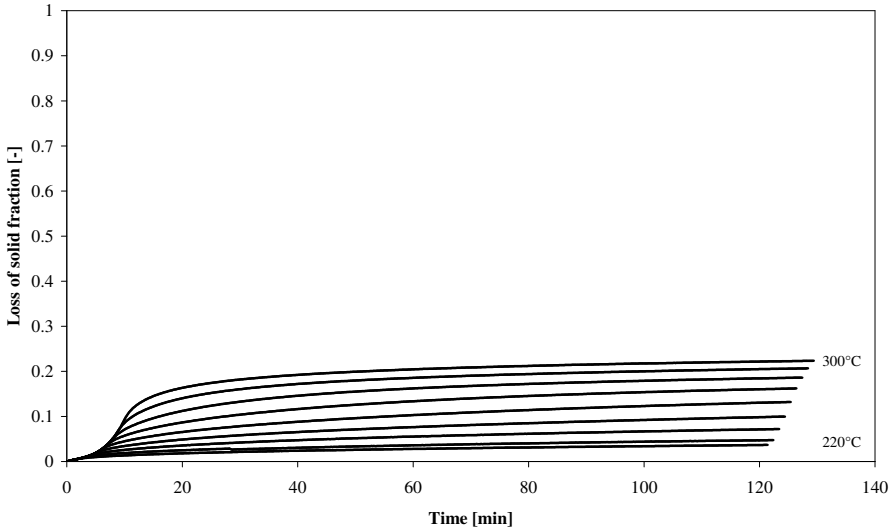


**Figure 4.12:** Isothermal TGA of alkali lignin at 220 - 300°C with heating rate 10°C/min until isothermal temperature. The mass loss is normalized at 200°C which is according the definition the starting temperature for torrefaction

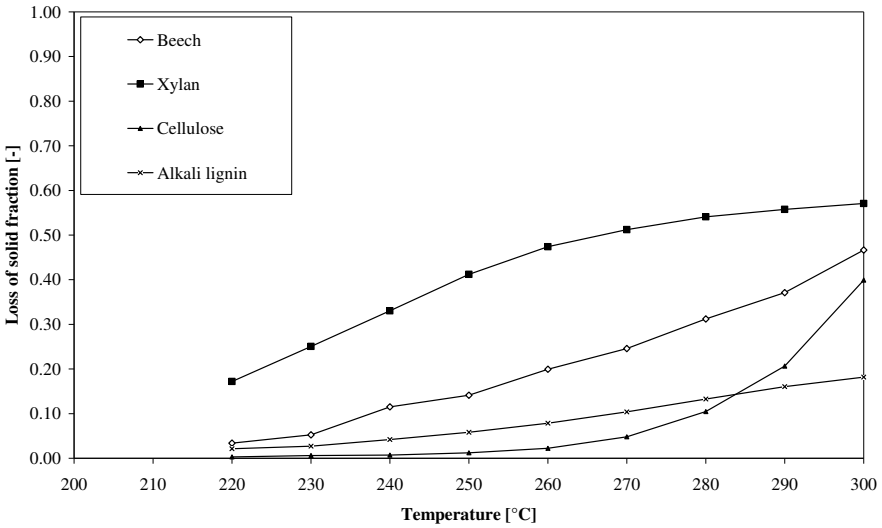


**Figure 4.13:** Mass loss of beech, xylan, cellulose and alkali lignin after 30 min. of torrefaction at different reaction temperatures

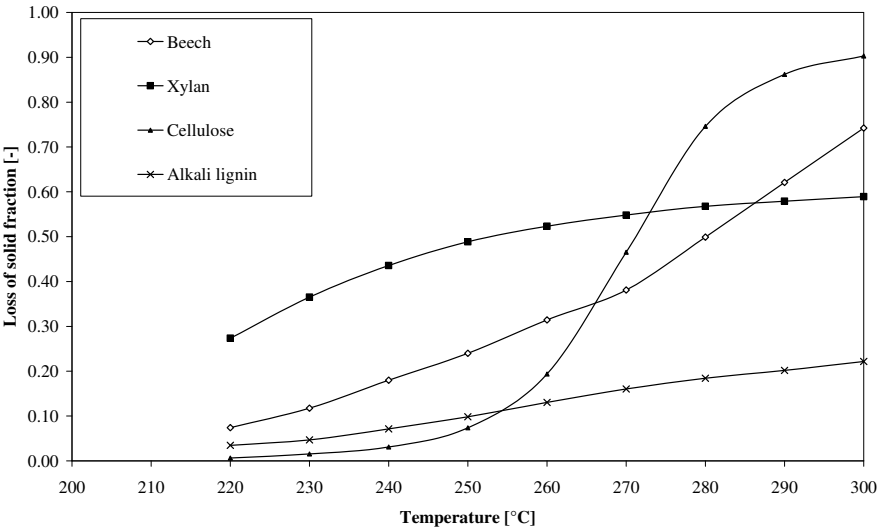


**Figure 4.14:** Final Mass loss of beech, xylan, cellulose and alkali lignin after 120 min. of torrefaction at different reaction temperatures

### 4.4.2 Domain 1: Fitting of weight loss curves in heating up stage

The TGA curves are also fitted in the first ten minutes to study the reactivity behaviour as described by equations (4.30) – (4.35c). In the first ten minutes the reactor is heated up to torrefaction temperature; the particle heats up and mass loss occurs. Curve fitting with equation (4.35c) shows that the mathematics for causal effect describes accurately the mass loss in the heating up stage to 300°C.

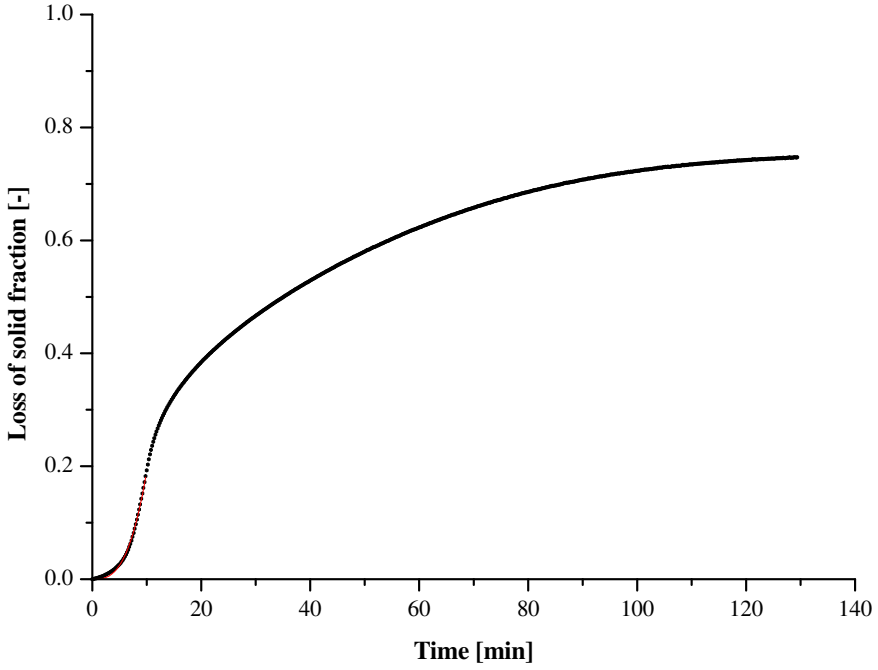


**Figure 4.15:** Mass loss curve fit of the first ten minutes if the torrefaction reactor is heated up and causal effects occur like biomass particle heat up and thermal degradation. The curve fit is carried out with equation (4.35c) at 300°C

### 4.4.3 Domain 2 and 3: Fitting of weight loss curves at isothermal conditions

After obtaining the TG curves for the several biomass feedstocks the kinetic analysis is carried out according the model selection and description for the four different models. The experimental results were fitted with the equations to obtain the values for the parameters "*a", "b", "c" and "d"*. The best curve fit was achieved by the least square methods.

Figure 4.16 shows the curve fitting of the weight loss kinetics of beech wood at temperatures between 220 - 300°C at isothermal conditions. Model i and model iii are shown in green and fitted with equation (4.5). These models describe the reactivity of biomass as a one phase reaction with either one global step reaction or two competitive reactions. Model ii and iv are shown in purple and fitted with equation (4.11). The models describe the reactivity of biomass as a two phase reaction mechanism that consists of two parallel or two consecutive reactions. The blue line in the graph shows model ii and model iv where the slow exponential part is described as a linear time dependence.

It is shown that a one phase reaction mechanism described by equation (4.5) is not accurate enough to describe the mass loss. At low temperatures between 220 – 250°C the curve fit is still accurate, but at higher temperatures between 250 - 300°C another reaction mechanism is necessary to describe the mass loss accurately. A two phase reaction mechanism is a solution to describe the mass loss more accurately. Equation (4.11) comprises four parameters that represent the thermal decomposition of the biomass during torrefaction. The results of the different parameter fits are shown in Figure 4.17.

In Figure 4.17 it can be seen that too much degrees of freedom are given to the system, because the *a,b,c and d parameters* do not show structured trends. The values that are found make it difficult to interpret the results. It is observed that at higher temperatures the *c-value* is satisfied around 0.6. From this the conclusion is drawn that the values for "*a"* and "*c"* are parameters that describe the amount of material that could react during torrefaction out of the phases that are described by a & b or c & d. After these observations more limitations are applied to the system.

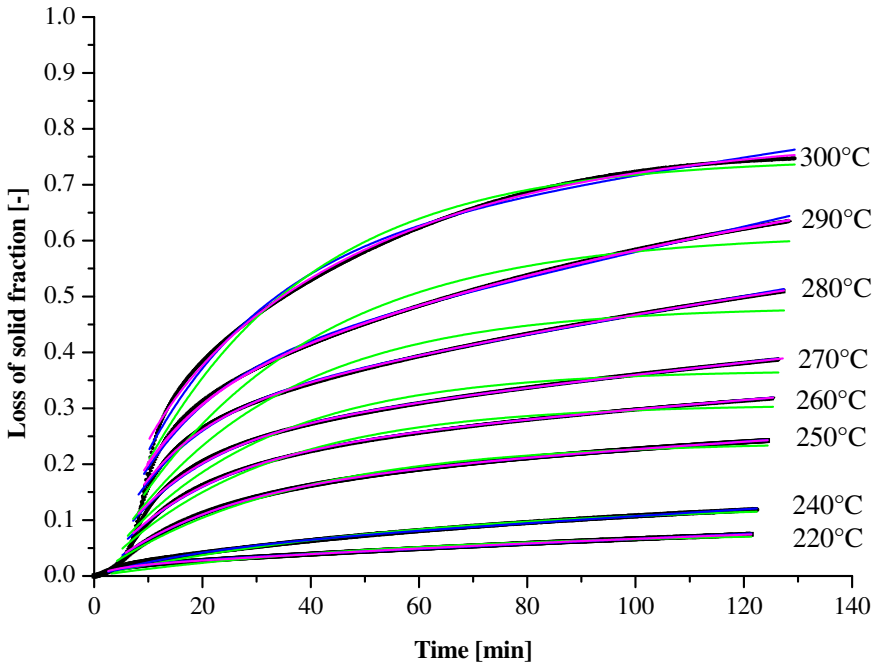


| | | |
|---|---|---|
| ---- | Experimental | |
| ---- | one phase model curve fit | Equation (4.5) |
| ---- | two phase model curve fit | Equation (4.11) |
| ---- | two phase model with one term developed in First term of series | Equation (4.23) |

**Figure 4.16:** Experimental and modeled relative mass loss of beech wood versus time for isothermal temperature conditions between 220 - 300°C. Model i and model iii are shown in green and fitted with equation (4.5). Model ii and iv are shown in purple and fitted with equation (4.11). The blue line is equation (4.11) developed into the first term of the series.

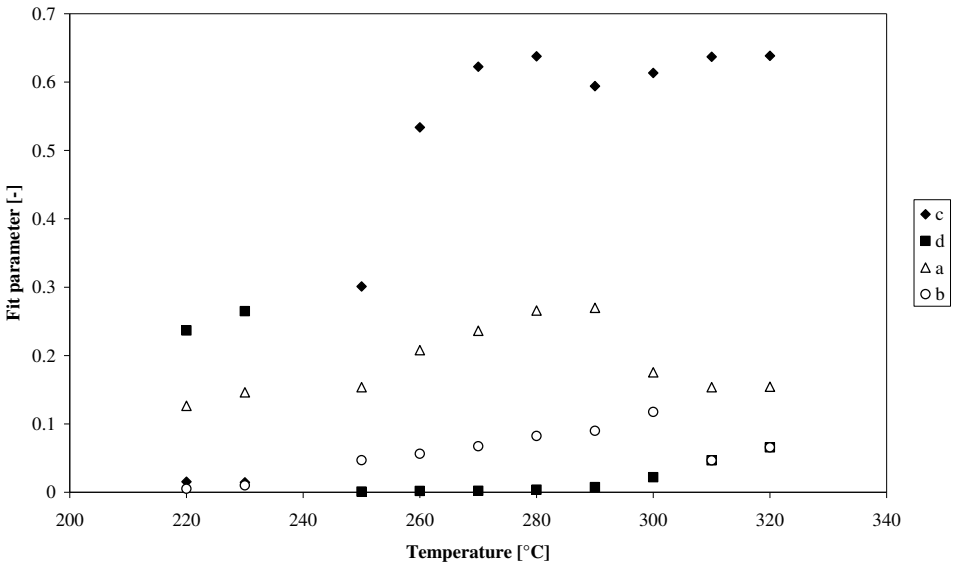


**Figure 4.17:** determined parameters a,b,c & d for beech wood by curve fitting between 220 - 320°C according equation (4.11)

## 4.4.4 Quantitative numbers of derived parameters

If too much degrees of freedom are given to the model that describes the biomass decomposition during torrefaction it is found that the results are difficult too interpret, so more limitations are applied to the model. These limitations are based on the satisfaction of the "c" parameter around 0.6 shown in Figure 4.17.

Figure 4.19 and Figure 4.20 show the absolute values for the fitted parameters for the curve fitting of beech wood between 250 - 300°C after restrictions to the model are applied. The graphical representation is shown in Figure 4.18. It is found that the best correspondence is obtained if the value for "*a"* is increasing with temperature and that "*c"* is a constant factor. This means that the availability of the phase (the amount of material that can react) that is described by parameters *"a"* and *"b"* is depended on the temperature. The parameters *"b"* and *"d"* are slightly increasing with temperature. In paragraph 4.4.5 an explanation is given about the temperature dependence of the "*a"-value*.

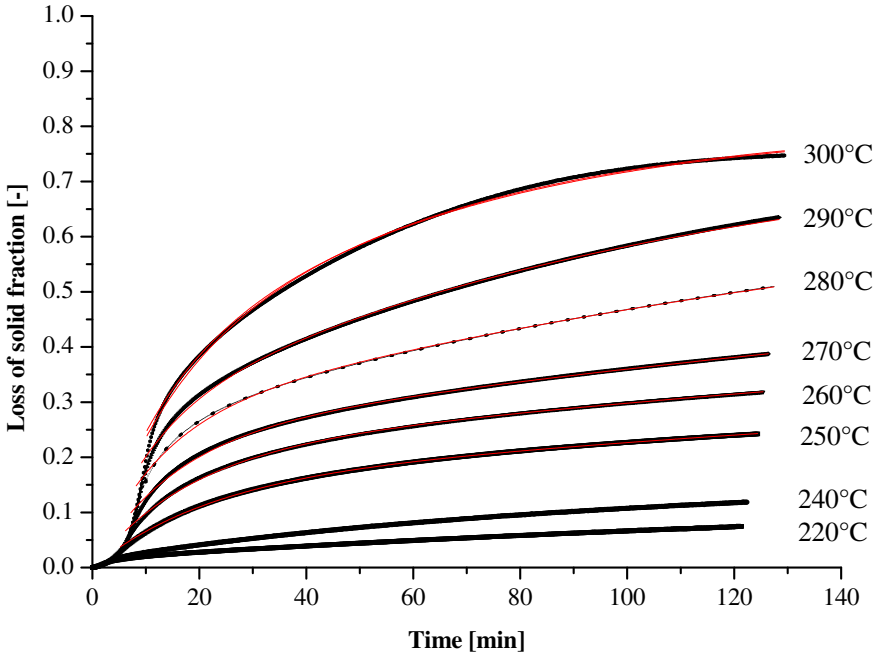


**Figure 4.18:** Experimental and modeled relative mass loss of beech wood versus time for isothermal temperature conditions between 220 - 300°C after restrictions to the model. The c-parameter in equation (4.11) is restricted to a fixed number

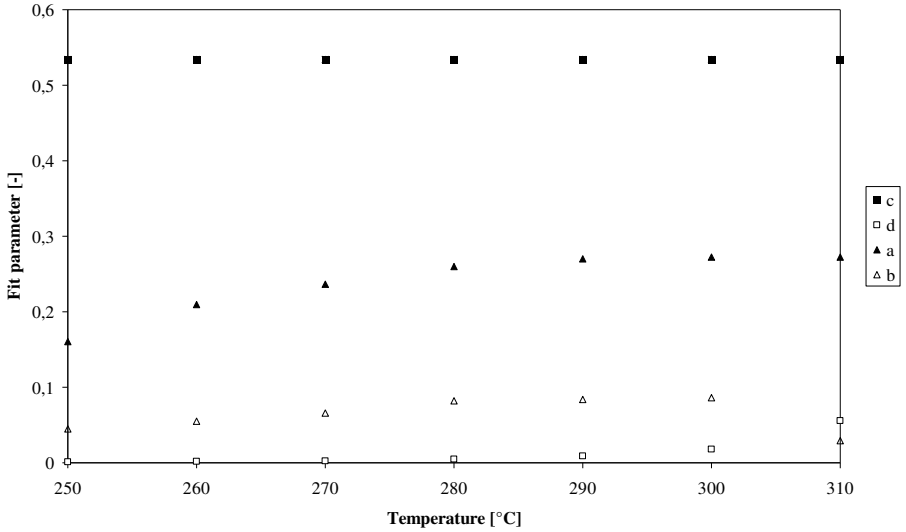


**Figure 4.19:** determined parameters a,b,c & d for beech wood by curve fitting between 250 - 310°C according equation (4.11)

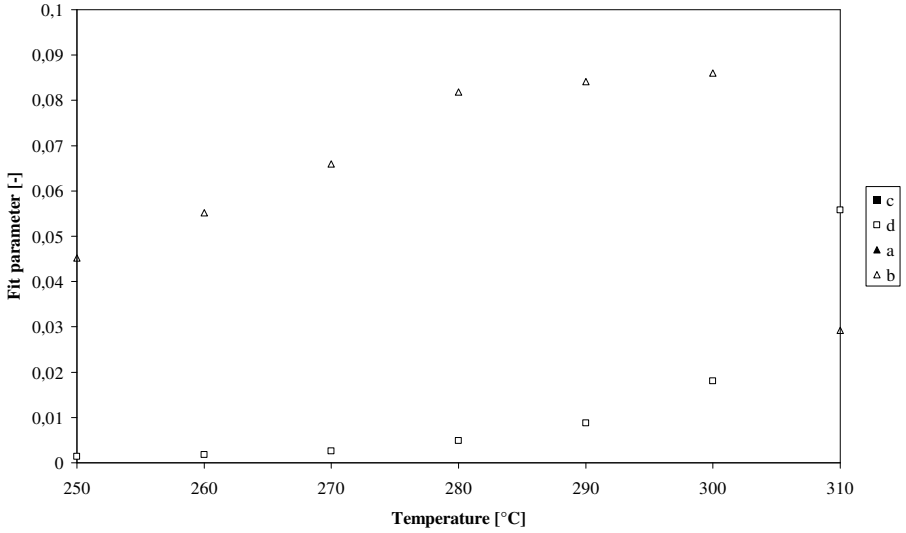


**Figure 4.20:** determined paramaters a,b,c & d for beech wood by curve fitting between 250 - 310°C according equation (4.11) zoomed in at the b & d values

### 4.4.5 Model verification

To verify the model that describes the torrefaction reactivity of different wood feedstocks the mass loss of beech wood in time is plotted for different temperatures between 250 - 300°C. In the figures the experimental TGA mass loss curves are shown together with the curve fit of the experiments and the independent curves that can be described with the parameters a & b and c & d. The plots are shown in Figure 4.21 - Figure 4.26. The values that are used for the plots are shown in Figure 4.19 and Figure 4.20.

It is shown that the summation of the plots that is described with the parameters "a" & "b" and of the plot that is described by the parameters "c" & "d" represents quite accurately the experimental values for beech wood. Only the heating up stage shows some errors, because of a constant lower temperature in the biomass than is modeled with the derived parameter values.

At (low) temperatures between 250 - 280°C the mass loss that is represented by the *c,d-plot* is shown with an almost linear trend up to 10 – 30% organic weight loss. At 290 and 300°C the c,d-plot shows already some exponential behaviour with a mass loss up to 40 – 50% based on the total mass of dry and raw beech wood. Finally, the *c,d-plot* shows that the reactivity of the beech wood is still present. After two hours of torrefaction the biomass mass still figures a linear trend in Figure 4.21 - Figure 4.26.

The *a,b-plot* shows a small increase in the mass loss with rising temperature. The mass loss that occurs due to the *a,b-curve* is almost 20% at 250°C and is increased up to 30% at 300° for beech wood. At all temperatures the major part is lost already in the first 30 minutes which is also the commercial residence time for torrefaction [Bergman et al., 2005].

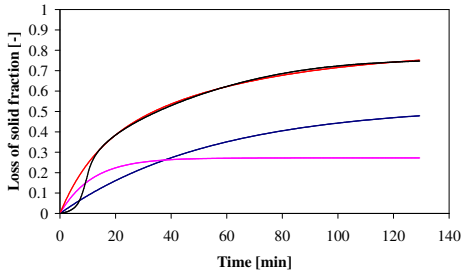


**Figure 4.21:** plot of experimental and modelled data of determined ab and cd values for beech wood at 300°C.
Experimental/curve fit/ab plot/cd plot

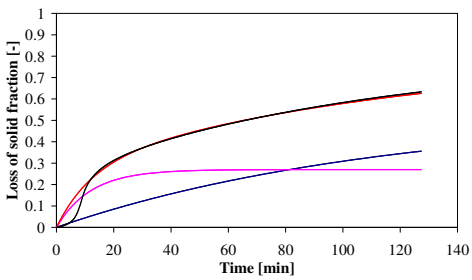


**Figure 4.22:** plot of experimental and modelled data of determined ab and cd values for beech wood at 290°C
Experimental/curve fit/ab plot/cd plot

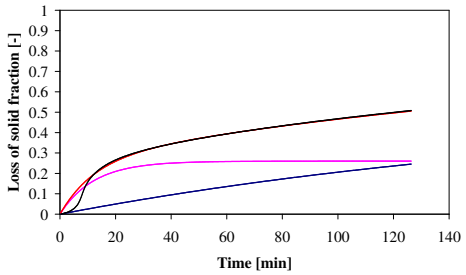


**Figure 4.23:** plot of experimental and modelled data of determined ab and cd values for beech wood at 280°C
Experimental/curve fit/ab plot/cd plot

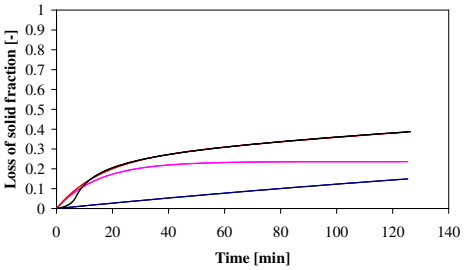


**Figure 4.24:** plot of experimental and modelled data of determined ab and cd values for beech wood at 270°C
Experimental/curve fit/ab plot/cd plot

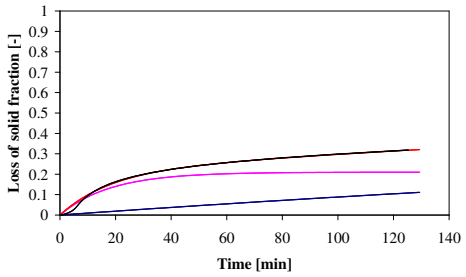


**Figure 4.25:** plot of experimental and modelled data of determined ab and cd values for beech wood at 260°C
Experimental/curve fit/ab plot/cd plot

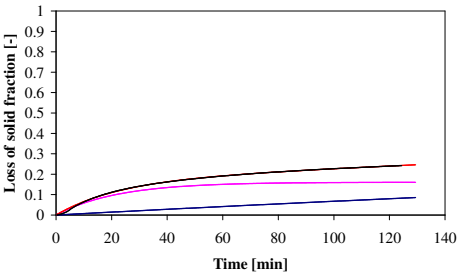


**Figure 4.26:** plot of experimental and modelled data of determined ab and cd values for beech wood at 250°C
Experimental/curve fit/ab plot/cd plot

Also the sensitivity of the "*a*" and "*b*" values is analyzed to study the effect of the temperature dependency of the "*a*"-value. It is possible that the increase of parameter "*a*" with increasing temperature (as is shown in the curve fitting of the wood species) is because of a set of reactions with different activation energies. At higher reaction temperatures it is possible that more organic material in the biomass could react. At a certain temperature two curves are plotted with different "*a*" and "*b*" values. A high "$a_1$" value is combined with a low "$b_1$" value and a low "$a_2$" value is combined with a high "$b_2$" value. After plotting these two curves the summation of these two plots is curve fitted over different time scales. This is carried out to study the influence of the combination of different "$a_i$" and "$b_i$" values on the influence of a combined "*a*"-*value*. This method shows how the a-value is build up if it depends on more parameters than only one a-value. The method that is used to research this dependency and describe the plots can be described with the following equations:

Figure 4.27
$$\frac{M_v(a,b)}{M_0} = a_1\left(1-e^{-b_1 t}\right)+a_2\left(1-e^{-b_2 t}\right) \tag{4.37}$$

Figure 4.28
$$\frac{M_v(a,b)}{M_0} = a_1\left(1-e^{-b_2 t}\right)+a_2\left(1-e^{-b_1 t}\right) \tag{4.38}$$

Figure 4.29
$$\frac{M_v(a,b)}{M_0} = a\left(1-e^{-b_1 t}\right)+a\left(1-e^{-b_2 t}\right) \tag{4.39}$$

The values that are chosen to study the influence of the temperature on the a,b curve at 260°C for beech wood are shown in Table 4.2. These plots are shown in Figure 4.27 - Figure 4.29. The $a_1$ curves are shown in red, the $a_2$ curves are shown in blue and the summation is shown in black. After plotting these curves with different a,b values the summation curves are fitted for different time scales to get more information about temperature dependency. The time scales used are 0 – 30 min, 0 – 60 min and 0 – 90 min. These results are shown in Table 4.3.

**Table 4.2:** a,b values used to construct different a,b curves for beech wood at 260°C that are shown in Figure 4.27 - Figure 4.29

| Figure | $a_1$ | $b_1$ | $a_2$ | $b_2$ |
|---|---|---|---|---|
| Figure 4.27 - 4.30 | 0.05245 | 0.027585 | 0.15735 | 0.165510 |
| Figure 4.29 | 0.10500 | 0.027585 | 0.10500 | 0.165510 |

**Table 4.3:** a,b values found after fitting the curve that has been constructed by the summation of "$a_i$" and "$b_i$" parameters as is shown in Table 4.2

| Figure | fitted a | | | fitted b | | |
|---|---|---|---|---|---|---|
| | 30 min | 60 min | 90 min | 30 min | 60 min | 90 min |
| Figure 4.27 | 0.18589 | 0.19559 | 0.19979 | 0.14079 | 0.11857 | 0.10990 |
| Figure 4.28 | 0.16370 | 0.18542 | 0.19578 | 0.06518 | 0.05038 | 0.04422 |
| Figure 4.29 | 0.16794 | 0.18624 | 0.19448 | 0.02063 | 0.07851 | 0.06869 |

It is shown by these curves that the process that is described with the a,b-parameters is a mix of different dissociation processes in the thermal degradation of the beech wood. Since parameter b is a parameter that represents the activation energy of the first reaction in the system the dependency can be described with Arrhenius:

$$b = \gamma.\exp\left(-\frac{E_a}{RT}\right) \tag{4.40}$$

The term in the exponent (–b·t) of equation (4.11) is a constant factor which means that the following equation is constant:

$$t.\gamma.\exp\left(-\frac{E_a}{RT}\right) = \text{constant} \tag{4.41}$$

From this derivation it can be concluded that with increasing time the temperature should also increase.

Also by fitting with equation (4.23) in which the c,d parameter in the equation is developed into the first term in the series, almost the same process can be observed.

$$\frac{M_v}{M_0} = a \cdot \left(1 - e^{-bt}\right) + c \cdot t \tag{4.23}$$

The first term of the series is derived if the following mathematical operation is carried out:

$$\sum c_i \left(1 - e^{-dt}\right) = t \sum c_i d_i = c \cdot t \tag{4.42}$$

This can be carried out if a linear term is found that can describe a part of the dissociation process. By applying this relation it can also be concluded that the thermal decomposition of the slow reactive phase, which has high availability to react described by the “c” and “d” parameter, can be a process of different dissociation processes. This leads to different activation energies for the components released during thermal decomposition of biomass by means of torrefaction.

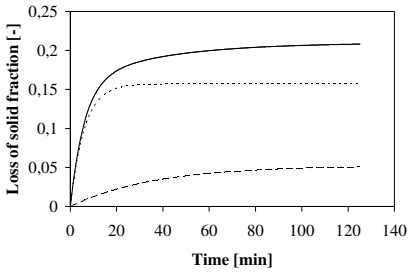


**Figure 4.27:** sensitivity analysis of a,b values for the analysis of temperature dependency with $a_1$ $b_1$ + $a_2$ $b_2$ for beech wood at 260°C. In the dotted curve the $a_1$ curve, in the dotted-striped curve the $a_2$ and in full black the summation

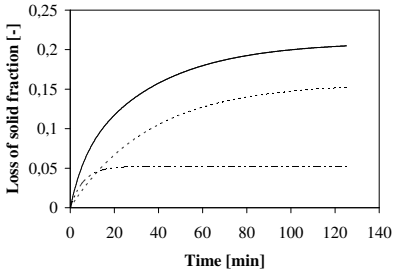


**Figure 4.28:** sensitivity analysis of a,b values for the analysis of temperature dependency with $a_1$ $b_2$ + $a_2$ $b_1$ for beech wood at 260°C. In the dotted curve the $a_1$ curve, in the dotted-striped curve the $a_2$ and in full black the summation

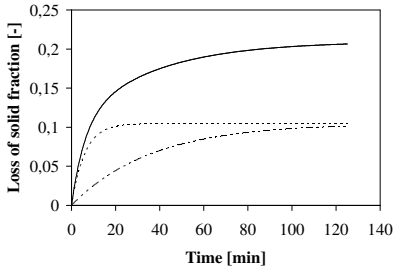


**Figure 4.29:** sensitivity analysis of a,b values for the analysis of temperature dependency with $ab_1$ + a $b_2$ for beech wood at 260°C. In the dotted curve the $b_1$ curve, in the dotted-striped curve the $b_2$ and in full black the summation

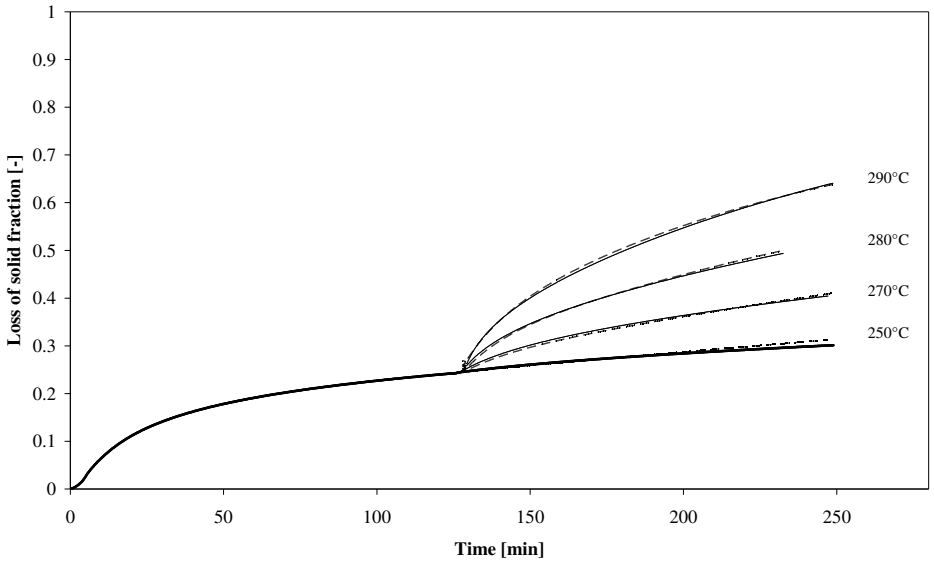


**Figure 4.30:** Two different heating stages are shown. In full black the isothermal TGA curves of thermal treated beech wood (that was first torrefied at 250°C for 2 hrs that can be seen in the graph from 0 – 130 min) at 250 - 290°C are shown. The beech wood was torrefied in a fixed bed reactor as described in Chapter 5. The striped curves describe the reaction kinetics model for beech wood at 250°C from 0 – 130 min and at 250 - 290°C for two hours between 130 – 250 min.

To verify the model also a TGA experiment with torrefied beech wood has been carried out. The beech wood was torrefied for two hours at 250°C and then analyzed with TGA for around four hours at isothermal conditions between 250 - 290°C. So in total the beech wood was torrefied for two hours. After the experiment the several mass loss curves were fitted with the kinetic data that has been found for beech wood. The results are shown in Figure 4.30.

It is seen that the model describes quite accurately the mass loss of the beech wood that was first torrefied for two hours at 250°C when it is again torrefied at even higher isothermal conditions. The reactivity almost super poses at the temperatures between 250°C and 290°C. A small difference of a few percentage of the mass loss is shown between the experimental and theoretical values. The superposition

of the mass loss curve at the temperatures 250°C - 290°C means that the two phases react independently.

It can be concluded that both reactions of $A_1$ and $A_2$ to form volatiles ($V_1$ and $V_2$) are independent from each other, because both reactions describe two different systems. The starting point of the reaction can be chosen independent from earlier reactions as is shown by Figure 4.30. Superposition of the two independent reactions is possible since it is possible to heat up to higher temperature at any moment in the process.

## 4.5 Conclusion and discussion

Describing four different thermal decomposition models for biomass torrefaction at isothermal conditions in a mathematical formulation shows they formally lead to the two mathematical descriptions. A global one step reaction model is mathematically similar to a two competitive reactions model and two steps in series reaction model is mathematically similar to a two parallel reaction model. Further it is shown that two different phases in the biomass react independently of each other. The slow reacting phase has high availability and the fast reacting phase has an apparent temperature dependence of the availability. The wood species beech, willow, spruce and oregon show similar thermal behaviour according a two parallel reaction model.

## References

Bergman PCA, Boersma, AR, Zwart RWR, Kiel JHA (2005). Torrefaction for biomass co-firing in existing coal-fired power stations “Biocoal”. Report ECN-C--05-013, 2005, ECN, Petten, The Netherlands

Chorkendorff I, Niemantsverdriet JW (2003). Concepts of modern catalysis and kinetics. Wiley-VCH Verlag GmbH & Co. KGaA, Weinheim

Di Blasi C, Lanzetta M (1997). Intrinsic kinetics of isothermal xylan degradation in inert atmosphere. Journal of Analytical and Applied Pyrolysis; 40; 287-303

Di Blasi C (2008). Modelling chemical and physical processes of wood and biomass pyrolysis. Progress in Energy and Combustion Science; 34; 1; 47-90

Ferro DT, Vigouroux V, Grimm A, Zanzi Z (2004). Torrefaction of agricultural and forest residues. Cubasolar, April 12-16 2004, Guantanamo, Cuba

Gaur S, Reed TB (1998). Thermal data for natural and synthetic fuels. Marcel Dekker, New York

Heikkinen JM, Hordijk JC, De Jong W, Spliethoff H (2004). Thermogravimetry as a tool to classifiy waste components to be used for energy generation. Journal of Analytical and Applied Pyrolysis; 71; 2; 883-900

Prins MJ, Ptasinski KJ, Janssen FJJG (2006a). Torrefaction of wood Part: 1. Weight loss kinetics. Journal of Analytical and Applied Pyrolysis; 77; 1; 28- 34

Prins MJ, Ptasinski KJ, Janssen FJJG (2006b). Torrefaction of wood Part: 2. Analysis of products. Journal of Analytical and Applied Pyrolysis; 77; 1; 35-40

Pyle DL, Zaror CA (1984). Heat transfer and kinetics in the low temperature pyrolysis of solids. Chemical Engineering Science; 39 1; 147-158

Repellin V, Govin A, Rolland M, Guyonnet R (2010). Modelling anhydrous weight loss of wood chips during torrefaction in a pilot kiln. Biomass and Bioenergy

Veringa HJ (1981). Intrinsic stability of technical superconductors. PhD thesis; Technische Hogeschool Twente; Enschede

## Nomenclature Chapter 4

| | |
|---|---|
| $\alpha$ | heating rate [°C/min] |
| a | availability factor [-] |
| $a_1$ | availability factor 1 [-] |
| $a_2$ | availability factor 2 [-] |
| b | activation energy derivative |
| $b_1$ | activation energy derivative |
| $b_2$ | activation energy derivative |
| c | availability factor [-] |
| d | activation energy derivative |
| A | reacting phase A in biomass [-] |
| $A_1$ | reacting phase $A_1$ in biomass [-] |
| $A_2$ | reacting phase $A_2$ in biomass [-] |
| $\beta_1$ | relaxation effect 1 constant [-] |
| $\beta_2$ | relaxation effect 2 constant [-] |
| B | reacting and/or intermediate phase B in biomass [-] |
| $B_1$ | reacting/produced phase $B_1$ in biomass [-] |
| $B_2$ | reacting/formed phase $B_2$ in biomass [-] |
| C | reacting/formed phase C in biomass [-] |
| $E_a$ | activation energy [J mole $^{-1}$] |
| $k_1$ | reaction constant [kg/s] |
| $k_2$ | reaction constant [kg/s] |
| $k_{v1}$ | reaction constant [kg/s] |
| $k_{v2}$ | reaction constant [kg/s] |
| $K_1$ | reaction constant [kg/s] |
| $K_2$ | reaction constant [kg/s] |
| M | total solid mass [kg] |
| $M_L$ | Mass loss fraction [-] |
| $M_0$ | initial mass [kg] |
| $M_t$ | solid mass at time t [kg] |
| $M_v$ | volatile mass at time t [kg] |
| $r_A$ | reaction rate [kg/s] |
| $r_{A1}$ | reaction rate [kg/s] |
| $r_{A2}$ | reaction rate [kg/s] |

| | |
|---|---|
| $r_B$ | reaction rate [kg/s] |
| $r_{B1}$ | reaction rate [kg/s] |
| $r_{B2}$ | reaction rate [kg/s] |
| $r_C$ | reaction rate [kg/s] |
| R | gas constant [J/K] |
| t | time [s] |
| $\tau$ | residence time [s] |
| T | Temperature [°C] or [K] |
| V | volatile fraction [-] |
| $V_1$ | volatile fraction [-] |
| $V_2$ | volatile fraction [-] |
| $W_{ash}$ | ash weight in biomass [kg] |
| $W_{initial}$ | initial weight biomass [kg] |
| $W_{TGA}$ | measured weight biomass [kg] |

# APPENDIX CHAPTER 4

In this appendix the kinetic parameters found for other biomass resources (willow and oregon) than beech wood are presented. It shown that the model is also applicable for these resources. The same trend is observed.

| Willow | a | b | c | d |
|---|---|---|---|---|
| 250°C | 0.46 | 0.002 | 0.157 | 0.058 |
| 260°C | 0.46 | 0.002 | 0.183 | 0.069 |
| 270°C | 0.46 | 0.004 | 0.207 | 0.082 |
| 280°C | 0.46 | 0.007 | 0.215 | 0.091 |
| 290°C | 0.46 | 0.010 | 0.281 | 0.059 |
| 300°C | 0.46 | 0.021 | 0.301 | 0.053 |

| Oregon | a | b | c | d |
|---|---|---|---|---|
| 250°C | 0.20 | 0.041 | 0.001 | series |
| 260°C | 0.20 | 0.065 | 0.001 | series |
| 270°C | 0.20 | 0.068 | 0.257 | 0.007 |
| 280°C | 0.20 | 0.091 | 0.328 | 0.012 |
| 290°C | 0.20 | 0.124 | 0.410 | 0.017 |
| 300°C | 0.20 | 0.127 | 0.530 | 0.017 |

# Chapter 5

# Product formation during torrefaction


## Abstract

*This chapter describes the product formation during torrefaction at isothermal conditions between 220 – 300°C for several biomass resources such as beech, willow, straw and poplar. In Chapter 4 a reaction mechanism has been proposed to describe the kinetics of torrefaction. In this chapter the products that belong to the mechanism are characterized by fixed bed experiments coupled with offline product analysis such as micro GC, GC/MS and elemental analysis. Also TG-MS and TG-FTIR experiments have been carried out with dynamic temperature conditions between 100 - 400°C to determine the product formation as function of time/temperature. Finally, the energy balance is constructed based on the mass balances found with the fixed bed experiments.*

## 5.1 Introduction

In the previous chapter it is shown that the biomass decomposition during torrefaction occurs in two independent steps. Two exponential terms which are related with the activation energy can describe the kinetics of the weight loss during the decomposition. These different activation energies belong to different sets of reactions that occur and the two reaction steps form several products. It is important to find out which products are formed in these two different steps so that a better understanding about the torrefaction mechanism can be achieved. In Chapter 2 an overview is given about the thermo chemical conversion of biomass and the main principles of pyrolysis mainly above 350°C. In this chapter a closer look is given at the product formation in the temperature range 200 - 300°C. A fixed bed reactor and different analytical techniques are applied to determine the product formation in these two steps.

In order to understand the torrefaction mechanism of biomass particles it is important to understand the torrefaction behaviour of the individual fractions hemicellulose, cellulose and lignin. In Chapter 4 it is found that hemicellulose is the most reactive fraction in the torrefaction of biomass resources, but cellulose and lignin also react at very low rate. [Gaur & Reed, 1998] mention that hemicellulose pyrolysis involves three competing reactions: i) low-temperature polymerization process to form components such as polysaccharides with the formation of char, CO, $CO_2$ and $H_2O$ ii) high-temperature decomposition reactions to generate volatile anhydrosugars and related monomeric compounds and iii) competitive degradation of some xylan. [Gaur and Reed , 1998] and [Prins et al., 2006] summarize the degradation of hemicellulose in the temperature range 200 - 300°C as a two step reaction where volatiles are formed in the first step followed by their catalytic degradation. It is also mentioned that mineral compounds catalyze the exothermic decomposition of levoglucosan.

Primary pyrolysis (and so also torrefaction) is the random cleavage of chemical bonds by the application of heat. [Diebold, 2000] mentions even the formation of secondary products at room temperature if there is no thermodynamic equilibrium. The condensable volatiles are multi-component mixtures of different molecular weight species derived from depolymerization and fragmentation. The degradation of a molecule is caused by the breakage of a chemical bond and the production of

free radicals. De Wild et al. used different subgroups to classify the several organic liquids that are produced during the staged thermal degradation of wood [De Wild et al., 2009]. These different liquid products are water, methanol, acids, furans, phenols and other oxygenates.

Physically bound water is derived in the process by drying and chemically bounded water by acid catalyzed dehydration reactions. Hydroxyl groups linked to the hemicellulose are released and contribute significantly to the amount of water produced. Also the degradation of cellulose contributes to the formation of water. Glucose chains in cellulose are first cleaved into glucose and in a second stage glucosan is formed by splitting off a molecule of water [Demirbas, 2000]. The decomposition of lignin starts with the cleavage of aliphatic hydroxyl and ether groups leading to the formation of water [Jakab et al., 1997].

A second important group of degradation products are carboxylic acids like formic, acetic and propionic acid. It is generally believed that the formation of formic acid is stemming from the carboxylic group of the pentosan-glucoronic chain. Acetic acid formation could also be caused by the thermolysis of acetyl radicals linked to the xylose units of hemicellulose [Demirbas, 2000].

The next important product of pyrolysis/torrefaction reactions is methanol. The formation of methanol is assigned to the degradation of methoxy groups which belong to the side chains of hemicellulose [Demirbas, 2000] [Prins et al., 2006] [Bourgois & Doat, 1984]. Alcohols could also be formed by the breakdown of both cellulose and lignin. Methanol is released out of methoxy groups of uronic acid [Demirbas, 2001]. Methyl-esters and or ethers from pectin can also degrade and form methanol [Demirbas, 2005].

Another important group of decomposition products originated from hemicellulose is the collection of furan derivatives [Demirbas, 2000] [Alen et al., 1996]. Furfuraldehyde is formed by dehydration of the xylose unit which is a hemicellulose component [Demirbas, 2005]. Furfural can also be formed by the degradation of cellulose via levoglucosan dehydration next to formaldehyde degradation.

**Table 5.1:** Organic vapour products of pyrolysis of birch and willow wood between 200 - 300°C adopted from [Lievens, 2007]

| | Birch | | Willow | |
|---|---|---|---|---|
| µg/g | 200-300°C | 300-400°C | 200-300°C | 300-400°C |
| Aliphatic hydrocarbons | 13 | 20 | - | 15 |
| Aromatic hydrocarbons | 17 | 64 | 40 | 363 |
| Acids | 47 | 87 | 131 | 710 |
| Aldehydes/ketones | 77 | 230 | 114 | 576 |
| Esters | 9 | 18 | 131 | 90 |
| Ethers/Alcohols | 6 | 16 | 103 | 50 |
| N-compounds | 0 | 0 | - | 21 |
| S-Compounds | 4 | 1 | - | 6 |
| Phenols | 2 | 2 | 36 | 170 |

The formation of phenol derivatives is mainly due to lignin degradation during biomass torrefaction. Decomposition at high temperatures occurs by dehydration, decarboxylation and decarbonylation reactions, where C-C linkages between lignin monomeric units also cleave to form radicals [Lievens, 2007] [Murwanashyaka et al., 2001]. Recombination reactions produce syringols and guaiacols. Aromatics are formed by the degradation of lignin. Depending on the side groups like hydroxyl- and methoxy-substituted phenyl propane units, connected by ether and carbon-carbon bridges a range of aromatic derivatives are formed. Polycyclic aromatic hydrocarbons are the result of secondary and tertiary gas phase reactions [Milne and Evans, 1998]. It is expected that phenol derivatives and polyaromatic hydrocarbons are hardly formed during torrefaction.

The formation of other oxygenates, like aldehydes and ketones, proceeds by a mixture of reactions that occur and is a result of the decomposition of all biomass constituents.

During torrefaction most of the oxygenates consist of one to three carbon atoms and one to two oxygen atoms. The difference between for example the $C_2 - C_4$ oxygenates is due to the internal arrangement and stereochemistry like retro aldol reactions [Prins et al., 2006]. [De Wild et al., 2009] determined the condensables acetaldehyde, methylformate, methylacetate, ethylacetate, propanol, acetone, 2-

**Table 5.2:** Decomposition of different hemicelluloses during pyrolysis

| Hemicelluloses | Decomposition effects |
|---|---|
| Rich of: | |
| Uronic acid | Extensive release of CO2 |
| 4-O-Methyl (poplar) | Extensive release of methanol |
| Acetyl groups | Extensive release of acetic acid |
| | carboxidation important after 240°C |
| Ester groups | Extensive release of acetic acid |
| Arabinose (poplar + coniferous) | Extensive release of water |
| Galactan (coniferous) | Fast decomposition in two steps |
| Mannan (coniferous) | Fast decomposition at basic temperatures |
| | that prolonge at high temperatures |
| Xylan (deciduous) | Fast decomposition with total disapearence |
| | before mannan is decomposed |

butenal and acetol). Depending on the type of hemicellulose different products are formed during pyrolysis, see Table 5.2 [Couhert, 2007].

Demirbas states that the formation of aliphatic hydrocarbons is due to initial degradation of products of lignin [Demirbas, 2000]. Side chains of lignin are thermally cleaved because of random scission by applying heat on the biomass feedstock. Cleavage of the aromatic C-O bond in lignin led to the formation of one oxygen atom products, and the cleavage of the methyl C-O bond to form two oxygen atom products is the first reaction to occur in the thermolysis at 300-350°C. Cleavage of the side chain C-C bond occurs between the aromatic ring and the α-carbon atom.

Yang et al. studied the gas product releasing properties of the three biomass components during pyrolysis [Yang at al., 2007]. It was found that the releasing of $CO_2$ was mainly caused by the cracking and reforming of functional groups of carboxyl (COOH) during hemicellulose decomposition. Also the formation of CO was mainly the result of hemicellulose decomposition by cracking of carbonyl (C=O), carboxyl (COOH) and ether groups (C-O-C). It is also shown that hemicellulose can release $CH_4$ at 280°C mainly caused by the cracking of methoxyl (OMe), but only at very low rate. Also the characteristics of hemicellulose,

cellulose and lignin pyrolysis are researched extensively. Li et al. analyzed the formation characteristics of gas compounds from cellulose pyrolysis by using FTIR at various conditions including heating rates, residence time, temperature and gas flow [Li et al., 2001]. Ferdous et al. researched the gas product property from lignin pyrolysis at changing temperatures and heating rates [Ferdous et al., 2002]. Bassilakis et al. investigated the gas product releasing from D-glucose, chlorogenic acid and xylan pyrolysis [Bassilakis et al., 2001].

[Lievens, 2007] studied TG/MS for the pyrolysis of contaminated biomass feedstocks such as birch, sunflower and willow. The amount of products formed is quantified in different temperature zones. A selection of the results is presented in Table 5.1. [Cornelissen, 2009] applied TG/MS in the research of flash pyrolysis of biomass and co-pyrolysis with biopolymers. The major components of the gaseous fraction are CO, $CO_2$ and $CH_4$. The major components of the liquid fraction are water, alcohols/ethers, acids, ketones/aldehydes and phenolics [Diebold, 2003]. [De Wild et al., 2009] quantified the amount of certain staged degasification reaction products.

[DeGroot et al., 1988] studied the first chemical events in pyrolysis of cottonwood at 250°C by TG FTIR which is shown in Figure 5.1. About 60% of the weight loss (volatilized) is accounted for by five compounds, which are the only products deteced in the gas by FTIR. These products are water, carbon dioxide, methanol, acetic acid and formic acid. The other 40% was already condensed before reaching the FTIR. It is concluded that uronic acids (a sugar with a carbonyl and carboxyl acid function) in the hemicelluloses and pectic substances decompose readily to yield carbon dioxide, water, char and some methanol. Uronic acid is attached to the xylose units in the biomass. After this the acetyl groups of the xyloses in the hemicelluloses, are released slowly as acetic acid, but are much more resistant to pyrolysis.

The research reported in this chapter focuses on the formation of the biomass degradation products during the two independent steps. The aim is to give a good insight into the overall mass balance of the process. The effect of different parameters on the product yield and composition is analyzed such as biomass feedstock, torrefaction temperature and residence time.

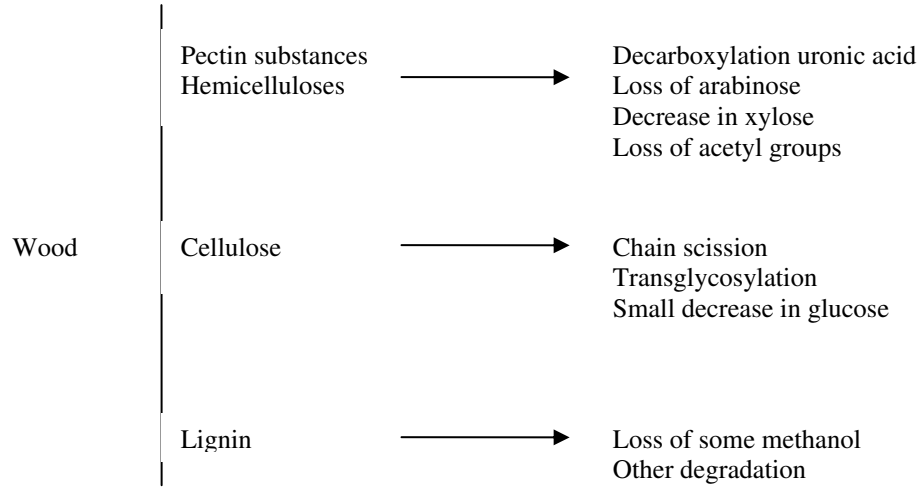


**Figure 5.1:** First chemical events in pyrolysis of wood at 250°C

## 5.2 Experimental

### 5.2.1 Materials

The experiments in the fixed bed reactor have been carried out with beech, willow, poplar, straw, cellulose and xylan. The TG-MS experiments have been carried out with beech, willow, xylan and straw. The biomass feedstock is supplied by the Energy Research Centre of The Netherlands (ECN) and the constituents are delivered from Sigma Aldrich. The particle size of the feedstock was a powder with maximum length of 2 mm. Knowledge of the composition of the biomass is important, because these parameters have an influence on the torrefaction process and hence on the torrefaction products. The elemental composition together with the calculated heating values of the several biomass feedstocks are shown in Table 5.3.

**Table 5.3:** Ultimate analysis of raw biomass samples for the torrefaction experiments in the fixed bed reactor and the TG-MS analysis

| Ultimate (wt%, dry basis) | Beech | Willow | Poplar | Straw |
|---|---|---|---|---|
| Carbon | 46.92 | 45.73 | 46.17 | 41.80 |
| Hydrogen | 5.85 | 6.09 | 6.06 | 5.56 |
| Nitrogen | 0.01 | 0.07 | 0.00 | 0.32 |
| Oxygen | 46.62 | 46.51 | 47.37 | 45.22 |
| Ash | 0.60 | 1.60 | 0.40 | 7.10 |
| Heating values (MJ/kg, dry basis) | | | | |
| HHV | 18.44 | 18.30 | 18.35 | 16.31 |
| LHV | 17.19 | 17.00 | 17.06 | 15.13 |

## 5.2.2 Fixed Bed Reactor setup

The biomass samples are torrefied at different temperatures in a quartz tube fixed bed reactor that is placed in a Carbolite vertical split tube oven which is electrically heated. Argon is used as inert and sweep gas to keep the system in absence of oxygen and remove the formed products to a coldtrap or gasbag. The coldtrap is a glass tube cooled with ice water and is used to collect the condensable volatiles and a gas bag is used to collect the permanent gases. The biomass is heated by the argon gas flowing through the reactor. The temperature in the bed of biomass is measured by a thermocouple which is placed into a quartz temperature wall.

Due to the temperature overshoot of the oven the reactor is heated up to the experimental temperature between 200 and 300°C. After stabilization of the temperature the biomass is dropped into the quartz tube reactor. The reactor bed is a porous ceramic plate. A batch of 5 – 10 gram of biomass is loaded in the reactor. The reactor is heated up to the desired temperature around 10°C/min before the isothermal temperature is reached. After the experiment the reactor is cooled down within 5 minutes to 200°C which is according the definition the lowest torrefaction temperature. In order to prevent the condensation of products the tube to the

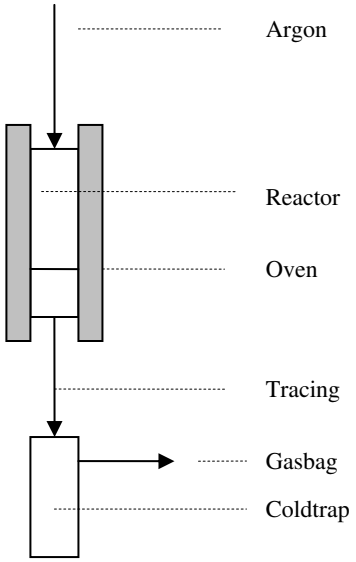


**Figure 5.2:** Schematic fixed bed torrefaction reactor setup

coldtrap is traced around 180°C. After the experiment the tracing is kept at this temperature for another 15 minutes.

### 5.2.3 Analyses Fix Bed Reactor experiments

All the reaction products in the fixed bed reactor experiments (a solid torrefied biomass, liquid product from the coldtrap and a permanent gas) are collected and weighed in order to make an overall mass balance. The torrefied wood, the liquid product and the gas are analyzed by using different techniques.

The composition of the (modified) solid product is analyzed by ultimate and proximate analysis. The heating values of the torrefied biomass (LHV and HHV) are calculated. The calculated HHV and LHV are calculated out of the results of elemental analysis [Channiwala et al., 2002]. The following formula is reported for the heating values of solid, liquid and gaseous fuels:

$$HHV_{dry} = 0.3491C + 1.1783H - 0.1034O - 0.015N - 0.0211Ash \quad (5.1)$$

$$LHV_{dry} = HHV_{dry} - 2.442\left(\frac{8.936H}{100}\right) \quad (5.2)$$

In which C, H, O, N, S, N and ash are the weight percentages of carbon, hydrogen, oxygen, sulphur, nitrogen and ash on dry basis.

The composition of the liquid product was analyzed with GC-MS by using two different columns on a Shimadzu QP5000. The liquid samples are prepared with isopropanol solutions and an internal standard of fluoranthene is used. Calibration lines have been constructed to quantify the amount of an organic fraction in the torrefaction condensables. The columns that are used are a Varian VF5 and a Varian CP-Wax 52. The method used and column parameters are found in Table 5.4 and Table 5.5 The produced permanent gas is collected in gasbags. The composition of the produced gas is analyzed by using a Varian Micro GC with a Poraplot and a Molsieve column.

**Table 5.4:** GC-MS analytical set up and parameters for analysis of condensable volatile products by using a Varian VF 5 column

| GC MS setup and parameters | |
|---|---|
| Gas chromatograph model | Shimadzu QP 5000 |
| GC column | Varian VF 5ms, 25m x 0.25 mm x 0.25µm |
| Injection method | 1.0µl split (dilution 1:4) |
| Temperature program | 40°C (5min), 10°C/min up to 250°C (15min) |
| Carrier gas | Helium |
| Source temperature | 250°C injection, 250°C interface |
| Mass range, scan rate | m/z 30 – 500, 0.1 s interval, 6000 amu/sec |

**Table 5.5:** GC-MS analytical set up and parameters for analysis of condensable volatile products by using a Varian CP Wax 52 column

| GC MS setup and parameters | |
|---|---|
| Gas chromatograph model | Shimadzu QP 5000 |
| GC column | Varian CP Wax 52, 25m x 0.32mm x 0.2 µm |
| Injection method | 1.0µl split (dilution 1:40) |
| Temperature program | 40°C (5min), 10°C/min up to 250°C (5min) |
| Carrier gas | Helium |
| Source temperature | 250°C injection, 250°C interface |
| Mass range, scan rate | m/z 30 – 500, 0.1 s interval, 6000 amu/sec |

### 5.2.4 Thermogravimetry – Mass Spectroscopy

Next to the experiments with the fixed bed setup, experiments have been carried out with thermogravimetry – mass spectroscopy. TG-MS is at the same time an "experimental" setup that torrefies the biomass and equipment that analyses the composition of the volatile fractions. TG/MS results in information concerning the thermal degradation of the input materials and the formation of torrefaction gases as a function of a temperature profile. The samples of 1- 5 mg are placed into a crucible and torrefied under a helium flow of 100 ml/min at a heating rate of 10°C/min from room temperature to 400°C.

In comparison to the TGA experiments that have been carried out for the development of the kinetic model in Chapter 4 no isothermal conditions are applied in the TG-MS experiments. The small sample size makes it impossible to analyze the mass of the volatile fractions that are formed during torrefaction at isothermal conditions. Small amounts of volatiles are not detectable. Dynamic heating conditions are required to determine the volatiles that are formed. Operating with larger amounts of sample will block the line to the mass spectrometer because of the formation of hydrocarbons with large molecular weight. The evolution of organic compounds as a function of the temperature is analyzed in a scan range m/z 10 – 150. The quadruple mass spectrometer operates with electron impact ionization at 70 eV electron energy. Ion-kinetograms of different ion-fragments are selected for the characterization of the evolved fragments, see Table 5.6.

**Table 5.6:** Compounds assigned to specific mass ion

| m/z values | Assigned to |
|---|---|
| 13,14, 15, 16 | CH, $CH_2$, $CH_3$, $CH_4$ |
| 17,18 | Water |
| 28 | Carbon monoxide |
| 29,31, 32, 43, 45, 58 | Alcohols and ethers |
| 44 | Carbon dioxide |
| 55, 56, 57, 58, 69, 70, 71 | Aliphatic hydrocarbon chains |
| 46, 59, 60, 74 | Acids |
| 29, 43, 58 | Ketones/aldehydes |
| 77,78, 91, 92 | Aromatic hydrocarbons |
| 93, 94, 107, 108, 109, 110 | Phenolics |
| 84, 98, 105, 110, 112, 114 | Other components |

### 5.2.5 Thermogravimetry – Fourier Transfer Infrared Spectroscopy (TG-FTIR)

The aim of performing TG-FTIR is to obtain qualitative information of the liquid and gas phase functional group composition of the evolved gasses of biomass as a function of the torrefaction temperature. The TG-FTIR analysis is carried with a TA Instruments 951 Thermogravimetric Analyzer and Bruker IFS 48 FTIR spectrometer. The sample is heated up to 400°C with a heating rate of 10°C/min in a $N_2$ inert atmosphere. The volatile products are transferred towards a heated gas cell into the FTIR spectrometer. The measurements are conducted betweed 3330 – 1025 $cm^{-1}$. Interferograms are continuously collected and transformed via a Gram Schmidt algorithm. Spectral windows, dedicated to functional groups are selected according to Table 5.7. The intensity within a spectral range as a function of the time and/or temperature describes the evolution of the functional groups during torrefaction of the biomass.

**Table 5.7:** Functional groups in the volatile fractions of biowaste torrefaction

| Wavenumber range ($cm^{-1}$) | Functional group |
|---|---|
| 3330 – 3050 | $H_2O$ |
| 3050 – 3000 | Methane, $C_{sp2}$-H stretch vibration (aromatic hydrocarbons) |
| 2990 – 2775 | C-H stretching aliphatic hydrocarbons |
| 2410 – 2235 | $CO_2$ |
| 2235 – 2050 | CO |
| 1830 – 1700 | carbonyl functional groups |
| 1140 – 1025 | C-O functional groups |

## 5.3 Results

### 5.3.1 Mass balances

This section describes the torrefaction yield of different biowaste streams as a function of time and temperature. The influence of different temperatures between 200 - 300°C and different residence times between 15 – 60 minutes have been researched. The overall mass balances of the fixed bed experiments for torrefaction of different biomass feedstock are shown in Figure 5.3 and Figure 5.4. The overall mass balance of the torrefaction experiments could be closed quite well in the range of 90 – 100%. There is some lost material because of gas leakages and condensable volatiles. From the same figures it is clear that with increasing temperature and residence time the amounts of gas and condensable volatiles increase while the yield of the solid product is decreasing. The impact of temperature is stronger than the impact of time as is shown in Figure 5.3. Between 10 and 30% of the willow is volatilized between 230 and 280°C. At 250°C also the influence of the residence time is researched. It is shown that the impact of the residence time on the total product yield is not very strong. The increase of volatilization from a residence of 15 minutes to a residence time of 60 minutes is about 6%. This means that the process is mainly heat transfer limited.

Figure 5.4 shows the overall mass balance of different woody feedstock, namely willow, poplar and beech.

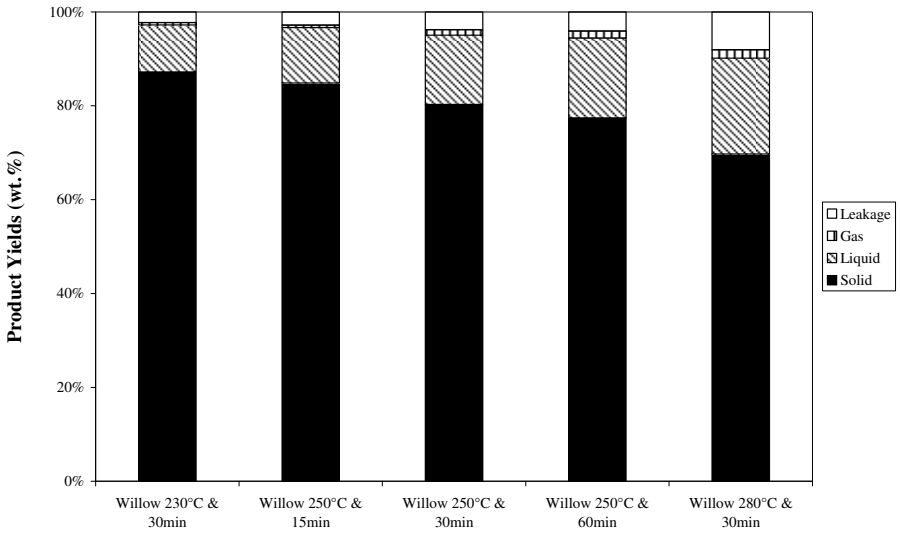


**Figure 5.3:** Overall mass balance for willow torrefaction experiments between 230 - 280°C and 15 – 60 min residence time

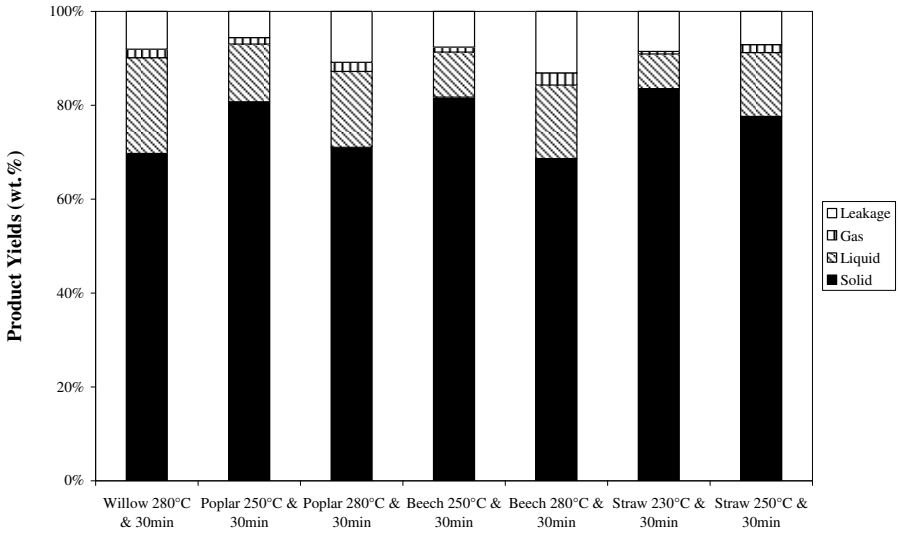


**Figure 5.4:** Overall mass balance for different biomass feedstock torrefaction experiments between 250 - 280°C and 30 min residence time

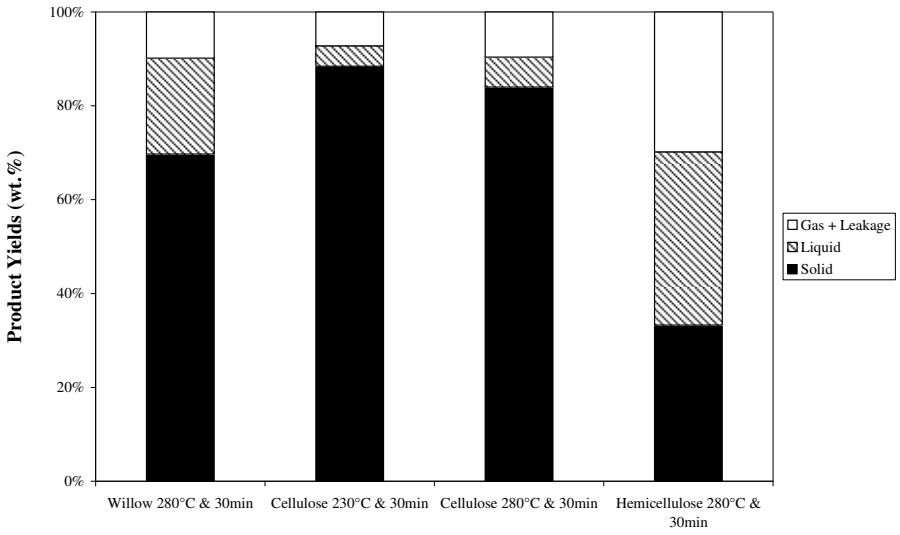


**Figure 5.5:** Overall mass balance for torrefaction of different biomass constituents at conditions between 230 and 280°C and 30 min residence time

The overall mass balances for cellulose and hemicellulose are given at different conditions and compared with the overall mass balance of deciduous wood willow at 280°C in Figure 5.5. It is shown that cellulose has a higher solid product yield which is approximately 84 wt % and still forms some condensable volatiles of around 10 wt % at 280°C. However, the solid product yield for willow is 70 wt% and the solid product yield of hemicellulose is 33 wt%. Moreover, there is a significant difference between the liquid product yields of cellulose, willow and hemicellulose. The liquid product yield of cellulose is only small, but willow and hemicellulose have higher liquid yields such as 20 wt % and 37 wt%, respectively. It is shown that almost 50% in the volatile phase comprises the condensable fraction. This indicates that the formation of liquid products can mainly be attributed to the hemicellulose degradation.

## 5.3.2 Kinetic model versus fixed bed results

In Chapter 4 a kinetic model for (beech) wood has been presented to observe the mass loss as function of time and temperature, which is the biomass that volatilizes to the gas phase. Figure 5.6 presents experimentally determined weight loss as a

function of time together with values calculated with the kinetic model given in Chapter 4. The upper data points show the loss of solid fraction into the gas phase for willow and beech after 30 minutes derived by the kinetic model. The lower data points show the the loss of solid fraction into the gas phase for willow and beech after 30 minutes after experiments in the fixed bed reactor. It is shown that there is good agreement between the model and the fixed bed experiments at the lower temperatures 230 and 250°C. At 280°C the model predicts a higher loss of solid fraction into the gas phase than is achieved in the fixed bed experiments. Secondary reactions and heat transfer effects may play a role for this lower the loss of solid fraction into the gas phase.

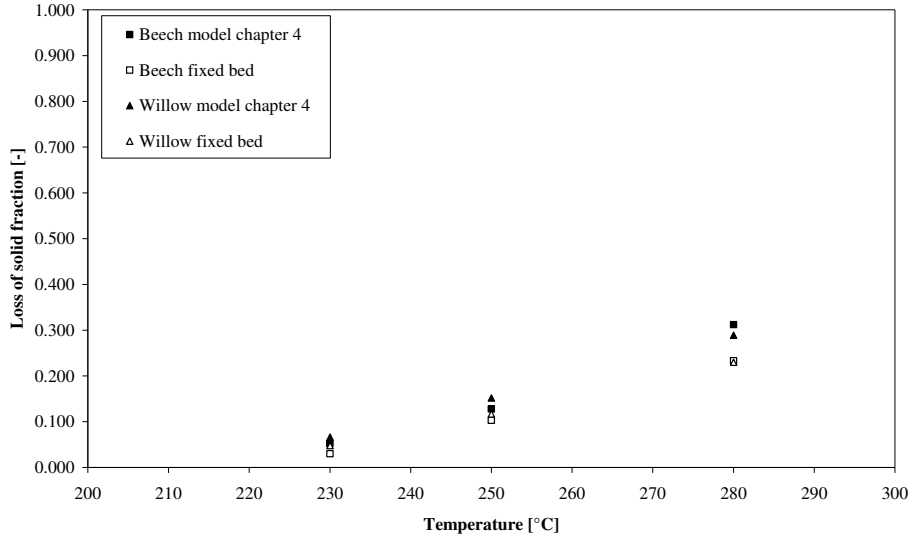


**Figure 5.6:** Yield of torrefied beech and willow in the fixed bed reactor as a function of temperature including the calculated values for the kinetic model for 30 minutes of torrefaction based on dry basis

## 5.3.3 Solid product composition

The modified solid product properties are the most important characteristics of the torrefaction process. It is important that during torrefaction the oxygen content

decreases. The chemical properties of the solid product are analyzed by using ultimate and proximate analysis and are shown in Figure 5.7. It is shown that the carbon percentage is significantly increased with increasing temperature and residence time. On the other hand, the hydrogen and oxygen content are decreasing. These changes in the elemental composition improve the heating values of the biomass (LHV and HHV). This trend shows that the atomic O/C and H/C ratio become more like coal (O/C around 0.5; H/C around 0.2).

In Figure 5.8 the lower heating values are given for the torrefaction of willow, beech, poplar wood and straw as function of temperature and residence time. It is shown that with increasing temperature the LHV of the different resources increase. It is shown that the LHV increases from 17 MJ/kg to 19.36 MJ/kg for torrefaction at 280°C and 30 min residence time. The LHV of beech and poplar are also increased from 17.20 MJ/kg to 20.30 MJ/kg and from 17.06 to 19.70 MJ/kg at the same reaction conditions, respectively. The LHV of straw is increased from 15.13 MJ/kg to 17.23 MJ/kg at 250°C and 30 min residence time. From these calculated lower heating values the energy densification can be derived, which is the LHV of the torrefied biomass divided by the LHV of the virgin biomass. In Figure 5.10 these values are shown. The maximum energy densification which is 1.16 is calculated for beech at 280°C and 30 min residence time. At 230°C and 30 min residence time, the energy densification values of willow, beech, poplar and straw are only a few percentages between 4 and 8 %, but at 280°C values around 15% are reached. Although, for the different biomass feedstock the lower heating values and energy densification show some small differences, the general trend is the same. The lower heating value is increasing with increasing torrefaction temperature. In Figure 5.9 it is shown how much of the energy is retained in the solid fraction and which LHV is related with it. It is shown that between 80 and 99% of the energy can be retained in the modified solid fraction depending on the conditions. Mild conditions do not lead to a major loss of energy instead of more extreme temperatures and residence times. Moreover, during the experiments it is observed that the volume of grinded straw is a factor 8 – 10 smaller than the raw straw. This is not further quantified, but it is clear that grinded biowaste has an enormous effect on the volumetric energy densification. As shown in Chapter 3 pelletization can increase the energy densification even more.

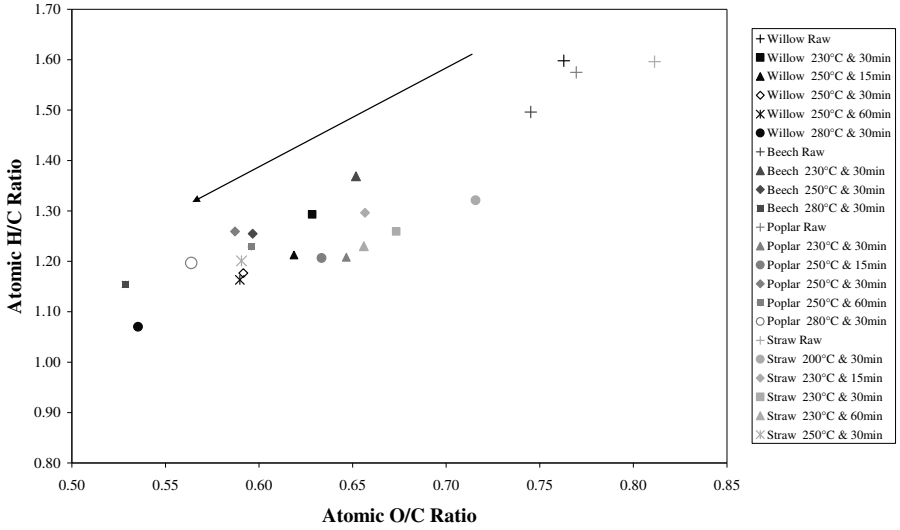


**Figure 5.7:** Van Krevelen diagram for raw and torrefied biomass at different reaction conditions

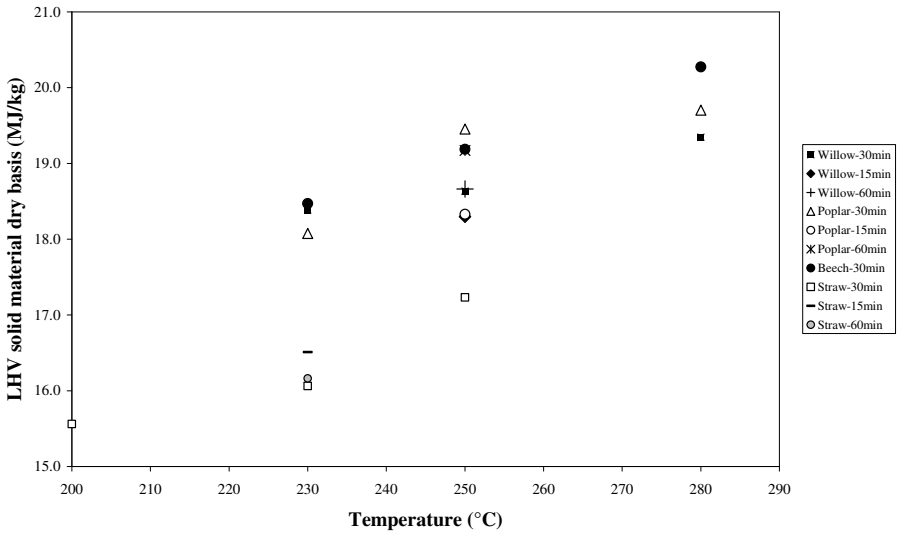


**Figure 5.8:** Lower heating value of torrefied wood as a function of temperature and residence time for different biomass feedstock. The LHV for the raw biomass feedstocks are for willow 17 MJ/kg, beech 17.2 MJ/kg, straw 15.13 MJ/kg and poplar 17.06 MJ/kg.

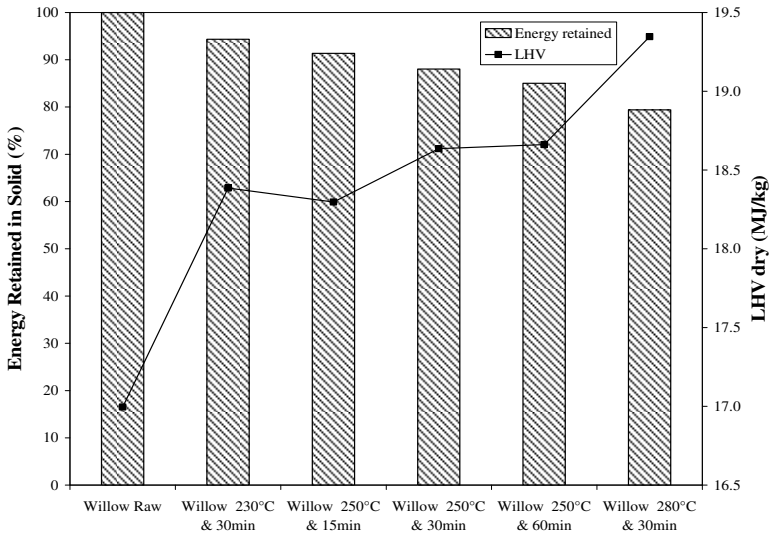


**Figure 5.9:** Energy retained in the solid product for willow torrefaction at different reaction conditions

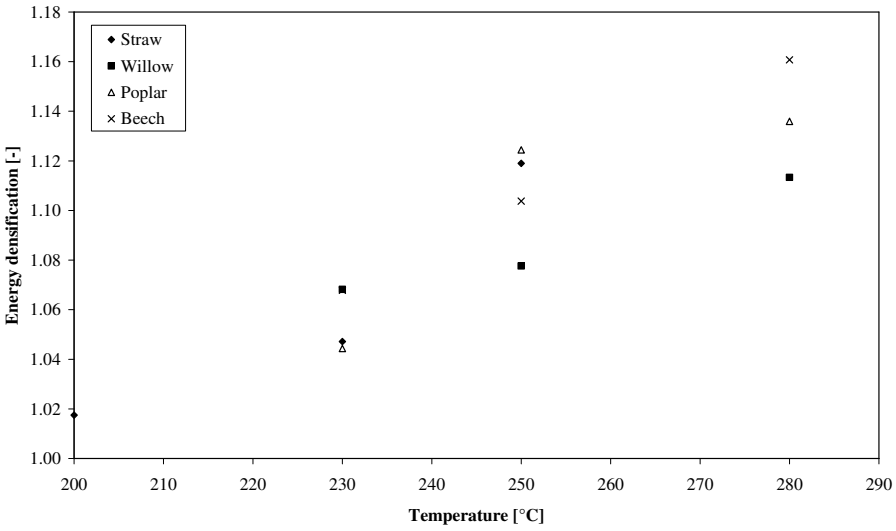


**Figure 5.10:** Energy densification during torrefaction of different biomass resources with residence time of 30 min at different reaction temperatures.

### 5.3.4 Liquid product composition

The liquid product which is the volatile fraction that condenses in the coldtrap is a complex mixture of various oxygenated organic compounds and water. In the torrefaction process design these volatiles can be combusted to produce heat to sustain the process at the right torrefaction temperature. The product yields of the condensable volatiles are shown in Figure 5.11. It is seen that the product yields increase with temperature and residence time. Acetic acid and water are the main liquid torrefaction products of willow, poplar and beech. However, small quantities of methanol, furfural and phenol are found. It is seen that the yields of furfural and phenol are very small compared to the yields of acetic acid and methanol. This is expected due to the fact that the degradation rates of lignin and cellulose are very low at temperatures below 300°C. In Chapter 4 it is shown that lignin and cellulose are reactive at these temperatures, but only with long residence time a certain mass loss is shown. Since it is known that phenol (and other aromatic compounds) is mainly coming from the lignin fraction of the biomass, the very low yield is expected under these conditions with low temperature and residence times smaller than 30 min. The formation of furfural is observed for willow and beech, because the dehydration of xylose in the hemicellulose fraction is the main reason for the furfural degradation.

In Figure 5.12 a more detailed composition of the torrefaction liquid is given for different types of biomass at different conditions. It is already observed that the maximum condensable yield belongs to acetic acid compared to the yields of other products. The yield of methanol is lower than the yield of the acetic acid, but higher than the yield of the other condensables. Next to acetic acid it is observed that the condensable fraction of the torrefaction gas contains other carboxylic acids like formic acid and propionic acid. The yields of acetic acid, methanol, furfural, formic acid and acetone are the most pronounced condensables and increasing in amount with increasing temperature. On the other hand, though small also the amounts of products such as propionic acid, 1-hydroxy-2-propanone, furfuryl alcohol, phenol, ethyl acetate and oxalic acid could be quantified.

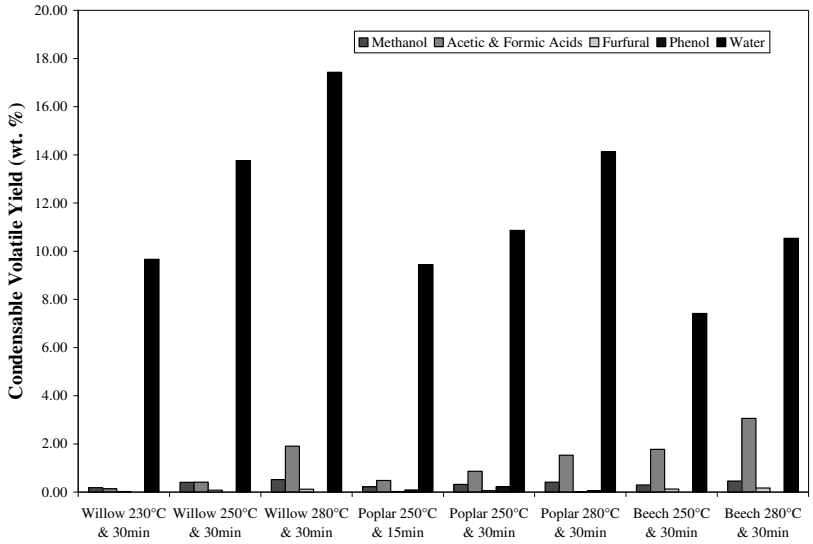


**Figure 5.11:** Product yields of condensable volatiles at different reaction conditions for willow, poplar and beech wood, including around 6% moisture

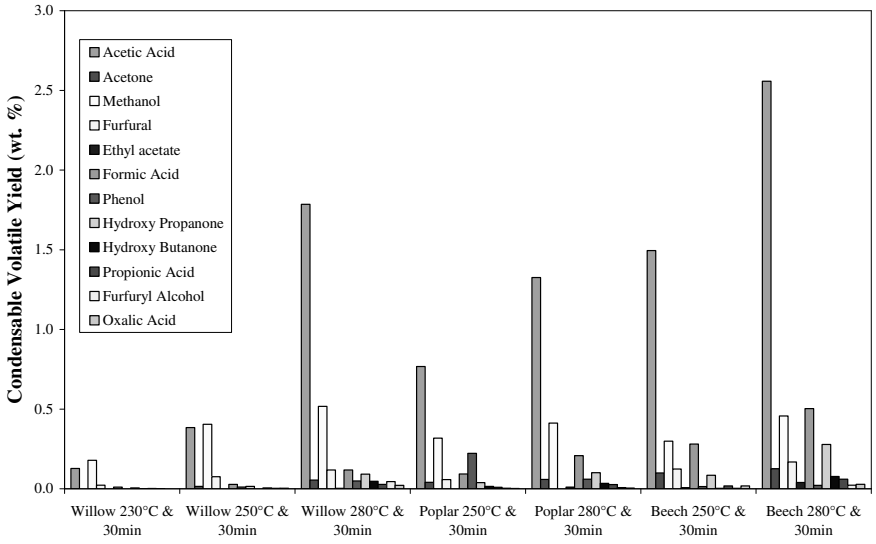


**Figure 5.12:** Product yields of condensable organic volatiles at different reaction conditions for willow, poplar and beech wood

### 5.3.5 Gas product composition

The composition of the permanent gas products for each type of biomass is presented in Figure 5.13. Besides CO and $CO_2$ traces of hydrogen and methane are found in the torrefaction gas. It is seen that carbon dioxide is more dominanct in the gaseous product. The weight percentages of carbon dioxide and carbon monoxide are increasing with temperature and residence time. When the temperature is increased to 280°C, the summation of the weight percentages of CO and $CO_2$ become 1.7 wt%, 1.8 wt% and 2.5%wt for willow, poplar and beech, respectively. When the different biomass resources are compared with each other, it is seen that they have nearly the same gas compositions at the same conditions. This is expected because of the deciduous character of the biomass resources.

In Figure 5.15 and Figure 5.16 the formation of carbon dioxide and carbon monoxide is shown for willow, beech, straw and poplar as a function of time. It is observed that the amount of produced carbon dioxide and carbon monoxide is higher for straw compared to the other biomass types. Since it is known from literature that inorganic material enhances the formation of CO and $CO_2$ it is expected that straw torrefaction leads to higher CO and $CO_2$ weight percentages during time. The general trend for the evolution of CO and $CO_2$ is the same for the different biomass resources. Looking at the profiles of the overall weight loss curves in Chapter 4 it is shown that the patterns are comparable. The production rate of carbon dioxide and carbon monoxide becomes smaller in time after 25 min. It can be concluded that torrefaction is mainly finished after this time. Further it is shown in the same figures that the production of the permanent gases reaches a certain saturation point. Finally, it is observed that the ration $CO_2$/CO decreases in time, see Figure 5.14. The increased carbon monoxide production can be explained by secondary reactions that occur in the gas phase by the reaction of carbon dioxide and steam with porous char to carbon monoxide. As the reaction proceeds more carbon dioxide is reacting to carbon monoxide.

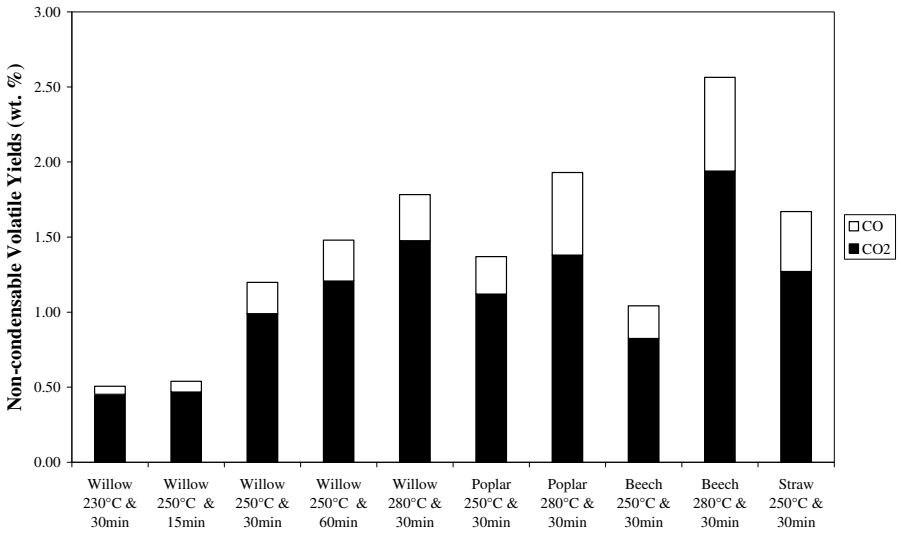


**Figure 5.13:** Non-condensable yields for willow, poplar and beech wood at different torrefaction reaction conditions

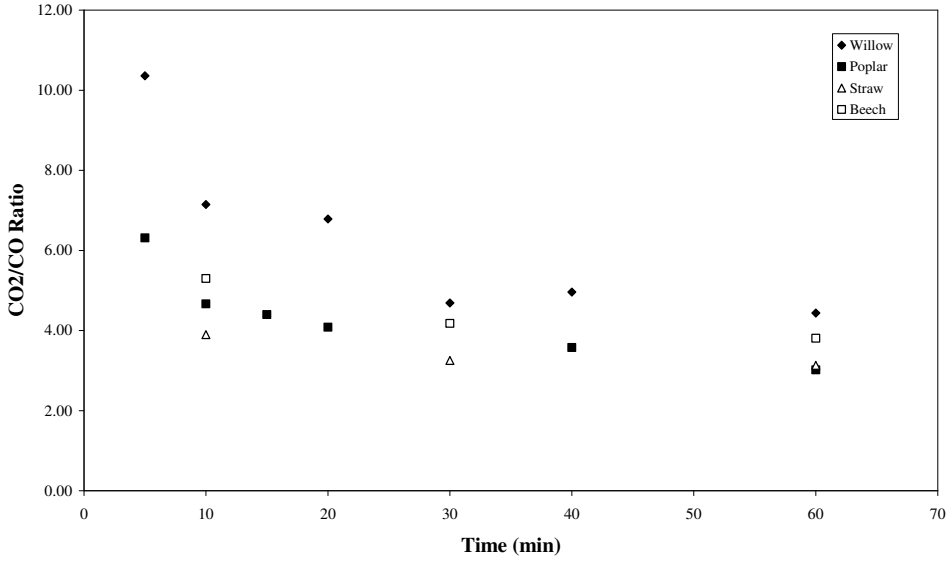


**Figure 5.14:** $CO_2$/CO ratio for different biomass feedstock at 250°C

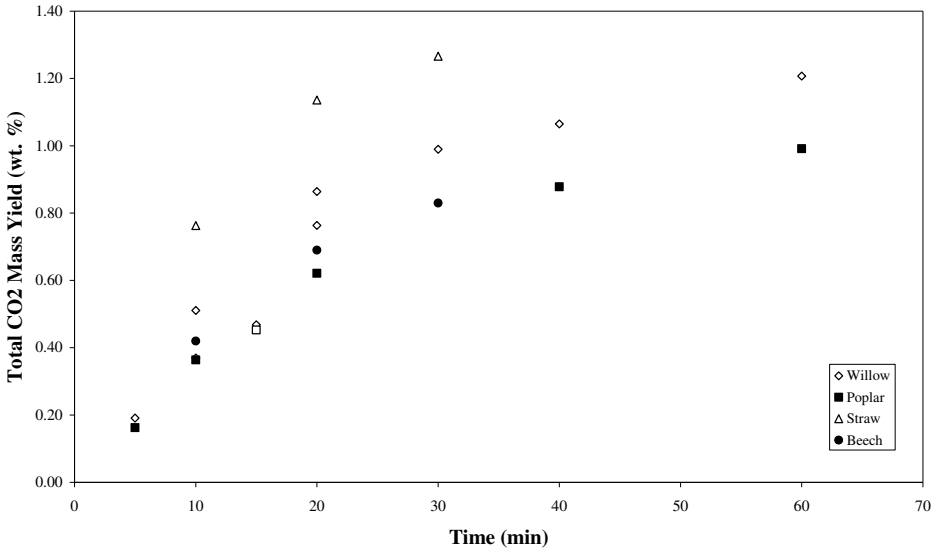


**Figure 5.15:** $CO_2$ production profile for different biomass feedstock at 250°C

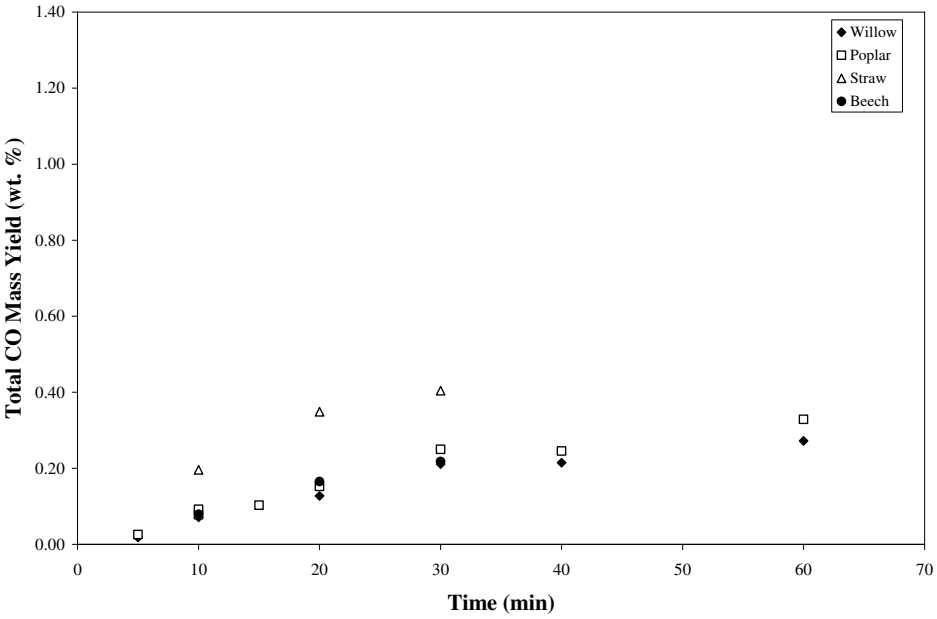


**Figure 5.16:** CO production profile for different biomass feedstock at 250°C

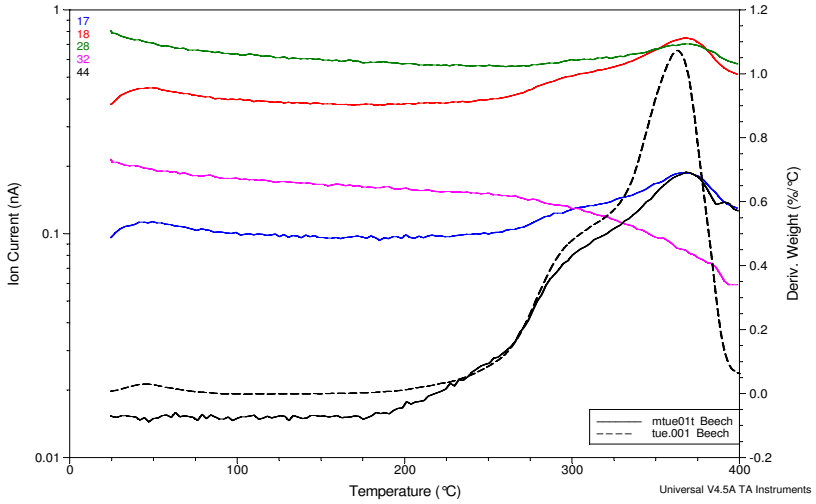


**Figure 5.17:** Derivative of the weight loss of beech wood and the evolution of the mass fragment ions 17, 18, 28, 32 and 44 in function of temperature (25 - 400°C)

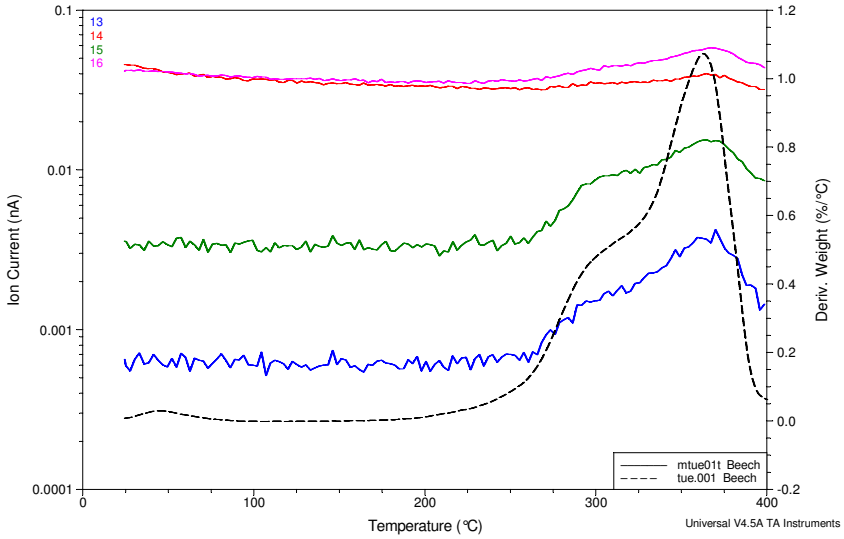


**Figure 5.18:** Derivative of the weight loss of beech wood and the evolution of the mass fragment ions 13, 14, 15 and 16 in function of temperature (25 - 400°C)

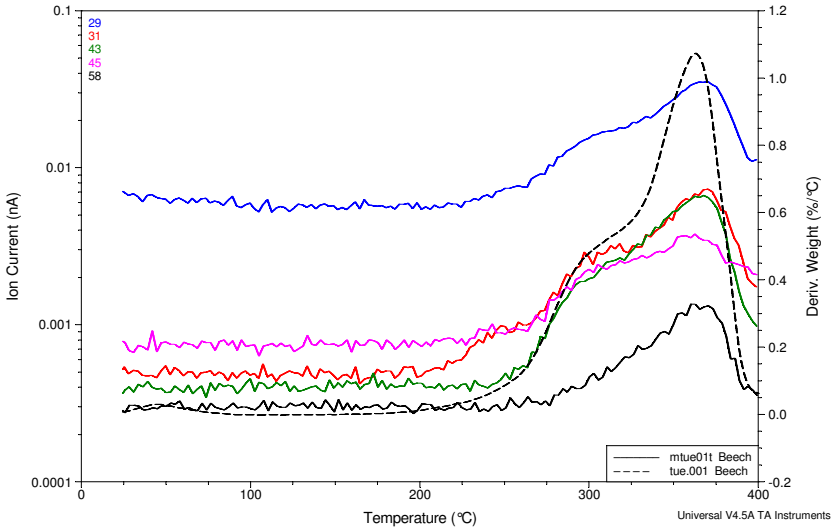


**Figure 5.19:** Derivative of the weight loss of beech wood and the evolution of the mass fragment ions 29, 31, 43, 45 and 58 in function of temperature (25 - 400°C)

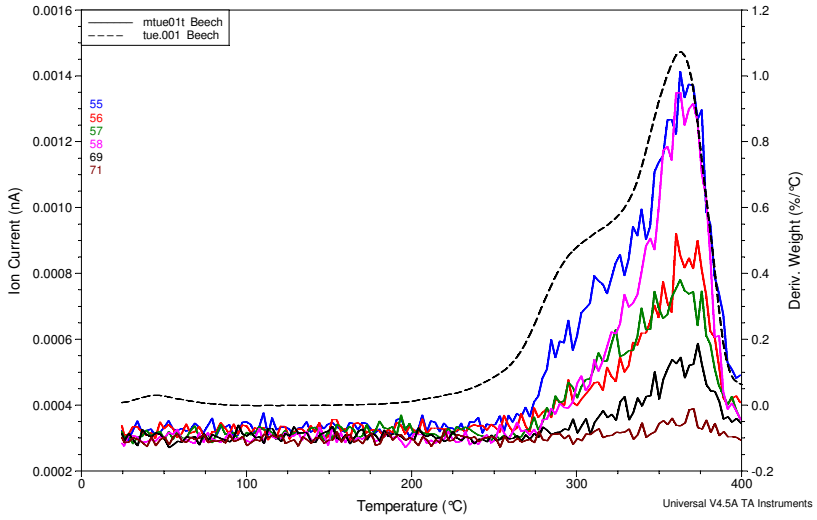


**Figure 5.20:** Derivative of the weight loss of beech wood and the evolution of the mass fragment ions 55, 56, 57, 58, 69 and 71 in function of temperature (25 - 400°C)

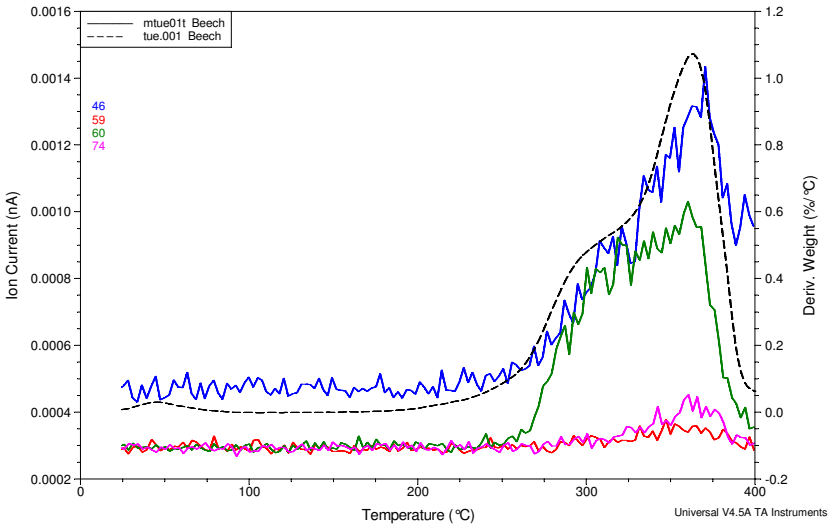


**Figure 5.21:** Derivative of the weight loss of beech wood and the evolution of the mass fragment ions 46, 59, 60 and 74 in function of temperature (25 - 400°C)

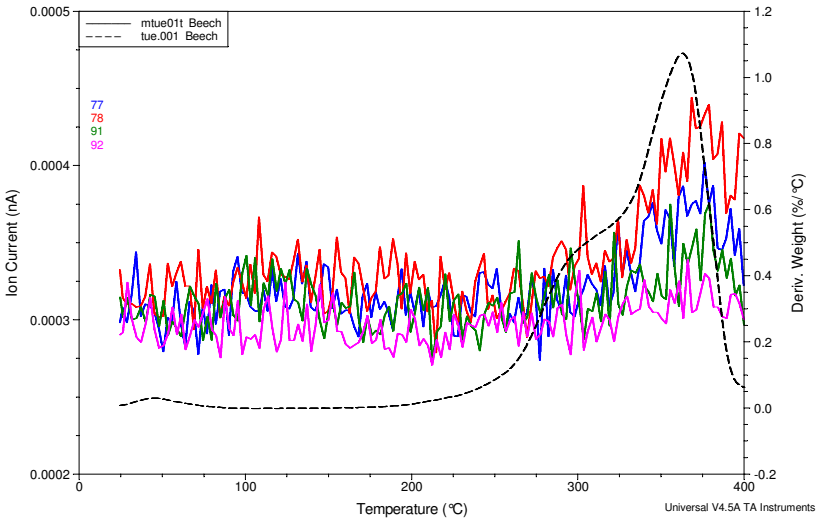


**Figure 5.22:** Derivative of the weight loss of beech wood and the evolution of the mass fragment ions 77, 78, 91 and 92 in function of temperature (25 - 400°C)

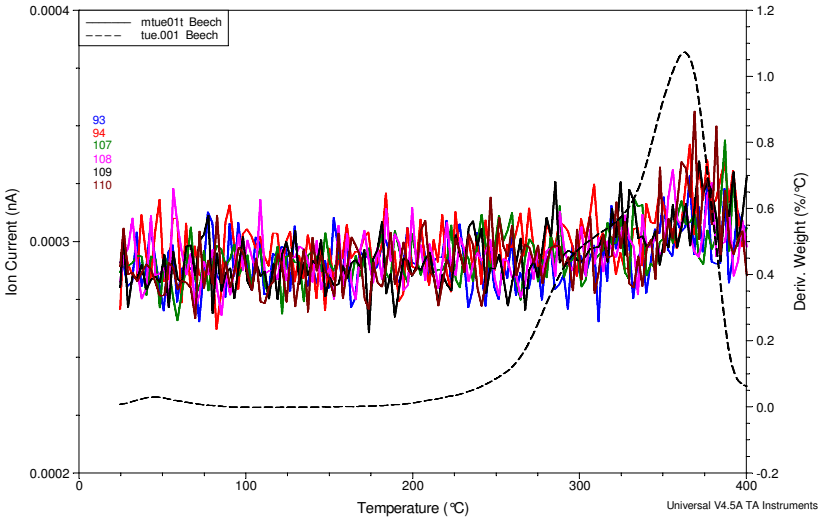


**Figure 5.23:** Derivative of the weight loss of beech wood and the evolution of the mass fragment ions 93, 94, 107, 108, 109, 110 in function of temperature (25 - 400°C)

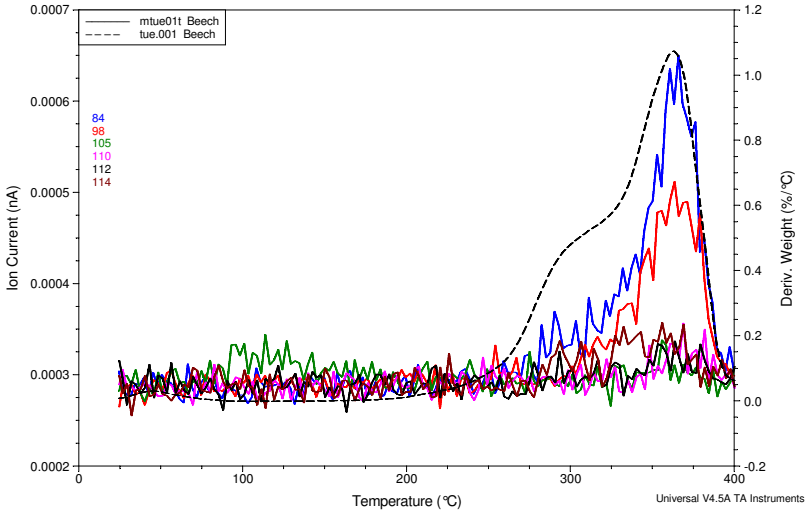


**Figure 5.24:** Derivative of the weight loss of beech wood and the evolution of the mass fragment ions 84, 98, 105, 110, 112 and 114

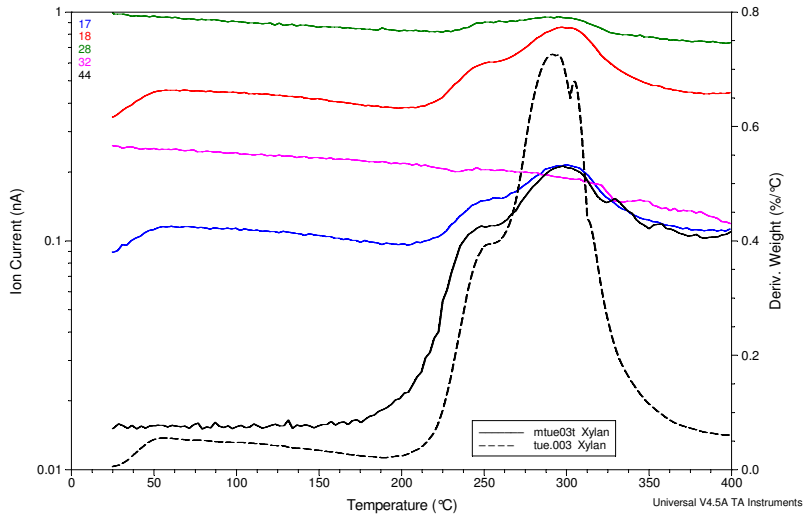


**Figure 5.25:** Derivative of the weight loss of xylan and the evolution of the mass fragment ions 17, 18, 28, 32 and 44 in function of temperature (25 - 400°C)

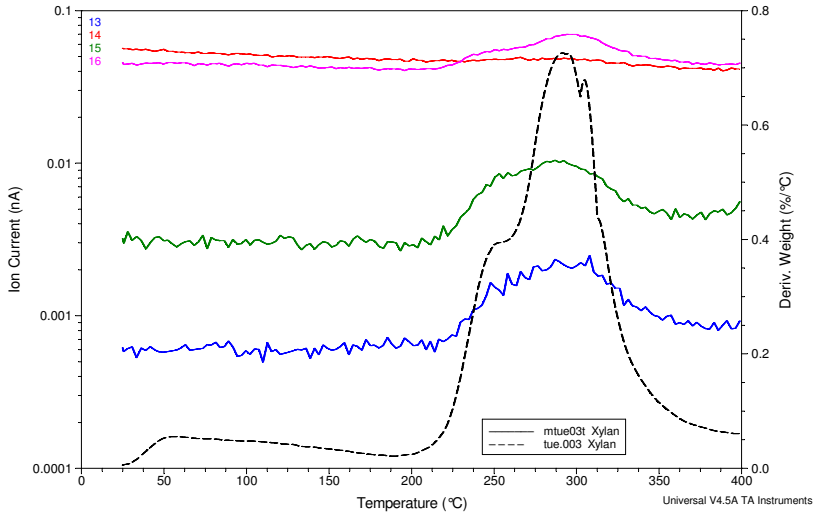


**Figure 5.26:** Derivative of the weight loss of xylan and the evolution of the mass fragment ions 13, 14, 15 en 16 in function of temperature (25 - 400°C)

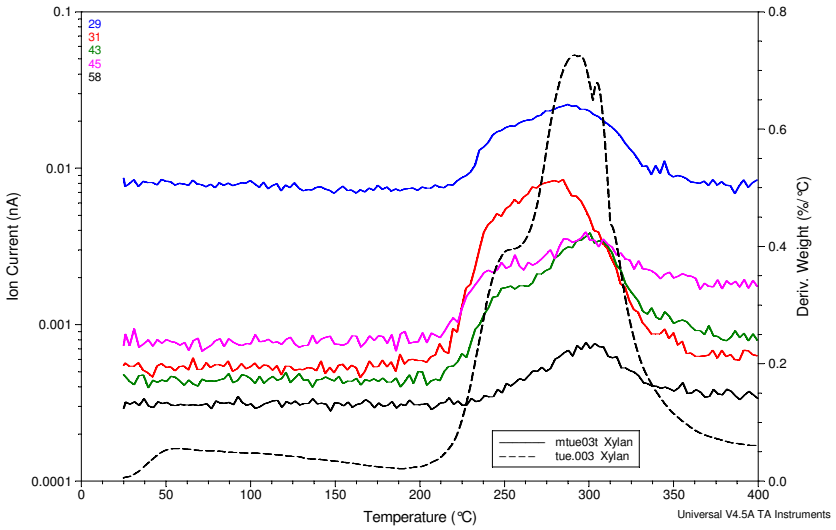


**Figure 5.27:** Derivative of the weight loss of xylan and the evolution of the mass fragment ions 29, 31, 43, 45 and 58 in function of temperature (25 - 400°C)

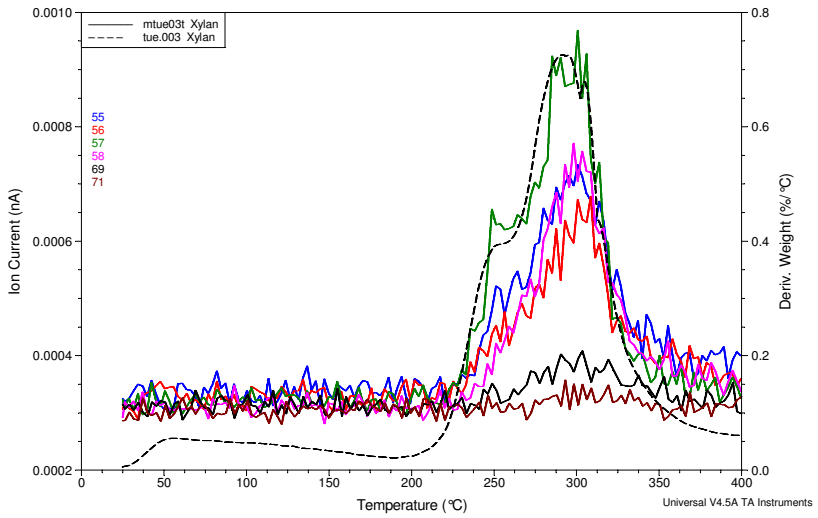


**Figure 5.28:** Derivative of the weight loss of xylan and the evolution of the mass fragment ions 55, 56, 57, 58, 69 and 71 in function of temperature (25 - 400°C)

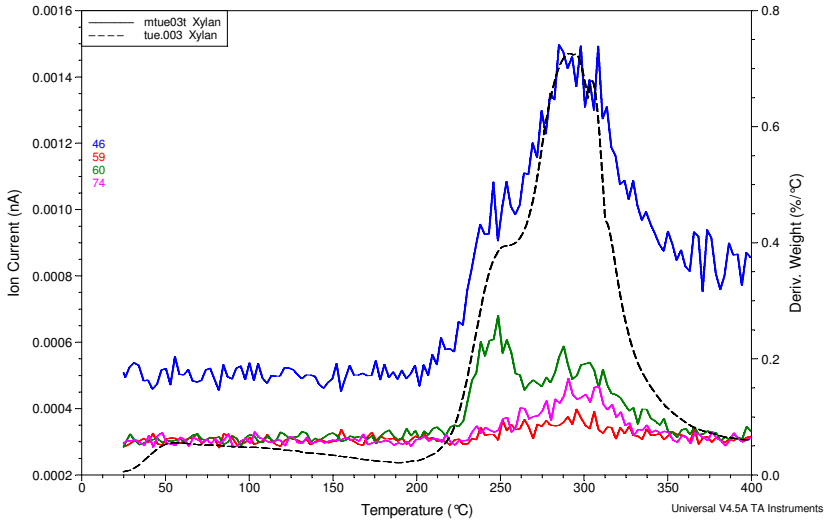


**Figure 5.29:** Derivative of the weight loss of xylan and the evolution of the mass fragment ions 46, 59, 60, 74 in function of temperature (25 - 400°C)

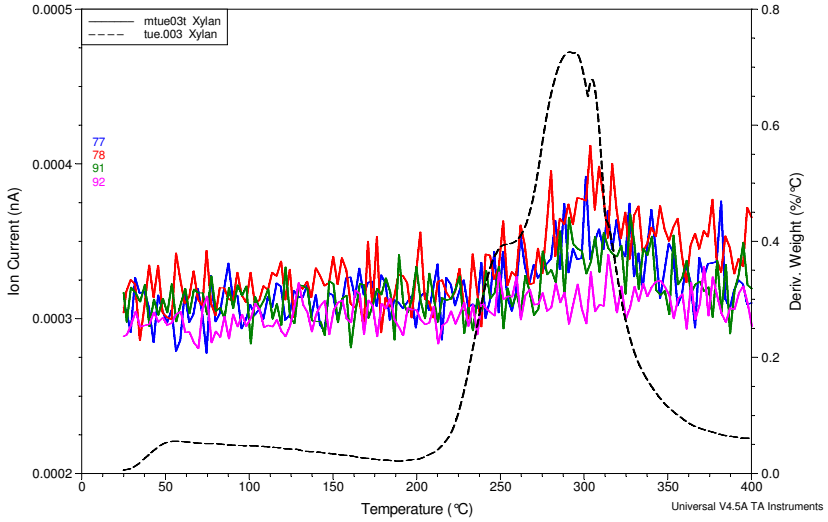


**Figure 5.30: :** Derivative of the weight loss of xylan and the evolution of the mass fragment ions 77, 78, 91 and 92 in function of temperature (25 - 400°C)

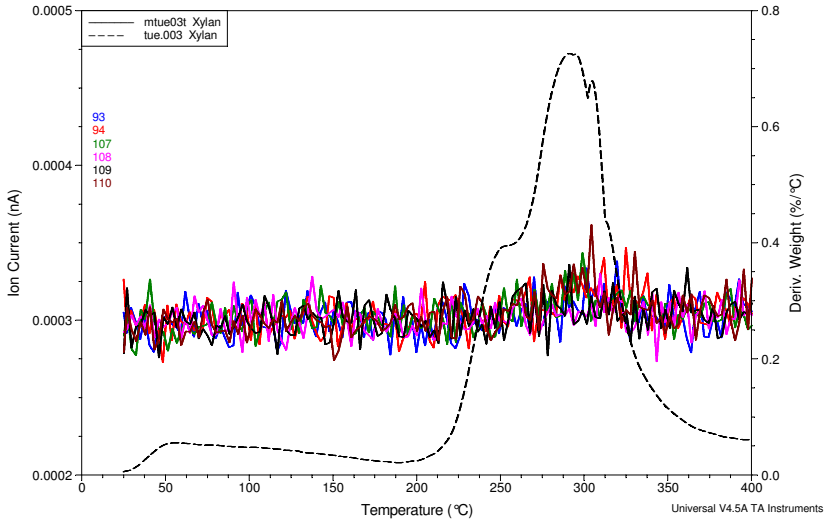


**Figure 5.31:** Derivative of the weight loss of xylan and the evolution of the mass fragment ions 93, 94, 107, 108, 109 and 110 in function of temperature (25 - 400°C)

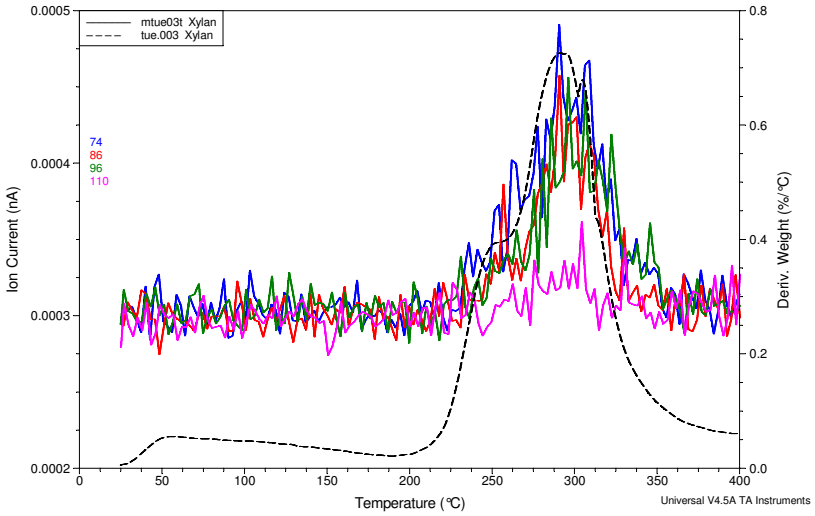


**Figure 5.32:** Derivative of the weight loss of xylan and the evolution of the mass fragment ions 74, 86, 96 and 110 in function of temperature (25 - 400°C)

### 5.3.5 TG MS of beech wood

The aim of performing thermogravimetric/mass spectroscopy is to gain qualitative information on the liquid and gas composition of the torrefaction of biomass as a function of the temperature up to 400°C. TG analysis provides valuable information on the kinetics which is studied in Chapter 4, but it does not provide unique information about the nature of the evolving volatile components [Lievens, 2007]. The nature and the identification of the formed compounds can be investigated by TG-MS. TG-MS experiments have been carried out for beech wood, willow, xylan and straw. A close look is given to the thermal degradation of beech wood and xylan. The degradation of willow and straw is comparable with each other and beech wood.

Figure 5.17 - Figure 5.24 show the ion-kinetograms and the relating derivative thermogravimetry (DTG) of beech wood between 25 - 400°C. The DTG curve shows the degradation profile of beech wood by its thermal stability. The evolution of the m/z values is shown as function of the temperature. Two distinct thermal events can be observed just before 100°C and 400°C, together with a plateau at 300°C and a peak at around 350°C. The first peak before 100°C is assigned to the drying of the beech wood. Free residual water is released and corresponds with a weight loss of around 3%. The decomposition of the beech wood starts around 180 - 200°C with a first plateau at 280 - 300°C and corresponds to a weight loss of around 25%. This mass loss can be mainly assigned to the degradation of the hemicellulose in the beech wood. The decomposition of beech wood up to 400°C coincides with the formation of different degradation products which can be identified partially with TG-MS and by GC-MS of the products that are formed in the fixed bed experiments.

Figure 5.17 shows the derivative of the weight loss of beech wood and the evolution of the mass fragment ions 17, 18, 28, 32 and 44 in function of the temperature between 25 - 400°C. The intensity of the curve is not in relation with the quantitative amount of product that is formed. It is shown that in the first part of the curve below 100°C moisture is evaporated, but at higher temperatures from 200°C also chemical water is formed in two steps. The broad peak means that different mechanisms occur to release the water. The two steps superpose with the two steps in which the beech wood decomposes, but there is a difference in the

intensity. Also the mass fragments that correspond with the formation of CO and $CO_2$ are formed during two steps.

Figure 5.18 shows the derivative of the weight loss of beech wood and the evolution of the mass fragment ions 13, 14, 15 and 16 as function of temperature. It is difficult to appoint the mass fragments to certain molecules since these mass fragments could be secondary degradation products of formed primary products. Ion fragment 16 ($CH_4$) is often ascribed to the formation of methane, but micro GC analysis does not confirm the formation of methane in the temperature range of torrefaction. With TG-MS the ion fragment m/z = 16 can also mean the formation of methanol (m/z divided by $2e^-$ because of ionisation) which is also related with ion fragment m/z = 31. It can be seen that the methanol is also formed during two decomposition steps of the beech wood. Fragments 13, 14 and 15 can be side groups of molecules that are released.

Polar components like alcohols, glycols and carbonyl compounds are released from 225°C. Figure 5.19 shows the derivative of the weight loss of beech wood and the evolution of the mass fragment ions 29, 31, 43, 45 and 58 as function of temperature. The figure shows the release of the alcohols, ketones and aldehydes like methanol and acetaldehyde, because carbonyl functionalities are observed. There is a good relation between the evolution of compounds with carbonyl functionality. The ion fragments with m/z values 29, 43 and 58 are formed around 250 - 400°C. According to [Lievens, 2007] the assignment of masses 29, 43 and 58 can be explained by a cleavage reaction of an ether with rest groups H, $CH_3$, $C_2H_5$. The formation of these fragments is shown in Figure 5.18 and Figure 5.19. Just like m/z = 16 it is shown that methanol is released in two steps. Fragment m/z = 58 can mean the release of a few oxygenated isomers like acetone and propanol. The m/z = 29 confirms the formation of propanol during the TG-MS experiments. These products are also formed in two steps during the degradation of beech wood.

Figure 5.20 shows the derivative of the weight loss of beech wood and the evolution of the mass fragments 55, 56, 57, 58, 69 and 71 as function of the temperature. These fragments could be assigned to aliphatic saturated and unsaturated hydrocarbon chains. The formation of these compounds is probably the result of side chain cleavages. The ion fragments 57 and 71 are saturated

hydrocarbon chains and 55,56 and 69, 70 unsaturated hydrocarbon chains. The ion kinetograms of 55, 66, 57 and 58 ($C_4$) are very similar to each other and are first formed at around 270°C with a maximum formation around 350 - 370°C. The formation of mass fragments with values m/z of 69, 71 (C5) starts at a little higher temperatures. Also the maximum formation is at a little higher temperature. It can be concluded that $C_4$ and $C_5$ are probably formed from the side chains of different fragments in the biomass.

Figure 5.21 shows the derivative of the weight loss of beech wood and the evolution of the mass fragment ions 46, 59, 60 and 74. These fragments could be assigned to the formation of the hydrocarbon acids, namely formic acid, acetic acid, propionic acid. The ion fragment evolution is almost the same for all components although m/z values 59 and 74 have a smaller temperature range in which they are formed. Mass fragments m/z 46 and 60 have a broad range in which the formation occurs. It is shown that both fragments are formed from the same constituent in the biomass. Different fragmentation reactions occur for the evolution of fragments 46 and 60 in comparison with 59 and 74.

The formation of aromatic structures is tried to assign to the mass fragments with values m/z 77, 78, 91 and 92 in Figure 5.22. It is shown that these components are formed starting around 300°C, but a lot of noise in the measurement is observed. It is difficult to separate two different steps in the reaction mechanism for these mass fragments. Aromatic structures are mainly formed due to the degradation of lignin. Figure 5.23 shows the derivative of the weight loss of beech wood and the evolution of the mass fragment ions with m/z values 93, 94, 107, 108, 109 and 110. These m/z values are assigned to the formation of phenolic derivatives due to the lignin decomposition. Although a lot of noise is shown in the figure it looks like that the phenol derivatives are formed in one step in the higher temperature range.

In Figure 5.24 the derivative of the weigh loss of beech wood and the evolution of mass fragment ion with m/z value 84, 98, 105, 110, 112, 114 is shown. The m/z values are assigned to the formation of furan derivatives. It is shown that some furan derivatives are formed in a broad temperature range and others in a single step at the higher temperatures.

### 5.3.6 TG MS of xylan

Figure 5.25 – Figure 5.32 show the ion-kinetograms and the relating derivative thermogravimetry of xylan between 25 - 400°C. The DTG curve shows that the degradation of xylan is a stepwise degradation with initial moisture loss. As it is already shown in Chapter 4, xylan is more reactive than beech wood at lower temperatures. At higher temperatures the possible mass loss of beech wood is higher than the mass loss of hemicellulose model compound xylan. The ion-kinetograms for xylan are comparable to the mass loss of beech wood. An extended description about all the effects is given in the paragraph about the beech wood decomposition.

Two distinct thermal events can be observed in the DTG curve of xylan around 100°C and between 200 - 350°C. A shoulder in the reaction pattern is observed at 250°C which means that the degradation of the xylan occurs in two steps. This shoulder is at a lower temperature than the one for beech wood which is at 300°C. This means that two different steps in the reaction mechanism do not automatically result in the conclusion that more constituents in the biomass react. The decomposition of the xylan up to 350°C coincides with the formation of different degradation products which can be identified partially with TG-MS. A big difference with the product formation between xylan and beech wood is the formation of aromatics and phenolics. Figure 5.31 shows so much noise in the signal that it is impossible to observe if phenolics are formed in the thermal degradation of xylan. Also the formation of aromatic hydrocarbons is difficult to observe during torrefaction of xylan, see Figure 5.30.

The formation of smaller molecules by the thermal decomposition of xylan is more clear to observe. Figure 5.25 shows the derivative of the weight loss of xylan and the evolution of the mass fragment ions 17, 18, 28, 32 and 44 in function of the temperature between 25 - 400°C. The intensity is not in relation with the quantitative amount of the product that is formed. From 200°C it is shown that $CO_2$ is formed together with CO. The production of moisture is shown over the full temperature range (physical and chemical water).

Figure 5.25 - Figure 5.32 show the formation of alcohols, aldehydes, ketones, ethers, aliphatic hydrocarbons and acids. It is shown that the formation of alcohols,

aldehydes, ketones and ethers occur in a broad temperature range. The formation of aliphatic hydrocarbons occur in two steps, but a difference can be seen in the intensity at which $C_4$ and $C_5$ hydrocarbons are formed from the side chains due to thermal cleavage. It is seen in Figure 5.29 that the formation of acids occur in two steps, but the intensity for formic acid (m/z value 46) is increasing with temperature, but fragment with value m/z = 60 becomes less intense with temperature. The release of aromatic compounds is observed at enhanced temperature (Figure 5.30).

### 5.3.7 TG-FTIR of beech wood

Dynamic TG/FT-IR experiments have been performed on the torrefaction of beech wood. The temperature range is extended to 200 - 400°C since it is not possible to study isothermal conditions. To investigate the changes in functional groups during the torrefaction, the FTIR analysis was employed qualitatively in this work. TG analysis coupled with Fourier transformed infrared spectroscopy has been applied to study the compounds evolving in the pyrolysis of biomass. It provides important information on the devolatilisation of materials, that is, the identification of major volatile species and the typical temperature range of release, with a continuous measurement [Biagini et al., 2006]. The dynamic heating rate is 10°C/min which means that time is directly connected with temperature. Figure 5.33 - Figure 5.40 show the evolution of different spectral ranges of wave numbers between 1000 and 3000 $cm^{-1}$ as a function of time and/or temperature. In this work, the organic compounds released during the Devolatilization are grouped in classes. Compounds with characteristic C-H bond are classified in the saturated hydrocarbon group (wavenumber interval 2775 – 2990 $cm^{-1}$). Compounds with characteristic carbonyl bond typical of acids, esters, aldehydes, and ketones (wavenumber interval 1700 – 1830 $cm^{-1}$) are C=O compounds with general formula R-(C=R)-Y with Y is OH, OR, H or R and correspond to the C=O stretching. The other compounds that are released are mainly $H_2O$ (wavenumber interval 3050 – 3330 $cm^{-1}$), $CH_4$ and C-H stretch vibration (aromatic hydrocarbons, unsaturated hydrocarbons) (wavenumber interval 3000 – 3050 $cm^{-1}$), $CO_2$ (wavenumber interval 2235 – 2410 $cm^{-1}$), CO (wavenumber interval 2050 – 2235 $cm^{-1}$) and C-O functional groups (wavenumber interval 1025 – 1140 $cm^{-1}$).

It should be noted that the Figure 5.33 - Figure 5.40 have a different scale at the y-axis to describe the absorbance intensity of evolving gases due to torrefaction. Comparing different peaks with other is difficult because of the response factor of different components with the equipment. Figure 5.33 shows the evolution of C-O functional groups as a function of temperature. It is shown that with increasing temperature the intensity of C-O functionality also increases having its maximum intensity around 300 - 330°C. The DTG curve has its maximum weight loss at a little higher temperature around 350 - 375°C which is seen in Figure 5.17 - Figure 5.24. After its maximum intensity is reached the intensity of the evolution of C-O functionality decreases and stabilizes. Only a single reaction step is observed in the evolution of C-O functionalities. Figure 5.34 shows the evolution of carbonyl functionalities during the torrefaction of beech wood as function of temperature. It is shown that with increasing temperature the intensity of carbonyl functionalities increases having a maximum at around 300 - 330°C. It is clearly seen that the evolution of carbonyl functionalities as function of temperature has the same profile as the DTG of beech wood. It is clearly shown that C-O functionalities and carbonyl functionalities do not have the same evolution profile. It can be concluded that different mechanisms are responsible for the formation of both functionalities.

Figure 5.35 and Figure 5.36 show the evolution of CO and $CO_2$ during the torrefaction of beech wood as function of temperature. It is clearly shown that both the evolution of CO and $CO_2$ has two different peaks at the same temperature. Both have a maximum (local) intensity around 300 - 330°C and around 400°C. The intensity of CO is higher at 300°C than at 400°C and $CO_2$ intensity is higher at 400 than at 300°C.

Figure 5.37 and Figure 5.38 show the evolution of C-H stretching of aliphatic saturated hydrocarbons and the C-H stretch vibration of aromatic hydrocarbons and/or unsaturated hydrocarbons as function of the temperature. C-H stretching of saturated hydrocarbons starts already between 200 - 300°C, but C-H stretch vibration of aromatic hydrocarbons and unsaturated hydrocarbons only occurs above 300°C.

Finally, Figure 5.39 shows the evolution of $H_2O$ during the torrefaction of beech wood as function of temperature. It is shown that the intensity of the absorbance of the evolution of $H_2O$ is increasing over the whole temperature range from 100 - 400°C. Comparing this with Figure 5.17 the derivative of the weight loss of beech wood and the evolution of the mass fragment ion 18 the experiments confirm each other. Physical and chemical bounded water are formed over the temperature range 100 - 400°C.

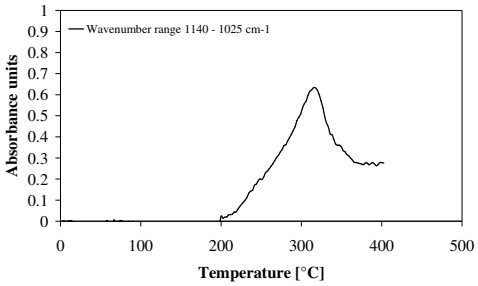


**Figure 5.33:** FTIR spectrum of beech wood torrefaction including the temperature range 200 - 300°C with wavenumber 1140 – 1025 $cm^{-1}$ which is ascribed to C-O functional groups

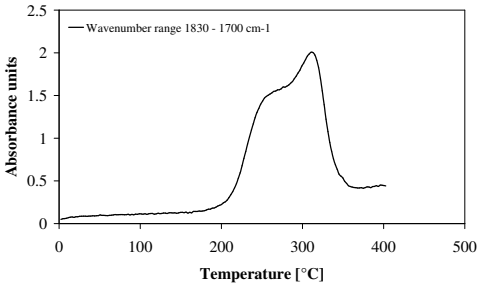


**Figure 5.34:** FTIR spectrum of beech wood torrefaction including the temperature range 200 - 300°C with wavenumber 1830 - 1700 $cm^{-1}$ which is ascribed to carbonyl functional groups

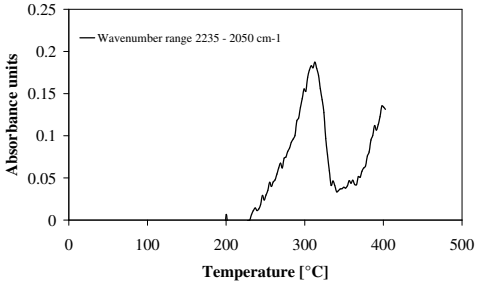


**Figure 5.35:** FTIR spectrum of beech wood torrefaction including the temperature range 200 - 300°C with wavenumber 2235 - 2050 $cm^{-1}$ which is ascribed to CO

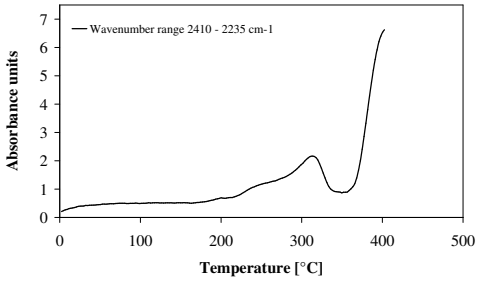


**Figure 5.36:** FTIR spectrum of beech wood torrefaction including the temperature range 200 - 300°C with wavenumber 2235 - 2050 $cm^{-1}$ which is ascribed to $CO_2$

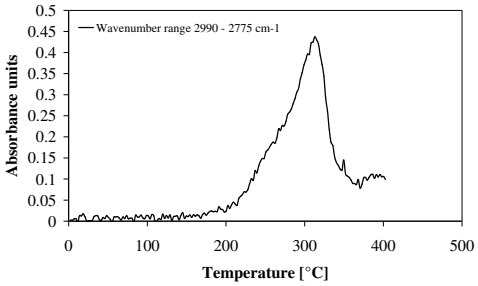


**Figure 5.37:** FTIR spectrum of beech wood torrefaction including the temperature range 200 - 300°C with wavenumber 2900 - 2775 $cm^{-1}$ which is ascribed to C-H stretching of aliphatic saturated hydrocarbons

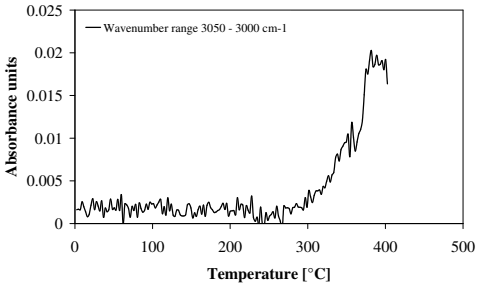


**Figure 5.38:** FTIR spectrum of beech wood torrefaction including the temperature range 200 - 300°C with wavenumber 3050 - 3000 $cm^{-1}$ which is ascribed to $CH_4$ and C-H stretch vibration of aromatic hydrocarbons and/or unsaturated hydrocarbons

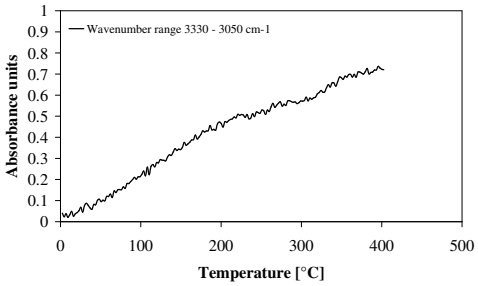


**Figure 5.39:** FTIR spectrum of beech wood torrefaction including the temperature range 200 - 300°C with wavenumber 3050 - 3000 $cm^{-1}$ which is ascribed to $H_2O$

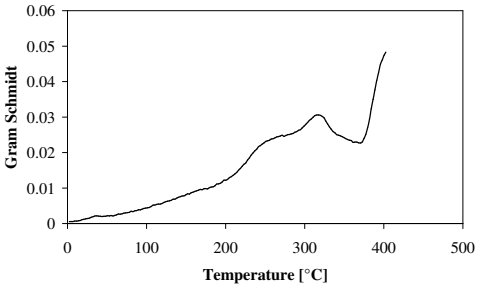


**Figure 5.40:** Gram Schmidt diagram of beech wood in the torrefaction temperature range

**Table 5.8:** Overview of qualitative product formation by applying different techniques in the torrefaction temperature range for beech wood

| Component | Fixed Bed | TG-MS | TG-FTIR |
|---|---|---|---|
| $H_2O$ | 100 - 300°C<br>Increasing with T | Two steps<br>Increasing with T<br>Similar with DTG | One broad peak<br>Increasing with T |
| CO | 100 - 300°C<br>Increasing with T | Two steps<br>Increasing with T<br>Similar with DTG | Two steps<br>Increasing with T<br>Maximum ± 330°C |
| $CO_2$ | 100 - 300°C<br>Increasing with T | Two steps<br>Increasing with T<br>Similar with DTG | Two steps<br>Increasing with T<br>Maximum ± 330°C<br>$2^{nd}$ Max. ± 400°C |
| Methanol | 200 - 300°C<br>Increasing with T | Two steps<br>Increasing with T<br>Similar with DTG | C-O functionality<br>Increasing with T<br>Maximum ± 330°C |
| Formic acid<br>Acetic acid<br>Propionic acid | 230 - 300°C<br>Increasing with T | Two steps<br>Increasing with T<br>Similar with DTG | Carbonyl function.<br>Increasing with T<br>Similar with DTG<br>Maximum ± 330°C |
| Furfural<br>Furfuryl alcohol | 230 - 300°C<br>Increasing with T | Two steps<br>Increasing with T<br>Similar with DTG<br>Maximum at 330°C | |
| Acetone<br>Hydroxy propanone<br>Hydroxy butanone | 230 - 300°C<br>Increasing with T | | Carbonyl function |
| Phenol<br>Aromatics | 250 - 300°C | Single step<br>Increasing with T<br>300°C<br>Maximum ± 330°C | Single step<br>C-H aromatics<br>> 300°C<br>Maximum 400°C |
| Aliphatic saturated | | Two steps<br>Increasing with T<br>> 280°C<br>Maximum ± 360°C | |

## 5.3.8 Energy balances

The energy balance is made for the different beech wood experiments to determine the heat of reaction, see Figure 5.41. The heat of reaction is calculated by the difference of the lower heating values between the output and input streams. Including the sensible heat of the feed ($Q_f$) and product ($Q_p$) streams information can be collected for engineering purposes, which is the heat that is absorbed in the material; to heat up from 25°C to torrefaction temperature. The sensible heat is calculated as the product from the heat capacity, the temperature difference and the amount of material.

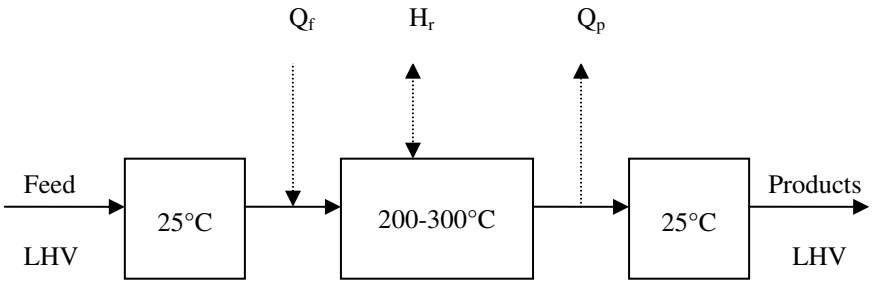


**Figure 5.41:** Energy balance calculation for heat of reaction during biomass torrefaction, where $H_r$ is the heat of reaction, $Q_f$ and $Q_p$ the sensible heat of the feed and the products. Feed and product streams contain certain lower heating values which are calculated by the relation of [Channiwalla, 2002] for the solids or tabulated for the volatilized products.

During the experiments the mass balance could not be closed for 100% due to material that leaks away or condenses in the reactor. The problem is that these products cannot be characterized. Due to this leaked and/or condensed material in the fixed bed experiments some assumptions should be made about this material so that an energy balance can be derived. Six scenarios have been developed to get a good idea about the total energy balance of the torrefaction experiments. These different scenarios are:

1. The leaked away and/or condensed material in the reactor has a LHV of zero, which means that this material is water and/or $CO_2$.

2. The leaked away and/or condensed material in the reactor has the same condensable and gas composition as that has been determined in the mass balance, but has leaked away. This means that the mass balance is normalized to 100% over the leaked and/or condensed material.
3. The leaked away and/or condensed material in the reactor has a LHV of 14 MJ/kg which corresponds with het LHV of acetic acid. All leaked and/or condensed material consists of organics.
4. The leaked away and/or condensed material in the reactor is assumed to be the solid raw material which is lost by introducing in the reactor system.
5. The leaked away and/or condensed material in the reactor is an equivalent of solid raw material, leaked and/or condensed condensable fraction (LHV is 14 MJ/kg) and leaked gas fraction.
6. The leaked away and/or condensed material in the reactor based on the elemental balance contains mainly C and O leading to the assumption that some $CO_2$ and CO is lost. The ratio between the leaked CO and $CO_2$ is taken from the identified CO and $CO_2$ ratio as been trapped in the gas bag.

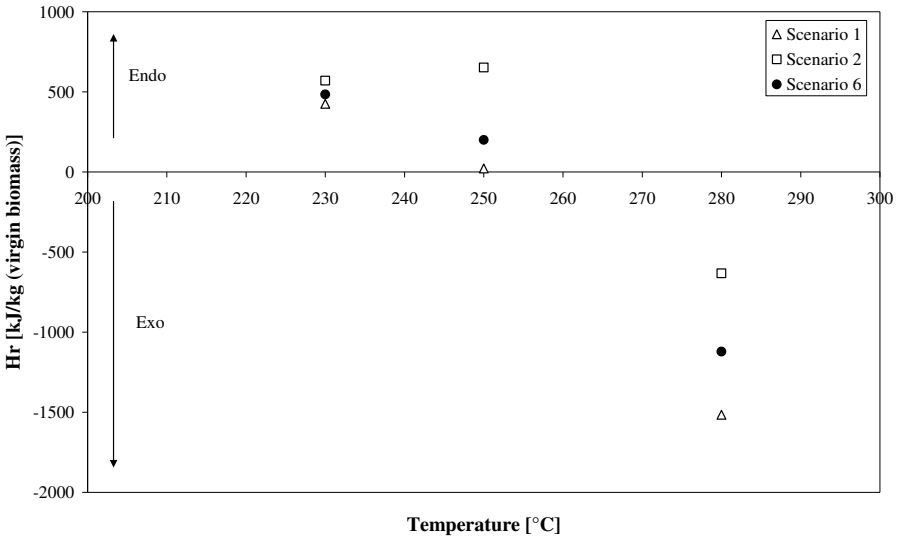


**Figure 5.42:** Heat of reaction ($H_r$) for the different energy scenarios as described above for beech wood torrefaction at temperatures of 230, 250 and 280°C and residence time 30 minutes

From the six different assumptions that have been made the most reasonable option is the sixth scenario. Based on the elemental balance, mainly C and O are lost in the overall balance. Also the LHV of the formed volatile fraction is in line with previous research as is shown in Chapter 3 [Prins et al., 2006] [Bergman et al., 2005]. As an example the more detailed mass and energy balance for beech wood torrefaction at 280°C and a reaction time of 30 min are presented for scenarios 6 is shown in Table 5.9.

A summary of the heat of reactions for beech wood torrefaction at temperatures of 230, 250 and 280°C and residence time of 30 min for the different energy scenarios one, two and six is shown in Figure 5.42. The main results for the heat of reaction are shown in the Appendix behind the references of this chapter. It is shown that a wide variety in results exists leading to an endothermic and/or exothermic torrefaction process. The results that have been found are between 1.5 MJ/kg biomass endothermic and -1.2 MJ/kg raw biomass exothermic. It is clear that with rising temperature the torrefaction process becomes less endothermic or more exothermic. In Chapter 6 it will be shown that the intra particle temperature profile increases with radius. It is also confirmed that with increasing temperature the exothermal behaviour in the particle is increased.

**Table 5.9:** Detailed mass and energy balance according assumption 6 for beech wood torrefaction at 280°C and 30 min residence time. The mass balance is presented as a fraction of a certain product in kg /kg raw biomass.

| Scenario 6 | Mass (kg/kg) | LHV (kJ) | Sensible Heat (kJ) |
|---|---|---|---|
| Wood | 1.00 | 17190.00 | 264.20 |
| TW | 0.73 | 14884.19 | 192.86 |
| Volatiles | 0.27 | 1183.84 | 101.68 |
| Steam | 0.04 | 0.00 | 21.27 |
| Acetic Acid | 0.03 | 390.75 | 9.71 |
| Other Organics | 0.02 | 325.98 | 6.98 |
| CO | 0.01 | 72.73 | 1.80 |
| CO2 | 0.02 | 0.00 | 5.04 |
| Leaked away | 0.15 | 394.38 | 56.88 |
| Heat of Reaction | -1121.97 | kJ/kg biomass | |

For the different scenarios also the energy content of the gaseous phase has been calculated. These values are important for the design of an auto thermal operational process. The combustion of the torrefaction gases produces heat to sustain the process at temperature. The results about the lower heating value of the volatile fraction are shown in Figure 5.43 and Figure 5.44. Figure 5.43 shows the LHV of volatile fraction per kg produced gas (Loss of solid fraction to the volatile phase) and Figure 5.44 shows the LHV of the volatile fraction per kg raw biomass. The main difference is that in Figure 5.43 the LHV is divided by the fraction of volatiles that is produced compared to Figure 5.44 in which the values are based on the raw biomass. It is shown that with increasing torrefaction temperature the lower heating value of the gas phase increases, but flattens out at higher temperature if calculated in kJ/kg raw biomass.

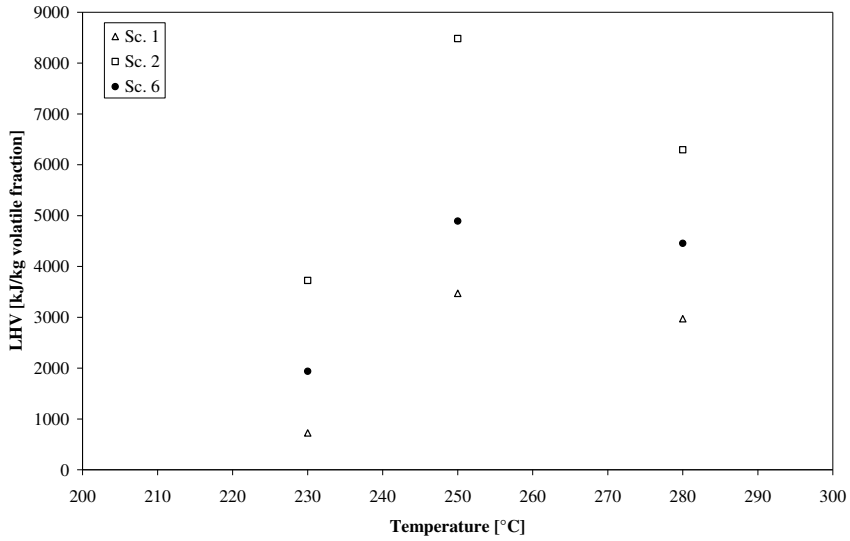


**Figure 5.43:** LHV of the volatile fraction per kg produced gas depending on the various scenarios that have been developed for the leaked and/or condensed material during the experiments

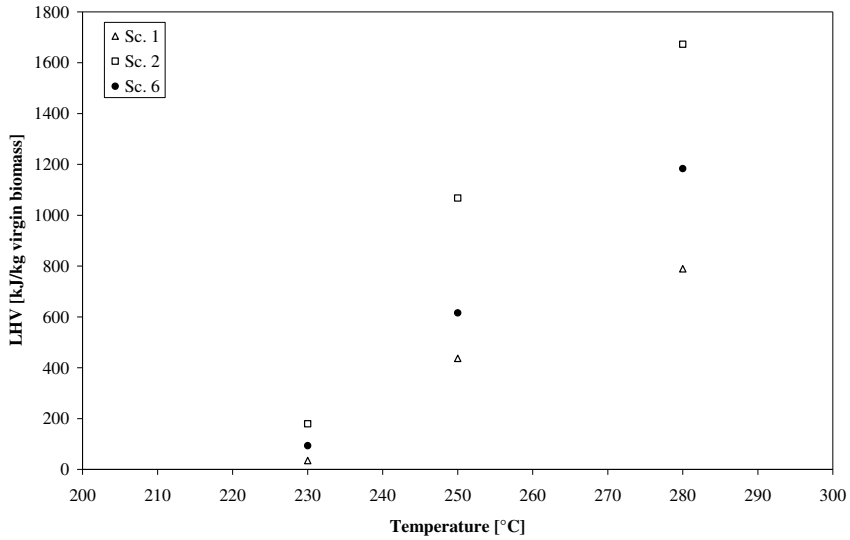


**Figure 5.44:** LHV of the volatile fraction based on the mass (kg) of the raw biomass depending on the various scenarios that have been developed for the leaked and/or condensed material during the experiments. Scenario 1 and 2 show overlap with each other.

## 5.4 Conclusion and discussion

In Chapter 4 it is shown that two independent phases in the biomass react; a slow reacting phase which has high availability and a fast reacting phase that has an apparent temperature dependence of the availability. In this chapter it is confirmed by TG-MS and TG-FTIR that two different steps can be identified. Almost all the components identified (except the phenol and aromatic compounds) are formed during the fast and slow reacting phase, but the rate in which the components are formed is different looking at the TG-FTIR figures.

It can be concluded that the fast reacting step with low availability produces small molecular products even as the slow reacting phase with high availability which also produces aromatic compounds. This slow reacting phase comprises the reactivity of lignin. It is shown that carboxylic acids and water are the main condensable torrefaction products while smaller quantities of other oxygenates with different functionality are formed. CO and $CO_2$ formation comprise an important part of the mass balance based on the assumptions made.

The energy balance of the torrefaction process shows that with increasing reaction temperature the process becomes less endothermic and/or more exothermic. The heat of reaction that has been found is between 1.5 MJ/kg biomass endothermic and -1.2 MJ/kg biomass exothermic. The formation of acetic acid (and other organics) has the highest influence on the energy balance. The lower heating value of the gas phase increases with temperature and biomass conversion, but at higher temperatures the LHV of the gas phase flattens out. Probably the organic fraction is cracked to energetically less valuable products.

It is recommended to obtain more insight into the torrefaction reactions as function of time at constant reaction temperature. In the development of the experimental setup it should be taken into account that the biomass can be feed at constant torrefaction temperature with analytical equipment connected to the setup so that in-situ measurements about the product characteristics are possible including the relative weight loss profile.

## References

Alen R, Kuoppala E, Oesch P (1996). Formation of the main degradation compound groups from wood and its components during pyrolysis. Journal of Analytical and Applied Pyrolysis; 36; 137-148

Bassilakis R, Carangelo RM, Wójtowicz MA (2001). TG-FTIR analysis of biomass pyrolysis. Fuel 80; 12; 1765-1786

Bergman PCA, Boersma, AR, Zwart RWR, Kiel JHA (2005). Torrefaction for biomass co-firing in existing coal-fired power stations “Biocoal”. Report ECN-C--05-013, ECN, Petten, The Netherlands

Biagini E, Barontini F, Tognotti L (2006). Devolatilization of biomass fuels and biomass components studied by TG/FTIR technique. Industrial and Engineering Chemistry Research 45; 13; 4486-4493

Bourgois JP, Doat J (1984). Torrefied wood from temperate and tropical species, advantages and prospects. In: Egeneus H, Ellegard A. Bioenergy 84. London: Elsevier Applied Science Publishers; 153 - 159

Channiwalla SA, Parikh PP (2002). An unified correlation for estimating HHV of solid, liquid and gaseous fuels. Fuels 81; 1051-1063

Cornelissen T (2009). Flash pyrolysis of biomass and co-pyrolysis with biopolymers. PhD thesis, Hasselt University; Belgium

Couhert C (2007). Pyrolyse flash a haute temperature de la biomass ligno-cellulosique et de ses composes – production de gas de synthese. PhD Thesis; l'Ecole des Mines de Paris

De Wild PJ, Uil H, Reith JH, Kiel JHA, Heeres HJ (2009). Biomass valorisation by staged degasification. A new pyrolysis-based thermochemical conversion option to produce value-added chemicals from lignocellulosic biomass. Journal of Analytical and Applied Pyrolysis 85; 1-2; 124-133

Degroot WF, Pan WP, Rahman MD, Richards GN (1988). First chemical events in pyrolysis of wood. Journal of Analytical and Applied Pyrolysis 13; 221-231

Demirbas A (2000). Mechanism of liquefaction and pyrolysis reactions of biomass. Energy Conversion & Management 41; 633 – 646.

Demirbas A (2001). Conversion of biomass to a pyrolytic oil for blending gasoline as an alternative fuel in internal combustion engines. Energy Sources 23; 553-662

Demirbas A (2005). Pyrolysis of ground beech wood in irregular heating rate conditions. Journal of Analytical and Applied Pyrolysis 73; 29-33

Diebold JP (2000). A review of the chemical and physical mechanisms of the storage stability of fast pyrolysis bio-oils; NREL;1-51

Diebold JP (2003). A review of the toxicity of biomass pyrolysis liquids formed at low temperatures. In Fast Pyrolysis of Biomass: A Handbook; Volume 1; Bridgwater AV (Ed.); CPL Press

Ferdous, D., Dalai, A.K., Bej, S.K., Thring, R.W (2002). Pyrolysis of lignins: Experimental and kinetics studies. Energy and Fuels 16 (6), pp. 1405-1412

Gaur S, Reed TB (1998). Thermal data for natural and synthetic fuels. Marcel Dekker, New York

Jakab E, Faix O, Till F (1997). Thermal decomposition of milled wood lignins studied by thermogravimetry/mass spectroscopy. Journal of Analytical and Applied Pyrolysis; 40 – 41; 171-186

Li XD, Poon CS, Sun H, Lo IMC, Kirk DW (2001). Heavy metal speciation and leaching behaviours in cement based solidified/stabilized waste material. Journal of Hazardous Material 82; 215 - 230

Lievens, C. (2007). Valorization of heavy metal contaminated biomass by fast pyrolysis. PhD thesis; Hasselt University; Belgium

Milne TA, Evans RJ (1998). Biomass gasification "tars": their nature, formation and conversion. NREL, Golden, Colorado, USA. Report no. NREL/TP-570-25357

Prins MJ, Ptasinski KJ, Janssen FJJG (2006). Torrefaction of wood Part: 1. Weight loss kinetics. Journal of Analytical and Applied Pyrolysis; 77; 1; 28- 34

Prins MJ, Ptasinski KJ, Janssen FJJG (2006d). Torrefaction of wood Part: 2. Analysis of products. Journal of Analytical and Applied Pyrolysis 77; 1; 35-40

Yang H, Yan R, Chen H, Lee DH, Zheng C (2007). Characteristics of hemi-cellulose, cellulose and lignin pyrolysis. Fuel 86; 12-13; 1781-1788

# APPENDIX CHAPTER 5

In the appendices 5.1 – 5.3 the detailed mass and energy balance according the different assumptions for beech wood torrefaction at 230, 250 and 280°C are shown on dry basis. The mass balance is presented as a fraction of a certain product based on $kg_i$ / $kg_{\text{raw biomass}}$

## Appendix 5.1 Beech wood torrefaction at 230°C and 30 min

| *Scenario 1* | Mass (kg/kg) | LHV (kJ) | Sensible Heat (kJ) |
|---|---|---|---|
| Wood | 1.00 | 17190.00 | 211.15 |
| TW | 0.952 | 17580.30682 | 200.98 |
| *Volatiles* | 0.048 | 35.000 | 14.266 |
| Steam | 0.004 | 0.00 | 7.599 |
| Acetic Acid | 0.002 | 21.93 | 2.172 |
| Other Organics | 0.001 | 8.34 | 0.930 |
| CO | 0.000 | 4.73 | 0.480 |
| CO2 | 0.003 | 0.00 | 3.085 |
| Leaked away | 0.039 | 0.000 | 0.000 |
| Heat of Reaction | 425.31 | kJ/kg biomass | |

| *Scenario 2* | Mass (kg/kg) | LHV (kJ) | Sensible Heat (kJ) |
|---|---|---|---|
| Wood | 1.00 | 17190.00 | 211.15 |
| TW | 0.952 | 17580.30682 | 200.98 |
| *Volatiles* | 0.048 | 179.415 | 26.189 |
| Steam | 0.004 | 0.00 | 7.599 |
| Acetic Acid | 0.002 | 21.93 | 2.172 |
| Other Organics | 0.001 | 8.34 | 0.930 |
| CO | 0.000 | 4.73 | 0.480 |
| CO2 | 0.003 | 0.00 | 3.085 |
| Leaked away | 0.039 | 144.416 | 11.923 |
| Heat of Reaction | 569.72 | kJ/kg biomass | |

| *Scenario 3* | Mass (kg/kg) | LHV (kJ) | Sensible Heat (kJ) |
|---|---|---|---|
| Wood | 1.00 | 17190.00 | 211.15 |
| TW | 0.952 | 17580.30682 | 200.98 |
| *Volatiles* | 0.048 | 577.82 | 26.189 |
| Steam | 0.004 | 0.00 | 7.599 |
| Acetic Acid | 0.002 | 21.93 | 2.172 |
| Other Organics | 0.001 | 8.34 | 0.930 |
| CO | 0.000 | 4.73 | 0.480 |
| CO2 | 0.003 | 0.00 | 3.085 |
| Leaked away | 0.039 | 542.82 | 11.923 |
| Heat of Reaction | 968.13 | kJ/kg biomass | |

| *Scenario 4* | Mass (kg/kg) | LHV (kJ) | Sensible Heat (kJ) |
|---|---|---|---|
| Wood | 0.96 | 16502.40 | 202.96 |
| TW | 0.95 | 17580.30682 | 200.98 |
| *Volatiles* | 0.009 | 35.00 | 14.27 |
| Steam | 0.004 | 0.00 | 7.599 |
| Acetic Acid | 0.002 | 21.93 | 2.172 |
| Other Organics | 0.001 | 8.34 | 0.930 |
| CO | 0.000 | 4.73 | 0.480 |
| CO2 | 0.003 | 0.00 | 3.085 |
| Leaked away | 0.00 | 0.00 | |
| Heat of Reaction | 1112.91 | kJ/kg biomass | |

| *Scenario 5* | Mass (kg/kg) | LHV (kJ) | Sensible Heat (kJ) |
|---|---|---|---|
| Wood | 0.99 | 16967.83 | 208.42 |
| TW | 0.95 | 17580.30682 | 200.98 |
| *Volatiles* | 0.035 | 264.08 | |
| Steam | 0.009 | 0.00 | 18.05 |
| Acetic Acid | 0.004 | 52.10 | 5.16 |
| Other Organics | 0.001 | 19.81 | 2.21 |
| CO | 0.001 | 11.23 | 1.14 |
| CO2 | 0.007 | 0.00 | 7.33 |
| Leaked away | 0.013 | 180.94 | 3.97 |
| Heat of Reaction | 876.55 | kJ/kg biomass | |

| Scenario 6 | Mass (kg/kg) | LHV (kJ) | Sensible Heat (kJ) |
|---|---|---|---|
| Wood | 1.00 | 17190.00 | 211.15 |
| TW | 0.952 | 17580.30682 | 200.98 |
| *Volatiles* | 0.048 | 93.389 | 26.189 |
| Steam | 0.004 | 0.00 | 7.599 |
| Acetic Acid | 0.002 | 21.93 | 2.172 |
| Other Organics | 0.001 | 8.34 | 0.930 |
| CO | 0.000 | 4.73 | 0.480 |
| CO2 | 0.003 | 0.00 | 3.085 |
| Leaked away | 0.039 | 58.39 | 11.923 |
| Heat of Reaction | 483.70 | kJ/kg biomass | |

## Appendix 5.2 Beech wood torrefaction at 250°C and 30 min

| *Scenario 1* | Mass (kg/kg) | LHV (kJ) | Sensible Heat (kJ) |
|---|---|---|---|
| Wood | 1.00 | 17190.00 | 231.75 |
| TW | 0.874 | 16774.48 | 202.58 |
| *Volatiles* | 0.126 | 436.99 | 41.35 |
| Steam | 0.010 | 0.00 | 4.24 |
| Acetic Acid | 0.016 | 228.44 | 4.91 |
| Other Organics | 0.010 | 183.22 | 3.20 |
| CO | 0.002 | 25.33 | 0.55 |
| CO2 | 0.009 | 0.00 | 1.87 |
| Leaked away | 0.079 | 0.00 | 26.58 |
| Heat of Reaction | 21.46 | kJ/kg biomass | |

| *Scenario 2* | Mass (kg/kg) | LHV (kJ) | Sensible Heat (kJ) |
|---|---|---|---|
| Wood | 1.00 | 17190.00 | 231.75 |
| TW | 0.87 | 16774.48 | 202.58 |
| *Volatiles* | 0.126 | 1067.62 | 31.86 |
| Steam | 0.026 | 0.00 | 11.34 |
| Acetic Acid | 0.043 | 610.38 | 13.12 |
| Other Organics | 0.027 | 389.56 | 0.93 |
| CO | 0.006 | 67.69 | 1.48 |
| CO2 | 0.024 | 0.00 | 5.00 |
| Leaked away | 0.000 | 0.00 | 0.00 |
| Heat of Reaction | 652.10 | kJ/kg biomass | |

| *Scenario 3* | Mass (kg/kg) | LHV (kJ) | Sensible Heat (kJ) |
|---|---|---|---|
| Wood | 1.00 | 17190.00 | 231.75 |
| TW | 0.87 | 16774.48 | 202.58 |
| *Volatiles* | 0.126 | 1565.92 | 41.35 |
| Steam | 0.010 | 0.00 | 4.24 |
| Acetic Acid | 0.016 | 228.44 | 4.91 |
| Other Organics | 0.010 | 183.22 | 3.20 |
| CO | 0.002 | 25.33 | 0.55 |
| CO2 | 0.009 | 0.00 | 1.87 |
| Leaked away | 0.079 | 1128.94 | 26.58 |
| Heat of Reaction | 1150.40 | kJ/kg biomass | |

| *Scenario 4* | Mass (kg/kg) | LHV (kJ) | Sensible Heat (kJ) |
|---|---|---|---|
| Wood | 0.92 | 15836.03 | 213.50 |
| TW | 0.87 | 16774.48 | 202.58 |
| *Volatiles* | 0.047 | 436.99 | 14.77 |
| Steam | 0.010 | 0.00 | 4.24 |
| Acetic Acid | 0.016 | 228.44 | 4.91 |
| Other Organics | 0.010 | 183.22 | 3.20 |
| CO | 0.002 | 25.33 | 0.55 |
| CO2 | 0.009 | 0.00 | 1.87 |
| Leaked away | 0.000 | 0.00 | 0.00 |
| Heat of Reaction | 1375.44 | kJ/kg biomass | |

| *Scenario 5* | Mass (kg/kg) | LHV (kJ) | Sensible Heat (kJ) |
|---|---|---|---|
| Wood | 0.97 | 16674.30 | 224.80 |
| TW | 0.87 | 16774.48 | 202.58 |
| *Volatiles* | 0.102 | 1134.00 | 32.99 |
| Steam | 0.013 | 0.00 | 5.66 |
| Acetic Acid | 0.021 | 304.58 | 6.55 |
| Other Organics | 0.014 | 244.29 | 4.26 |
| CO | 0.003 | 33.78 | 0.74 |
| CO2 | 0.012 | 0.00 | 2.49 |
| Leaked away | 0.039 | 551.35 | 13.29 |
| Heat of Reaction | 1234.18 | kJ/kg biomass | |

| Scenario 6 | Mass (kg/kg) | LHV (kJ) | Sensible Heat (kJ) |
|---|---|---|---|
| Wood | 1.00 | 17190.00 | 231.75 |
| TW | 0.874 | 16774.48 | 202.58 |
| *Volatiles* | 0.126 | 615.98 | 41.35 |
| Steam | 0.010 | 0.00 | 4.24 |
| Acetic Acid | 0.016 | 228.44 | 4.91 |
| Other Organics | 0.010 | 183.22 | 3.20 |
| CO | 0.002 | 25.33 | 0.55 |
| CO2 | 0.009 | 0.00 | 1.87 |
| Leaked away | 0.079 | 178.99 | 26.58 |
| Heat of Reaction | 200.46 | kJ/kg biomass | |

## Appendix 5.3 Beech wood torrefaction at 280°C and 30 min

| *Scenario 1* | Mass (kg/kg) | LHV (kJ) | Sensible Heat (kJ) |
|---|---|---|---|
| Wood | 1.00 | 17190.00 | 264.20 |
| TW | 0.73 | 14884.19 | 192.86 |
| *Volatiles* | 0.27 | 789.46 | 101.68 |
| Steam | 0.04 | 0.00 | 21.27 |
| Acetic Acid | 0.03 | 390.75 | 9.71 |
| Other Organics | 0.02 | 325.98 | 6.98 |
| CO | 0.01 | 72.73 | 1.80 |
| CO2 | 0.02 | 0.00 | 5.04 |
| Leaked away | 0.15 | 0.00 | 56.88 |
| Heat of Reaction | -1516.35 | kJ/kg biomass | |

| *Scenario 2* | Mass (kg/kg) | LHV (kJ) | Sensible Heat (kJ) |
|---|---|---|---|
| Wood | 1.00 | 17190.00 | 264.20 |
| TW | 0.73 | 14884.19 | 192.86 |
| *Volatiles* | 0.27 | 1673.03 | 86.82 |
| Steam | 0.10 | 0.00 | 48.31 |
| Acetic Acid | 0.06 | 887.43 | 22.05 |
| Other Organics | 0.04 | 620.42 | 0.93 |
| CO | 0.02 | 165.18 | 4.09 |
| CO2 | 0.05 | 0.00 | 11.44 |
| Leaked away | 0.00 | 0.00 | 0.00 |
| Heat of Reaction | -632.78 | kJ/kg biomass | |

| *Scenario 3* | Mass (kg/kg) | LHV (kJ) | Sensible Heat (kJ) |
|---|---|---|---|
| Wood | 1.00 | 17190.00 | 264.20 |
| TW | 0.73 | 14884.19 | 192.86 |
| *Volatiles* | 0.27 | 2920.92 | 101.68 |
| Steam | 0.04 | 0.00 | 21.27 |
| Acetic Acid | 0.03 | 390.75 | 9.71 |
| Other Organics | 0.02 | 325.98 | 6.98 |
| CO | 0.01 | 72.73 | 1.80 |
| CO2 | 0.02 | 0.00 | 5.04 |
| Leaked away | 0.15 | 2131.46 | 56.88 |
| Heat of Reaction | 615.10 | kJ/kg biomass | |

| *Scenario 4* | Mass (kg/kg) | LHV (kJ) | Sensible Heat (kJ) |
|---|---|---|---|
| Wood | 1.00 | 17190.00 | 264.20 |
| TW | 0.86 | 17484.27 | 226.55 |
| *Volatiles* | 0.14 | 865.35 | 52.99 |
| Steam | 0.05 | 0.00 | 24.99 |
| Acetic Acid | 0.03 | 459.01 | 11.41 |
| Other Organics | 0.02 | 320.90 | 8.56 |
| CO | 0.01 | 85.44 | 2.12 |
| CO2 | 0.02 | 0.00 | 5.92 |
| Leaked away | 0.00 | 0.00 | 0.00 |
| Heat of Reaction | 1159.62 | kJ/kg biomass | 52.99 |

| *Scenario 5* | Mass (kg/kg) | LHV (kJ) | Sensible Heat (kJ) |
|---|---|---|---|
| Wood | 1.00 | 17190.00 | 264.20 |
| TW | 0.77 | 15660.48 | 202.92 |
| *Volatiles* | 0.23 | 2535.59 | 87.26 |
| Steam | 0.03 | 0.00 | 16.38 |
| Acetic Acid | 0.02 | 300.82 | 7.48 |
| Other Organics | 0.01 | 210.31 | 5.61 |
| CO | 0.01 | 55.99 | 1.39 |
| CO2 | 0.02 | 0.00 | 3.88 |
| Leaked away | 0.14 | 1968.47 | 52.53 |
| Heat of Reaction | 1006.07 | kJ/kg biomass | |

| Scenario 6 | Mass (kg/kg) | LHV (kJ) | Sensible Heat (kJ) |
|---|---|---|---|
| Wood | 1.00 | 17190.00 | 264.20 |
| TW | 0.73 | 14884.19 | 192.86 |
| *Volatiles* | 0.27 | 1183.84 | 101.68 |
| Steam | 0.04 | 0.00 | 21.27 |
| Acetic Acid | 0.03 | 390.75 | 9.71 |
| Other Organics | 0.02 | 325.98 | 6.98 |
| CO | 0.01 | 72.73 | 1.80 |
| CO2 | 0.02 | 0.00 | 5.04 |
| Leaked away | 0.15 | 394.38 | 56.88 |
| Heat of Reaction | -1121.97 | kJ/kg biomass | |

# Chapter 6

# Torrefaction of large wood particles


## Abstract

*This chapter describes the influence of torrefaction on large cylindrical wood particles with diameter between 10 and 28 mm for beech and willow wood. Fixed bed experiments have been carried out at temperatures between 200 - 300 ℃ to determine the product composition and the intra particle temperature profile depending on location, time and temperature. The condensable products have been characterized and the exothermal effect quantified. Finally an analytical model has been developed based on the reaction mechanism found in Chapter 4. Some modifications are applied regarding reaction kinetics, reaction coordinates and the heat transfer. The model describes the temperature profile in the particle as function of time, temperature, location and the progress of the reaction.*

## 6.1 Introduction

In the previous chapters it is shown that the biomass decomposition during torrefaction occurs in two independent steps and which components do belong to these different steps. Chapters 4 and 5 deal with the torrefaction of small particles with negligible temperature gradient within the solid, where the chemical kinetics is the rate controlling process.

In real (industrial) processes torrefaction will be carried out with larger particles than these that have been researched. In this chapter larger single cylindrical particles with diameter between 10 mm and 28 mm are applied to investigate their torrefaction behavior. It is expected that with larger single wood particles the intra particle physical and chemical effects play an important role in the biomass torrefaction. Torrefaction itself is a complex phenomenon which involves heat transfer, drying, flows of liquids and gases, anisotropy, surface recession and a large number of chemical reactions [Bellais, 2007]. In this case, the chemistry of decomposition is influenced by heat and mass transfer effects. The key factor in torrefaction is the heat transfer phenomenon into and in the (large) wood particle. Reactivity of and volatile product formation from the biomass depend on the temperature at which torrefaction takes place. The reaction rate of the constituents of biomass hemicellulose, cellulose and lignin differ with temperature, residence time and matrix structure of the biomass material. Internal heat transfer limitations result in a temperature profile which leads to different reactivity rates and heterogeneous material characteristics in the biomass particle itself. Endo and exothermal biomass decomposition reactions can enlarge the effect of the temperature profile and therewith influence the product quality, but also the process design and process operation regarding temperature set point. The application of larger wood particles offers the opportunity to study the temperature profile inside the wood particle and draw conclusions about the homogeneity of the torrefied material

In order to design a reactor the understanding of the interaction between chemical and physical phenomena during biomass torrefaction is of fundamental importance. Coupled transport and reaction models are developed to investigate the effects of various parameters on biomass pyrolysis and/or torrefaction. This will also be the subject of this chapter, where theoretical and experimental work on the torrefaction

of large wood particles will be presented. The chapter contains three topics that are important for working with large particles, like basic mass balances, temperature profiles in the large particles and tar formation (due to secondary reactions). The chapter comprises a literature review about single large particle pyrolysis. An experimental paragraph consists of torrefaction by fixed bed experiments with cylindrical beech wood particles measuring the temperature profile. A qualitative explanation about the observed effects is given by the development of a theoretical analytical model. The connection is made between the (primary and secondary) kinetic model and the heat transfer process.

## 6.2 Large particle modelling

### 6.2.1 Intra particle process description

Figure 6.1 explains schematically the thermal degradation process during biomass pyrolysis. The processes of drying, pyrolyzing and charring follow, or even overlap each other depending on temperature, time, particle size, heat and mass transfer. A temperature profile moves through the porous solid biomass particle resulting in the mentioned processes in one and the same biomass particle. As volatiles from the pyrolysis and water vapour formed during drying flow out through this temperature affected layer, secondary reactions may occur both homogeneously and heterogeneously which can be endo and/or exothermic [Gronli, 1996] [Milne & Evans, 1998] [Morf, 2001].

Although torrefaction is a rather new technology (in development), pyrolysis research can teach us about the physical processes in wood such as: heat transfer by convection, conduction and radiation and convective transport of volatile species. Torrefaction is the result of heat transfer to the particle (external heat transfer), heat transfer in the particle (internal heat transfer) and chemical reactions. In short, it is the interaction between chemistry and transport phenomena at the level of the biomass particle and the reaction environment. Therefore a mathematical large particle model comprises the conservation equations for mass and energy, boundary conditions, a kinetic model, property relations and thermo-physical data, like moisture content, pressure relations, heat of evaporation, permeability's, thermal conductivity, specific heat, diffusion coefficients and dynamic viscosity [Bellais et al., 2003] [Larfeldt et al., 2000] [Di Blasi, 1994 & 1996] [Gronli & Melaaen, 2000] [Chan et al., 1988].

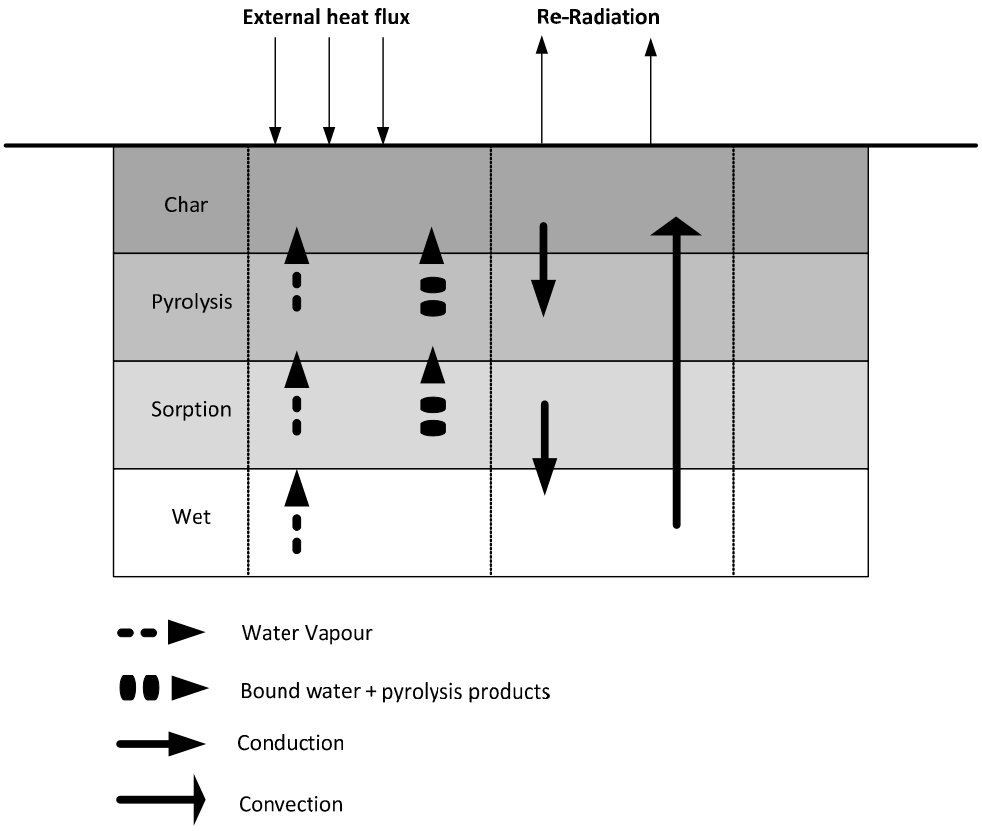


**Figure 6.1:** Schematic diagram of the thermal degradation process of wood during pyrolysis

A lot of effort has been done to better understand the complex mechanisms interacting in the thermal decomposition of wood particles and its substances. [Gronli, 1996] made an extensive review about pyrolysis of large biomass particles controlled by heat and mass transfer. It is concluded that there are common used simplifying assumptions applied by modellers, namely:

- No shrinkage and cracks of the solid
- No heat transfer by convection within the solid
- No heat transfer by radiation within the solid
- Local thermal equilibrium between the solid and gas phase
- Constant thermo-physical properties (specific heat, thermal conductivity)
- Unrestricted outflow of gas species from the solid
- No secondary reactions
- No moisture effect

By assuming all above possibilities it is suggested that the transient temperature response could be described by a one-dimensional heat conduction equation with a source term to account for the heat of decomposition. Depending on the shape of the particle a spherical, polar or cylindrical coordinate system is chosen. [Grønli and Melaaen, 2000] state that a quantitative comparison between model predictions and experimental data has to be proved difficult for three reasons:

- The heterogeneity of the biomass resources used in the experiments.
- The high uncertainty in the kinetic model and rate constants used for global reaction mechanisms and
- The large uncertainty on the properties of the charred product.

In the model that is worked out in this thesis all above assumptions are taken into account to quantify the heat of reaction in large particle torrefaction. After quantification of the heat another analytical description is given about the endo/exothermal effect that has been measured during torrefaction as function of time, temperature and location in the particle.

### 6.2.2 Heat of reaction

An important parameter in the torrefaction process is the heat of reaction. In Chapter 5 it is shown that the heat of reaction for small particles varies between 1.6 MJ/kg biomass (endothermic) and -1.2 MJ/kg biomass (exothermic) based on the product composition. With increasing temperature torrefaction becomes less endothermic or more exothermic. In this paragraph a small overview of the

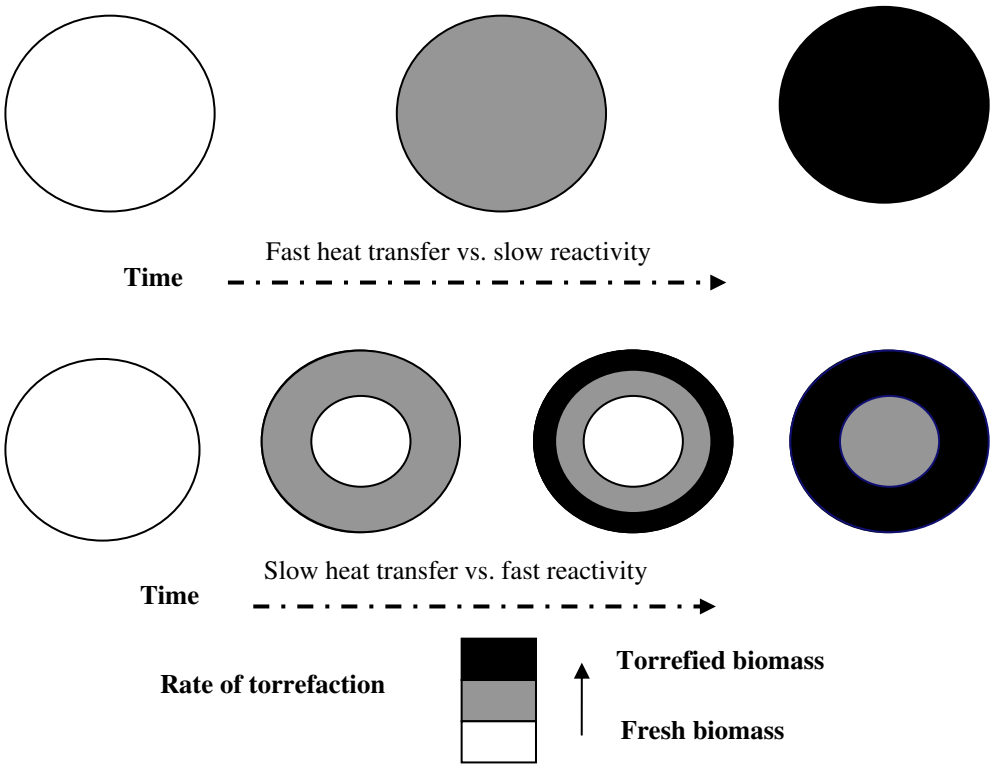


**Figure 6.2:** Fast and/or slow heat transfer versus slow and/or fast reactivity determines the temperature profile in the wood and so the rate of torrefaction which is a indicator for the quality of the particle

literature is discussed. Most of the literature does not consider the heat of torrefaction directly, but rather a generic heat of pyrolysis. The reported values for wood, cellulose, hemicellulose and lignin vary widely as reported by [Rousset, 2004]. It is reported that the heat of pyrolysis for wood varies between -2300 kJ/mole (exothermic) to 450 kJ/mole (endothermic), -510 to 120 kJ/kg for cellulose, -455 to 79 kJ/kg for lignin and -363 to 42 kJ/kg for hemicellulose. [Cowdery, 1987] reports heats of pyrolysis between 240 kJ/mole and -2100 kJ/mole. [Park et al., 2010] studied experimentally heat and mass transfer processes during wood pyrolysis. It is concluded that both endothermic and exothermic reactions have been observed previously, however the explanation for this behavior differs significantly, Mechanisms for exothermicity that are mentioned are lignin

decomposition, secondary tar cracking reaction, de-hydroxy-cellulose decomposition. [Di Blasi et al., 2001] attributes this to the exothermic secondary reaction between volatiles and char. Studies show that exothermic behaviour in biomass pyrolysis is related to the formation of char [Rath et al., 2003] [Milosavljevic, 1996] [Mok et al., 1983]. [Rath et al., 2003] investigated the heat of pyrolysis of beech and spruce wood by means of a differential scanning calorimeter. Among the wide variations for the heat of the primary pyrolysis processes a linear correlation was found with the final char yield. It is assumed that there is an exothermic primary char formation process competing with an endothermic volatile formation process.

[Prins et al., 2006] is the only study that shows an energy balance for torrefaction quite directly. It is found that the overall mass and energy balances show that torrefaction at 250 and 300°C is mildly endothermic. The error analysis shows that the process could also be exothermic. At 250°C and a reaction time of 30 minutes the heat of torrefaction is 87 (±449) kJ/kg and 124 (±400) kJ/kg at 300°C and 10 minutes of reaction time for torrefaction of (dry) willow. If drying of the biomass is also taken into account the heat to evaporate moisture will make the overall process certainly endothermic.

It is also found that thermal analysis shows endothermic behaviour of the biomass pyrolysis at temperatures of up to 230°C, beyond which the reactions were predominantly exothermic [Strezov et al., 2007]. At temperatures above 230°C the reactions shifted to an exothermic behaviour, which was significantly complex consisting of series of endothermic peaks and exothermic troughs. It is found that hemicellulose decomposes exothermally at about 200°C. Cellulose decomposes endothermally at 290°C with sometimes an exothermal peak at 350°C. Lignin is supposed to decompose exothermally. Finally, [Yang et al., 2007] also studied the pyrolysis characteristics of the three main components (hemicellulose, cellulose and lignin) of biomass using TGA with differential scanning calorimetry (DSC). It is shown that from the viewpoint of energy consumption in the course of pyrolysis, cellulose behaves differently from hemicellulose and lignin. The pyrolysis of the former is endothermic while that of the latter is exothermic. The DSC values of hemicellulose and lignin are above zero between 150 and 500°C with two peaks at

275 and 365°C, respectively, indicating that their pyrolysis reactions are exothermic. Cellulose showed an endothermal peak at 355°C.

The differences in exothermicity reported in the literature may be due to many factors. Those authors who have tried to identify the most important underlying mechanism agree that it is likely that there is a primary pyrolysis step involving volatilisation that is endothermic and another step that is exothermic involving secondary reaction between the released vapours and the remaining solid matrix. Exothermicity increases with pressure, sample weight and sample thickness. In a series of dedicated experiments it correlates well with final char yield [Rath et al., 2003]. So, in this chapter the experiments on the heat of reaction are focused on the low temperature pyrolysis range between 200 - 300°C.

## 6.3 Experimental

### 6.3.1 Materials

The large particle experiments in the fixed bed reactor have been carried out with beech and willow. The particle size of the feedstock was a 10 cm long cylinder with a diameter between 10 and 30 mm delivered by a carpenters company. An example of the material before and after torrefaction is seen in Figure 6.3.

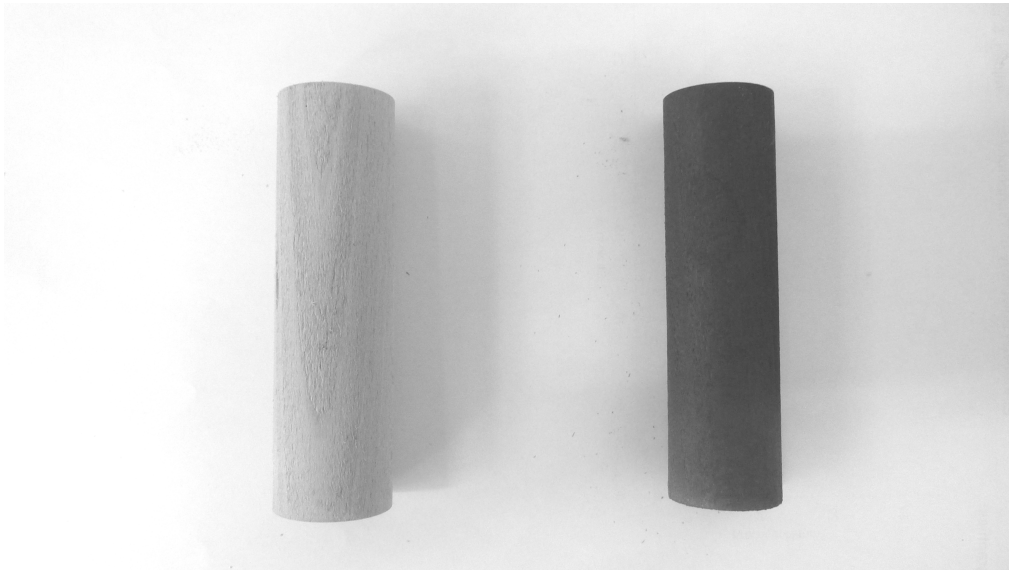

**Figure 6.3:** Raw (left) and torrefied beech wood (right) as applied in the large particle experiments

## 6.3.2 Fixed Bed Reactor setup

The biomass samples are torrefied in a fixed bed reactor that is placed in a Carbolite vertical split tube oven which is electrically heated. Argon is used as inert gas to keep the system in absence of oxygen and remove the formed products to the coldtrap, which is a glass tube cooled with ice water, or gas bag. The coldtrap is used to collect the condensable volatiles and the gas bag is used to collect the permanent gases. The biomass particle is placed in the reactor at room temperature. Thermocouples are positioned in the middle of the biomass particle so the temperature profile in the particle can be measured, see Figure 6.4. In this figure exothermic and/or endothermic effects can be observed. The reactor is heated up to the desired temperature around 10°C/min before the isothermal temperature is reached. After the experiment the reactor is cooled down within 5 minutes to 200°C which is according the definition the lowest torrefaction temperature. In order to prevent the condensation of products the tube to the coldtrap is traced to around 180°C. After the experiment the tracing is kept at this temperature another 15 minutes. A picture of the experimental setup is shown in Chapter 5.

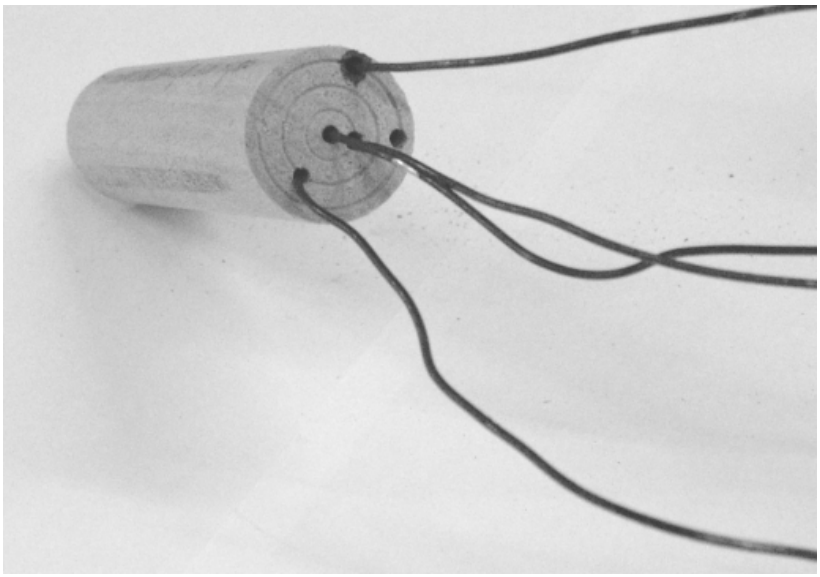

**Figure 6.4:** Single cylindrical beech wood particle including the positions of several thermocouples

### 6.3.3 Analyses Fix Bed Reactor experiments

The main focus in this chapter is to measure the endo- and/or exothermic effect. This is done by measuring the temperature profile in the biomass cylindrical particle by several thermocouples at different radial positions. In Figure 6.5 these positions of the several thermocouples in the beech wood particles is shown. If the particle size becomes smaller than 28 mm radius the number of thermocouples becomes smaller than six, but the positions will be the same starting with thermocouple $T_1$, $T_2$ etc. The method is verified by applying the torrefaction conditions to self prepared gypsum cylinders.

In this chapter also information about the mass balances and (condensable) product formation is gained. All the reaction products in the fixed bed reactor experiments (a solid torrefied biomass, condensable product from the coldtrap and a permanent gas) are collected and weighed in order to make an overall mass balance. The condensable product and the gas are analyzed by using different techniques. The solid fraction is not analyzed in detail after torrefaction.

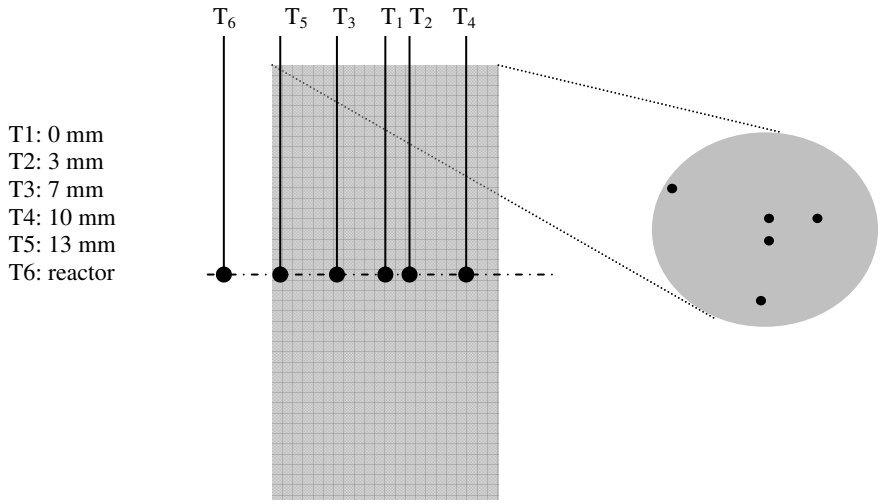


**Figure 6.5:** positioning of thermocouples in the cylindral beech wood particle in the vertical and horizontal axis

The composition of the condensable product was analyzed with GC-MS by using two different columns on a Shimadzu OP5000. The condensable samples are prepared with isopropanol solutions and an internal standard of fluoranthene is used. Calibration lines have been constructed to quantify the amount of a fraction in the torrefaction condensables. The columns that are used are a Varian VF5 and a Varian CP-Wax 52. The method used and column parameters are described in the experimental part of Chapter 5.

## 6.4 Results

In this paragraph the main results are presented about the mass balances that can be created for the torrefaction of cylindrical particles. Also examples of temperature profiles in the biomass particles are shown. The results will be used to develop an analytical model that describes the torrefaction behaviour for cylindrical particles.

### 6.4.1 Mass balances

The normalized mass balances for torrefaction at 240 and 280°C for particles with different diameter (between 10 – 28 mm) are shown in Figure 6.6 and Figure 6.7. The mass balances are normalized, because the mass balance could not get closed. The gas and condensable volatile fractions are normalized to 100% so that a closed balance is derived. The ratio between the gas and condensable fraction is chosen the same as that has been quantified before normalizing the mass loss. The loss of material is around 15%, because of gas leakages and condensation of volatiles in the reactor or in the lines to the cold trap. An example of this condensation of products is shown in **Figure 6.11**. High oxygen content in the condensable volatiles makes the product sensitive for secondary reactions and so tar formation. This will be studied further in this chapter.

It is shown that with increasing particle size the formation of char yield is also increasing at both 240 and 280°C, respectively. Together with this increasing char yield the formation of the condensable fraction is decreasing with increasing particle size. The increasing char yield with increasing particle radius can be explained by heat transfer limitations or by secondary pyrolysis reactions. It is well known that gas – solid reactions are important chemical reactions during pyrolysis [Gomez et al., 2009] [Hosoya et al., 2009]. As the particle diameter increases, the residence time of gases and volatiles are longer inside the particle which will result in char formation [Ahuja et al., 1996].

In Figure 6.8 the comparison of the product yields during torrefaction at 250℃ and 280℃ of small particles (<< 2mm) and the cylindrical particles (28 mm diameter) is shown. When solid, condensable and gas product yields are compared at two different temperatures it is observed that there is not a significant difference in the solid yields between small particles and cylindrical particle with 28 mm diameter. Comparing the powder (<<2mm) with the 10, 15 and 20 mm diameter particles it is observed that the cylindrical particles have a lower char yield. A possible explanation is that with small particles (powder) secondary reactions occur in the gas phase and with larger particles solid-gas reactions leading to charring and gas-gas reactions to recondensation.

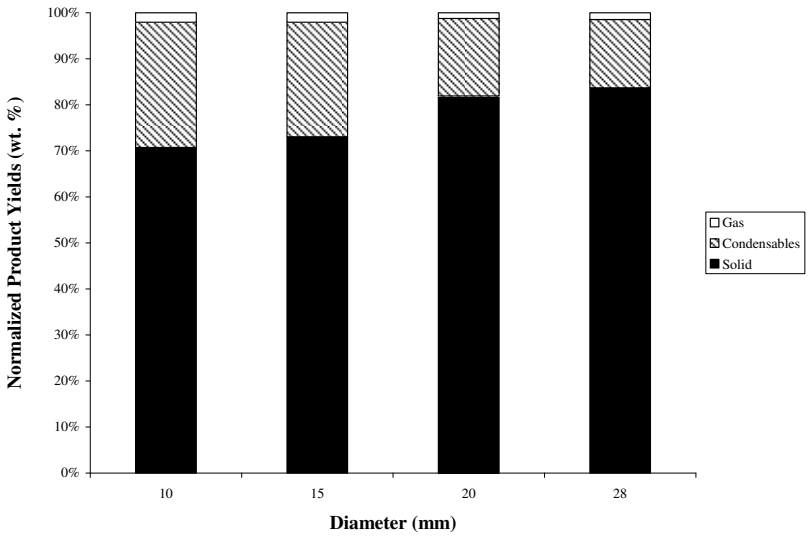


**Figure 6.6:** Normalized overall mass balance for large particle beech experiments at 240°C and 30 minutes residence time

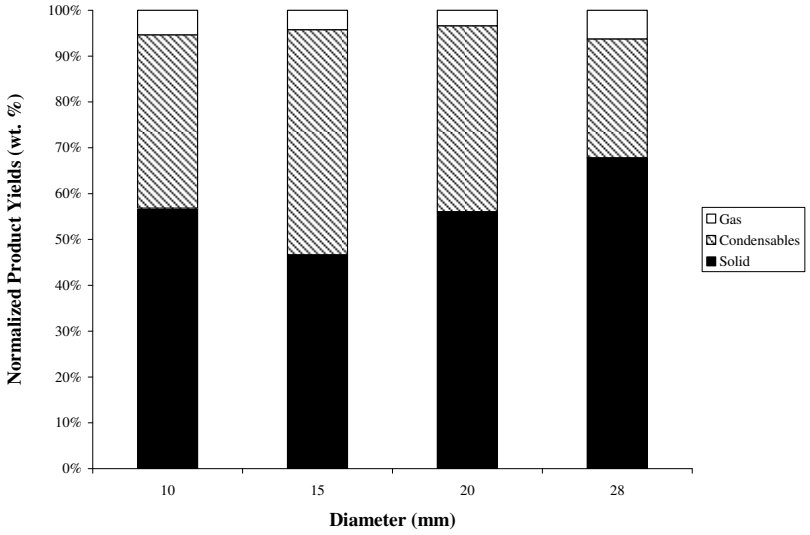


**Figure 6.7:** Normalized overall mass balance for large particle beech experiments at 280°C and 30 minutes residence time

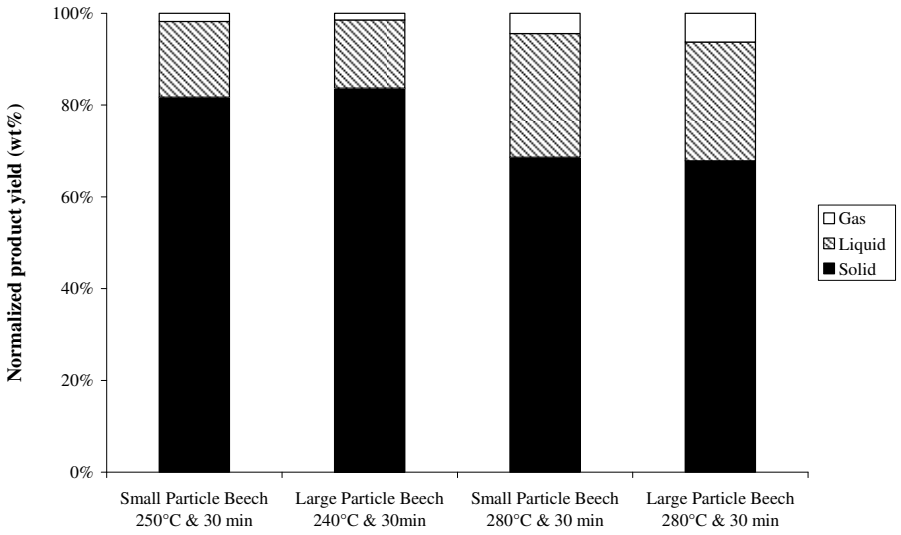


**Figure 6.8:** Overall mass balance for small & large particle (diameter size 28 mm) experiments at 240°C and 280°C with 30 minutes residence time

## 6.4.2 Condensable products

Figure 6.9 and Figure 6.10 show the product yields of the characterized condensable volatiles during large particle beech wood torrefaction at 240°C and 280° as function of the particle diameter. It is shown that with increasing temperature the yields of the condensable products based on wt% feedstock also increases. It is shown that also larger particles produce mainly acetic acid and methanol. Increasing the particle diameter means a decrease in the yield of the different condensable products. It is clearly observed that the amount of acetic acid is decreased from almost 2.5 wt% to around 1.3 wt% by 10 mm and 28 mm diameter at torrefaction conditions of 280°C. For the other components it is not very clear to observe a decrease in yield. The permanent gas composition is not determined during large particle torrefaction.

This condensable product which is trapped in the coldtrap is heated up to 100°C and after that again analyzed with GC – MS. Most of the water is evaporated after this treatment. Next to the products that are shown in Figure 6.9 and Figure 6.10

larger fragments with maximum $C_{12}$ - $C_{13}$ are detected with the method described in the experimental part in Chapter 5. These organic fragments are both linear and/or aromatic structures. It means that some oligomerization can occur during torrefaction. Also the stability of the condensable product is analyzed after heating up again to 100°C with thermo gravimetry as described in the experimental part of Chapter 4. The results are shown in Figure 6.12 and Figure 6.13. It is shown that at torrefaction temperature the condensable products are sensitive for degradation and can lead to coke formation which is shown in Figure 6.11.

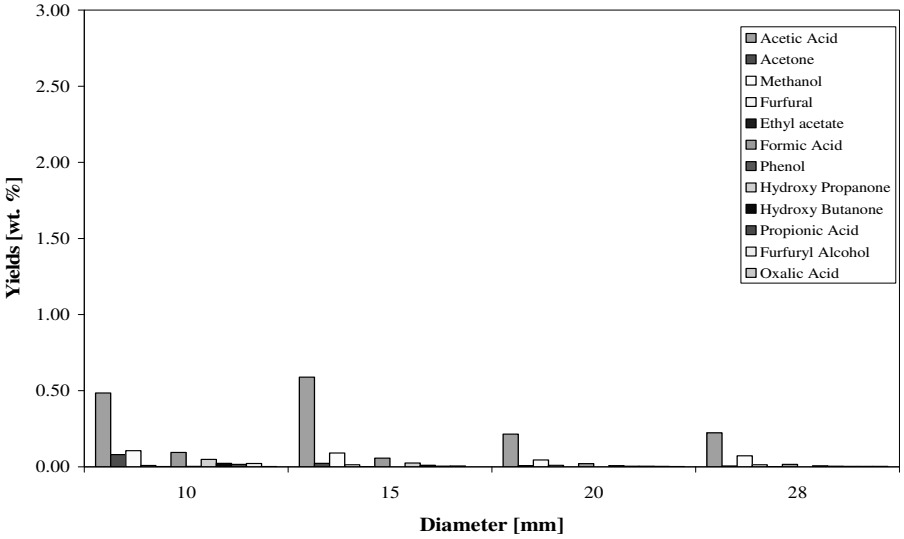


**Figure 6.9:** Product yields in wt% of the feedstock for torrefaction at 240℃ of cylindrical beech wood particles with diameter between 10 and 28mm

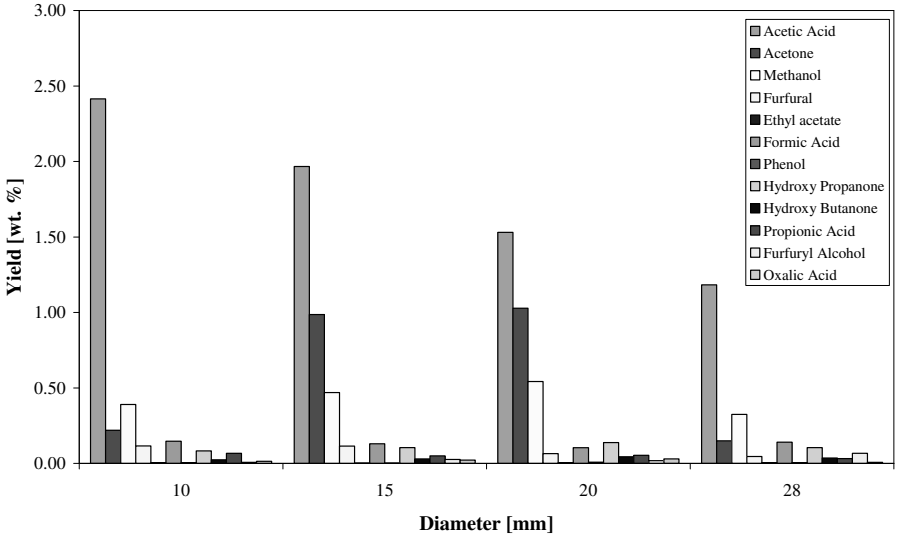


**Figure 6.10:** Product yields in wt% of the feedstock for torrefaction at 280℃ of cylindrical beech wood particles with diameter between 10 and 28 mm

**Figure 6.11:** Formation of tars during biomass torrefaction in a lab scale fixed bed reactor after several experiments. The sticky tars in the reactor are shown by the black areas

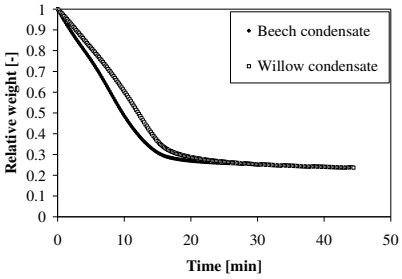


**Figure 6.12:** Thermogravimetric Analysis of beech and willow wood condensate (obtained above 100℃) and thermally treated for a second time at 250℃ to study coke formation

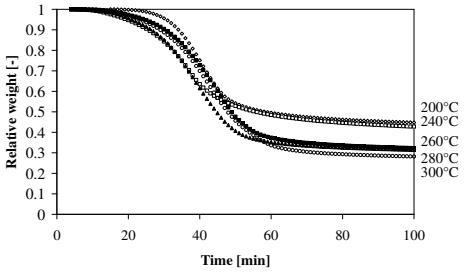


**Figure 6.13:** Thermogravimetric Analysis of beech wood condensate (obtained above 100℃) and thermally treated for a second time between 200 - 300℃ to study coke formation

## 6.4.3 Temperature profiles and heat of reaction

Figure 6.14 - Figure 6.16 show the temperature profile in a cylindrical beech wood particle as measured during torrefaction. The experiments are carried out at 230°C and 280° with or without glass wool insulation. It is shown that after a certain heating period an exothermal temperature profile is found. At 230°C the exothermal effect is not that large yet, but the exothermal effect is clearly shown for torrefaction at 280°C. In paragraph 6.5 a model is developed that describes the temperature profile mathematically as function of time, temperature, location and reaction coordinate. The model is developed into two different parts. The first mathematical description of the temperature focuses on the profile before the maximum intra particle temperature is reached; this is defined as time $\tau$. The second description of the temperature focuses on the profile after the maximum intra particle temperature is reached. This means that a temperature profile is described on time intervals $t_1 < \tau$ and $t_2 > \tau$. An example is that in Figure 6.15 this would mean that $\tau$ is reached around 40 min. At this time $\tau$ a temperature of maximum 340°C is reached.

During heating up of the biomass an internal temperature gradient over the radius is measured. A decreasing temperature gradient is observed in the direction of the center of the particle. After a certain time the intra particle exothermic effect occurs which means that the temperature in the particle becomes higher than the reactor temperature. At the moment this effect starts, it is observed that the temperature increase in the center of the particle is higher than at the circumference. Temperature gradients in the particle probably lead to heterogeneous quality characteristics of the modified torrefied solid.

Figure 6.16 shows the temperature profile if the biomass is insulated with glass wool. An extra heat resistance is constructed before the biomass is heated up. At first sight insulation affects the evolution of the isothermal profile, but not the total exothermal effect.

The observed exothermal effect in the particle is calculated by the following simplified equations as described below.

$$\lambda\left(\frac{\partial^2 T}{\partial r^2}+\frac{1}{r}\frac{\partial T}{\partial r}\right)=P(t)=\frac{\partial Q}{\partial t} \tag{6.1}$$

where $\lambda$ is the conductivity, $T$ is the intra particle temperature, $r$ is the radius, $P(t)$ is the heat production.

It is assumed that the exothermal temperature profile in the biomass is parabolic.

$$T=ar^2+c \tag{6.2}$$

where $a$ and $c$ are undefined parameters and just describe the profile.

If these equations are solved the result of the exothermal effect over time is:

$$Q = \left( \frac{4\lambda}{r^2} (T - T_0) \right) \Delta t \tag{6.3}$$

In which Q is the exothermal effect, T the exothermal temperature, $T_0$ the reactor temperature at steady state condition and $\Delta t$ the time over which the exothermal effect occurs. The thermal conductivity $\lambda$ is determined experimentally. The radius r is chosen for the cylindrical particle size. It can be expected that with smaller radius the maximum $\Delta T$ above the reactor temperature is smaller which is related by $r^{-2}$ vs T. The exothermal effect due to chemical reactions is not a function of particle size.

The results about the exothermal effects for torrefaction between 200 - 280°C are shown in Figure 6.17 for beech wood and in Figure 6.18 for willow wood. In the figures the heat production in the particle and the maximum temperature rise above the torrefaction temperature is shown. It is shown that heat production in the beech wood particle starts around 210°C. With increasing temperature the heat production in the particle increases. The maximum temperature increase in the wood cylinder is shown on the right y-axis. It is observed that with increasing torrefaction temperature also the maximum temperature in the center of the wood cylinder rises.

Also some experiments have been carried out with beech wood at 320°C, 340° and 350°C, but these are not shown in the figure. At 320 and 340°C the maximum $\Delta T$ is stabilized at around 40℃. If the temperature is raised to higher temperatures it is observed that the biomass particle cracks and the temperature increases with 100°C. It is difficult to observe whether this temperature rise is due to the destruction of the particle or that the temperature increase is the reason for the cracking of the particle. Since the experimental system changes due to the cracking it is difficult to compare these results with the observations between 200 and 300°C.

The results confirm the work of [Rousset, 2004] who studied the validation of an experimental model for the pyrolysis of wood at low temperatures up to 300°C. Temperature profiles in the cylindrical biomass particle during the pyrolysis are measured with several thermocouples resulting in an exothermal temperature profile due to the wood pyrolysis. Also the particle size is varied between 5 and 45 mm diameter. Low temperature experiments show a systematic increase in heat of reaction with increasing distance from the centre of the surface [Roberts and Clough, 1963]. The increasing residence time and secondary exothermic reactions are probably the main reason for this effect. But [Blackshear and Kanury, 1965] show that for most of the reactions in the interior of the cellulose cylinder the heat of pyrolysis is endothermic.

It is shown that with increasing particle size the temperature in the particle increases more due to exothermic reactions. [Mok et al., 1983] researched the exothermic behaviour of pyrolysis dependent on pressure. With increasing pressure the heat of reaction due to pyrolysis becomes more exothermic or less endothermic. [Tinney, 1965] observed a pressure increase in the single wood particle. The pressure increase is higher with increasing pyrolysis temperature. After the particle cracks the pressure drops to normal pressure. Recondensation of condensable volatiles is mentioned as a possible explanation for an exothermic effect due to the increase of pressure in the particle by volatile formation. Pressure increase in the biomass particles is presented as a reason for the destruction of the cylinder. [Rousset, 2004] states that if the permeability of the biomass increases the exothermal effect will be smaller.

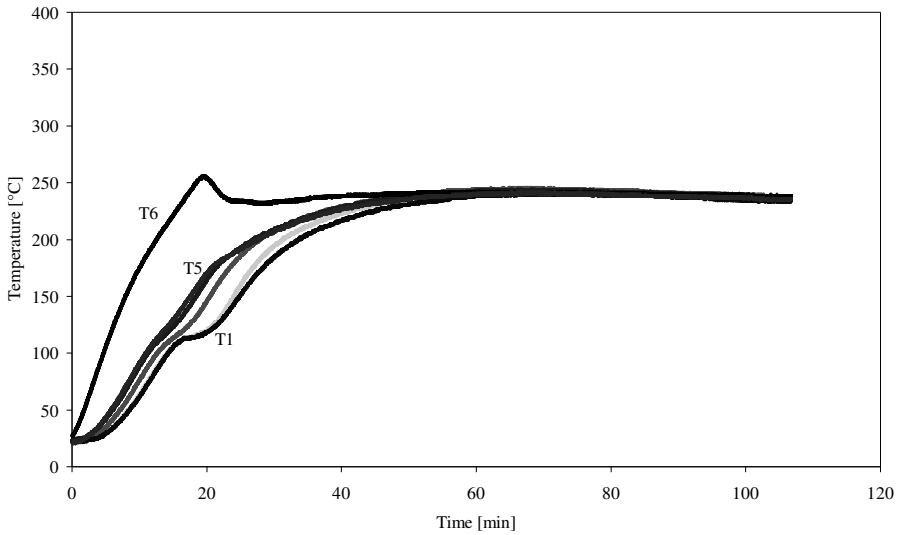


**Figure 6.14:** Temperature profile inside a cylindrical beech wood particle with diameter of 28 mm during torrefaction at 230°C. $T_1$, $T_2$, $T_3$, $T_4$, $T_5$ and $T_6$ describe the temperatures at different location as shown in paragraph 6.3.3.

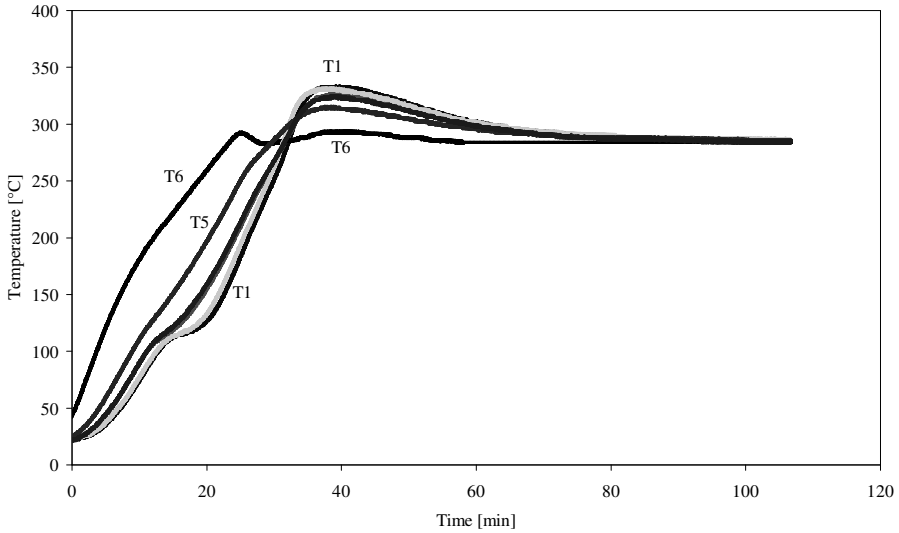


**Figure 6.15:** Temperature profile inside a cylindrical beech wood particle with diameter of 28 mm during torrefaction at 280°C. $T_1$, $T_2$, $T_3$, $T_4$, $T_5$ and $T_6$ describe the temperatures at different location as shown in paragraph 6.3.3.

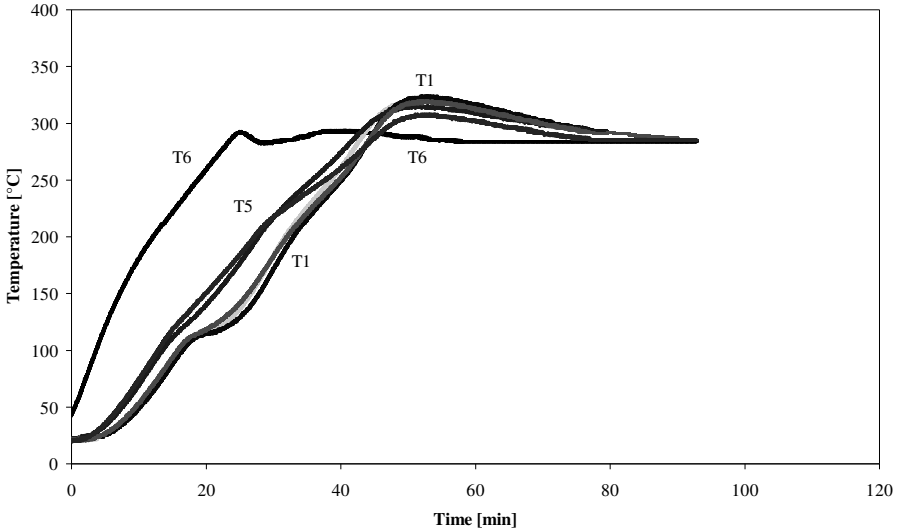


**Figure 6.16:** Temperature profile inside an insulated cylindrical beech wood particle with diameter of 28 mm during torrefaction at 280°C. The insulation is carried out by packing the beech wood particle with 2 mm thick glass wool. $T_1$, $T_2$, $T_3$, $T_4$, $T_5$ and $T_6$ describe the temperatures at different location as shown in paragraph 6.3.3

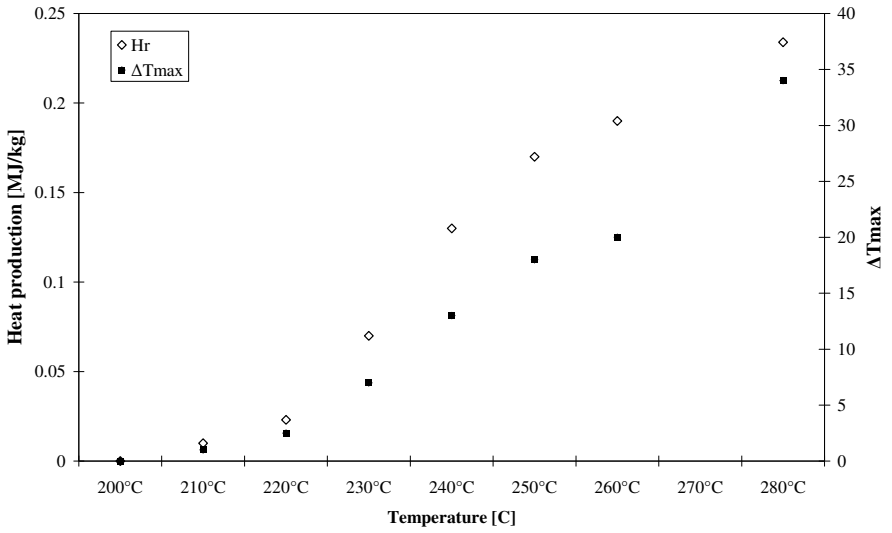


**Figure 6.17:** Heat production in a cylindrical biomass particle with radius 28 mm during beech wood torrefaction

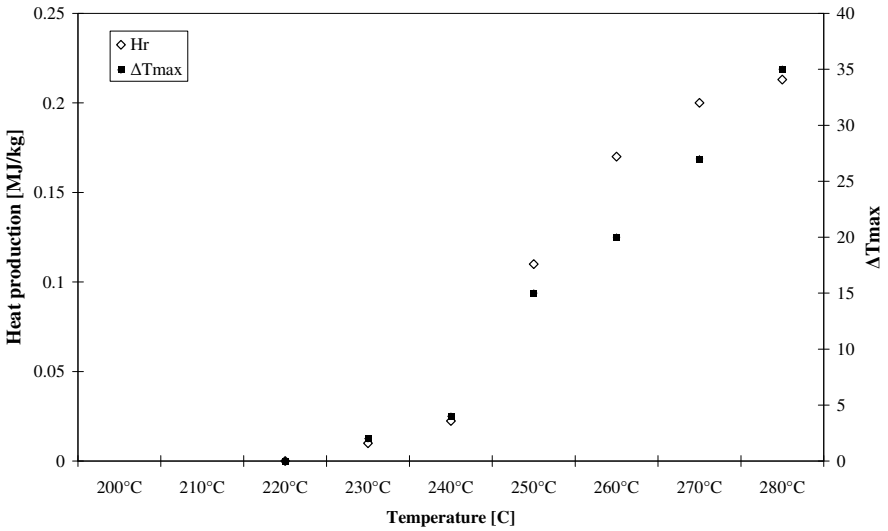


**Figure 6.18:** Heat production in a cylindrical biomass particle with radius 28 mm during willow wood torrefaction

## 6.5 Development of an analytical model for the torrefaction of a beech wood particle

### 6.5.1 Approach

In this paragraph the exothermal effect in the cylindrical particle is described by an development of an analytical model. This model describes the temperature profile in the particle as function of time, temperature, location and reaction coordinate. In general the development of a reaction model for the pyrolysis (or torrefaction) of large wood particles consists of the following parts, namely i) the set of torrefaction reactions used for the chemical reactions occurring in the wood, ii) extended formulation of heat and mass transfer in porous media, which accounts for the heat and production of volatiles due to the chemical reactions and iii) a strategy for the numerical validation to solve the set of transport equations [Turner et al., 2010].

In this chapter only the first two parts of the reaction model for torrefaction are developed regarding heat transfer phenomena. The extended amount of required numerical parameters limits the numerical validation of the torrefaction model, though the exothermal effect can be quantified. There are only a limited number of models used to investigate this process at low pyrolysis temperature [Felfli et al., 1998] [Rahjohnson et al., 1994]. [Rousset, 2004] developed a model for low temperature biomass pyrolysis that contained a i) pyrolysis reaction model based on the biomass constituents between 200 and 260°C, ii) conservation equations of heat and mass transfer comprising solid, liquid and gas conservation, volatile matters produced by the chemical reactions and energy conservation, iii) several relations such as gas and liquid velocities described by the generalised Darcy's Law, and enthalpy – temperature description. Sometimes also porosity of the biomass is taken into account [Bellais, 2007].

In the development of an analytical model for the torrefaction of a beech wood particle the following assumptions have been made in this chapter:

- One dimensional
- Only heat conduction, no convection and radiation
- No shrinkage of the particle
- Secondary recondensation taken into account
- Constant thermo-physical properties
- No mass transfer relations used
- Reaction kinetics derived in chapter 4 are modified

In the remainder of this chapter the modified reaction kinetics, its reaction coordinates and heat transfer model are worked out. Combining this information leads to the proper analytical description of beech wood torrefaction.

## 6.5.2 Reaction kinetics

In Chapter 4 the reaction kinetics for biowaste are derived and so far in this Chapter it is found that torrefaction includes an exothermal effect. In this paragraph the reaction mechanism is modified to take into account exothermal effects. The two independent reaction steps are enlarged with an exothermal reaction. The exothermal effect that has been considered in the modified reaction scheme is the recondensation of the condensable volatiles.

The reaction mechanism of coupled reactions as is shown in Figure 6.19 is a standard phenomenon in catalysis. It is assumed that all participants are well mixed and concentration gradients do not occur. Further it is assumed that the coupled reactions proceed only in the forward direction such that the sequence of elementary steps is reduced.

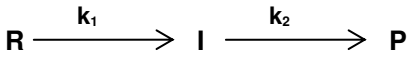


**Figure 6.19:** Reaction scheme of coupled reactions in well mixed batch reactors

Coupling the reaction scheme of above coupled reactions with the reaction mechanism during torrefaction gives a description of the exothermal effect. The derived mechanism of Chapter 4 and the coupled reactions together give the reaction mechanism as is shown in Figure 6.20.

Figure 6.21 shows the combination of the modified two independent steps minimized to a single step including the exothermal effect. It is assumed that one single step from the reaction mechanism derived in Chapter 4 contributes to the heat production in the large particle. A fraction $\xi$ in the biomass phase "A" reacts via recondensation to B and shows emission. Phase "B" shows the formation of volatiles via emission and reacts further to a final char "C". It is also shown in the figure that fraction 1-$\xi$ reacts via the formation of volatiles and a final char "C" in a direct mechanism.

In the next paragraph the related reaction coordinates with the different energy states are proposed as a theory behind the exothermal effect. To make the link between the energy production due to the reactions that occur and the reaction coordinates first the reaction kinetics of the modified reaction mechanism are necessary. The reaction model is explained in Figure 6.20. The different reactivity rates are described as follow:

$$\frac{\partial A}{\partial t} = -K_1 A \tag{6.4}$$

$$\frac{\partial B}{\partial t} = k_b A - K_{1B} B \tag{6.5}$$

$$\frac{\partial C}{\partial t} = k_{c1} A + k_{c1^*} B \tag{6.6}$$

Solving these equations lead to the following solution:

$$A = A_0 e^{-K_1 t} \tag{6.7}$$

$$B = A_0 \frac{k_b}{K_{1B} - K_1} \left( e^{-K_1 t} - e^{-K_{1B} t} \right) \tag{6.8}$$

$$C = A_0 \left( -\frac{k_{c1^*} k_b + k_{c1} \left( K_{1B} - K_1 \right)}{K_1 \left( K_{1B} - K_1 \right)} e^{-K_1 t} + \frac{k_{c1^*} k_b}{K_{1B} \left( K_{1B} - K_1 \right)} e^{-K_{1B} t} + \frac{k_{c1} K_{1B} \left( K_{1B} - K_1 \right) + k_{c1^*} k_b K_{1B} - k_{c1^*} k_b K_1}{K_{1B} K_1 \left( K_{1B} - K_1 \right)} \right) \tag{6.9}$$

A general concentration profile as function of time of the different reactive and produced phases A, B and C is constructed. Figure 6.23 is an example how the profile can look like which is based on the reaction mechanism of Figure 6.19. R, I and P can be replaced in the figure by A, B and C. Depending on the reaction rate constants decomposition and/or formation of A, B and C will show a different slope.

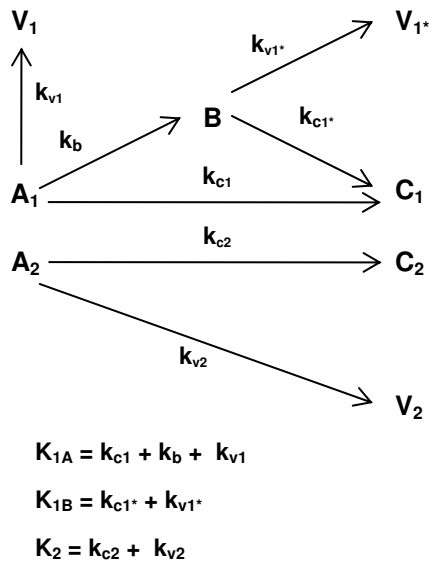


**Figure 6.20:** Modified reaction mechanism including the recondensation of the primary volatiles. The reaction mechanism is extensively described in Chapter 4.

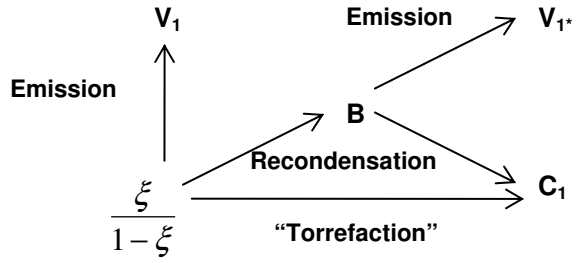


**Figure 6.21:** Reaction scheme for biomass conversion during torrefaction including recondensation and emission reactions during the "a,b" reaction as explained in Chapter 4. The mechanism is modified with a fracion ξ which is responsible for the exothermal effect during torrefaction

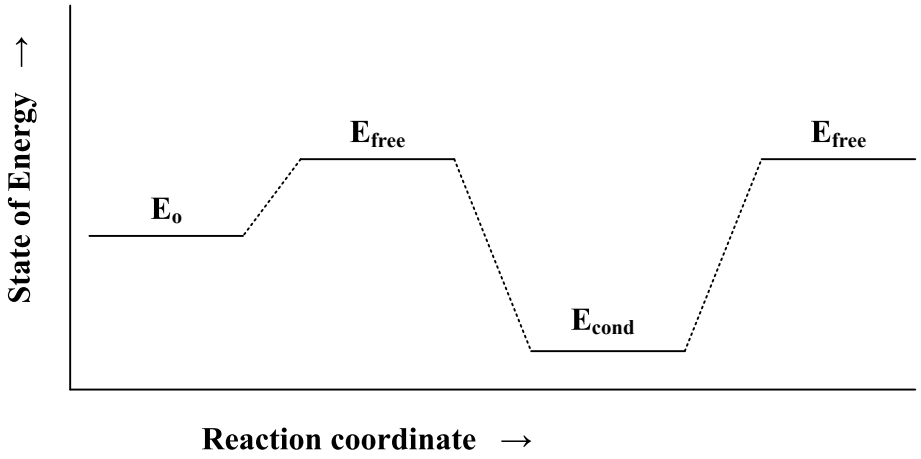


**Figure 6.22:** Reaction states of beech wood torrefaction during the "ab" reaction (as described in Chapter 4) with emission of volatiles and secondary recondensation

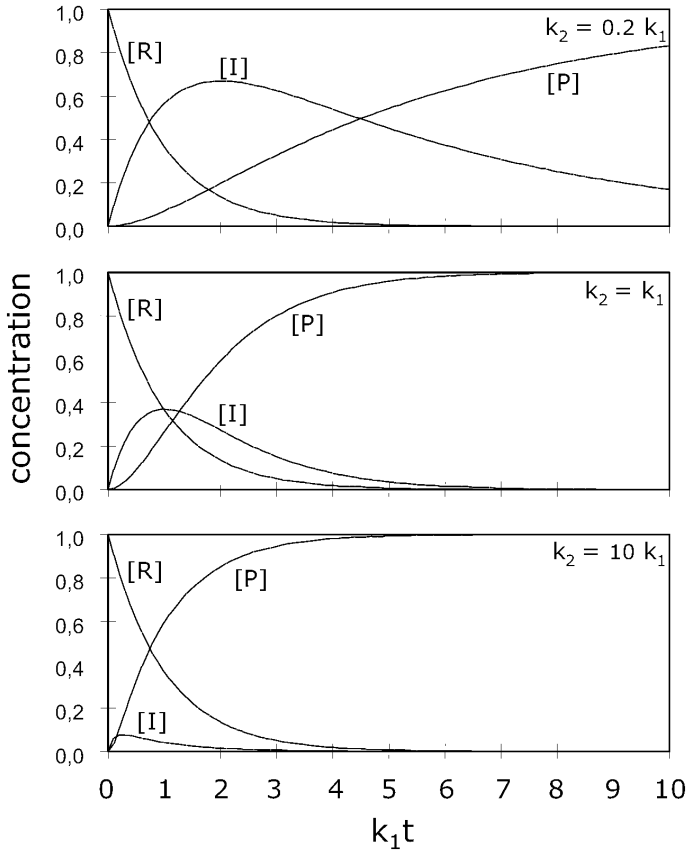


**Figure 6.23:** General concentration profile of the different phases [R], [I] and [P] as function of time which represent the reaction mechanism of Figure 6.19. [R], [I] and [P] can be replaced by [A], [B] and [C]

## 6.4.3 Reaction coordinates

In this paragraph the reaction coordinates, reaction mechanism and reaction rates are coupled to describe the exothermal effect depending on its coordinates. Figure 6.21 shows that a fraction ξ of phase "A" (or [R]) is responsible for the exothermal effect in the cylindrical biomass particle by for example recondensation. Figure 6.22 explains the reaction states of beech wood torrefaction during the *"ab"* reaction as explained in Chapter 4 and modified above. $E_0$ is the state of energy of the fraction that is responsible for the exothermal effect, $E_{free}$ is the state of energy of molecules in the volatile state. These molecules can recondensate ($E_{cond}$) and

again go to the volatile state. By coupling the reaction states and the reaction mechanism a mathematical relation is derived.

The reaction state of the beech wood during torrefaction could give an explanation about the exothermal effect that occurs. Three effects determine whether the overall reaction is exothermic. These three different terms are described with equations (6.10) – (6.12):

$$P_1 = -\xi\left(E_{free} - E_o\right)A_0 e^{-t/\tau} \tag{6.10}$$

$$P_2 = \left(1-\xi\right)\left(E_{free} - E_{cond}\right)A_0 e^{-t/\tau} \tag{6.11}$$

$$P_3 = -\left(1-\xi\right)\left(E_{free} - E_{cond}\right)C\left((t)\right) \tag{6.12}$$

The overall reaction is exothermal if the result of (6.12) – (6.11) – (6.10) is positive. This means that $\xi$ is high or the behaviour of *C(t)* in equation (6.12) is small. The factor $\xi$ is a certain value that determines the amount of recondensation of volatiles.

$$P = \sum_n P_n = \xi\left(E_1\right)e^{-t/\tau_1} + \left(1-\xi\right)\left(E_2\right)e^{-t/\tau} + \left(1-\xi\right)\left(E_2\right)e^{-t/\tau_2} \tag{6.13}$$

The exothermal effect is the biggest in the beginning of the process, so it is assumed that the exothermal effect is only dependent on a single exponential term which means that $t<<\tau_2$. At low concentrations of C (t) there is only heat transfer with the oven. The time dependency is then a function like $P(t)=P_0\exp(-t/\tau)$.

### 6.5.4 Heat transfer model

If the heat production profile depending on time is known (via a decreasing exponential power) the question arises how the temperature profile develops in

time in the cylindrical experiments. Earlier it was assumed that the temperature distribution is parabolic in time that follows the heat production proportional. If the heat production is now via a decreasing exponential power this is not completely correct and a correction is necessary. This is also shown by the experiments.

By using cylindrical coordinates in the case that the differential dT/dt is not zero, complicated Besselfunctions are derived. To simplify the problem with cylindrical coordinates perpendicular coordinates are applied to describe the temperature profile depending on time. The accuracy when shifting to square surfaces instead of cylindrical is not significantly affected and simple analytical solutions are possible and proposed. The error that is made by this assumption is small if the radius R is chosen that belongs to the same surface as for a square surface.

The heat production follows an exponential power $e^{-t/\tau}$ which is derived from the kinetics in the previous step. It is important that also the heat production is postulated with the same time dependency. A cosine function fits at first sight best with the temperature profile in the cylindrical beech wood particle. At the centre of the particle the highest temperature is observed at exothermal conditions and at the boundaries of the wood particle a lower temperature is found.

To come to a proper analytical description of the exothermal effect as a function of the temperature profile in time some assumptions have been made. The following assumptions are made:

1. It is applied to the time scale where the function of $f_3$ that describes the concentration of $C(t)$ is still very small.

2. There is no feedback effect of the exothermal effect on the kinetics. It is assumed that the description of the kinetics stays the same by the exothermal reactions that occur during the torrefaction with the large cylindrical particle.

The uniformity throughout the biomass particle can be determined by the heat conduction law of Fourier applied in a non-stationary system and for a simple

geometry. Thermal gradients often happen during wood pyrolysis since wood is a poor heat conductor and it is indeed difficult to be in kinetically controlled pyrolysis [Bellais, 2007]. The simplest 2D mathematical model which describes both heat transfer and thermo chemical decomposition is given by the set of equations for spherical coordinates:

$$P(t) = C_p \frac{\partial T}{\partial t} - \lambda\left(\frac{\partial^2 T}{\partial x^2} + \frac{\partial^2 T}{\partial y^2}\right) \tag{6.14}$$

It is assumed that the heat production in time has the same relation as the decomposition of chemical component “A” as written above and follows a decreasing exponential term. A general concentration profile for “A” is shown in Figure 6.23. The heat production profile follows the general concentration profile of phase “A”, described by the following equation:

$$P(t) = P_0 e^{-t/\tau} \tag{6.15}$$

As described already in paragraph 6.4.3 the model is developed into two different parts. The first mathematical description of the temperature focuses on the profile before the maximum intra particle temperature is reached, this is defined as time $\tau$. The second description of the temperature focuses on the profile after the maximum intra particle temperature is reached. The temperature profiles in Figure 6.14 - Figure 6.16 show a maximum temperature at $t = \tau$. For this reason the model is divided into two parts with:

- $t_1 << \tau$
- $t_2 >> \tau$

Firstly, the temperature profile in the second part is analyzed. The temperature profile in this part if $t >> \tau$ is stated by :

$$T_2 = \alpha_2 e^{-t/\tau}\left(\cos kx \cdot \cos ky - \beta_2\right) \tag{6.16}$$

Introducing this in (6.14) means that:

$$P_0 e^{-t/\tau} = -C_p \alpha_2 \frac{1}{\tau} e^{-t/\tau}\left(\cos kx \cdot \cos ky - \beta_2\right) + 2\lambda\alpha_2 e^{-t/\tau} k^2 \left(\cos kx \cdot \cos ky\right) \tag{6.17}$$

The cosine dependency is removed from the equation by stating the factors in the equation equal to zero:

$$C_p - 2\lambda\tau k^2 = 0 \tag{6.18}$$

This gives the result for k:

$$k = \pm\sqrt{\frac{C_p}{2\lambda\tau}} \tag{6.19}$$

Introducing this result in equation (6.17) gives the following formula:

$$\frac{P_0}{C_p} = \frac{\beta_2\alpha_2}{\tau} \tag{6.20}$$

If it is assumed that the cylindrical coordinates are related to spherical coordinates by stating that the contours for both spheres are equal; this means that:

$$2\pi r = 4l \tag{6.21}$$

The boundary conditions are:

$$T = 0 \text{ at } x, y = \pm\frac{1}{2}l \tag{6.22}$$

$$\left.\frac{\partial T}{\partial x}\right|_{center} = 0 \tag{6.23}$$

$$\left.\frac{\partial T}{\partial y}\right|_{center} = 0 \tag{6.24}$$

To get the total exothermal effect over the total volume of the cylinder integration is necessary. It is assumed that at the boundaries the temperature is equal to the environmental temperature. Since it is worked with delta functions the boundary coundition of T=0 is valid. A contour integral over the contour S is solved which is shown in Figure 6.24 this can be integrated by:

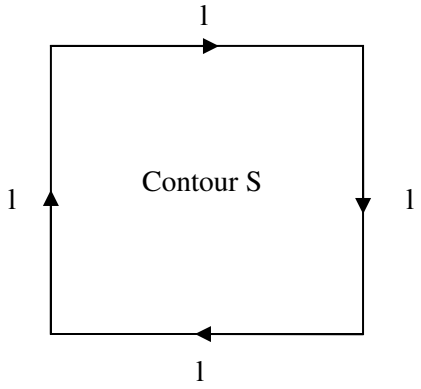


**Figure 6.24:** description of contour integral S over a square with length l

$$\oint_S TdS = 0 \tag{6.25}$$

Which becomes:

$$4 \int_{x,y=-\frac{1}{2}l}^{x,y=\frac{1}{2}l} Tdx' = 0 \tag{6.26}$$

Resulting into:

$$4 \int_{x-\frac{1}{2}l}^{x\frac{1}{2}l} \alpha_2 e^{-t/\tau}\left(\cos kx \cos ky - \beta_2\right)dx = 4\alpha_2 e^{-t/\tau}\frac{1}{k}\left(\sin kx \cos ky - \beta_2 x\right)\Big|_{-\frac{1}{2}l}^{+\frac{1}{2}l} = \tag{6.27}$$

With y = ½ l this leads to:

$$4\alpha_2 e^{-t/\tau}\frac{1}{k}\left(\sin kx\cos ky-\beta_2 x\right)\Big|_{-\frac{1}{2}l}^{+\frac{1}{2}l}=0 \tag{6.28}$$

$$4\alpha_2 e^{-t/\tau}\frac{1}{k}\left(\sin\left(\frac{1}{2}kl\right)\cos\left(\frac{1}{2}kl\right)-\sin\left(-\frac{1}{2}kl\right)\cos\left(\frac{1}{2}kl\right)\right)-4\alpha_2 e^{-t/\tau}\beta_2 l=0 \tag{6.29}$$

Which means that

$$\beta_2=\frac{2}{kl}\left(\sin\left(\frac{1}{2}kl\right)\cos\left(\frac{1}{2}kl\right)\right) \tag{6.30}$$

Including this means that:

$$\alpha_2=\frac{P_0\tau}{C_p\beta_2}=\frac{P_0 kl}{2C_p}\frac{1}{\left(\sin\left(\frac{1}{2}kl\right)\cos\left(\frac{1}{2}kl\right)\right)} \tag{6.31}$$

Secondly, the temperature profile in the first part if $t_1 << \tau$ is stated by :

$$T_1=\alpha_1\left(1-e^{-t/\tau}\right)\left(\beta_1-k^2\left(x^2+y^2\right)\right) \tag{6.32}$$

Which means that:

$$P = P_0 e^{-t/\tau} = C_p \alpha_1 \frac{1}{\tau} e^{-t/\tau} \left(\beta_1 - k^2 \left(x^2 + y^2\right)\right) + 4\lambda\alpha_1 k^2 \left(1 - e^{-t/\tau}\right) \tag{6.33}$$

Substitution of:

$$r^2 = x^2 + y^2 \tag{6.33}$$

$r = R$ and T=0 (6.34)

$$T_1 = \alpha_1 \left(1 - e^{-t/\tau}\right)\left(\beta_1 - k^2 r^2\right) \tag{6.35}$$

Means that:

$$\beta_1 = k^2 R^2 \tag{6.36}$$

To derive the value for $\alpha_1$ the following surface integration is carried out:

$$\int_0^R P_0 e^{-t/\tau} 2\pi r dr = \frac{C_p \alpha_1}{\tau} e^{-t/\tau} \left(\beta_1 \pi R^2 - \left(\int_0^R k^2 \pi r^3 dr\right)\right) + 4\lambda\alpha_1 k^2 \left(1 - e^{-t/\tau}\right)\pi R^2 \tag{6.37}$$

Which is:

$$P_0 e^{-t/\tau}\pi R^2 = \frac{C_p \alpha_1}{\tau} e^{-t/\tau}\left(\beta_1 \pi R^2 - \left(\frac{1}{4}k^2 \pi R^4\right)\right) + 4\lambda\alpha_1 k^2\left(1 - e^{-t/\tau}\right)\pi R^2 \tag{6.38}$$

This means that:

$$\alpha_1 = \frac{P_0 e^{-t/\tau}}{\frac{C_p}{\tau} e^{-t/\tau}\left(\frac{3}{4}k^2 R^2\right) + 4\lambda k^2\left(1 - e^{-t/\tau}\right)} \tag{6.39}$$

In the end two different terms have been derived that describe the exothermal temperature profile of beech wood torrefaction. These two terms are:

$$T_1 = \alpha_1\left(1 - e^{-t/\tau}\right)\left(\beta_1 - k^2 r^2\right) \tag{6.35}$$

With:

$$\alpha_1 = \frac{P_0 e^{-t/\tau}}{\frac{C_p}{\tau} e^{-t/\tau}\left(\frac{3}{4}k^2 R^2\right) + 4\lambda k^2\left(1 - e^{-t/\tau}\right)} \tag{6.39}$$

$$\beta_1 = k^2 R^2 \tag{6.36}$$

$$k = \pm\sqrt{\frac{C_p}{2\lambda\tau}} \tag{6.19}$$

And:

$$T_2 = \alpha_2 e^{-t/\tau}\left(\cos kx \cdot \cos ky - \beta_2\right) \tag{6.16}$$

With:

$$\alpha_2 = \frac{P_0\tau}{C_p\beta_2} = \frac{P_0\tau kl}{2C_p}\frac{1}{\left(\sin\left(\frac{1}{2}kl\right)\cos\left(\frac{1}{2}kl\right)\right)} \tag{6.31}$$

$$\beta_2 = \frac{2}{kl}\left(\sin\left(\frac{1}{2}kl\right)\cos\left(\frac{1}{2}kl\right)\right) \tag{6.30}$$

$$k = \pm\sqrt{\frac{C_p}{2\lambda\tau}} \tag{6.19}$$

Both temperature functions can be simplified to the following equations:

$$T_1 = C_1\left(1 - e^{-t/\tau}\right) \tag{6.40}$$

$$T_2 = C_2 e^{-t/\tau} \tag{6.41}$$

And are equal at the moment when the constants describe the level of the temperature and if:

$$t = \tau \ln 2 \tag{6.42}$$

$T_1$ and $T_2$ are equal at the moment that the maximum temperature is reached so that a mathematical description about the exothermal effect is derived in which it is expected that the maximum temperature increase flattens out at higher torrefaction temperatures. The main assumption is that the system should be the same which means that the biomass particle should not crack. This cracking is observed at higher temperatures. A feedback effect of the increased heat production in the particle is the main reason that the temperature increase stabilizes. In Figure 6.17 and Figure 6.18 this can already slightly be observed.

## Conclusions

It can be concluded that with increasing particle size more char is formed during torrefaction. Heat transfer limitations and recondensation of volatiles in the particle are the main contributors to this effect. It can be concluded that secondary reactions as recondensation and gaseous polymerization reactions influence the heat production during torrefaction. An increasing exothermal effect with increasing reaction temperature is shown. The exothermal effect is quantified between 200 and 300°C and is found to be between 0 – 0.25 MJ/kg beech wood raw material. A maximum temperature increase of 40°C is shown in the beech wood particle with particle diameter 28 mm. Above 300°C it is observed that the particle cracks, probably due to pressure build up in the wood, and higher temperature increases than 40°C are reached into the system.

Finally, an analytical model can be developed that describes the temperature profile in the particle as function of time, temperature, location and the progress of the reaction. Temperature profiles in the particle are finally dependent on an exponential term which describes the heat production and which is dependent on the reactivity of the biomass as shown in Chapter 4.

## References

Ahuja P, Kumar S, Singh PC (1996). A model for primary and heterogeneous secondary reactions of wood pyrolysis. Chemical Engineering and Technology 19; 3; 272-282

Bellais M, Davidsson KO, Liliedahl T, Sjöström K, Pettersson JBC (2003). Pyrolysis of large wood particles: A study of shrinkage importance in simulations. Fuel 82; 12; 1541-1548

Bellais M (2007). Modelling of large particle pyrolysis. PhD Thesis; KTH Stockholm

Blackshear PL, Kanury AM, (1965). On the Combustion of Wood I: A Scale Effect in the Pyrolysis of Solids. Combustion Science and Technology 2; 1; 1 - 4

Chan WCR, Kelbon M, Krieger BB (1988). Single-particle biomass pyrolysis: Correlations of reaction products with process conditions. Industrials and Engineering Chemistry Research 27; 12; 2261-2275

Cowdery C., Measurement of the Mass and Energy Balance in Contact Fast Pyrolysis of Wood. MS Thesis T-3459; University of Colorado

Di Blasi C (1994). Numerical simulation of cellulose pyrolysis. Biomass and Bioenergy 7; 1-6; 87-98

Di Blasi C (1996). Heat, momentum and mass transport through a shrinking biomass particle exposed to thermal radiation. Chemical Engineering Science 51; 7; 1121-1132

Di Blasi, C., Branca, C., Santoro, A., Gonzalez Hernandez, E. (2001). Pyrolytic behavior and products of some wood varieties. Combustion and Flame 124; 1-2; 165-177

Felfli FF, Luengo CA, Beaton PA (1998). Bench unit for biomass residues torrefaction. in Kopetz, H., (ed.), Biomass for Energy and Industry, Proc. Int. Conf.; Wurzburg; Germany; 1593-1595.

Hosoya T, Kawamoto H, Saka S (2008). Pyrolysis gasification reactivities of primary tar and char fractions from cellulose and lignin as studied with a closed ampoule reactor. Journal of Analytical and Applied Pyrolysis 83; 1; 71-77

Hosoya T, Kawamoto H, Saka S (2008). Secondary reactions of lignin-derived primary tar components. Journal of Analytical and Applied Pyrolysis 83; 1; 78-87

Hosoya T, Kawamoto H, Saka S (2009). Solid/liquid- and vapor-phase interactions between cellulose- and lignin-derived pyrolysis products. Journal of Analytical and Applied Pyrolysis 85; 1-2; 237-246

Gomez C, Velo E, Barontini F, Cozzani V. (2009). Influence of secondary reactions on the heat of pyrolysis of biomass. Industrial and Engineering Chemistry Research 48; 23; 10222-10233

Grønli MG (1996). A theoretical and experimental study of the thermal degradation of biomass. PhD Thesis; Norwegian University of Science and Technology; Trondheim

Grønli MG, Melaaen MC (2000). Mathematical model for wood pyrolysis-comparison of experimental measurements with model predictions. Energy and Fuels 14; 4; 791-800

Kansa EJ, Perlee HE, Chaiken RF (1977) Mathematical model of wood pyrolysis including internal forced convection. Combustion and Flame 29; 311-324

Larfeldt J, Leckner B, Melaaen MC (2000). Modelling and measurements of the pyrolysis of large wood particles. Fuel 79; 13; 1637-1643

Larfeldt J, Leckner B, Melaaen MC (2000). Modelling and measurements of heat transfer in charcoal from pyrolysis of large wood particles. Biomass and Bioenergy 18; 6; 507-514

Milne TA, Evans RJ (1998). Biomass gasification “tars”: their nature, formation and conversion. NREL, Golden, Colorado, USA. Report no. NREL/TP-570-25357

Milosavljevic, I., Oja, V., Suuberg, E.M (1996). Thermal effects in cellulose pyrolysis: Relationship to char formation processes. Industrial and Engineering Chemistry Research 35; 3; 653-662

Mok WSL, Antal Jr MJ (1983). Effects of pressure on biomass pyrolysis. I. Cellulose pyrolysis products. Thermochimica Acta 68; 2-3; 155-164

Mok WSL, Antal Jr MJ (1983). Effects of pressure on biomass pyrolysis. I. Cellulose pyrolysis products. Thermochimica Acta 68; 2-3; 165-186

Morf P (2001) Secondary reactions of tar during thermochemical biomass conversion. PhD Thesis; Swiss Federal Institute of Technology; Zurich

Park WC, Atreya A, Baum HR (2010). Experimental and theoretical investigation of heat and mass transfer processes during wood pyrolysis. Combustion and Flame 157; 3; 481-494

Prins MJ, Ptasinski KJ, Janssen FJJG (2006). Torrefaction of wood Part: 2. Analysis of products. Journal of Analytical and Applied Pyrolysis 77; 1; 35-40

Rahjohnson JR, Guyonnet R, Guilhot B (1994). Experimental study and modelling of the wood retification process. in: Bimbenet J.J., Dumoulin E., Trystam G. (Eds.), Automatic Control of Food and Biological Process; 227–235

Rath, J, Wolfinger MG, Steiner G, Krammer G, Barontini, F, Cozzani V (2003). Heat of wood pyrolysis. Fuel 82; 1; 81-91

Roberts AF, Clough G (1963). Thermal decomposition of wood in an inert atmosphere. Symposium (International) on Combustion 9; 1; 158-166

Rousset P (2004). Choix et validation experimentale d’un modele de pyrolyse pour le bois traite parr haute temperature: de la micro-particule au bois massif. PhD Thesis; ENGREF; Nancy

Strezov V, Patterson M, Zymla V, Fisher K, Evans TJ, Nelson PF (2007). Fundamental aspects of biomass carbonization. Journal of Analytical and Applied Pyrolysis 79; 1-2 SPEC. ISS. ; 91-100

Tinney ER (1965). The combustion of wooden dowels in heated air. Symposium (International) on Combustion 10; 1; 925-930

Turner I, Rousset P, Remond R, Perre P (2010). An experimental and theoretical investigation of the thermal treatment of wood in the range 200 - 260°C. International Journal of Heat and Mass transfer 53; 715 - 725

Yang H, Yan R, Chen H, Lee DH, Zheng C (2007). Characteristics of hemicellulose, cellulose and lignin pyrolysis. Fuel 86; 12-13; 1781-1788

## Nomenclature

| | |
|---|---|
| $\alpha_1$ | modelling constant |
| $\alpha_2$ | modelling constant |
| $A_1$ | reacting phase in biomass [-] |
| $A_2$ | reacting phase in biomass [-] |
| $\beta_1$ | modelling constant |
| $\beta_2$ | modelling constant |
| B | reacting phase in biomass [-] |
| $C_1$ | formed phase in biomass [-] |
| $C_2$ | formed phase in biomass [-] |
| $C_p$ | heat capacity [J $kg^{--1}$ $°C^{-1}$] |
| $E_0$ | reaction coordinate [-] |
| $E_{free}$ | reaction coordinate [-] |
| $E_{cond}$ | reaction coordinate [-] |
| $k_b$ | reaction constant [kg/s] |
| $k_{c1}$ | reaction constant [kg/s] |
| $k_{c1*}$ | reaction constant [kg/s] |
| $k_{c2}$ | reaction constant [kg/s] |
| $k_{v1}$ | reaction constant [kg/s] |
| $k_{v1*}$ | reaction constant [kg/s] |

| | |
|---|---|
| $k_{v2}$ | reaction constant [kg/s] |
| l | length [m] |
| $\lambda$ | conductivity [$W \cdot K^{-1} \cdot m^{-1}$] |
| $K_{1A}$ | reaction constant [kg/s] |
| $K_{1B}$ | reaction constant [kg/s] |
| $K_2$ | reaction constant [kg/s] |
| $P_0$ | Energy production term [J/s $kg^{-1}$] |
| $P_{n=1,2,3}$ | Energy production [J/s $kg^{-1}$] |
| r | radius [m] |
| t | time [s] |
| T | temperature [°C] or [K] |
| $V_1$ | volatile fraction formed [-] |
| $V_{1*}$ | volatile fraction formed [-] |
| $V_2$ | volatile fraction formed [-] |
| $\zeta$ | exothermal reactive fraction [-] |

# Chapter 7

# Overview of torrefaction initiatives


## Abstract

*In this chapter an overview is presented about the torrefaction initiatives in The Netherlands. This chapter focuses on the commercialization developments that take place with the several torrefaction technologies. Also some remarks will be given about the advantages and disadvantages stated by the several torrefaction developers about their technology. Finally, the different agreements between electricity producers and torrefaction developers are mentioned.*

## 7.1 Introduction

Nowadays several initiatives on torrefaction research and commercialisation make The Netherlands a key centre for the development of torrefaction. A central role is ascribed to the activities of the Energy Research Centre in The Netherlands (ECN) located in Petten, Noord-Holland. ECN initiated the world wide torrefaction research (again) in 2002 and is the main contributor to (scientific) knowledge development from industrial point of view. Further in this chapter an overview is presented about the detailed role of ECN.

With the founding of the Dutch Torrefaction Association (DTA) by three developers of torrefaction systems in 2010 The Netherlands stay on the frontline of torrefaction development. DTA is supported by the foundations AgentschapNL and Energy Valley. The three companies that are part of DTA are; FoxCoal, Topell Energy BV and TorrCoal Technology. The goal of DTA is to develop the torrefaction technology as an important factor in the Dutch energy structure and by this as a stimulator for the Dutch employability. Dutch electricity companies expect a revolutionary change in the biomass industry by commercial applications of torrefaction [Essent, 2010]. Another goal of DTA is to give information about torrefaction and work together as developers on shared interests like product recognition, acceptation and licensing. The three companies each developed their own torrefaction system with different characteristics. Other companies that are not part of the DTA, but also invest in the development of torrefaction as key technology for the Dutch energy economy are Biolake and Stamproy Green Investments.

In this chapter an overview is given about initiatives that are taken to commercialize several torrefaction systems. Although a lot of information is still confidential it is tried to give a good overview about the available information. Most of the information is taken from the companies' websites or by oral communication with the responsible persons.

**Table 7.1:** Overview of reactor technologies and torrefaction initiators in The Netherlands

| Reactor technology | Company |
|---|---|
| Rotating drum | Torrcoal |
| Torbed reactor | Topell |
| Auger reactor | BTG, Biolake, FoxCoal |
| Moving bed | ECN |
| Belt dryer | Stramproy |

## 7.2 Torrefaction reactor technologies

### 7.2.1 Rotating drum

The rotating drum continuous reactor system has proven itself already in different applications. If this technology is applied for torrefaction the biomass can be heated up directly or indirectly by steam or other gases. Parameters that can control the torrefaction process are temperature, rotation speed, length and the angle of the drum. Rotation of the reactor causes mixing of the biomass and good heat transfer, but resistance with the wall increases the amount of dust that is formed. The limitation of rotating drum reactors is the difficulty for scaling up; a maximum product capacity of 5t/hr can be reached.

### 7.2.2 Auger reactor

An auger reactor is a continous reactor that comprises one or more screws that move the biomass through the reactor. The screw is often heated indirectly by a medium that heats up the reactor wall, but can be heated directly. A disadvantage of these systems is that coal and coke formation can occur at the reactor wall if the biomass is not well mixed; this can also lead to weak heat transfer in the system. The residence time in the reactor is determined by the length of the screw. An auger type of technology is a relatively cheap option that has limitations to be scaled up since the ratio surface of the screw versus biomass can become limited. The principle of economies of scale is not valid for auger reactors.

### 7.2.3 Moving bed

A moving bed is continuous reactor that consists of a tube in which the biomass falls down. This tube is completely filled with biomass resources, feeding from the top, and the biomass moves slowly to the bottom of the system. Heating is by a medium that moves in counter current direction from the bottom to the top of the reactor. At the top of the reactor the gaseous phase products are removed and lead to a combustor. A disadvantage of this system is that the heating medium is looking for a way through the biomass bed which has the least amount of resistance. Channel formation is a possibility leading to a heterogenic biomass product quality.

The volume of the reactor can be filled almost completely with biomass, but the presence of very small particles can cause a high pressure drop in the reactor lead. This pressure drop means that the reactor can shut off itself. Sieving before the biomass is feed to the reactor is an option. Pressure of the biomass bed itself can also lead to smaller particles in the reactor.

### 7.2.4 Belt dryer

The belt dryer torrefaction reactor system is a proven continuous design for the drying of biomass resources. The biomass is transported on a belt while it is heated by a heating medium. A proven method is the injection of the medium through holes in the belt while the biomass drops from one belt on the other; at the same time mixing occurs. The moving rate of the belt controls at the same time the transport of the biomass and the residence time. Coal and/or coke formation of the biomass is not possible, but the formation of tars can block the holes in the belt leading to a bad heat transfer. Another disadvantage is that the space of the belt allows only a limited amount of biomass in the system. Finally, the temperature can only be controlled by the heating medium and the speed of the belt.

## 7.3 Gas - solid heat transfer

### 7.3.1 ECN

The Energy Research Centre of The Netherlands has been working on torrefaction with wood as main feedstock since early 2002. The activities mainly focused on the scientific research on topics such as mass – and energy balance with respect to the

influence of different reaction parameters such as temperature and residence time. Also research has been carried out on physical properties such as grindability, hydrophobicity and pelletization behaviour. Since 2006 the research also focused on the application of different (bio) waste feedstocks from mainly agriculture.

At that moment ECN also started with the development of a proto-type pilot plant scale torrefaction unit with a capacity of 50 – 100 kg/h. The combination of torrefaction and pelletization delivered a torrefied pellet, called $BO_2$. The reactor developed by ECN is a moving bed reactor in which the central element is the heating up of the biomass by using recycled torrefaction gases. The recycle consists of re-pressurization of the torgas to compensate for the pressure drop in the recycle-loop and of the heating of the recycle gas to deliver the required heat demand in the torrefaction reactor [Kiel et al. 2008]. In this reactor gas-solid heat transfer is the heating principle which means that the thermal buffer is determined in the fuel itself. An excess of heat must be corrected by the thermal capacity of the wood which means that probably the temperature of the recycled torrefaction gas will run away to higher temperatures by the exothermal reactions. Also the introduction of wood with still a reasonable amount of moisture can cause a temperature drop in the reactor, because the heat capacity of the gas is too small to correct for this.

ECN entered into an agreement with two Dutch industrial parties, Econcern and Chemfo, to bring the technology to the market, but with the bankrupt of Econcern early 2009 this deal came to an end. It was planned to build a demonstration plant with a capacity of around 100 ktonne annual product of $BO_2$ pellets. At the moment of writing ECN has been looking for new investors, a party that wants to develop the project and a party for the engineering. It is expected that the ECN technology will not be operational before 2014.

Finally, [Kiel et al, 2008] mentions that with 10% biomass co-firing of all coal-fired plants in the EU-27 requires 70 Mtonne/a dry biomass. This requires 700 $BO_2$-plants with a size of 100 ktonne/a biomass input. In the EU-15 43 Mtonne/a dry biomass is available for energy processes and in the EU-27 10% biofuels had to be introduced in 2010. To make this chain more efficient from biomass-to-biofuel many plants of 100 ktonne/a can be build.

### 7.3.2 Topell Energy BV

Topell Energy BV is a small Dutch start up company that uses the Torbed ® reactor system that is developed by Polow energy systems. According the website of Topell the system can by used in both continuous and batch processes for drying, combustion, gasification and flue gas cleaning. Also a few advantages are mentioned for the Torbed reactor system, which are the following [Topell, 2010]:

- **Highly efficient heat transfer** : The generated turbulence inside the reactor causes intense contact between the material and the process air, thus facilitating good heat transfer rates. This, in combination with the small bed volume, provides excellent control of the process within small limits inside the reactor.

- **Heat recycling and heat recovery** : By recycling a large amount of the process air when drying the material, enormous energy savings can be achieved. Should recycling not be an option for some reason or other, a heat exchanger can be used to heat up the fresh process air.

- **No moving parts in the reactor** : As the functioning of the Torbed® reactor is completely based on the displacement of air, it does not feature any moving parts inside the reactor chamber. As a result, the reactor has very low maintenance costs. It goes without saying that all additional parts, such as the burner and fans, require the normal amount of maintenance.

Just like the moving bed reactor of ECN in this reactor gas-solid heat transfer is the heating principle which means that the thermal buffer is determined in the fuel itself. An excess of heat must be corrected by the thermal capacity of the wood which means that probably the temperature of the recycled torrefaction gas will run away to higher temperatures by the exothermal reactions. Also the introduction of wood with still a reasonable amount of moisture can cause a temperature drop in the reactor, because the heat capacity of the gas is too small to correct for this.

In May 2008 Topell Energy BV made a deal with RWE Innogy for cooperation for converting biomass into biocoal pellets on larger scale. The deal is based on the following agreements:

- First transaction in the venture capital business – 25% equity in Dutch start-up company Topell
- Ground-breaking process for producing biocoal pellets as fuel for conventional power plants
- Effective method of reducing $CO_2$ emissions through co-firing of coal and biocoal pellets

Topell Energy BV and RWE Innogy together aimed at building the first commercial plant in The Netherlands for producting biocoal pellets to be realized in 2009. In February 2010 it is decided to build a torrefaction plant of 60,000 ton biocoal on yearly basis in Duiven. The company aims at the application of wood as feedstock, but a provincial subsidy of 1M€ for a drying installation should make it possible to use difficult grass resources as torrefaction material.

## 7.4. Belt dryer and drum reactors

### 7.4.1 Stramproy Green Investments

Stramproy Green Investments (SGI) is a company that develops for torrefaction a belt dryer that can be used for continuous processes. In Februari 2009 SGI together with 4 Energy Invest made a deal about the construction of a torrefaction unit for the production of BioCoal pellets in Amel in Belgium. In August 2009 Essent Energy Trading B.V. and Stramproy already made a deal about the construction of 90,000 tonne capacity torrefaction plant. The Stramproy biocoal production plant will be located in Steenwijk and will be combined with a small scale combined heat and power to reduce the impact on the environment and increase the energy efficiency.

### 7.4.2 Torrcoal

Torr-Coal is a relatively small company with 6 – 8 employees which develop their own torrefaction system based on a rotating drum technology. The company has been involved in the developed of waste to fuel for electricity power stations for a long time. It already developed a process in which the biomass is washed so that chlorine and sulfur are removed. Torr-coal aims at the development of waste stream torrefaction for the production of pellets with 60% organic material. At the moment Torr-coal develops a torrefaction installation in Dilsen-Stokkem in Belgium with a production capacity of 35kton. Torr-coal is involved in standardization of the final product by the Dutch Torrefaction Association and develops its own Hard Grove Index for biomass grinding.

## 7.5 Auger reactors

### 7.5.1 BioLake

BioLake is a company that focuses on the development and the commercialization of sustainable fuels from dry organic feedstocks by torrefaction. It is founded by a consortium of five agrarian companies and ATO-NH (an association for technology commercialization in the North of Netherlands) in the end of 2006. At the moment the technology is in its testing phase and if succeeded more torrefaction installations will be build in the rest of Europe.

The process of BioLake focuses on the combination of torrefaction with pelletization. The torrefaction technology that is applied by BioLake is based on existing technology, but is applied for other production processes. A long tube is directly heated by installations that are already applied in the ceramic and cement industry or for drying processes in industry. The biomass feedstock (straw) is transported by a rotating screw or auger in the tube that is positioned in a small angle which enforces the transportation. Another possibility is the rotation of the tube itself [BioLake, 2010]. An important aspect of the BioLake technology is that the focus is also on the development of a transportable reactor concept that can be placed close to the biomass harvest location.

An important side product of the torrefaction is the volatile phase that is formed. In the BioLake technology this gas is used to heat up the tube reactor directly, but the

biomass indirectly, by combustion of the formed gases. The combustion flames heat up the reactor tube and keep it at constant temperature. The heat of combustion is enough to keep the process running.

### 7.5.2 Foxcoal

Foxcoal developed a torrefaction system based on an auger reactor. At the moment the activities of Foxcoal are focused on the installation of an up-scaled system and are there plans to build a second torrefaction system.

## References

BioLake (2010). www.biolake.nl last checked at 16th of March 2010

Essent (2010). Essent Trading. January 2010

Kiel JHA, Verhoeff F, Gerhauser H, Meuleman B (2008). $BO_2$-technology for biomass upgrading into solid fuel – pilot-scale testing and market implementation. 16th European Biomass Conference & Exhibition, 2-6 June 2008, Valencia, Spain.

Topell (2010). www.topell.nl last checked at 16th of March 2010.

# Chapter 8

## Conclusions

## 8.1 Main conclusions

The main objective of this study was to identify how the different reaction parameters influence the reaction mechanism of biowastes during torrefaction for the production of solid biofuels. Furthermore, the thesis aimed to answer the question **how the chemistry and reaction kinetics of torrefaction are influenced by its reaction conditions and what effects occur during the thermo chemical reactions.** This research question can be more specified with the subquestions such as, how are the kinetics during torrefaction and what does this mean, which products are formed, what are the mass - and energy balances, what is the endo- and or exothermal behaviour. The information gained in this study can be applied to make a proposal for an improved torrefaction reactor within a process design. The main conclusions are:

- Some biomass properties, particularly high O/C ratio and difficulty to get small particle size, form problems for technological application of biomass. Torrefaction has the potential to become an important biomass pretreatment technology and so improve the biomass to a high quality solid fuel with good characteristics in energy density, homogeneity, grindability and hydrophobic behavior. The main advantage of torrefaction is improvement of energy density and grindability. It is shown that torrefaction offers efficiency advantage when used as a pretreatment step before entrained flow gasification (Chapter 3).

- Describing four different thermal decomposition models for biomass torrefaction at isothermal conditions in a mathematical formulation shows they formally lead to two mathematical descriptions. A global one step reaction model is mathematically similar to a two competitive reactions model and two steps in series reaction model is mathematically similar to a two parallel reaction model. Further it is shown that two different phases in the biomass react independent of each other. The slow reacting phase has high availability and the fast reacting phase has an apparent temperature dependence of the availability (Chapter 4).

- It is confirmed with TG-MS and TG-FTIR that two different steps can be identified. All the components identified, except the phenol and aromatic compounds, collected during the fixed bed experiments, TG-MS and TG-FTIR

are at the same time formed during the fast and slow reacting phase, but the rate in which the components are formed show a different profile looking at the TG-FTIR figures (Chapter 5).

- It can be concluded that the fast reacting step with low availability produces small molecular products even as the slow reacting phase with high availability which also produces aromatic compounds. This slow reacting phase comprises the reactivity of lignin. It is shown that carboxylic acids and water are the main condensable torrefaction products while smaller quantities of other oxygenates with different functionality are formed. CO and $CO_2$ formation comprise an important part of the mass balance based on the assumptions made (Chapter 5).

- The energy balance of the torrefaction process shows that with increasing reaction temperature the process becomes less endothermic and/or more exothermic. The heat of reaction that has been found is between 0.7 MJ/kg biomass endothermic and -0.8 MJ/kg biomass exothermic. The formation of acetic acid (and other organics) has the highest influence on the energy balance. The lower heating value of the gas phase increases with temperature and biomass conversion, but at higher temperatures the LHV of the gas phase flattens out. Probably the organic fraction is cracked to energetic less valuable products (Chapter 5).

- It can be concluded that with increasing particle size more char is formed during torrefaction. Heat transfer limitations and recondensation of volatiles in the particle are the main contributors to this effect. It can be concluded that secondary reactions as recondensation and gaseous polymerization reactions influence the heat production during torrefaction. An increasing exothermal effect with increasing reaction temperature is shown. The exothermal effect is quantified between 200 and 300°C and is found to be between 0 and 0.25 MJ/kg beech wood raw material, depending on the temperature. A maximum temperature increase of 40°C is shown in the beech wood particle with particle diameter 28 mm. Above 300°C it is observed that the particle cracks, probably due to pressure build up in the wood, and higher temperature increases than 40°C are reached into the system (Chapter 6).

## 8.2 Recommendations for future work

The understanding of biomass chemistry and reaction kinetics during torrefaction has been growing fast last years. Recommendations for further torrefaction research can be made on different levels. So the following recommendations are presented:

- It is recommended to obtain more insight into the torrefaction reactions as function of time at constant reaction temperature. In the development of the experimental setup it should be taken into account that the biomass can be feed at constant torrefaction temperature with analytical equipment connected to the setup so that in-situ measurements about the product characteristics are possible including the relative weight loss profile. In this way a better understanding can be obtained about the energy content in the gaseous phase as function of the relative biomass weight which has reacted during torrefaction.

- Further research on the product characteristics is recommended. Characteristics such as pelletization, biological degradation and dust forming of the solid biomass need more attention in relation to reaction conditions during torrefaction. An interesting topic is the formation of condensable tar products and its applicability as binder in pelletization.

- Challenges in torrefaction research can be found in the up scaling of the technology to commercial scale. The potential of torrefaction is recognised, but the lack of available mature technology blocks market implementation of a torrefied biomass pellet. Each biomass resource has its own technological and economical optimum for torrefaction.

- Product standardization is an important step in the recognition of torrefied biomass. The development of product specifications about the sustainable production of a high quality product is an important step for the market implementation of torrefied biomass.

- Further it is recommended that the production of chemicals during torrefaction will be researched more extensively and that wise concepts are thought about.

During torrefaction of biomass the main products that have been found are carboxylic acids in an aqueous solution. These acids are mixed with small fractions of other oxygenated functions such as alcohols, aldehydes, ketones, furans and lignin derivates. [De Wild et al., 2009] studied the staged degasification of lignocellulosic biomass resources for the production of chemicals. Staged degasification is carried out to fractionate condensable volatiles on their functionality. Torrefaction is proposed as first step in the production of chemicals. Between 200 - 300° the condensable volatiles produced from thermo chemical conversion are isolated and upgraded to biobased chemicals. This staged degasification may contribute to the BIOCOUP project that focuses on the separation and purification of bio-chemicals for several applications.

## List of Publications

### Journal publications

Stelt, M.J.C. van der, Gerhauser, H., Kiel, J.H.A., Ptasinski, K.J. (2010). Biomass upgrading by torrefaction for the production of biofuels: a review. Biomass and Bioenergy, submitted / in press.

Stelt, M.J.C. van der, Leenders, T.M., Veringa H.J. (2010). Chemistry and reaction kinetics of biowaste torrefaction: mechanistic pathway for biomass decomposition during torrefaction at isothermal conditions, to be submitted / in press

Stelt, M.J.C. van der, Bolkent, E., Carleer, R., Veringa H.J. (2010). Chemistry and reaction kinetics of biowaste torrefaction: product formation during biowaste torrefaction, to be submitted / in press

Stelt, M.J.C. van der, Veringa H.J. (2010). Chemistry and reaction kinetics of biowaste torrefaction: large particle beech wood torrefaction, to be submitted / in press

### Book chapter

Ptasinski, K.J., Stelt, M.J.C. van der (2010). Extended Exergy Accounting (EEA) of the Dutch Society. In A. Solovyov, I. Kuznetosv (Eds.), International accounting in the 21st century. (pp. accepted) Hauppauge, NY: Nova Publishers.

### Conference Proceeding

Stelt, M.J.C. van der, Ptasinski, K.J., Veringa, H.J. (2009). Biomass upgrading for the production of biofuels from biowastes; Modelling of (large particle) torrefaction. Netherlands Process Technology Symposium 2009 (NPS-9),26-28 October, Veldhoven. (pp. p.-95). Netherlands, Veldhoven: Netherlands Research School of Process Technology (OSPT) / Nederlandse Procestechnologen (NPT).

Stelt, M.J.C. van der, Ptasinski, K.J. (2008). Biomass upgrading for the production of biofuels from biowastes; weight loss kinetics of biomass torrefaction. From Research to Industry and Markets proceedings of the 16th European Biomass

Conference & Exhibition, 02-06 June 2008, Feria Valencia, Spain. Florence: ETA-Florence Renewable Energies.

Stelt, M.J.C. van der, Ptasinski, K.J. (2007). Biomass upgrading by torrefaction for the production of biofuels. Netherlands Process Technology Symposium. (pp. pp.-1). Netherlands, Veldhoven.

Stelt, M.J.C. van der Stelt, Ptasinski, K.J., Koymans, M.N., Sciubba, E., Performance of the Dutch Society Based on Energy, Exergy and Extended Exergy Accounting, in ECOS 2007 20th International Conference on Efficiency, Cost, Optimization, Simulation and Environmental Impact of Energy Systems; Editors: -, Padova, Italy, 1477-1484, (2007)

## Dankwoord - Acknowledgements

Graag wil ik vanaf deze plek iedereen bedanken die heeft bijgedragen aan de ontwikkeling van mijn torrefactie onderzoek, de totstandkoming van dit proefschrift en iedereen die mij de laatste jaren heeft aangemoedigd, gemotiveerd en gesteund; niet alleen tijdens het promotieonderzoek, maar ook tijdens de mooie en afwisselende tijd aan de TU en de activiteiten en het leven daarbuiten. Eindhoven is als een thuis voor mij geworden; een plek waar ik me als mens heb mogen vormen. Het is een zegen om zoveel goede collega's, vrienden en familie om je heen te mogen hebben, elkaar op te bouwen en te mogen genieten. Sommige mensen wil ik hieronder graag persoonlijk noemen en bedanken.

Mijn promotor Hubert Veringa wil ik bijzonder bedanken voor de vele interessante discussies en gesprekken, de nodige input en de waardevolle correcties van mijn proefschrift. Hubert, zeer veel dank voor je tussentijdse komst naar Eindhoven, en voor de totstandkoming van dit proefschrift.

Krzysztof Ptasinski wil ik mijn waardering uitspreken voor het eerste anderhalfjaar begeleiding na het te vroeg overlijden van Frans Janssen. Je hebt mij immers de kans gegeven om binnen SET dit onderzoek te starten na mijn afstuderen.

Jaap Schouten wil ik bedanken voor de gastvrijheid om binnen SCR gebruik te mogen maken van alle faciliteiten. Het was een mooie tijd om in deze groep actief te zijn en van dichtbij compleet ander onderzoek te mogen aanschouwen. Succes bij het verder bouwen aan mooie en creatieve onderzoeksgroep.

De samenwerking met ECN heb ik ook als zeer prettig ervaren. Jaap Kiel, Heiko Gerhauser en Fred Verhoef enorm veel dank voor de input in het onderzoek en de praktische onderzoeksideeen. Ook wil ik Jasper Lensselink en Alex Adell bedanken voor de samenwerking en hun enthousiasme tijdens het Tortech onderzoek. Veel succes bij de (creatieve) wegen die jullie opslaan. Mijn dank gaat ook uit naar Patrick Bergman die mij stimuleerde met torrefactie verder te gaan tijdens mijn stage bij ECN.

Ik ben ook veel dank verschuldigd aan Jan Meuldijk. Jan, jouw liefde voor het vak en studenten is onevenaarbaar! De TU mag trots op je zijn! Bedankt voor de autoritjes naar Hasselt en de leuke en waardevolle gesprekken. In Hasselt wil ik

graag Robert Carleer en Guy Reggers bedanken voor de praktische mogelijkheden die zij mij geboden hebben.

Tim Leenders, Eralp Bolkent, Jordy Franssen en Fernanda Neira D'Angelo wil ik graag bedanken voor hun input in het onderzoek door een (afstudeer) project aan torrefactie uit te voeren. Het was plezierig en leerzaam om met jullie samen te werken. Succes met jullie verdere loopbaan! Guus Pemen en Johan Wijers bedankt voor het plaatsnemen in de commissies.

Ook zijn er een aantal mensen actief geweest om mijn kwalitatieve en kwantitatieve analyses te doen slagen. Maria Eriksson en Chunxia Sun wil ik bedanken voor het oneindige aantal TGA analyses die gedaan zijn. Ingeborg en Hester, bedankt dat ik van het analytisch lab gebruik kon maken.

Ik ben voor ook veel dank verschuldigd aan Anton Bombeeck, Erik van Herk, Chris Luykx, Wim Groenland, Marlies Coolen, Peter Lipman, Carlo Buijs, Madan Bindraban en Dolf van Liempt. De technische en analytische ondersteuning heb ik zeer gewaardeerd. Het is goed om te weten dat er met jullie vaardigheden veilig gewerkt kan worden. Gelukkig is er voor jullie op de werkplaats met het verschijnen van dit proefschrift een einde gekomen aan het draaien van wel erg korte bezemstelen.

Zonder Denise Tjallema zou mijn administratie een chaos geworden zijn. Daarom heb ik zeer veel waardering voor de secretariele ondersteuning bij het halen van deadlines (vooral bij het afronden van alle formulieren op het eind en de in mijn ogen veelal nutteloze bureaucratie)! Martin Timmer wil ik bedanken voor het financiele overzicht tijdens het project

Mijn kantoorgenoten Anna Sues, Carlos Vilela en Martin Jurascik wil ik bedanken voor de prettige sfeer, de fijne gesprekken, het bezoeken van conferenties en de veiligheid op het lab ☺! Anna, het was goed om jou als kantoorgenoot te hebben met zoveel kennis. Je stond altijd klaar een vraag te beanwoorden. Het was ook erg handig om een Catalaanse tijdens de conferentie Valencia erbij te hebben zodat je niet afgezet wordt! Veel succes bij het vervolg van je loopbaan in Barcelona! Carlos, bedankt voor je levendigheid en gezelligheid in het kantoor, op het lab of op het voetbalveld (Alleen moet je meer overspelen!). Succes met het afronden van

je onderzoek en het vervolg daarna! Martin, bedankt voor je aangename aanwezigheid op kantoor en natuurlijk voor je rondleiding door Bratislava.

Natuurlijk wil ik ook mijn waardering uitspreken aan mijn Zuid-Afrikaanse vrienden en collega's Jack Fletcher en Gregory Govender voor de vele gezellige koffies, lunches, bezoekjes aan de stad en andere sociale activiteiten. We hebben veel kunnen lachen. Jack, wanneer gaat die meesterlijke Zuid-Afrikaanse "Braai" er nou komen? Succes bij Sasol jullie beiden!

Ook wil ik Frans Visscher, Tom Jansen, Marco Meeuwse, Joost Rooze, Stijn de Loos en Kevin van Eeten bedanken voor een mooie tijd tijdens het promotieonderzoek en de vele koffies. Hoop jullie in de toekomst nog geregeld te zien bij fijne filosofische lezingen, pubquizen, voetbalwedstrijden of bepaalde proeverijen. Succes bij het voltooien van jullie projecten!

Ook wil ik mijn overige collega's van harte bedanken voor een onvergetelijke tijd. Beste koffiedrinkers, bedankt! Vele afstudeerders zijn gekomen en gegaan bij SET en SCR, maar toch wil ik ook hen bedanken voor een goede tijd aan de TU. Speciaal wil ik toch nog even Tomas, Rene, Harro, Bas, Mark, Sander, Jan-Jaap, Michiel en Rik noemen.

Jeroen Ramakers wil ik bij deze graag bedanken voor het ontwerp van de cover om mij zo bij te staan met computerkwaliteiten die ik absoluut niet bezit.

Naast de drukke bezigheden was het altijd een waar genot om in wisselende samenstelling even stoom af te blazen in de F.O.R.T en in de stad meer of minder kwalitatief te dineren. Totelos N4, Cup-a-Soup-Tigers, De Vlakkers en Spartak wil ik graag bedanken voor de sportieve ontspanning in de zaal.

ChristenUnie en PerspectieF Brabant bedankt om een plek te zijn waar mijn maatschappelijke interesse kon aarden en de komende tijd verder vorm gegeven mag worden. Uit overtuiging hebben jullie goud in handen, maar helaas ziet nog niet iedereen dat! Ik kijk uit naar een verdere samenwerking met jullie, Gerben en Mathijs. En in moderne tijden kun je natuurlijk ook niet meer om Social Media heen. Tweeps, bedankt!

Ralf Verhaegh wil ik bedanken voor het aanhoren van al mijn frustraties en irritaties tijdens het onderzoek (al kon jij er ook wat van). Het was goed om een luisterend oor te hebben en af en toe lekker cynisch te zijn over het nut van wat we doen!

Mijn dank gaat ook uit naar Andrey Dvortsov voor zijn enthousiasme en interesse in mijn bezigheden. Je enorme interesse in vele onderwerpen verbazen mij iedere keer weer. Ook jij bedankt voor het luisterende oor tijdens de (vele) dipjes ☺.

Fokko Haveman wil ik bedanken voor al zijn boekentips en uitgebreide conversaties. Je hebt enorm veel talent Fokko, maar geniet van alles dat je gegeven is. Ik hoop dat we samen met Frans nog vele CU activiteiten gaan bezoeken! Jeroen Klijn, Marco Krielen, Jesper van Berkel, Chris Gits en Tim van Acker, bedankt voor het contact via de Chemiewinkel, onze Zwedentripjes, kerstdiners, filmavonden, etc. Het was goed om de nodige ontspanning te hebben aan de TU.

Graag wil ik ook Mathijs, Dorien, Marcel, Joska, Kees, Albert, Annemarie, Basjan, Sharon, Sandra, Steven, Erik, Sandra, Leslie en Rene bedanken voor vele jaren diepgang en oppervlakkigheid, vriendschap, interesse, liefde en steun.

Als laatste wil ik mijn ouders en broers en zus en overige familie bedanken voor hun liefde, vertrouwen en ondersteuning in tijden dat het goed ging, maar zeker ook dat ik jullie aanwezigheid zeer goed kon gebruiken, vooral tijdens de laatste loodjes. Pa en ma, Arnoud, Annelies, Robin en Christiaan, bedankt voor al het geduld, de warmte en geborgenheid. Het is goed om te weten altijd bij jullie terecht te kunnen.

*Wat er was, zal er altijd weer zijn,*
*wat er is gedaan, zal altijd weer worden gedaan.*
*Er is niets nieuws onder de zon.*
*Wanneer men van iets zegt: 'Kijk, iets nieuws,'*
*dan is het altijd iets dat er sinds lang vervlogen tijden is geweest.*
*De vroegere generaties zijn vergeten,*
*en ook de komende zullen weer worden vergeten.*

*(Prediker 1 : 9 - 11)*

## About the Author

Michiel van der Stelt was born on the 15th of April 1983 in Werkendam. He graduated from the Gymnasium Camphusianum in Gorinchem in 2001. In the same year he started his study Chemical Engineering at the Eindhoven University of Technology, from which he obtained his M.Sc. degree in 2006 on the topic of "The performance of the Dutch society based on energy, exergy and extended exergy accounting". In October 2006 he started his Ph.D. research at the Laboratory of Environmental Technology at the Eindhoven University of Technology initiated by late prof.dr.ir. F.J.J.G. Janssen and under temporary supervision of dr.ir. K.J.Ptasinski and promoter prof.dr. H.J. Veringa. Communication with the author is possible by email: michielvanderstelt@hotmail.com